Universitat Autònoma de Barcelona

FACULTAT DE CIÈNCIES
DEPARTAMENT DE GENÈTICA I DE MICROBIOLOGIA

CARACTERIZACIÓN ECOLÓGICA DE COMUNIDADES DE MICROORGANISMOS PLANCTÓNICOS MARINOS, BASADA EN RELACIONES ENTRE LA DISTRIBUCIÓN DE TAMAÑOS, COMPOSICIÓN QUÍMICA Y TAXONOMÍA

M. Laura Arin Carrau

Tesis Doctoral
Universitat Autònoma de Barcelona
Facultat de Ciències – Departament de Genètica i de Microbiologia

Caracterización ecológica de comunidades de microorganismos planctónicos marinos, basada en relaciones entre la distribución de tamaños, composición química y taxonomía

Memoria presentada por M. Laura Arin Carrau para optar al título de Doctora en Biología en el Departamento de Genética y de Microbiología – Facultad de Ciencias, Universidad Autónoma de Barcelona, bajo la tutoría del Dr. Jordi Mas y la dirección de la Dra. Marta Estrada i Miyares del Departamento de Biología Marina y Oceanografía del Instituto de Ciencias del Mar (CMIMA, CSIC) de Barcelona.

M. Laura Arin Carrau
Barcelona, Septiembre de 2002

La directora de la tesis
Dra. Marta Estrada i Miyares
Profesora de Investigación
Institut de Ciències del Mar
CMIMA, CSIC

El tutor de la tesis
Dr. Jordi Mas
Profesor titular
Facultad de Ciències
Universitat Autònoma de Barcelona

A mi familia

Todo lo que vivamente imaginamos,
ardientemente deseamos,
sinceramente creemos y
entusiastamente emprendemos,
inevitablemente sucederá

Anónimo

ÍNDICE

AGRADECIMIENTOS

En verdad, me parece mentira estar en esta fase de agradecer sobre el papel a todas aquellas personas que ya sea de manera directa o indirecta me han apoyado y ayudado para que este trabajo llegara - ¡ por fin ! - a su fin.

En primer lugar, quiero agradecer a mi directora de tesis, la Dra. Marta Estrada, no sólo por haberme dirigido este trabajo sino también por haberme dado la oportunidad y la confianza de poder llevarlo a cabo. Por sus sabias y rápidas correcciones, sus consejos y tener siempre un lugar para escucharme dentro de su apretada agenda.

Una vez iniciado este camino, he tenido la suerte de trabajar también con Cèlia Marrasé. A ella mi muy especial agradecimiento por permitirme elaborar y discutir gran parte de esta tesis a su lado, por su gran apoyo y por los muchos, muchísimos ánimos que me ha dado en todo momento. Con ella no sólo he compartido el "turbulento" mundo de la turbulencia sino otros "turbulentos" ires y venires de la vida. En esta etapa he de agradecer a todos y cada uno de los integrantes del "MEDEA-SERET-NTAP team" (Elisa, Montse S, Cesc, Montse V, Rafel S, Miquel, Andrea, Òscar, Cristina, Mercedes y … a esa persona que seguro me olvido), y a los que han participado en algunos de los experimentos (thank you Marie!) ya que de una manera u otra me han ayudado en la realización de este trabajo; con todos he compartido, con "buen rollo" (y a veces pastitas), muchos experimentos de microcosmos (aunque en esta tesis sólo esté reflejado uno de ellos). En especial agradezco a Elisa todas sus enseñanzas en bioquímica y su apoyo principalmente cuando esta tesis aún era un proyecto. Además, entre ella y Lluïsa me han enseñado el ABC en lo que se refiere a cultivos de fitoplancton. Con Cesc, he aprendido muchas cosas sobre los Macintosh (aunque después acabé trabajando con PC… cosas de la vida!), y me ha echado más que una mano con los cálculos de turbulencia, con la estadística y en mil dudas que fueron surgiendo por el camino. A Montse S he acudido muchas veces con textos para que me los corrigiera o me diera su punto de vista. Muchas gracias a todos!!

En realidad fueron muchas las personas del Departamento con quienes he aprendido las metodologías y discutido muchos puntos que están reflejados en esta memoria. Las bases para analizar clorofilas y contar fitoplancton me las dio Marta pero luego he recurrido a mucha más gente preguntando dudas y/o consejos como a Lluïsa, Cèlia, Elisa, Maxi, Magda, Dolors B, Renate, Mikel, Esther… El contar flageladitos al microscopio de epifluorescencia se lo debo principalmente a

Dolors V, el contar bacterias y picoeucariontes por citometría de flujo a Pep, el utilizar el Coulter a Elisa y Enric …, el sistema de análisis de imagen a Cesc, Enric, Pep … Además, muchas personas han respondido a mis dudas (sería muy larga la lista), ya sean metodológicas o conceptuales en momentos críticos y no tan críticos durante esta etapa de tesis. A todos, muchas gracias!!!

En realidad, mi agradecimiento va dirigido a todas las personas del Departamento que de una manera u otra me han ayudado para que esta tesis se hiciera realidad y que han creado un buen ambiente de trabajo y también a veces de distensión ya sea por las comidas en la terraza o los encuentros en el "rincón del café". A Pep, Dolors V, Cèlia, Rafel S, Nagore, Mariona, Òscar, Cristina, Andrea, Montse V., Giorgious, Alejandro, Montse S., Jarone, Kees, Lluïsa, Pili, Carles, Marta E, Elisa, Jordi C, Jordi F, Vanessa, Eva, Dacha, Laura, Maria, Fernando, Eli, Sergi, Cristina L, Renate, Marta R, Esther, Magda, Albert, J Maria, Miquel, Mikel, Francesc P, Meme, Isabel, Enric, Ramon, Cesc, Ted, Dolors B, Ana … y a los más nuevos o los que están por aquí por un tiempo. A las personas que ahora ya no están (sea por el motivo que sea) pero con las que también he compartido un trozo de este camino: Antonia, Luisa, Juani, Núria, Emilio, Angela, Xelu, Xabier, Cova, Patricia, Maxi, Evaristo, Michael, Laure, Aramis, Eduardo, Octavio, Josep, Gloria, Bea, Rafel C, Susana, Maria, Alícia, Víctor, Carme, Eduard, Akira, Madda ...

Dentro del Departamento el despacho ha sido un mundo aparte y siempre me he sentido muy a gusto con las personas con quienes lo compartí. A mis compañeros del antiguo ICM (Marta R, Cesc, Xabier, y más tarde Andrea y Albert) y del nuevo ICM-CMIMA (Lluïsa y Pili), gracias por haberme escuchado tanto en momentos de agobio y desespero como en momentos de alegría y festejo durante estos años de tesis. Con Marta R recuerdo con cariño compartir mis primeras etapas en el ICM en un despacho que en principio parecía enorme pero que luego no lo fue tanto. Con Andrea, recuerdo que entre "gráfica y gráfica" nos fuimos contando la vida y compartiendo nuestras dudas existenciales (y la paciencia de Albert al tenernos de compañeras!). En esta última etapa en el antiguo ICM no han faltado, sobre todo en las últimas horas del día, aquellos visitantes (Xelu, Ramon, Eli, Bea, …) que ya sea con el motivo de alguna pregunta, en busca de datos o simplemente por una "galleta o chocolate", me permitían levantar la vista del ordenador y compartir con ellos momentos muy agradables.

A todos los que me han contratado (Marta, Cèlia, Miquel, Jordi C), por dejarme (sobre todo al final) un lugar para que esta tesis pudiera constituirse y llegar así a su fin, y a Nagore, Magda, Mariona, … porque en este último año parte de mis tareas las habéis hecho vosotras. Muchas gracias!

A las bibliotecarias, informáticos, recepcionistas, personal de la UTM y personal administrativo en general, gracias por toda la ayuda otorgada. En especial a Marta E por explicarme muy pacientemente cosas que "ya debería saber", a Àlex y Evilio por solucionarme problemas informáticos (sobre todo cuando me pasé al PC). A José Maria por redibujar las Fig. 1, 2 y 3 del Capítulo IV, a Roser por todos los análisis de nutrientes.

A la gente de otros departamentos con muchos de los cuales más de una vez ha salido el tema "tesis": Montse R, Montse D, José Manuel, Jordi S, Jordi F, Mikhail, Jordi S, Pili O, Joan, Alicia, Enrique, Anita, Mohamed, Marc, Sergi, Anna S, Isabel P, Marta R, Maribel, Laura, Toni, Jorge, Pere, Jacobo, …

Esta tesis se ha completado gracias a los trabajos realizados en determinadas campañas oceanográficas en las que he participado. A todos los participantes, ya sean colegas, jefes de campaña o tripulación, os estoy muy agradecida, no sólo por vuestra ayuda sino también por la buena compañía que me habéis brindado. Tengo muchos buenos recuerdos de las campañas vividas gracias al buen ambiente que se respiraba …, sobre todo la MATER I, donde tuve la oportunidad de festejar un especial cumpleaños en alta mar!

A todos con los que he compartido muy buenos momentos también fuera del Instituto ya sea en excursiones, cenas, cines, bailando, o simplemente hablando o "filosofando" sobre cosas de la vida: A Nuri, Rosanna, Anna y Roger, Graziella, Marvin, Paolo, Hugo, Gabriel y Censi, Ma Àngels y Andrea B, Agustín y Tina, Nancy y Aurelio, César, Nuria, Juani, Emilio, Marta R, Xabier, Angela, Cova, Andrea, Xelu, Ramon, Eli, Bea, Albert, Jarone, Magda, Pastora, Carles, Mariona, Òscar, Vanessa, Jordi F …

A Anna y Graziella, porque sois mis "hermanas" de Barcelona. Gracias por vuestra amistad y cariño, por todas las horas y horas compartidas hablando y hablando y hablando …

A Lluïsa, por su incondicional apoyo en todo momento. Gracias por tu más que amistad, tu cariño y tus siempre muy buenos consejos.

A Carles, ¡ noi ! me has conocido en el agobio final de la tesis !!! Gracias por tu enorme paciencia y comprensión, por tu saber escuchar y aconsejar, por leerte la Introducción y la Discusión General y por tus correcciones y sugerencias (y responder siempre a mi pregunta: ¿se entiende?), por tu "tesis" dentro de esta tesis. Y por hacerme pasar tantos y tantos buenos momentos.

A mi familia de Irún, a quien he tenido la suerte de conocer. En especial a Junkal y Candi por recibirme tan bien cada vez que estuve allí.

A mi gente de Uruguay a la que quiero tanto y siempre tengo presente. A mis padres por haberme dado TODO lo que me han dado. Gracias por vuestro cariño, vuestro apoyo y vuestra comprensión en todo momento. Por las siempre esperadas llamadas cada 15 días y por recibirme y mimarme tanto cuando estoy allí. A mis hermanos, Javier, Gonzalo y Daniel, por ser tan buenos hermanos y tratarme tan (demasiado) bien siempre. Por vuestros mails (a veces "chats") poniéndome al día con cosas de allí. Por hacerme ver, en momentos de desaliento, lo importante que es todo esto para mi. A mis sobrinos, Lucía, Mauricio, Santiago, Diego, Ale, Romina, Nico y Gastón por darme tanto cariño cuando voy. A mis grandes amigas "de toda la vida" (Laura, Gabriela y Andrea). Gracias por hacerme sentir cada vez que voy, como si no me hubiera ido. Y a mucha más gente (Marta R, Ma Elena, René, Mabel, Negra, cuñadas, tíos, primos …) que siempre está allí para darme una buena bienvenida.

¡¡¡ GRACIAS A TODOS !!!

INTRODUCCIÓN GENERAL

El estudio de los flujos de materia y energía resulta básico para la comprensión del funcionamiento de cualquier ecosistema. El flujo de carbono es de especial importancia debido a su implicación en el cambio climático global (Siegenthaler & Sarmiento 1993) asociado al aumento antropogénico en las concentraciones de dióxido de carbono (CO_2) atmosférico. Este CO_2 atmosférico puede disolverse fácilmente en el medio marino. En este medio, la incorporación del CO_2 está dominada por la fotosíntesis del fitoplancton. Una gran parte de la biomasa producida es consumida por los organismos heterotróficos, con lo que el carbono fijado en la fotosíntesis es respirado o transportado a otros niveles de la cadena trófica. La vía de transferencia de materia y energía a través de los diferentes niveles de la cadena trófica y el tipo de red trófica predominante depende, entre otras cosas, de las condiciones ambientales en las que crecen los organismos. En términos generales, en aguas eutróficas (ricas en nutrientes), débilmente estratificadas, mezcladas o turbulentas, predominan células de fitoplancton de gran tamaño como pueden ser las diatomeas (Semina 1968, Margalef 1974, 1978, Malone 1980, Harris et al. 1987, Legendre 1990, Kiørboe et al. 1990). En cambio, en aguas oligotróficas (pobres en nutrientes) y estratificadas, la comunidad de fitoplancton está generalmente dominada por células pequeñas, como flagelados de diversos grupos o cianobacterias (Cushing 1989, Takahashi & Hori 1984). Esto determina básicamente dos vías de transferencia de energía y biomasa hacia los productores secundarios (Fig. 1). En el primer caso (aguas eutróficas - autótrofos grandes) se desarrollaría la llamada vía clásica (Fig. 1a): fitoplancton - mesozooplancton - peces (Steele 1974) y en el segundo caso (aguas oligotróficas - autótrofos pequeños) la llamada vía microbiana (Fig. 1b): fitoplancton - bacterioplancton - flagelados heterotróficos - ciliados (Azam et al. 1983). Por lo tanto, la estructura de tamaños de los productores primarios parece ser un factor fundamental para el establecimiento de una red trófica u otra (Legendre & Rassoulzadegan 1995) la cual, a su vez, determinará el destino final del carbono orgánico asimilado. El desarrollo de autótrofos grandes favorecerá la exportación del carbono a capas profundas del océano debido a que tienden a sedimentar más rápidamente (Smayda 1970, Smetacek 1980), ya sean las células intactas o al ser incluidas en paquetes fecales (mediante el mesozooplancton) o al acumularse en determinadas zonas y ser predadas por microfagos (Fig. 2). En cambio, los autótrofos pequeños (los cuales prácticamente no sedimentan o sedimentan muy despacio) han de agregarse entre ellos y/o a otros materiales para hacer posible su sedimentación, lo que hace más lento este proceso. Por otra parte, en una cadena trófica basada en autótrofos pequeños intervienen más pasos que en una basada en autótrofos grandes. El aumento del número

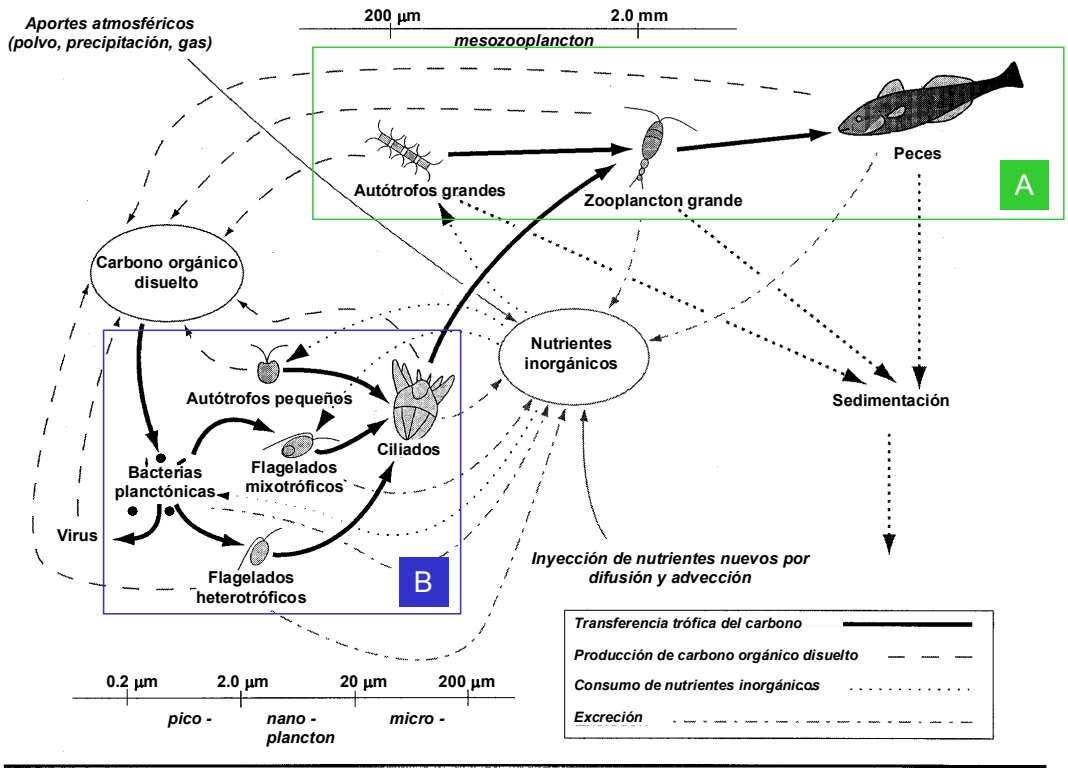

Fig. 1 – Representación esquemática de la red trófica clásica (A) y la microbiana (B). Modificado a partir del proyecto OEUVRE 1998 (realizado por P. Jonsson).

de intercambios tróficos y la lentitud del proceso de sedimentación hacen que aumente la proporción de carbono fijado fotosintéticamente que es respirado.

Así como los diferentes factores ambientales pueden determinar la estructura de tamaños de la comunidad fitoplanctónica, el desarrollo de una comunidad de fitoplancton u otra produce cambios a nivel de los otros grupos de microorganismos planctónicos (bacterias, flagelados heterotróficos, ciliados) según se favorezca la vía trófica clásica o la microbiana. Por ejemplo, las bacterias heterotróficas y el fitoplancton (considerados en esta memoria como organismos osmotróficos, ya que ambos grupos asimilan directamente los nutrientes inorgánicos disueltos en el agua y en el caso de las bacterias, además, los nutrientes orgánicos) compiten por el nutriente limitante ante una situación de limitación de nutrientes (Bratbak & Thingstad 1985, Wheeler & Kirchman 1986). Como veremos a continuación, la proporción relativa de un grupo u otro en un ambiente determinado dependerá de las condiciones en las cuales se desarrollen.

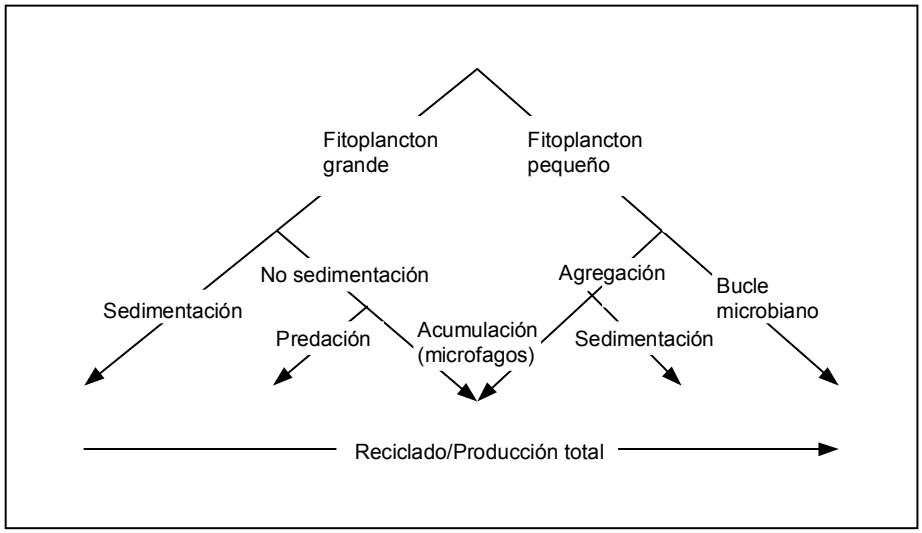

Fig. 2 – Modelo de exportación de la producción en los océanos. La longitud y la complejidad de la cadena trófica implicada en la exportación aumenta hacia la derecha. Modificado a partir de Legendre & Le Fèvre 1991.

¿QUE FACTORES DETERMINAN LA ESTRUCTURA DE TAMAÑOS DE LOS ORGANISMOS OSMOTRÓFICOS?

Diversas propiedades físicas (movimiento) y químicas (concentración de nutrientes) del agua juegan un papel fundamental en el establecimiento de una determinada estructura de tamaños de los organismos osmotróficos, especialmente del fitoplancton. Sin embargo, una vez establecida una determinada distribución de tamaños, factores biológicos como la predación, pueden cambiarla de manera significativa.

Hidrodinámica

Los organismos planctónicos están, por definición, sujetos al movimiento del agua. La energía mecánica derivada principalmente del calor solar y del viento (y en grandes masas de agua, también de la rotación de la tierra), produce movimientos del agua en forma de remolinos. La energía cinética asociada al remolino inicial se va disipando en otros cada vez más pequeños, hasta llegar a la viscosidad molecular (Ozmidov 1965). Existe un tamaño mínimo de remolino en donde las fuerzas inerciales y la viscosidad se igualan. Se trata de la escala de longitud de Kolmogorov (L_K, Tenekes & Lumley 1972) definida por:

(1) $$L_K = (\nu^3/\varepsilon)^{1/4} \quad ,$$

donde ν es la viscosidad cinemática y ε es la tasa de disipación de la energía cinética turbulenta. Por debajo de este tamaño mínimo de remolino la energía cinética se disipa como calor y el movimiento del agua pasa a ser laminar. El tamaño mínimo de remolino en los océanos es generalmente del orden de 1 mm o más (Lazier & Mann 1989). Muchos de los microorganismos del plancton (como bacterias y la mayoría de las células de fitoplancton) son mucho más pequeños que la microescala de Kolmogorov por lo que los gradientes alrededor de la célula son debidos fundamentalmente a cizallamiento laminar.

El efecto de la turbulencia sobre los organismos planctónicos puede darse a varias escalas. A nivel de mesoescala (del orden de 10 a 100 km), la presencia de giros, zonas de afloramiento o frentes puede ser un factor crítico en la selección y evolución de las especies. Por ejemplo, la respuesta del fitoplancton ante estas perturbaciones físicas estaría influenciada fundamentalmente por modificaciones en el abastecimiento de luz y nutrientes. La rotura de ondas internas a nivel de la termoclina puede inyectar nutrientes en la base de la zona fótica y originar pulsos de crecimiento de organismos de tasa de división elevada, como pueden ser las diatomeas. Además, la presencia de turbulencia de mesoescala puede, o bien reducir las pérdidas de material particulado por sedimentación fuera de la zona fótica (Kiørboe 1993), o bien favorecer su sedimentación mediante la formación de agregados con velocidades de sedimentación más altas (Smetacek 1985).

La tasa de sedimentación de los organismos planctónicos puede ser estimada mediante la ecuación de Stokes sobre la caída de partículas esféricas en un medio líquido:

(2) $$\nu' = 0.222 g \eta^{-1} r^2 (\rho' - \rho),$$

donde r es el radio celular, g es la aceleración debida a la gravedad, η es la viscosidad del líquido y $(\rho' - \rho)$ es la diferencia de densidad entre el fluido y la partícula. De acuerdo con esta expresión, las formas grandes y carentes de movimiento, como muchas diatomeas, tendrían una tasa de sedimentación alta y podrían beneficiarse de la turbulencia (en el caso de no formarse agregados) para mantener sus poblaciones suspendidas en la zona fótica de la columna de agua.

A pequeña escala, el movimiento turbulento del agua afecta al transporte de moléculas fuera y dentro de la célula y puede tener efectos directos en procesos como la división celular (Berdalet 1992, Thomas et al. 1995) y la predación por organismos herbívoros (Rothschild & Osborn 1988,

Marrasé et al. 1990). El efecto de la turbulencia a pequeña escala sobre la incorporación de nutrientes por parte de organismos osmotróficos (fundamentalmente fitoplancton) ha sido un tema de interés en las últimas décadas (Pasciak & Gavis 1975, Savidge 1981, Karp-Boss et al. 1996 entre otros); sin embargo, existen pocos trabajos al respecto.

Nutrientes y turbulencia

Ante una concentración baja de nutrientes, en ausencia de mecanismos de transporte activo, la tasa de difusión molecular a través de la membrana celular en las células osmotróficas puede limitar el suministro de nutrientes hacia la célula. Cuando el flujo de un nutriente determinado hacia el interior de una célula osmotrófica es menor que la tasa potencial de consumo metabólico de este nutriente, la célula pasa a estar limitada por difusión. La tasa específica de incorporación de un nutriente determinado por difusión molecular puede calcularse a partir de las leyes físicas. Consideremos el caso extremo en que la concentración del nutriente (C) es igual a 0 a nivel de la superficie celular (células esféricas). Esta concentración aumentará, a medida que nos alejamos de la célula, hasta alcanzar un valor igual a la concentración ambiental del nutriente, C_∞. (Fig. 3). Esta relación se puede describir según la siguiente ecuación (Berg & Purcell 1977):

$$C = - C_\infty r R^{-1} + C_\infty, \quad (3)$$

donde R es la distancia desde el centro de la célula hacia el exterior (Fig. 3). Consideremos ahora un número de capas imaginarias concéntricas a la célula. El flujo por área superficial (J) a través de cada capa estaría dado por la primera ley de Fick:

$$J = -D dC/dR, \quad (4)$$

donde D es el coeficiente de difusión del nutriente. El flujo total integrado para toda el área superficial a través de cada una de las capas sería igual a la tasa de incorporación (Q) de nutriente por la célula:

$$Q = 4J\pi R^2 = -4\pi R^2 D dC/dR \quad (5)$$

Combinando las ecuaciones (3) y (5) tendríamos:

$$Q = 4\pi r D C_\infty \quad (6)$$

y, por lo tanto, la tasa de incorporación específica estaría dada por la siguiente ecuación:

(7) $$Q/V = 4\pi rDC_\infty (4/3\pi r^3)^{-1} = 3DC_\infty r^{-2},$$

donde *V* corresponde al volumen celular. Puede observarse que la incorporación por difusión de un nutriente limitante es inversamente proporcional al cuadrado del radio celular. Por ello, cuando no existe movimiento alguno del agua o de las células y ante una situación de limitación de nutrientes, las células de menor tamaño tendrían ventajas sobre las grandes.

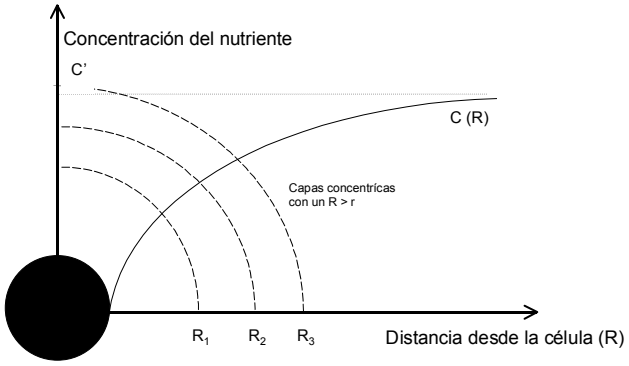

Fig. 3 – Estimación de la limitación por difusión de la incorporación de nutrientes en organismos osmotróficos. Modificado a partir de Kiørboe 1993, según una idea de T. Fenchel.

Un movimiento de las células (ya sea por sedimentación o por natación) o del agua circundante, produce una renovación del nutriente limitado que rodea a la célula, con lo que aumenta el gradiente de concentración entre el medio y la célula y la incorporación de nutriente por difusión se incrementa en una cantidad Q_{adv}, que se denomina “transporte advectivo”.

(8) $$Q_{adv} = 4\pi DrShC_\infty ,$$

donde Sh es el número de Sherwood el cual es el cociente entre el flujo de nutrientes total que llega a la célula y el transporte de nutrientes sólo por difusión. Si el transporte advectivo es cero, el número de Sherwood es igual a 1 y, por lo tanto, el transporte es sólo por difusión. A su vez, el número de Sherwood está relacionado con el número de Reynolds (el cual describe la importancia relativa de las fuerzas inerciales comparadas con la viscosidad) y con el número de Péclet (el cual indica la efectividad del transporte advectivo comparado con el transporte difusivo a través del fluido sobre una escala de longitud específica).

El número de Sherwood es dependiente del tamaño celular (Karp-Boss et al. 1996) ya que está relacionado directamente con el número de Péclet el cual, a su vez, se define como:

$$Pe = Er^2/D, \quad (9)$$

donde E es la tasa de cizallamiento, la cual se calcula a partir de ν (viscosidad cinemática) y ε (tasa de disipación de la energía cinética turbulenta):

$$E = (\varepsilon/\nu)^{1/2} \quad (10)$$

Por tanto, las células más grandes experimentarían un mayor aumento en el consumo de nutrientes debido a la turbulencia que las células más pequeñas. Según Karp-Boss et al. (1996) sólo las células mayores de 60 µm experimentarían un aumento significativo en términos de incorporación de nutrientes debido a la turbulencia.

Predación

En general, existe una cierta relación entre el tamaño de los depredadores y el de sus presas. Las células pequeñas de fitoplancton y las bacterias son comidas por pequeños depredadores (flagelados heterotróficos y ciliados), mientras que el fitoplancton de mayor tamaño es consumido por organismos de mayor tamaño (como los copépodos y otros grupos de metazooplancton). Sheldon et al. (1972) propone que una comunidad de organismos pelágicos en equilibrio presenta una distribución de tamaños en que la biomasa es más o menos constante en clases de tamaños logarítmicas iguales. Posteriormente, Platt (1985) observó que la pendiente en esta distribución era igual a - 0.25. Esto hace suponer que la presión de predación decrece con el tamaño de la presa. Además, parece haber una relación tamaño depredador-presa más o menos constante de 10:1 a 100:1 (escala lineal) (Fenchel 1987, Kiørboe 1993). La tasa de crecimiento de los pequeños flagelados es comparable a la de sus presas, por lo que la predación podría ser un mecanismo que mantuviese las poblaciones de picoplancton en rangos más o menos constantes, evitando así su concentración en grandes cantidades. Por otro lado, tras un pulso de crecimiento rápido de células grandes como muchas diatomeas, el incremento de la población de herbívoros tiene lugar con cierto retraso, por lo que no alcanzarían a controlar la población de sus presas y la mayoría de las células de fitoplancton sedimentarían directamente a las capas más profundas del océano.

Estructura de tamaños y ecosistemas

En ambientes estratificados y pobres en nutrientes, las células osmotróficas pequeñas tendrían ventajas sobre las células más grandes a la hora de competir por un nutriente limitante que no tuviese mecanismos de transporte activo y pudiese ser incorporado a la célula sólo por difusión (la cual es inversamente proporcional al cuadrado del radio celular). En zonas costeras, frentes o regiones de afloramiento con aporte de nutrientes y elevada intensidad de mezcla de las aguas, la turbulencia de pequeña escala daría lugar a un transporte advectivo de nutrientes hacia las células. En teoría, sin embargo, el incremento en la incorporación de nutrientes sólo sería significativo para células mayores de 60 µm. Por ello, en relación con la incorporación de nutrientes, las bacterias y el fitoplancton de tamaño pequeño tendrían ventajas competitivas sobre las células mayores en aguas tranquilas, mientras que, en aguas turbulentas sólo se beneficiarían las células de fitoplancton más grandes.

CLASIFICACIÓN DE LOS MICROORGANISMOS POR CLASES DE TAMAÑOS

Uno de los primeros en clasificar los organismos del plancton por tamaños fue Schütt (1892), que utilizó los prefijos “micro”, “meso” y “macro”. Posteriormente, se han ido agregando y/o modificando clases de tamaño a las definidas en esta clasificación. Lohmann (1911), por ejemplo, introdujo el prefijo “nano” para designar organismos de tamaños inferiores al “micro” de Schütt (1892). Hoy en día, la clasificación de tamaños más utilizada es la propuesta por Sieburth et al. (1978), en la que los organismos planctónicos se clasifican como: femtoplancton (0.02 - 0.2 µm), picoplancton (0.2 - 2 µm), nanoplancton (2 - 20 µm), microplancton (20 - 200 µm), mesoplancton (0.2 - 20 mm), macroplancton (2 - 20 cm) y megaplancton (20 - 200 cm). Además, muchas veces se utiliza el término ultraplancton para designar a los organismos menores de 8 - 10 µm (Murphy & Haugen 1985) o menores de 5 - 10 µm (Sverdrup et al. 1942).

El fitoplancton eucariótico (diatomeas, dinoflagelados, flagelados autotróficos y cocolitoforales) estaría ubicado en más de un compartimento de la clasificación de Sieburth (dentro del pico-, nano- y microplancton). Lo mismo ocurriría con los ciliados (nano- y microplancton) y los flagelados heterotróficos (pico- y nanoplancton). Otros microorganismos entrarían fundamentalmente dentro de un sólo compartimento, como las cianobacterias (*Prochlorococcus* y *Synechococcus*) y las bacterias heterotróficas (picoplancton), o también los virus (femtoplancton).

CONSIDERACIONES METODOLÓGICAS

Un método ampliamente utilizado para cuantificar a los organismos planctónicos por clases de tamaño es el de la filtración (Herbland & Le Bouteiller 1981, Takahashi & Bienfang 1983, Weber & El-Sayed 1987, Odate & Maita 1988, Montecino & Quiroz 2000, Teira et al. 2001). Mediante filtros de un determinado tamaño de poro es posible concentrar y/o separar a los diferentes organismos del plancton. Sin embargo, este método tiene como desventajas la de no discriminar la composición taxonómica de los organismos en cada clase de tamaño y, además (según sea el caso), la de no poder separar el material detrítico del vivo. El mismo problema se presenta con el uso de contadores electrónicos de partículas, los cuales también han sido utilizados para estudiar la estructura de tamaños de los organismos planctónicos (Kahru et al. 1991). El desarrollo de otras metodologías, como la citometría de flujo, ha representado un gran avance para estimar de manera más exhaustiva la abundancia de los organismos pertenecientes al picoplancton (como las bacterias heterotróficas, las cianobacterias y picoeucariontes autotróficos), en función de su tamaño y fluorescencia (Olson et al. 1985, Li et al. 1992, Simon et al. 1994). En general, cuando se desea conocer la composición taxonómica de los organismos, es necesaria la microscopía ya sea óptica, de epifluorescencia o electrónica.

En los trabajos desarrollados en esta memoria, el término fitoplancton incluye, en general, no sólo a los grandes grupos generalmente identificados mediante microscopía óptica, sino también a los grupos de tamaño típicamente inferior a 2 µm (picoeucariontes y cianobacterias). Para una adecuada cuantificación de todos estos grupos de fitoplancton por clases de tamaño (García et al. 1994) se requiere el uso de diferentes metodologías (microscopía invertida, electrónica y de epifluorescencia y citometría de flujo).

ESTRUCTURA DE TAMAÑOS EN COMUNIDADES FITOPLANCTÓNICAS

La estructura de tamaños de los productores primarios ha sido ampliamente estudiada debido a su gran importancia en el funcionamiento de las redes tróficas pelágicas y en el ciclo del carbono. Entre los estudios que se han llevado a cabo sobre el tema pueden señalarse los de Durbin et al. (1975), Malone (1977), Herbland & Le Bouteiller (1981), Bienfang (1984), Hopcroft & Roff (1990), Delgado et al. (1992), Raimbault et al. (1988a, b), Legendre et al. (1993) y Marañón et al. (2001), entre muchos otros. En base a muchos de estos trabajos se pueden hacer ciertas generalizaciones sobre la estructura de tamaños de las comunidades de fitoplancton.

En términos generales, se sabe que el picofitoplancton constituye más del 50 % de la biomasa y de la producción primaria en zonas oligotróficas, pero representa menos del 10 % de estos parámetros en aguas eutróficas (Agawin et al. 2000, revisión bibliográfica de aguas oceánicas y costeras). En el Mar Mediterráneo, por ejemplo, esta fracción del fitoplancton constituye, en promedio, un 59 % y un 65 % de la biomasa en términos de clorofila y de la producción primaria, respectivamente (Magazzù & Decembrini 1995). Las altas concentraciones de fitoplancton que pueden observarse en zonas costeras, frentes o regiones de afloramiento con elevado aporte de nutrientes a la zona fótica e importante movimiento turbulento de las agua, se deben principalmente a un aumento en la proporción de células de gran tamaño (Malone 1971, Marañón et al. 2001). Generalmente las diatomeas son el grupo que más contribuye a las proliferaciones de biomasa fitoplanctónica en zonas altamente productivas (Margalef 1978).

Típicamente, cuanto menor es la biomasa de fitoplancton, mayor es la contribución relativa de los organismos picoplanctónicos. Por otra parte, el picofitoplancton es considerado como la fracción con menor variabilidad espacio-temporal, mientras que las fracciones más grandes suelen ser las responsables de los cambios más importantes en la biomasa autotrófica total (Raimbault et al. 1988b, Magazzù et al. 1996, Rodríguez et al. 1998). Raimbault et al. (1988b) observaron que, en aguas del Mediterráneo y otros ambientes, la cantidad de clorofila en las fracciones < 1, < 3 y < 10 µm alcanzaba un límite superior que correspondía a 0.5, 1 y 2 µg l^{-1}, respectivamente. Sin embargo, la poca variabilidad del picofitoplancton parece ser relativa y es aparente sólo cuando se comparan determinaciones de biomasa que abarcan un amplio rango de valores. En este sentido, Marañón et al. (2001) encuentran que la mayor parte de la variabilidad del fitoplancton en un transecto meridional en aguas abiertas del Atlántico era debida fundamentalmente a cambios en la fracción picoplanctónica.

Dentro de los grandes grupos de fitoplancton, se han señalado ciertas regularidades con respecto a su estructura de tamaños. Por ejemplo, las diatomeas son consideradas muchas veces como típicamente microplanctónicas; sin embargo, dentro de este grupo existe un amplio rango de tamaños y hay especies con células de sólo 2 µm de diámetro (Hasle & Thomas 1995).

La distribución de tamaños y/o las diferentes morfologías que desarrollan las comunidades de fitoplancton según las condiciones ambientales están definidas en algunos modelos conceptuales. Margalef (1978), en base al suministro de nutrientes y a la intensidad de turbulencia (o energía externa), propone un modelo (el denominado “Mandala”, Fig. 4) en el cual las diatomeas carentes de movimiento y con una tasa de crecimiento potencial alta crecerían en aguas ricas en nutrientes y

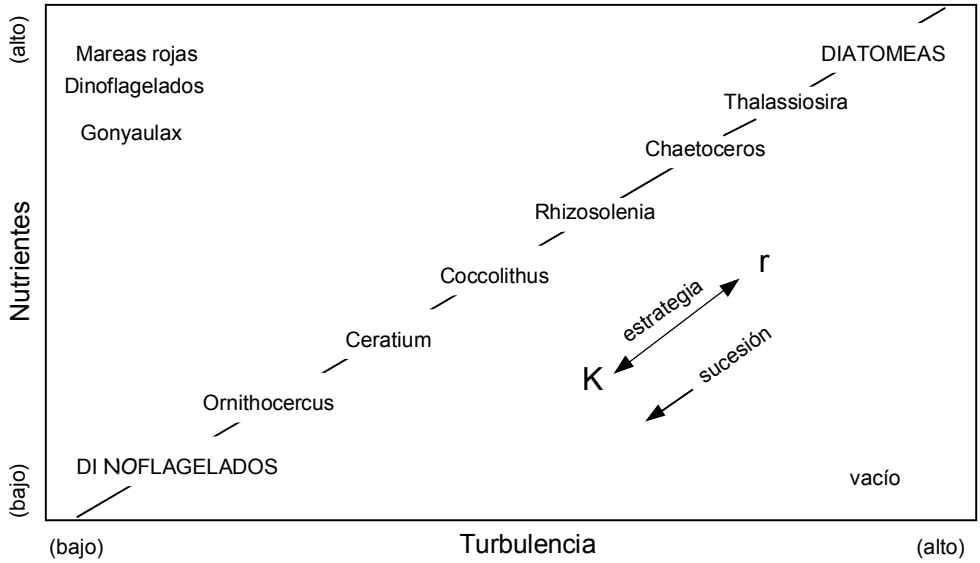

Fig. 4 – "Mandala" de Margalef. Los diferentes tipos biológicos del fitoplancton están graficados en función de la concentración de nutrientes y de la turbulencia del agua. Modificado a partir de Margalef 1978.

turbulentas y, en cambio, los dinoflagelados, que se mueven por medio de flagelos, podrían sobrevivir en aguas estratificadas debido a su capacidad de migrar y obtener nutrientes de aguas más profundas. Otros organismos del fitoplancton como los cocolitoforales aparecerían en posiciones intermedias. Legendre & Le Fèvre (1991), basándose en la hidrodinámica del ambiente, clasifican el ecosistema pelágico marino en cinco tipos según los diferentes tamaños de fitoplancton (Fig. 5). En esta clasificación, los ecosistemas extremos serían aquéllos en que predomina la vía trófica clásica (ecosistema 1 - producción y biomasa dominada por células grandes) y la vía trófica microbiana (ecosistema 5 - producción y biomasa dominada por células pequeñas). Entre medio estarían aquellos ecosistemas donde se combinan células grandes y pequeñas como dominantes en la producción y/o en la biomasa fitoplanctónica. Sin embargo, hay que considerar estas clasificaciones con precaución; puede ser que diferentes tipos de vía trófica dominen en distintas épocas del año o que varios de estos tipos coexistan en un ambiente determinado.

En las células del fitoplancton se ha observado que procesos fisiológicos tan importantes como el crecimiento y la respiración, así como el contenido en carbono, nitrógeno, proteína o clorofila *a* son dependientes del tamaño celular (Banse 1976, Blasco et al. 1982, Verity et al. 1992, Montagnes et al. 1994) y se relacionan, generalmente, mediante la ecuación alométrica:

(11) $M = aV^b$,

o, lo que es lo mismo: $\log M = \log a + b \log V$

donde M es el proceso metabólico, elemento o compuesto celular, V el volumen del organismo y "*a*" y "*b*" son constantes empíricas (Bertalanffy 1964). Así, por ejemplo, las células más pequeñas contienen más carbono y nitrógeno por unidad de volumen que las células grandes. Las primeras relaciones del crecimiento o la respiración con el tamaño celular revelaban un coeficiente *b* entre - 0.25 y - 0.30 (Eppley & Sloan 1965). Sin embargo, posteriormente se observó que la relación de alometría podría ser más débil de lo encontrado en un principio (Banse 1982, Blasco et al. 1982, Sommer 1989), de modo que podría ser más importante el potencial genético de crecimiento de un determinado grupo taxonómico de fitoplancton con respecto a otro (Furnas 1990). Por ello, tasas de crecimiento *in situ* de diatomeas de tamaño pequeño o medio podrían ser iguales o más altas que las de pequeños microflagelados o de comunidades ultraplanctónicas.

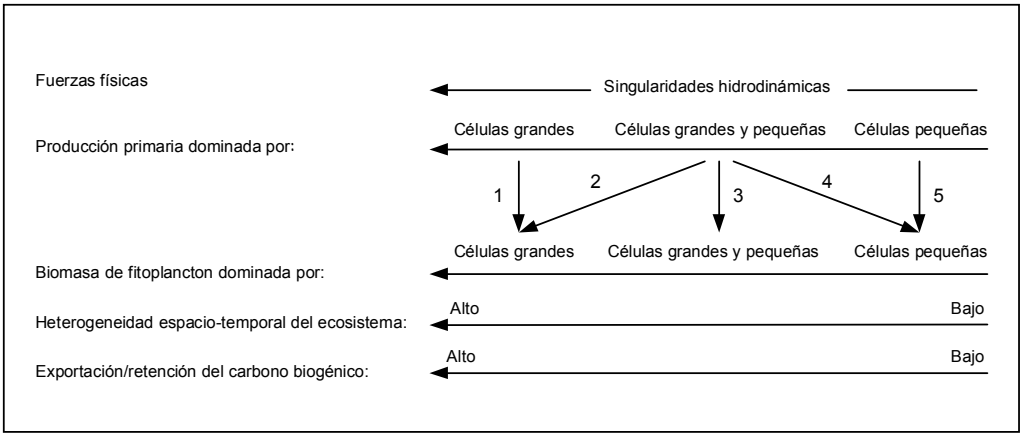

Fig. 5 – Cinco tipos de ecosistemas pelágicos definidos por la estructura de tamaños del fitoplancton según el dominio de células grandes o pequeñas en la producción y la biomasa, y en función de las características hidrográficas del ambiente y, como consecuencia, su importancia en la retención del carbono biogénico. El ecosistema 1 caracterizaría a la cadena trófica "clásica", mientras que el ecosistema 5 caracterizaría a la "microbiana". Modificado a partir de Legendre & Le Fèvre 1991.

IMPORTANCIA DE LA ESTRUCTURA DE TAMAÑOS Y LA COMPOSICIÓN TAXONÓMICA DE UNA COMUNIDAD DE MICROORGANISMOS EN RELACIÓN CON LA COMPOSICIÓN QUÍMICA DE LA MATERIA ORGÁNICA FORMADA

Como hemos visto anteriormente, la turbulencia puede afectar la estructura de tamaños del fitoplancton favoreciendo las células de mayor tamaño y su importancia relativa con respecto a otras más pequeñas como las bacterias heterotróficas. Estos dos compartimentos de biomasa tienen diferentes demandas de nutrientes con respecto a la formación de biomasa. Se suele aceptar que el fitoplancton asimila los elementos C:N:P en una relación 106:16:1 (Redfield 1963) aunque se han observado variaciones relacionadas con el estado trófico del ambiente (Harris 1986). En cambio, las bacterias heterotróficas poseen un cociente C:N:P más bajo, de alrededor de 50:9:1, que también puede variar según su actividad metabólica y disponibilidad de nutrientes (Chrzanowski et al. 1996). Por ello, la estructura de tamaños y la composición taxonómica de las comunidades de microorganismos del plancton se ven reflejadas en su composición química. Generalmente, cuando se habla en términos de biomasa de los diferentes componentes de la comunidad de microorganismos planctónicos se utiliza el carbono por ser el elemento base de muchos compuestos y estructuras celulares. Sin embargo, compuestos como el ADN y las proteínas son también utilizados como indicadores de biomasa (Holm-Hansen 1969b, Paul et al. 1985, Boehme et al. 1993, Dortch & Packard 1989) debido a su implicación en la división y crecimiento celular, respectivamente. Además, debido a su composición química, ambas macromoléculas son importantes en la dinámica del nitrógeno en ambientes marinos y el ADN participa, además, en la dinámica del fósforo. Las primeras medidas del ADN en la columna de agua fueron realizadas como una manera de cuantificar la biomasa fitoplanctónica (Holm-Hansen 1969a, b). Sin embargo, trabajos posteriores (donde se obtuvieron simultáneamente medidas de ADN, clorofila y bacterias), indicaron una buena correlación de esta macromolécula con la concentración bacteriana (Paul & Carlson 1984, Paul et al. 1985, Boehme et al. 1993) pero no con la de clorofila. Por ello, la mayor parte de la forma particulada de esta macromolécula en ambientes marinos es atribuida al bacterioplancton. El contenido proteico en las células de fitoplancton es menor en relación a su volumen en las células grandes que en las pequeñas (Montagnes et al. 1994). Por ello, la estructura de tamaños de la comunidad fitoplanctónica es importante a la hora de cuantificar su aporte en términos de proteína.

OBJETIVOS Y ESTRUCTURA DE LA TESIS

En la presente memoria se han estudiado diferentes aspectos de la relación entre la caracterización taxonómica, la composición química y la estructura de tamaños de comunidades de microorganismos planctónicos. Los principales objetivos han sido los siguientes:

A) Determinar experimentalmente la importancia de la turbulencia en el desarrollo de organismos osmotróficos (bacterias y fitoplancton) y en la estructura de tamaños y composición taxonómica del fitoplancton bajo diferentes condiciones iniciales de nutrientes.

B) Estudiar la estructura de tamaños de comunidades de fitoplancton y su composición taxonómica en sistemas naturales, así como su variabilidad espacio-temporal.

C) Estudiar cómo influye la estructura de tamaños y la composición taxonómica de la comunidad de microorganismos planctónicos en la composición química de la materia orgánica formada, ya sea en experimentos de laboratorio como en sistemas naturales.

A continuación, se presentan de forma detallada los trabajos desarrollados en los diferentes capítulos de que consta esta memoria.

Un estudio de la importancia del tamaño de los organismos osmotróficos como las bacterias y el fitoplancton en relación con la turbulencia y los nutrientes se presenta en los **Capítulos I** y **II** de esta memoria. La hipótesis de base para ambos trabajos fue que la turbulencia beneficiaría el crecimiento de las células grandes pero tendría un efecto insignificante sobre el crecimiento de células pequeñas. En el **Capítulo I**, el efecto de la turbulencia en el crecimiento de dos especies de diatomeas (*Thalassiosira pseudonana* y *Coscinodiscus* sp.) ha sido estudiado en cultivos limitados en fósforo. Ambas especies de diatomeas fueron elegidas debido a que tienen una forma similar pero son muy diferentes en tamaño, lo que permite separar las interacciones entre turbulencia y tamaño de efectos relacionados con la forma. Además, con el fin de predecir el papel de la turbulencia en el crecimiento algal, se ha utilizado un modelo simple para caracterizar el crecimiento de ambas diatomeas en presencia y ausencia de turbulencia. En el **Capítulo II**, se ha considerado el efecto de la combinación de nutrientes y turbulencia sobre la dinámica y la distribución de tamaños del plancton osmotrófico. Para ello, una comunidad planctónica de componentes capaces

de pasar a través de una malla de 150 µm, procedente de la costa catalana (Mediterráneo Noroccidental), fue cultivada en microcosmos sometidos a diferentes condiciones iniciales de nutrientes (sin adición inicial de nutrientes (N:P = "in situ") y con adición inicial de nutrientes (N:P igual y mayor que Redfield) y bajo condiciones de turbulencia y calma. A pesar de que no pueden considerarse como una "imitación" de sistemas naturales (Platt et al. 1981, Carpenter 1996) el uso de microcosmos permite aislar un factor (en este caso la turbulencia) de otros factores que covarían (como la luz y los nutrientes) con él en la naturaleza. Asimismo, los microcosmos permiten replicabilidad experimental y un mejor control de los factores ambientales. En el trabajo de ambos capítulos se ha considerado la limitación en fósforo como condición inicial de nutrientes (condición única en el experimento del **Capítulo I** y una de las tres condiciones de nutrientes en el experimento del **Capítulo II**) debido a que es considerado como el nutriente más a menudo limitante en las aguas oligotróficas del Mediterráneo (Berland et al. 1990, Krom et al. 1991, Thingstad et al. 1998, Sala 2002). Los trabajos realizados en estos dos capítulos están enmarcados dentro de los proyectos europeos MEDEA (MAS3-CT95-0016) y NTAP (EVK3-CT-2000-00022).

En los **Capítulos III** y **IV**, la distribución de tamaños del fitoplancton y su variación espacio-temporal ha sido observada en dos sistemas naturales del Mar Mediterráneo. En el **Capítulo III**, el escenario elegido para el estudio ha sido el Giro anticiclónico Occidental del Mar de Alborán. Este giro está formado por aguas superficiales que entran del Atlántico por el Estrecho de Gibraltar, las cuales se mezclan con las aguas Mediterráneas residentes formando un chorro de agua Atlántica modificada (Parrilla & Kinder 1985, Minas et al. 1991, Tintoré et al. 1991). El borde norte del giro se caracteriza por la presencia de un frente con afloramiento intermitente de aguas profundas que aportan nutrientes a las capas superficiales de la columna de agua (Packard et al. 1988, Minas et al. 1991), mientras que el centro del giro está ocupado por aguas oligotróficas. Estas diferencias físico-químicas entre sus distintas zonas hacen del giro un lugar idóneo para el estudio de la estructura de tamaños de la comunidad de fitoplancton y su variación a corto plazo. Se han estimado, además, las tasas de crecimiento de las comunidades de fitoplancton de las diferentes zonas del giro, así como sus respectivas relaciones carbono:clorofila, y se las ha relacionado con las correspondientes estructuras de tamaños. El trabajo formó parte de un "High Frequency Flux Experiment", cuyo objetivo era estudiar la variabilidad a corto plazo de las propiedades físico-químicas y biológicas de la zona occidental del Mar de Alborán, dentro del proyecto europeo MATER (MAS3-CT96-0051). En el **Capítulo IV**, la zona elegida para estudiar la variabilidad espacio-temporal de la estructura de tamaños de la comunidad de fitoplancton fue la plataforma del Delta del Ebro. En las capas superficiales de esta zona se observan masas de agua ligeramente diferentes: las aguas

Mediterráneas de mar abierto (más saladas) y las aguas de la plataforma continental (menos saladas) además de las aguas procedentes de la descarga del río Ebro, con una salinidad aún inferior (menos de 37.8, según Salat et al. 2002). La región se caracteriza por una gran variabilidad en cuanto a vientos y una importante actividad hidrográfica de mesoescala (Sánchez-Arcilla & Davies 2002). En esta área, una amplia red de estaciones (alrededor de 140) fue muestreada en otoño, invierno y verano, dentro del proyecto europeo FANS (Fluxes Across Narrow Shelves – MAST3-CT95-0037). Uno de los objetivos principales era el estudio de la influencia de los cambios estacionales en los parámetros fisico-químicos del agua sobre el fitoplancton. Debido a la variabilidad de esta zona, era factible esperar fluctuaciones en la estructura de tamaños en la comunidad fitoplanctónica en las diferentes estaciones muestreadas.

En los **Capítulos V** y **VI,** se examinan los resultados entre la estructura de tamaños, la composición taxonómica y la composición química de una comunidad de microorganismos planctónicos. El **Capítulo V** presenta resultados obtenidos en el mismo experimento considerado en el Capítulo II. Se estudiaron las variaciones producidas en la estequiometría de la materia orgánica y la dinámica del fósforo, en relación con los cambios en la estructura de tamaños y en la composición taxonómica observados en las diversas condiciones experimentales. En el **Capítulo VI,** se presenta un estudio de la contribución relativa de proteína y ADN particulados en la columna de agua, de los principales grupos de microorganismos (bacterias, flagelados heterotróficos, fitoplancton y ciliados) y del material detrítico. Las determinaciones se realizaron en dos estaciones de características distintas, ubicadas en el Mar Catalano-Balear (Mediterráneo Noroccidental). Esta zona del Mediterráneo se caracteriza por la presencia de tres tipos de aguas, separados por dos frentes, el frente Catalán y el frente Balear (Salat & Cruzado 1981, Font et al. 1988). El frente Catalán separa las aguas costeras, de salinidad relativamente baja debido a las descargas continentales (las cuales fluyen en dirección Sudoeste), del área central, con aguas más densas y frías (Font et al. 1988). El frente Balear separa esta zona central de las aguas de influencia Atlántica, menos saladas y más calientes, que fluyen en dirección Nordeste. Este estudio fue realizado en el marco del proyecto europeo MAS2-CT93-0063 cuyo objetivo principal era caracterizar las redes tróficas planctónicas en el Mar Catalán y examinar su relación con los procesos hidrográficos de mesoescala.

Después de los capítulos, se discute de manera general (**Discusión general**) cómo los resultados obtenidos han permitido responder a los objetivos propuestos al iniciar esta tesis y se enseñan las

conclusiones de la tesis. Finalmente, se incluye un **resumen de la tesis** (que resume la introducción, los resultados y la discusión general de la tesis).

Effects of small-scale turbulence on the growth of two diatoms of different size in a phosphorus-limited medium

ABSTRACT

The response on the growth of two marine diatoms of different size (*Thalassiosira pseudonana*, 6 µm diameter and *Coscinodiscus* sp, ca. 110 µm diameter) to turbulence was studied in phosphorus-limited cultures. The growth of both algae was followed for ca 5 Days under still and turbulent ($\varepsilon = 4.4 \times 10^{-2}$ cm^2 s^{-3}) cultures in two independent experiments. In agree with the theory, turbulence enhanced the growth of *Coscinodiscus* sp. but not the growth of *T. pseudonana*. At the end of the experiment there were about 1.7 times more *Coscinodiscus* sp. cells in the turbulent than in the still conditions, while for *T. pseudonana* almost the same cell numbers were found in both conditions. In addition, the *Coscinodiscus* sp. cells growing under still conditions presented a higher specific alkaline phosphatase activity than those growing in turbulent ones which indicates a higher phosphorus limitation of *Coscinodiscus* sp. cells in the still cultures. A dynamical model of phosphorus uptake and cell growth, implemented using literature parameters, fitted experimental results and showed that turbulence increased the growth rates of *Coscinodiscus* sp. and *T. pseudonana* in a 118 % and a 19 %, respectively.

INTRODUCTION

In nutrient-limited ecosystems the interaction between small-scale turbulence, phytoplankton cells and nutrients is important to understand whole ecosystem dynamics. Nutrients are transported to cells by diffusion or advection. In still water and for non-motile cells, the nutrient supply is by diffusion alone. When the nutrient uptake capacity of these cells is higher than the diffusional flux and in absence of active transport mechanisms, the cells become diffusion-limited and a nutrient-depleted region is created around them (Kiørboe 1993). Relative motion of the cells (either by swimming or sinking) with respect to the fluid, or laminar or turbulent movement of the water, will generate an advective transport of nutrients to renew the depleted zone. The relative importance between both kinds of nutrient transport is given by the Sherwood number (*Sh*), which is the ratio between the total flux of nutrients arriving to the cell surface and the transport of nutrients by diffusion alone. If the advective transport is zero (*Sh* = 1), the nutrient transport is purely diffusional. The Sherwood number is adimensional and increases with cell size. Thus, when a relative motion between the fluid and the cells is present, large cells experience a larger increase in nutrient flux to their cell surface than small cells (Karp-Boss et al. 1996). These authors concluded that the increase of advective transport owing to small-scale turbulence under normal oceanic conditions is only significant for cells larger than ca. 60 µm.

The different components of a phytoplankton community compete for the limiting nutrient. In theory, under still conditions, the smallest organisms would be better competitors for the limiting nutrient due to their high surface:volume ratio. In addition, motile organisms could have an advantage in calm waters by increasing nutrient flux through swimming. However, under turbulent conditions, the increase in the nutrient flux due to turbulence would mainly benefit, as mentioned above, the growth of the largest cells. In addition, turbulence could enhance the maintenance of large cells in suspension (Kiørboe 1993). Thus, turbulence could change the competition interactions of the different components of the phytoplankton community. This could have important implications in the trophic ecology of the whole ecosystem, as turbulence would favour the “classical” food web over a more microbial-based food web (Legendre & Rassoulzadegan 1995). In nature, the presence of particular life-forms of phytoplankton is related to the physico-chemical conditions of the medium (Margalef 1978). In upwelling areas, with active fluid dynamics and high nutrient concentrations, diatoms are usually the main component of the phytoplankton community and may form high biomass blooms. Most diatoms are non-motile and thus may be favoured by the enhancement of nutrient flux into the cells produced by the relative movement of water with respect to them. There

are few experimental studies that assess the effect of fluid motion on nutrient uptake and growth of diatoms. Savidge (1981) found different results on the nutrient uptake of the diatom *Phaeodactylum tricornutum* depending on whether the cultures were phosphate or nitrate limited. This author observed that, under turbulence, the uptake of nitrate was enhanced while that of phosphate was decreased. For *Ditylum brightwellii* growing in a nitrogen-limited medium, Pasciak & Gavis (1975) found that the transport limitation of nitrate and nitrite decreased with turbulence. Although theoretical approaches conclude that turbulence effects are only significant for cell sizes exceeding several tens of micrometers (Mann & Lazier 1991, Karp-Boss et al. 1996), no experimental work has been done assessing the effect of small-scale turbulence on the growth of diatoms of different sizes. This knowledge may be key to understand diatom bloom formations in marine ecosystems and a factor to be considered in the parameterisations of phytoplankton growth models.

In the present study we investigate the effect of small-scale turbulence on the growth of selected marine diatoms. Our approach combines dynamic modelling and laboratory experiments with batch cultures. Our main interest is to test the importance of turbulence effects depending on cell size. Two diatoms, *T. pseudonana* and *Coscinodiscus* sp. were chosen because they are similar in shape and other characteristics (both are centric diatoms and belong to the Order Biddulphiales, suborder Coscinodiscineae), but are very different in size. *T. pseudonana* has a diameter of around 6 µm and *Coscinodiscus* sp. is approximately twenty times larger (ca. 110 µm in diameter). The growth of both algae was monitored in a phosphorus-limited medium under still and turbulent conditions. From the calculations of *Sh* we expected that turbulence would increase the phosphate transport into *T. pseudonana* by 5.9 % and into *Coscinodiscus* sp. by 60 % and that this would be reflected in their respective growth.

MATERIAL AND METHODS

Experimental setup

We used batch cultures of the diatoms *Thalassiosira pseudonana* (original strain from Instituto de Ciencias del Mar de Andalucía - Puerto Real - Cádiz) and *Coscinodiscus* sp. (CCMP1584 strain from Provasoli-Guillard National Center for Culture of Marine Phytoplankton - Bigelow Laboratory for Ocean Sciences). These diatoms are regularly maintained in the culture collection of our laboratory growing in f/2 or f/20 media with silicate (Guillard 1975).

For this study, we used a phosphorus-limited medium for both stock cultures and experiments. It was prepared adding known quantities of sterile stocks of inorganic nutrients (as nitrate, phosphate,

silicate, metals and vitamins, Table 1) and TRIS buffer, to nutrient-depleted, aged, sea water, after filtering through Whatman GF/F and sterilizing at 121°C for 50 minutes. The medium was adjusted to have a phosphorus concentration of 1 µM and an N:P ratio of 88.2.

Two experiments were carried out (Experiment 1 and Experiment 2) with independent stock cultures.

Table 1 – Nutrients addition (µM) and N:P ratio.

Nutrient	Concentration (µM)
Phosphate (P)	1
Nitrate (N)	88.2
Silicate	125
Metals and vitamins	idem proportion to nitrate that for f/2
N:P	88.2

At the beginning of an experiment, known volumes of either *T. pseudonana* or *Coscinodiscus* sp. were inoculated into four 2.5 l Nalgene polycarbonate bottles to achieve starting concentrations of 0.037 µM P in algal biomass. This biomass was calculated from algal cell volumes (Table 2) and average literature values of cell carbon content (Mullin et al. 1966, Blasco et al. 1982, Brzezinski 1985, Moal et al. 1987, Montagnes et al. 1994) and Redfield C:P ratio (Redfield 1963). Theoretical initial concentrations resulted in 3200 cells ml^{-1} for *T. pseudonana* and 3.35 cells ml^{-1} for *Coscinodiscus* sp. and the measured initial cell numbers resulted, on average, in 7.0 cells ml^{-1} for *Coscinodiscus* sp. and 3118 cells ml^{-1} for *T. pseudonana*. Experiments were run in an environmental chamber at a temperature of 22 ± 1 °C and under a 12:12 hour light-dark period with a light intensity between 180 and 220 µmol photons m^{-2} s^{-1}. Two bottles of each species were grown under still conditions and the other two bottles were grown under turbulent conditions. Turbulence was generated with an orbital shaker at 130 revolutions per minute (rpm). From the measurements in Zirbel et al. (2000) we estimated an average turbulence intensity of 4.4 x 10^{-2} cm^2 s^{-3} with values ranging from 6.7 x 10^{-3} to 8.0 x 10^{-1} cm^2 s^{-3}.

Parameters measured

Samples for algal and bacterial cell numbers and inorganic nutrient concentration (one replicate) were taken at the beginning of the experiment and at four or five times more during the experiment

(which lasted for ca. 5 days). Cell numbers and biovolume of *T. pseudonana* were monitored with a Multisizer Coulter Counter (validated with simultaneous microscopy counts: y = - 4567.4 + 0.95443x, R^2 = 0.99, n = 13; y = coulter counts and x = microscopic counts). *Coscinodiscus* sp. cells were fixed with Lugol´s solution and counted each day using 10 ml settling chambers in an inverted microscope (Utermöhl 1958). The mean volume of these cells was obtained by measuring the diameter and height of twenty live cells and applying the formula of a cylinder.

Bacterial concentration and cell volume was estimated by flow cytometry following a methodology described in Gasol & del Giorgio (2000). Samples of 1.2 ml were fixed with 1 % paraformaldehyde + 0.05 % glutaraldehyde (final concentration), left in the dark at room temperature for 10 min and then stored frozen at - 70 °C. At a later date, samples were unfrozen and run through a FACS-calibur (Becton & Dickinson) flow cytometer with a laser emitting at 488 nm. A subsample of 200 µl was stained with Syto13 (Molecular Probes) at 1.6 µM (diluted in DMS), left in the dark for 15 min, and then run at low speed (approx. 12 µl min^{-1}). Data were acquired in log mode until 10000 events had been processed. As an internal standard, 10 µl of a 10^6 ml^{-1} solution of yellow-green 0.92 µm Polyscience latex beads were added to subsamples. Bacteria were detected by their signature in a plot of side scatter (SSC) vs. FL1 (green fluorescence).

Phosphate consumption by bacteria in the period of their exponential growth (Table 4) was calculated dividing the bacterial increase in this period in terms of phosphorus (using a carbon content of 0.35 pg C μm^{-3} (Bjørnsen 1986) and a C:P ratio = 50) and the difference in phosphate concentration between the same period.

Inorganic nutrients (phosphate, nitrate and silicate) were analyzed in an Evolution II (Alliance Instruments) autoanalyzer, using the methods of Grasshoff et al. (1983).

Alkaline phosphatase activity (APA) was determined by using a fluorogenic substrate (MUF) following the procedure described in Sala et al. (2001). In brief, 1 ml samples were incubated in replicates with the substrate 4-MUF-P-phosphate (100 µM final concentration). Fluorescence was measured at 365 nm excitation and 446 nm emission wavelengths before and after an incubation of 1 h in the dark at room temperature. The increase of fluorescence with time was converted to activity units using a standard curve prepared with the end product of the reactions. Specific activity, i.e. activity per cell, was calculated dividing activity by the number of algal cells in the culture. The limitation on phosphate uptake was estimated by the increase of the specific alkaline phosphatase activity. The activity of this ectoenzyme has been used in different environments as an indicator of

phosphorus limitation (Gage & Gorham 1985, Li et al. 1998, Sala et al. 2001). A higher alkaline phosphatase activity in the cells is expected when the cells are phosphorus-limited.

Dynamic model

We set up a numerical model of diatom growth based on phosphorus limitation to simulate population growth in the experimental containers. The model was developed with the computer package Stella (Stella Research 6.0, High Performance Systems, Inc.). The units tracked over time were µmol P ml^{-1}. The uptake flow of phosphorus by diatoms was computed as:

$$(1) \qquad \alpha_{P,B}\, PB$$

where $\alpha_{P,B}$ is the affinity constant (Table 2) for phosphorus, and P and B are the concentrations of phosphorus and of diatoms at a given time. The flux at a particular time step (*dt*) is determined by multiplying Eq. 1 times *dt*. The uptake can only reach a maximum value given by V_{max} (h^{-1}) from Moloney & Field (1989).

Table 2 – Parameter values in model runs.

Parameter	Units	*T. pseudonana*	*Coscinodiscus* sp.
Carbon content	fgC μm^{-3}	113 [a]	64 [b]
P affinity constant	ml $\mu molP^{-1}$ h^{-1}	56	20
Cell size (diameter)	µm	6.00	109
Cell volume	μm^{3}	106	390000
P diffusivity	cm^{2} s^{-1}	6.12×10^{-6}	6.12×10^{-6}
Viscosity	cm^{2} s^{-1}	10^{-2}	10^{-2}
Turbulent kinetic energy dissipation rate	cm^{2} s^{-3}	10^{-6} - 10^{-1}	10^{-6} - 10^{-1}
C:P	molC $molP^{-1}$	204 [c]	88 [d]

[a] Mullin et al. 1966
[b] Moal et al. 1987
[c] Perry 1976
[d] Blasco et al. 1982, Moal et al. 1987, Montagnes et al. 1994

The effect of turbulence on uptake is parameterized by the Sherwood number, which multiplies the uptake flow. The Sherwood number (*Sh*) was calculated from the estimations of the Péclet number (*Pe*) for spherical cells, as seen in Table 3. *Pe* is defined as:

$$Pe = Er^2/D, \quad (2)$$

where E (s^{-1}) is the shear rate, r is the radius of the cell (cm) and D is the diffusivity of solute ($cm^2\ s^{-1}$). In turn E, is calculated from the kinematic viscosity (ν, $cm^2\ s^{-1}$) of seawater and the turbulent kinetic energy dissipation rate (ε, $cm^2\ s^{-3}$).

$$E = (\varepsilon/\nu)^{1/2} \quad (3)$$

For the still condition, a background ε of 10^{-6} $cm^2\ s^{-3}$ produced simply by convection processes was used. This value was inferred considering the minimum values of ε measured in nature (Petersen et al. 1988, Peters & Marrasé 2000).

We used a combination of direct measurements and literature values for the different parameters (Table 2).

Table 3 – Equations utilized (from Karp-Boss et al. 1996) in order to calculate the *Sh* number according to the *Pe* number.

Pe range	Equation for Sherwood number	original equation in Karp-Boss et al. 1996
$Pe \leq 0.01$	$1 + 0.29\ Pe^{1/2}$	Eq. 48
$Pe \geq 100$	$0.55\ Pe^{1/3}$	Eq. 49
$0.01 < Pe < 100$	mean of $1.014 + 0.150\ Pe^{1/2}$ and $0.955 + 0.344\ Pe^{1/3}$	Interpolation

The model was run with a Runge-Kutta 4 integration method. We only ran the model for ca. 5 days (the duration of the experiments), and made no attempt to reach some equilibrium state since we wanted to simulate the transient batch culture.

Statistics

Results were analyzed with an analysis of covariance (ANCOVA) using sampling time as the covariate and cell concentration as the independent variable. Statistical significance was considered when $p < 0.05$. Comparison between model output and experimental data was done with regression analysis. Both the slope and the percentage of variance explained by the regression (R^2) for cell numbers and inorganic phosphorus were used to evaluate the goodness of fit of the dynamic model.

RESULTS

Experimental results

In both still and turbulent conditions, exponential growth of *T. pseudonana* was observed during the first 90 h of the experiment (Fig. 1a, c); then, the population started to reach stationary phase (Exp.1, Fig. 1a) or a lower growth rate phase (Exp. 2, Fig. 1c). Final concentrations averaged 324500 cells ml^{-1}. During the first 60 h, a slightly faster growth of *T. pseudonana* was observed in the still than in the turbulent conditions ($\mu = 1.39 \pm 0.076$ d^{-1} (still) and 1.30 ± 0.007 d^{-1} (turbulence) in Exp. 1 (mean ± SE) and 1.45 ± 0.007 d^{-1} (still) and 1.25 ± 0.092 d^{-1} (turbulence) in Exp. 2). In all containers, the inorganic phosphorus (with an initial concentration between 1 and 2 µM) was consumed during the first 70 h (Fig. 1a, c). The measured initial phosphate concentration was higher than foreseen, probably due to phosphate added as carryover with the inocula, although the inocula were from a phosphorus-limited medium as well. Nitrate and silicate decreased during the experiment until approximately half of their initial concentration (both nutrients in Exp. 2 and nitrate in Exp. 1) or until their total depletion (silicate in Exp. 1) (data not shown).

Exponential growth of *Coscinodiscus* sp. was observed during the experiment (Exp. 1 and 2, Fig. 1b, d) for the still and turbulent cultures. The growth rates in the first 40 - 70 h of the experiment were 0.52 ± 0.139 d^{-1} (still) and 0.48 ± 0.029 d^{-1} (turbulence) in Exp. 1 and 0.33 ± 0.033 d^{-1} (still) and 0.42 ± 0.085 d^{-1} (turbulence) in Exp. 2 (mean ± SE). In the last 50 h of both experiments higher growth rates in turbulent than in still conditions were observed. Final cell concentrations reached 33 cells ml^{-1} (still) and 55 cells ml^{-1} (turbulence) in Exp. 1 and 22 cells ml^{-1} (still) and 38 cells ml^{-1} (turbulence) in Exp. 2. In both conditions, phosphate concentration decreased during the first 70 hrs of the experiment and then remained at low levels (< 0.5 µM) until the end. Nitrate decreased smoothly over the duration of the incubation and approximately 13 % of the initial concentration had been removed by the end of the experiments (data not shown). A larger decrease in silicate was observed under turbulence than in still water (data not shown).

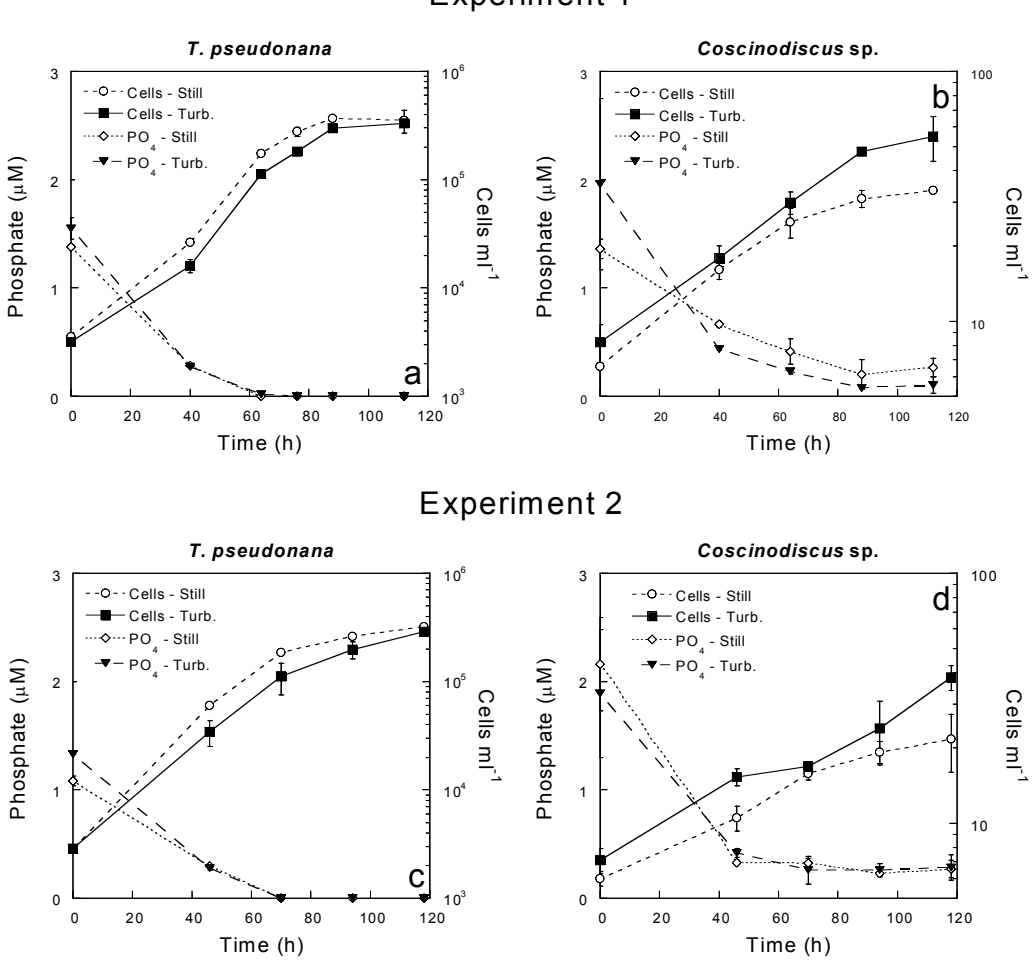

Fig. 1 – Growth curves (cells ml^{-1}) and phosphate concentration (µM) of *T. pseudonana* (a and c) and *Coscinodiscus* sp. (b and d) under still and turbulent conditions for Experiment 1 and 2.

Although we used sterile techniques throughout the experiments, none of the algal cultures was initially axenic. We took care in reducing bacteria carryover in the inocula for the experiments, achieving initial bacterial concentrations from 2.3×10^3 to 3.0×10^5 cells ml^{-1} (Table 4), depending on the experiment. This resulted in particulate-P contribution from bacteria of 10.38 ± 0.16 % (mean ± SE, Exp. 1) and 0.87 ± 0.03 % (Exp. 2) of the P-biomass in the *T. pseudonana* cultures and of 5.72 ± 0.10 % (Exp. 1) and 1.95 ± 0.11 % (Exp. 2) in the *Coscinodiscus* sp. cultures. There were no significant differences in bacterial abundance between the still and turbulent conditions for *T. pseudonana* and *Coscinodiscus* sp. cultures. In general, an increase in bacterial numbers was

observed during the first 40 or 75 h of the experiment; thereafter, they decreased (Exp. 1) or remained at a more or less constant concentration (Exp. 2, Table 4). Estimated phosphate consumption by bacteria was between 4.8 and 17.5 % (on average 9.1 %).

Table 4 – Initial, end of exponential phase, and final concentration of bacterial abundance at the different experimental conditions (mean ± SE). No replicate for *Coscinodiscus* sp.-turb. was available on the initial day of Exp. 2.

Experimental condition	Bacterial concentration cells ml^{-1} ($*10^6$)		
	Initial	End exp. phase (time-h)	Final
Exp. 1			
T. pseudonana-still	0.03 ± 0.002	2.28 ± 0.75 (40)	0.14 ± 0.009
T. pseudonana-turb.	0.03 ± 0.001	2.25 ± 0.31 (40)	0.11 ± 0.002
Coscinodiscus sp.-still	0.22 ± 0.02	2.06 ± 0.83 (76)	0.65 ± 0.23
Coscinodiscus sp.-turb.	0.29 ± 0.02	3.28 ± 0.87 (76)	0.65 ± 0.23
Exp. 2			
T. pseudonana-still	0.02 ± 0.0002	0.97 ± 0.04 (70)	0.77 ± 0.02
T. pseudonana-turb.	0.03 ± 0.0001	1.57 ± 0.55 (70)	0.99 ± 0.32
Coscinodiscus sp.-still	0.06 ± 0.007	2.99 ± 0.13 (70)	5.74 ± 2.08
Coscinodiscus sp.-turb.	0.06	5.07 ± 1.21 (70)	5.13 ± 2.05

The ratios of specific APA-still:specific APA-turbulence (APA_s:APA_t) for both experiments are shown in Fig. 2. In *T. pseudonana* cultures, these ratios were always near unity or slightly higher (CV = 11 %, Exp. 1, 31 %, Exp. 2). However, at the end of the *Coscinodiscus* sp. experiments, the ratio APA_s:APA_t reached values between 2.3 or 4.5 times higher than at the 40 or 46 h time point (Exp. 1 and Exp. 2, respectively), which was taken as reference.

Model predictions and parameter adjustment

The model was run with the measured initial cell numbers and phosphate concentrations measured in Exp. 1; the cell carbon content values and the C:P ratios were adjusted within ranges reported in the literature (Table 2). The P affinity constant was adjusted to optimize the statistics between model output and observed data. For *T. pseudonana* the model predicted an initial growth rate (first four hours of the experiment) of 1.86 d^{-1} (still) and 2.21 d^{-1} (turbulence). Cells reached stationary

phase in about 80 h in the turbulent condition and in about 100 h in the still condition (Fig. 3a). According to the model, maximum cell concentration was slightly higher under turbulence than under still conditions. For *Coscinodiscus* sp., the model predicted significantly higher cell numbers in the turbulent than in the still condition (Fig. 3b). Calculated initial exponential growth rates (first four hours) were 0.71 d^{-1} (still) and 1.55 d^{-1} (turbulence). According to the model, after the 5 d of the experiment we expected to find around 36 cells ml^{-1} in the still condition and 63.4 cells ml^{-1} in the turbulent one.

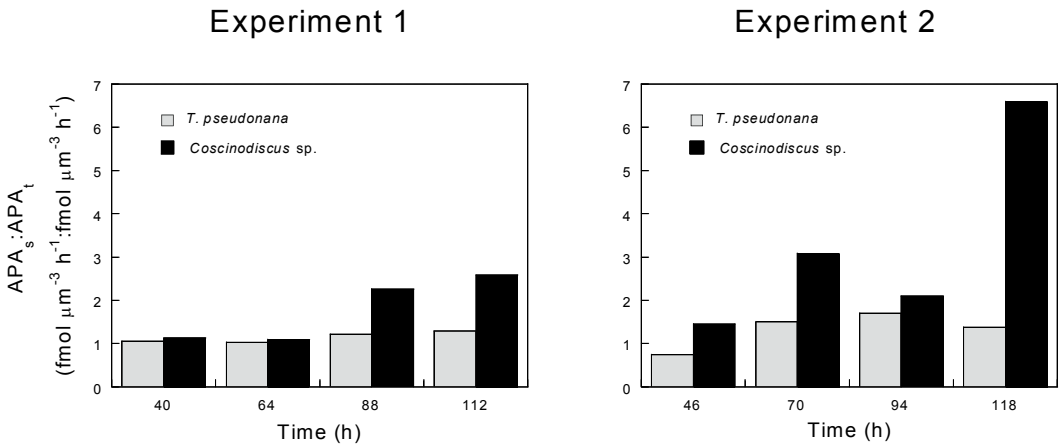

Fig. 2 – Ratios of specific alkaline phosphatase activity (APA) between still and turbulent conditions (APA_s:APA_t) for *T. pseudonana* and *Coscinodiscus* sp. cultures and for Experiments 1 and 2.

The model predicted exhaustion of phosphate after the first 110 h in both the still and turbulent conditions of *T. pseudonana* cultures (Fig. 3). For *Coscinodiscus* sp., a faster decrease of this nutrient was predicted under turbulence. At the end of the experiment, the model predicted lower phosphate concentration in the still than in the turbulent conditions.

Regression analyses of model output with respect to observed values are given in Table 5. In comparison with experimental data, the model predicted a faster initial growth rate of *Coscinodiscus* sp. in turbulent conditions and a somewhat lower phosphate consumption of both algae. In addition, the model predicted rather faster growth rates of *T. pseudonana* in turbulent than in still water.

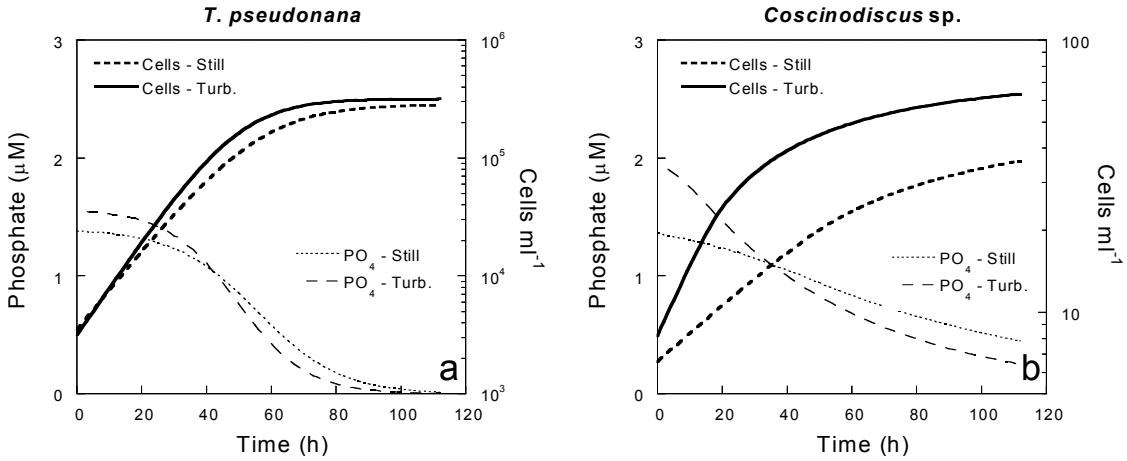

Fig. 3 – Model results on *T. pseudonana* (a) and *Coscinodiscus* sp. (b) growth and phosphate dynamics using parameters from Table 2.

Table 5 - Regression analysis of model output against observed values in phosphorus and cell number concentration. y = model values, x = experimental values

Thalassiosira pseudonana		[P]		Cell number	
		slope	R^2	slope	R^2
	S	0.85	0.64	0.70	0.94
	T	0.91	0.70	0.85	0.74
Coscinodiscus sp.		[P]		Cell number	
		slope	R^2	slope	R^2
	S	0.71	0.86	1.04	0.99
	T	0.82	0.92	1.01	0.71

DISCUSSION

Enhancement of *Coscinodiscus* sp. growth by turbulence was observed in the experiments and could be reproduced by the model (Fig. 1 and 3). However, experimentally, the enhancement of *Coscinodiscus* sp. growth was only observed in the last days of the experiment. In the case of *T. pseudonana* the model predicted a slightly enhanced growth under turbulence while experimental data showed the opposite, although almost the same cell numbers were found in both conditions at the end of the experiment. Phosphate depletion in *T. pseudonana* cultures was probably the reason of the decrease in their growth rates at the end of the experiment. However, in the *Coscinodiscus* sp. cultures phosphate was not completely consumed, allowing growth to continue until the end of the experiment.

The best adjustment of model and experimental values was obtained with C:P ratios of 204 for *T. pseudonana* and 88 for *Coscinodiscus* sp. Although the molar Redfield ratio would be 106, higher and lower C:P ratios have been reported in the literature. Perry (1976) found values as high as 665 in phosphorus-limited cultures of *T. pseudonana*. Cases where only measurements of diatom cell carbon and nitrogen are given, C:P ratios could be inferred considering an N:P ratio of 16. Using this approximation, a C:P of 88 would be also in the range of reported values (Blasco et al. 1982, Moal et al. 1987, Montagnes et al. 1994). The P-affinity rate has been estimated for nutrient concentrations tending to 0 (Vadstein & Olsen 1989). For larger P concentrations, the affinity should be lower. As we found no data on how much lower this affinity should be or a function of affinity with respect to P-concentration, the affinity was adjusted to optimize the statistics between model output and observed data.

Once the parameters in the model were tuned, experimental and modelling results agreed quite well with the theoretical observations of Karp-Boss et al. (1996). According to these authors, turbulence enhancement of the nutrient transport into the cells would be significant only for cell-sizes larger than 60 µm. Dynamic modelling results show a 118 % increase in growth rate for *Coscinodiscus* sp. and only a 19 % increase for *T. pseudonana*. According to the model, enhanced initial growth rate would have been expected in the *Coscinodiscus* sp. experiments but this was not the case. Only after later in the incubation were growth rates different owing to turbulence. At the end of the experiment, the biomass difference between turbulence and still water was of about 70 %.

The specific APA values were higher in the still than in turbulent conditions for *Coscinodiscus* sp., (between ca. 3 and 7 times higher at the end of the experiment, Fig. 2). This indicates a higher phosphorus limitation of *Coscinodiscus* sp. cells in the still cultures. However, for *T. pseudonana*,

the specific APA was very similar in both conditions or only slightly higher in the turbulent ones suggesting an almost equal phosphorus limitation in *T. pseudonana* cells growing in still and turbulent conditions. In addition, *Coscinodiscus* sp. reduced silicate faster under turbulence. All this accumulated evidence points towards the confirmation of the current theory of increasing nutrient flux through turbulent water motion and on the differential effect depending on the size of cells.

Phosphate consumption was slower in the model than in the experiments, especially in the case of *T. pseudonana*. Bacteria were present in the cultures and the fast increase of bacteria observed in the first hours of the experiment (Table 4) means that part of the phosphate in the medium was consumed by these organisms. This could explain a faster decrease of phosphate in the experiments compared to the model output (where bacteria were not considered). However, we estimated that no more than 17.5 % (average of 9.1 %) of the phosphate would have been consumed by bacteria. Moreover, the fact that bacteria did not continue growing to achieve much higher numbers suggests that they became C-limited, influencing still less the dynamics of P in the cultures. Since there were no statistical differences in the concentration of bacteria between turbulence and still treatments in any of the experiments, we assumed that the differences observed for the diatoms were due to turbulence. This agrees with theoretical expectations since the phosphate transport into a bacterial cell would increase only by 0.6 % due to turbulence (Karp-Boss et al. 1996). Therefore, as the bacterial nutrient consumption would be almost the same with and without turbulence, the differences observed in the phosphate concentration in the still and turbulent conditions would be due fundamentally to differences in the nutrient consumption of the algae. We did not consider including bacteria in the model because it would have increased unnecessarily the number of uncertain parameter values.

We observed some sedimentation in the experimental containers, especially in the still water ones with *Coscinodiscus* sp. If we use the data in Fig. 1 of Smayda (1970) to obtain a regression of sinking rate versus average cell diameter and then introduce the dimensions of *Coscinodiscus* sp. and *T. pseudonana*, we obtain sinking velocities of 2.36×10^{-3} and 1.12×10^{-4} cm s^{-1}, respectively. These sinking velocities are lower than the eddy velocities derived from the turbulence level introduced (18×10^{-2} cm s^{-1}) and even for still water (1×10^{-2} cm s^{-1}) if we consider a background ε of 10^{-6} cm^2 s^{-3} produced simply by convection. This means that, in principle, even if cells are sinking they would also be resuspended, so we would not expect cell accumulation at the bottom of the containers. But we did observe part of the population at the bottom of the containers. Presumably, settled cells would not be able to take up as much phosphate as cells in suspension (because of having one of their valves in contact with the bottom). Additionally, in the case of *Coscinodiscus* sp. we observed empty shells. These shells must have been produced at some point

and therefore they were accounted for to compute the total number of cells in the experimental results. However, comparing growth rates with model run output may be misleading since mathematically all cells are growing in the model. We do not know what triggered cells to die and generate empty shells. One hypothesis could be that as cells touched the bottom of the container, some of them would no longer be able to resuspend and would die. Thus, empty shells should be more abundant in still water conditions. Experimentally, we computed almost the same amount of empty shells in both the still and turbulent cultures, although the relative amount of these cells was higher in still water (around 80 % of the total population with respect to ca. 40 % under turbulence at the end of the experiment). Thus, even after excluding the empty shells from the total cell numbers, turbulent cultures would still show higher cell counts than still cultures. No empty shells were observed for *T. pseudonana*.

Sinking could also have enhanced the flux of nutrients towards the cells since this is one way to increase the relative motion between the cells and the fluid. The gain in nutrient flux towards the cells owing to sinking in still water can be computed following Karp-Boss et al. (1996) as:

$$Sh = ½ [1 + (1 + 2Pe)^{1/3}] \quad (4)$$

where Pe is the Péclet number calculated as Ur/D, r the radius of the cell and U the sinking velocity. This would give a *Sh* of 1.36 for *Coscinodiscus* sp. and of 1.0018 for *T. pseudonana*. Equation 4 applies for sinking in still water. Unfortunately, there are no theoretical equations that can resolve the increase in nutrient uptake due to sinking in a turbulent environment.

The turbulent intensity used in our experiments was in the range of intensities found in the ocean (Mackenzie & Legget 1993, Peters & Marrasé 2000). Thus, our results suggest that turbulence could favour larger diatoms in natural conditions because of increased nutrient flux towards the cells. However, the outcome of competition between large and small diatoms in the field may be modified by other factors such grazing, or by the redistribution of cells in the water column by turbulence. Additionally, phytoplankton cells in the open sea are subject to time-varying levels of turbulence and their growth conditions, in terms of turbulence, may be more complex than what we can currently generate in the laboratory.

The effects of turbulence on the sedimentation rate of phytoplankton are poorly studied. In natural waters, it is generally accepted that turbulence prevents the loss of phytoplankton cells from the mixed layer (Kiørboe 1993). However, Ruiz et al. (1996) observed that the sedimentation rate of phytoplankton cells could be affected by changes in turbulence levels only when their settling velocity was higher than 1 m d^{-1}. This was the case for *Coscinodiscus* sp. but not for *T.*

pseudonana. In addition, diatom cells may modify their sinking velocity by physiological control (e.g. fat accumulation and gas vacuoles) or by changes in their growth rates (Smayda 1970). Cells with low growth rate or senescent cells have higher sinking velocities than actively growing cells. One of the shortcomings of our model is that it did not consider sinking of the cells in the experimental vessels. This was done to avoid incrementing the number of uncertain mechanisms and parameters. However, the model needed only parameter tuning to fairly accurately match experimental results and theoretical predictions and we found it useful to constrain the possible importance interactions between turbulence and cell size concerning nutrient uptake. Clearly, further experiments assessing the effects of turbulence on diatoms need to address explicitly the sinking of cells. This is intrinsically difficult since stirring, aerating or otherwise trying to keep cells in suspension also introduces turbulence, and no still water control is possible.

ACKNOWLEDGEMENTS

We thank Marta Estrada for the helpful comments on the manuscript and Roser Ventosa for nutrient analysis. This work was supported by the European projects MEDEA (MAS3-CT95-0016) and NTAP (EVK3-CT-2000-00022).

Combined effects of nutrients and small-scale turbulence in a microcosm experiment. I. Dynamics and size distribution of osmotrophic plankton

ABSTRACT

The response of phytoplankton and bacterial dynamics to turbulence and nutrient availability interactions was studied in natural coastal waters enclosed in 15 L microcosms. The effect of turbulence was examined under three nutrient induced conditions: nitrogen-surplus (N - with initial addition of an excess of nitrogen, N:P ratio = 160), nitrogen:phosphorus ratio balanced (NP - with initial addition of nitrogen and phosphorus as Redfield ratio, N:P ratio = 16) and control (C - no nutrient addition). Turbulence (ε = 0.055 cm^2 s^{-3}) was generated by vertically oscillating grids. The experiment lasted for 8 days and samples were generally taken daily for nutrient and plankton measurements. Turbulence increased the relative importance of phytoplankton to bacteria when nutrients were added, while in the control the effect of turbulence was negligible. Turbulence also influenced the species' composition and the size distribution of the phytoplankton community. The relative contribution of diatoms to total phytoplankton biomass and the average cell size were higher under turbulence, particularly in N and NP treatments. The results of these experiments indicate the importance of considering the hydrodynamic conditions in studies addressing competition for nutrients among different osmotrophic organisms in plankton communities.

INTRODUCTION

In aquatic systems, an osmotrophic cell is said to be diffusion-limited when the uptake rate of the limiting nutrient is faster than the diffusive transport across the boundary layer surrounding the cell (Karp-Boss et al. 1996). Small-scale turbulence (including laminar shear) should theoretically disrupt this layer and thus increase the advective transport of nutrients into the cell. This phenomenon is especially important for non-motile planktonic cells, which need the movement of water to enhance their nutrient uptake. The increase in the nutrient flux into the cells due to small-scale turbulence varies from negligible to significant as cell size increases (Karp-Boss et al. 1996). Karp-Boss and coworkers concluded that small-scale turbulence is only significant for cells > 60 µm, while small cells should not be directly affected. Some properties of the organisms, such as chain formation in diatoms, could be a mechanism to enhance nutrient uptake due to turbulence when their length approaches the Kolmogorov scale (Karp-Boss et al. 1996, Karp-Boss & Jumars 1998, Pahlow et al. 1997) which is the smallest scale of eddy motion.

In a natural plankton community, both bacteria and phytoplankton compete for limiting nutrients. As mentioned above, small-scale turbulence has been predicted to have little effect on the nutrient flux to small planktonic organisms, such as bacteria and small phytoplankton, but could favour large cells in the competition for nutrients. Also, turbulence could select particular life-forms within the phytoplankton community. Frequently, diatoms dominate in turbulent and nutrient-rich waters, while dinoflagellates dominate in calm and nutrient-poor waters. Margalef (1978) suggested that this trend could be due to the different capability of movement of these organisms. In turbulent environments, non-motile and fast-growing life forms could be favoured as large-scale turbulence reduces sedimentation losses out of the photic zone, while dinoflagellates could take advantage in calm waters by increasing nutrient flux through swimming and migratory behaviour. In addition, dinoflagellates seem to be the most sensitive organisms to turbulence (Thomas & Gibson 1990, Estrada & Berdalet 1998). Changes in hydrodynamic conditions can affect cell processes like cell division (Berdalet 1992, Thomas et al. 1995), nutrient uptake (Karp-Boss et al. 1996) or swimming motion (Karp-Boss et al. 2000).

Few experimental studies have dealt with the effect of fluid motion on osmotrophic organisms (Pasciak & Gavis 1975, Canelli & Fuhs 1976, Savidge 1981, Thomas & Gibson 1990, Berdalet 1992, Thomas et al. 1995, Köhler 1997). Even fewer have been done with natural plankton communities confined in enclosures (Oviatt 1981, Estrada et al. 1987, 1988, Peters et al. 1998, Petersen et al. 1998, Svensen et al. 2001). Most of those studies show that the extent of turbulence

effects on phytoplankton dynamics depends on the initial conditions and nutrient inputs, but none of them reported the relative importance of bacteria versus phytoplankton during the experiment.

As changes in nutrient flux to cells induced by turbulence depend on cell size, we hypothesise that: (1) turbulence increases the relative importance of phytoplankton biomass with respect to bacterial biomass; (2) phytoplankton size distribution is affected by turbulence; and (3) the relative contribution of diatoms to phytoplankton biomass increases with turbulence. To test these hypotheses we enclosed coastal water from the NW Mediterranean Sea and added nutrients in order to achieve different initial N:P ratios, and then incubated them under still and turbulent conditions. We also expect that the response of plankton to turbulence will be reflected in the organic matter stoichiometry. Data on organic matter quality in relation to the degree of heterotrophy is reported elsewhere (Maar et al. see *Chapter V*).

MATERIAL AND METHODS

Experimental set-up

Surface water from the Catalan coast (Masnou, NW Mediterranean, ca 1 km offshore) was enclosed in twelve 15 L cylindrical plexiglass containers (24.2 cm inner diameter and 34.5 cm depth) on March 25, 1998. The water had previously been filtered through a 150 µm mesh net in order to remove the larger zooplankton.

The experiment was performed in an environmental chamber at 15 ± 1 °C under a 12:12 h light:dark cycle and a light irradiance of 225 µmol photons m^{-2} s^{-1}. Six of the twelve containers were subjected to turbulence (see below), and the remainder were left under still conditions. Within each group of containers, two were left as controls (C) with no nutrient addition, and four received nitrogen and phosphorus in different proportions. Of these four, two were enriched with a nitrogen-surplus addition (N) and two were enriched following the Redfield ratio (NP) (see Table 1). In the N and NP containers, metals and silicate were also added. The metal solution was added in the same proportion to nitrate as in the f/2 medium (Guillard 1975). All additions were done at the beginning of the experiment.

Small-scale turbulence was generated by vertically oscillating stainless steel grids coated with non-toxic plastic, with a mesh size of 0.6 cm and bar thickness of 0.35 cm (Peters et al. 2002). The grid moved down to 1 cm from the bottom. Stroke length was 20 cm and oscillation frequency was set to 3.7 rpm.

Table 1 – Nutrient concentration (µM) and N:P ratio in the initial water, and nutrient addition in the six (with replicate) different experimental conditions. A and B are replicates, letter combinations explain experimental conditions, e.g. SCA: still control replicate A.

	Still	Turbulent	PO_4	NH_4	NO_2	NO_3	SiO_3	N:P
Initial water			0.05	0.50	0.07	0.4	0.75	19.4
Control	SCA SCB	TCA TCB	----	----	----	----	----	19.4
N-surplus	SNA SNB	TNA TNB	0.1	----	----	16	30	160
Redfield ratio	SNPA SNPB	TNPA TNPB	1.0	----	----	16	30	16

Turbulence intensity was calculated from these parameters according to Peters & Gross (1994) giving an estimation of 0.055 $cm^2\ s^{-3}$. This value is within the range of turbulence intensities in coastal areas (Kiørboe & Saiz 1995). We also estimated turbulence intensity in the upper meters of the NW Mediterranean coastal zone from wind speed data following MacKenzie & Leggett (1993). Yearly averages fluctuate around 0.007 $cm^2\ s^{-3}$. It is not uncommon to have events with average intensities of the order of 0.01 $cm^2\ s^{-3}$ lasting for 4 days or more. When the volume of water decreased due to sampling, the stroke length was corrected to maintain the same energy dissipation rate. The final volume of the containers at the end of the experiment was approximately 5 litres.

The grids inside the turbulent containers increase the surface:volume ratio. To test for their possible effect on plankton, we set up a trial experiment with natural water and nutrient additions as in the real experiment. Two microcosms were left still without a grid, two had moving grids to reproduce the turbulence level (ε = 0.055 $cm^2\ s^{-3}$) and four microcosms were left still but with grids hanging in the middle of the containers. Changes in phytoplankton biomass were followed over 6 days. An analysis of covariance using the sampling times as covariate showed no statistical difference in chlorophyll *a* (chl *a*) concentrations between the still containers with and without grids. On the other hand, turbulence produced higher concentrations of chl *a* with respect to still containers ($p < 0.001$). Thus, the mere presence of grids inside the containers has no effect on plankton dynamics, at least as reflected by chl *a* concentrations.

Parameters measured

Changes in the measured parameters were monitored over eight days. Samples for nutrients, total and fractionated chl *a*, flow cytometry measurements (bacteria, picoeukaryotes, and cells in the *Synechococcus* and *Prochlorococcus* genera) and autotrophic flagellate counts were, for the most

part, taken daily. Samples for coccolithophorid, dinoflagellate and diatom counts were taken on Days 0, 4 and 8.

On Day 8, one replicate of the turbulent N-surplus (TN) and turbulent Redfield ratio (TNP) containers was sampled because the other replicate was left for another experiment. Further, after taking the routine samples on Day 8, each microcosm was strongly mixed until total resuspension of the settled material was achieved. Samples for chl *a* and bacteria were taken after resuspension. Differences in concentration before and after resuspension were used as an estimation of sedimented phytoplankton and bacterial biomass.

Data were analysed statistically with the analysis of covariance (ANCOVA) using the sampling times as a covariate. The data for time 0 was not considered as treatments had no time to affect the different variables. Statistical significance of a particular treatment was considered when $p \leq 0.05$.

Nutrients and chlorophyll a determinations

Concentration of nitrate, nitrite, ammonia, phosphate and silicate were determined by means of an Alliance Evolution II autoanalyzer, using the methods of Grasshoff et al. (1983) with minor modifications.

Total and fractionated chl *a* were estimated fluorometrically (Yentsch & Menzel 1963). For total chl *a*, 20 ml samples were filtered through Whatman GF/F filters. For the > 10 µm fraction, 40 ml samples were filtered through 10 µm pore size polycarbonate filters. To extract chl *a*, all the filters were ground in 90 % acetone and left in the dark at room temperature for at least two hours. The fluorescence of the extract was measured with a Turner Designs fluorometer.

Bacteria and autotrophic plankton enumeration

Bacterial and autotrophic picoeukaryotes, *Synechococcus* and *Prochlorococcus* abundances were determined by flow cytometry (Gasol & del Giorgio 2000). Samples of 1.2 ml were fixed with 1 % paraformaldehyde and 0.05 % glutaraldehyde (final concentration), left in the dark at room temperature for 10 min and then stored frozen at - 70 °C. Later, samples were unfrozen and run through a FACS-calibur (Becton & Dickinson) flow cytometer with a laser emitting at 488 nm. To determine bacterial abundance a subsample of 200 µl was stained with Syto13 (Molecular Probes) at 1.6 µM (diluted in DMS) and left to stain in the dark for 15 min. Subsamples were run at low speed (ca 12 µl min^{-1}) and data were acquired in log mode until 10000 events had been processed. As an internal standard, 10 µl of a 10^6 ml^{-1} solution of yellow-green 0.92 µm Polyscience latex beads

was added to subsamples. Bacteria were detected by their signature in a plot of side scatter (SSC) versus green fluorescence (FL1).

Subsamples of 600 µl were run at high speed (ca 60 µl min^{-1}) for the determination of autotrophic picoeukaryotes, *Synechococcus* and *Prochlorococcus*. As for bacteria, the data were acquired in log mode until 10000 events had been processed. A volume of 10 µl of a 10^5 ml^{-1} concentration of beads was used as an internal standard. *Synechococcus* was detected by its signature in a plot of orange fluorescence (FL2) versus red fluorescence (FL3). *Prochlorococcus* had a lower FL3 signal and no FL2 signal. Autotrophic picoplankton had higher FL3 signals and no FL2 signal.

Autotrophic nanoflagellate (ANF) samples were fixed with 10 % glutaraldehyde (final concentration 1 %). Twenty ml were filtered through 0.8 µm black polycarbonate filters and stained with DAPI (5 µg l^{-1} final concentration); the filters were kept at - 20 °C. ANFs were counted on a Nikon Labophot epifluorescence microscope at 1250x (Porter & Feig 1980), and sized using a calibrated ocular micrometer in 3 size classes (4 - 8 µm, 8 - 16 µm and > 16 µm).

For the identification and enumeration of the rest of the phytoplankton cells (mainly diatoms, dinoflagellates and coccolithophorids), samples were fixed with formalin-hexamine solution (0.4 % final concentration). Counts were made with the Utermöhl technique (Utermöhl 1958) using 50 cm^3 settling chambers. One transect of the chamber was observed at 400x magnification to count the smaller (< 20 µm) and more frequent organisms. Additionally, one transect or half of the chamber was observed at 200x to count cells of intermediate size (generally between 20 and 50 µm) and the whole chamber was scanned at 200x to count the large forms. The observed organisms were classified to the lowest possible taxonomic level.

Biomass calculations

Bacterial biomass was estimated by flow cytometry following the methodology described in Gasol & del Giorgio (2000), using a carbon conversion factor of 0.35 pg C μm^{-3} (Bjørnsen 1986). Chl *a* values were converted to carbon using a factor of 30 µg of carbon per µg of chl *a* (Strickland 1960) which correspond to the values observed in the upper layers of the water column (average = 32.5, SE = 4.6, n = 6) in the NW Mediterranean Sea (Delgado et al. 1992).

Literature cell volumes for March in the NW Mediterranean (Ribes et al. 1999) were used to calculated the biovolumes of *Synechococcus* and picoeukaryotes. A mean size of 0.7 µm (Vaulot et al. 1990) was used for *Prochlorococcus* volume calculations. A mean carbon content 0.357 pg C μm^{-3} for *Synechococcus* was derived from Bjørnsen (1986), Kana & Gilbert (1987) and Verity et al.

(1992). A conversion factor of pg C cell^{-1} = 0.433 x (µm^3)$^{0.863}$ was used for picoeukaryotes (Verity et al. 1992). For *Procholococcus* a conversion factor of 0.133 pg C µm^{-3} was used (Simon & Azam 1989).

Cell volume of ANFs was calculated from the mean size of each size class assuming ellipsoidal cell shape. The carbon conversion factor used in this case was the same as for picoeukaryotes.

Diatom, dinoflagellate and coccolithophorid biomass estimations were also done from size measurements. At least 20 individuals of the most abundant forms were recorded with a video camera (Hitachi KPC503) at 400x. Then, each organism was measured (length and width) using a NIH-Image software and its volume calculated using a geometrical approximation of its form. Carbon content was estimated from the conversion factor pg C cell^{-1} = 0.109 x (µm^3)$^{0.991}$ (Montagnes et al. 1994).

RESULTS

Data from replicated containers were highly consistent with each other. Nutrient concentrations, chl *a* and bacteria showed no statistical differences among replicates for all treatments.

Inorganic nutrients

Variations of the inorganic nutrient concentrations during the experiment for the different treatments, are shown in Figure 1. In the controls, the initial concentrations of phosphate, nitrate and silicate were 0.03, 0.08 and 0.2 µM, respectively, and they remained at low concentrations during the experiment. In this treatment, no significant differences in nitrate and phosphate concentrations between still-control (SC) and turbulent-control (TC) containers were found. Silicate was slightly lower in TC (0.26 µM) than in SC (0.48 µM).

In general, in the N and NP treatments a decrease in phosphate, nitrate and silicate concentrations was observed throughout the experiment which was more evident with turbulence. Turbulence had a statistically significant effects on nutrient concentrations for the N and NP treatments, with the exception of phosphate in the N treatment where no difference was found. In the NP treatments, a depletion of phosphate and nitrate was observed in the turbulent containers from Day 5.

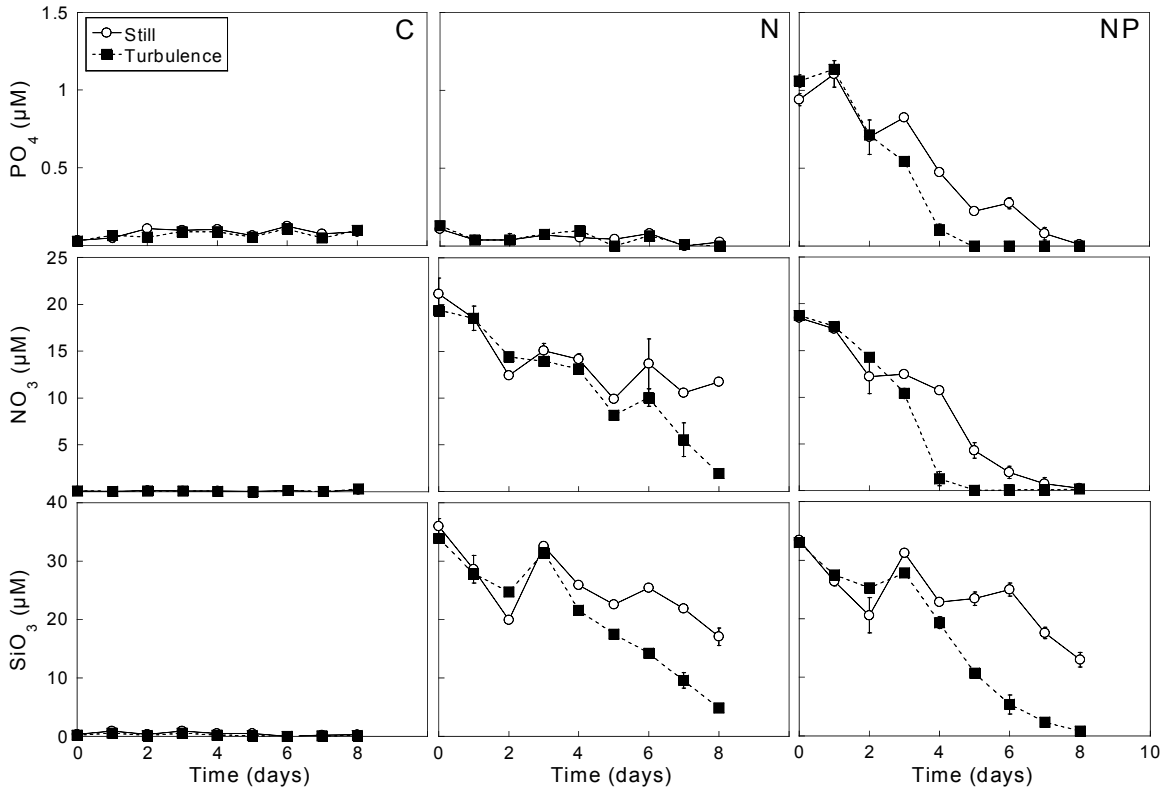

Fig. 1 – Phosphate (PO_4), nitrate (NO_3) and silicate (SiO_3) concentrations (µM) for the C (control), N (N-surplus) and NP (Redfield ratio) conditions (still and turbulent) during the experiment. Mean of two replicate microcosms per treatment ± SE. No replicates for TN and TNP were available on Day 8.

Chlorophyll a

The initial total chl *a* was around 1 µg l^{-1} in all the containers (Fig. 2). In the controls, no significant difference in total chl *a* was observed between still and turbulent containers. In both, total chl *a* increased slightly during the first two days of the experiment and thereafter it started to decrease to around 0.20 µg l^{-1} by Day 8.

In the N and NP treatments, significantly higher total chl *a* was observed in turbulent than in still containers from Day 2 ($p < 0.001$). In the turbulent N containers, total chl *a* increased until the end of the experiment (up to 10.2 µg l^{-1} of chl *a*), while in turbulent NP containers total chl *a* peaked on Day 4 with a concentration of 19.0 ± 1.1 µg l^{-1}. In the still containers, total chl *a* increased during the first two or three days, reaching a maximum of 3.7 ± 2.5 and 4.2 ± 0.2 µg l^{-1} in the N and NP treatments, respectively.

The ratio of the > 10 µm chl *a* fraction with respect to total chl *a* showed no significant differences owing to turbulence in C containers (Fig. 3). However, in the N and NP containers, significant higher values of >10 µm:total chl *a* ratio were found in the turbulent treatments after Day 2 or 3 ($p < 0.001$).

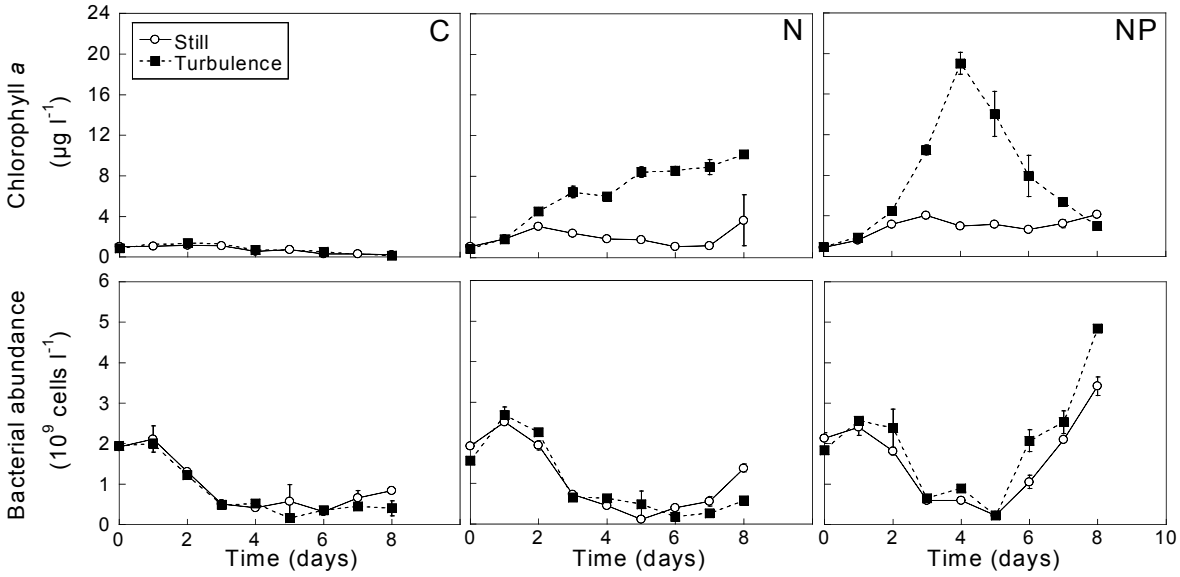

Fig. 2 – Chlorophyll *a* concentration (µg l^{-1}) and bacterial abundance (cells l^{-1}) for the C (control), N (N-surplus) and NP (Redfield ratio) conditions (still and turbulent) over the course of the experiment. Mean of two replicate microcosms per treatment ± SE. No replicates for TN and TNP were available on Day 8.

Bacterial abundance

No significant differences in bacterial abundance were observed between still and turbulent containers in all the treatments (Fig. 2). However, in the NP containers, the tendency in the last days of the experiments (from Day 5) was a higher bacterial abundance under turbulence. Initial bacterial number in all the incubators was around 1.88×10^9 cells l^{-1}. After an increase on Day 1, bacterial abundance decreased down to 5.12×10^8 cells l^{-1} on Day 5 or 6. Thereafter, the values increased again until the end of the experiment. The highest increase was in the NP treatments.

The relationship between bacteria and phytoplankton biomass (as derived from chl *a*) for the C, N and NP treatments during the experiment is presented in Figure 4. In C, the evolution of the phytoplankton and bacterial biomass during the experiment was similar in both, the still and the turbulent containers.

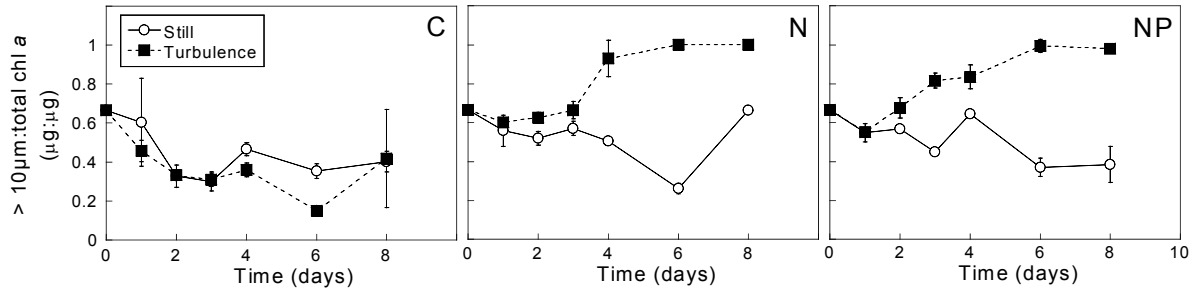

Fig. 3 – Ratio of the > 10 µm chlorophyll *a* fraction with respect to total chlorophyll *a* for the C (control), N (N-surplus) and NP (Redfield ratio) conditions (still and turbulent) during the experiment. Mean of two replicate microcosms per treatment ± SE. No replicates for TN and TNP were available on Day 8.

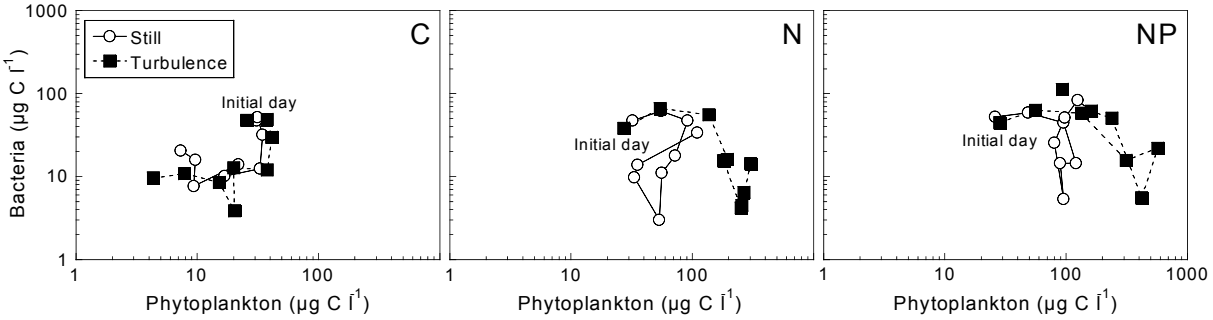

Fig. 4 – Relationship between bacterial and phytoplankton biomass (as derived from chlorophyll *a*) for the C (control), N (N-surplus) and NP (Redfield ratio) conditions (still and turbulent) for the nine days sampled. Initial day = initial day (Day 0) of the experiment.

However, in N and NP, from approximately the same bacterial biomass evolution, we found higher values of phytoplankton biomass under turbulence (from Day 2 and until the end of the experiment in the N treatments and between Days 3 and 6 in the NP ones).

Chl a and bacteria sedimentation

Table 2 shows the chl *a* concentration and bacterial abundance of the water column and of the water column plus the resuspended biomass at the end of the experiment (Day 8). Sedimented phytoplankton was higher in turbulent than in still treatments, while sedimented bacteria were, in general, similar in both treatments.

Table 2 – Chlorophyll *a* concentrations (µg l^{-1}) and bacterial abundance (cells l^{-1}) (mean of two replicate microcosms ± SE) at the end of the experiment (Day 8) in the water column and in the water column plus the resuspended biomass for the still (S) and turbulent (T) containers of the C (control), N (N-surplus) and NP (Redfield ratio). No replicates for TN and TNP were available on Day 8.

Treatment	Chl *a*		Bacteria	
	water column	water column + resuspended	water column	water column + resuspended
SC	0.25 ± 0.05	1.13 ± 0.09	8.41 ± 0.34 (x 10^8)	8.50 ± 1.09 (x 10^8)
TC	0.15 ± 0.02	1.94 ± 0.05	3.96 ± 1.88 (x 10^8)	4.58 ± 2.41 (x 10^8)
SN	3.68 ± 2.50	6.73 ± 0.19	1.38 ± 0.10 (x 10^9)	1.81 ± 0.37 (x 10^9)
TN	10.15	23.38	0.58 (x 10^9)	1.00 (x 10^9)
SNP	4.17 ± 0.21	13.47 ± 5.56	3.43 ± 0.23 (x 10^9)	6.37 ± 0.17 (x 10^9)
TNP	3.01	17.64	4.84 (x 10^9)	7.24 (x 10^9)

Phytoplankton size distribution and composition

In general, the highest percentage of large cells (> 50 µm) was observed in the turbulent containers, especially when nutrients were added (Fig. 5). The fraction > 50 µm represented more than 85 % of the autotrophic carbon in the turbulent N-surplus (TN) and turbulent Redfield ratio (TNP) containers and around 70 % in the TC containers on Day 8 although their contribution in absolute values (in terms of carbon) was very different (Table 3). This fraction was between 55 and 173 and between 131 and 178 times higher in TN and TNP than in TC containers, respectively. In all the treatments, the most abundant taxa in these fractions were species of two chain-forming diatom genera: *Chaetoceros* and *Pseudo-nitzschia*.

Among the three still containers, the highest percentages of autotrophic carbon < 20 µm were found in the C and NP treatments. On Day 8, the fraction < 2 µm was remarkably high (more than 30 % of the total autotrophic carbon) in these two treatments. *Prochlorococcus* was not observed in any of the treatments while *Synechococcus* decreased to undetectable concentrations by Day 4.

Independent of the percentage of each size fraction present in the different containers, almost 100 % of the cells > 50 µm corresponded to diatoms, while dinoflagellates were more frequent in the 10 - 50 µm size fraction (data not shown).

Table 3 – Carbon content (µg l^{-1}) in the different size classes (mean of two replicate microcosms ± SE) of the autotrophic biomass on Days 0, 4 and 8 for the still (S) and turbulent (T) containers of the C (control), N (N-surplus) and NP (Redfield ratio) conditions. No replicates for TN and TNP were available on Day 8.

Size-fraction (µm)	Day 0	Day 4					
	Initial water	SC	TC	SN	TN	SNP	TNP
< 2	5.2	2.45 ± 0.04	2.46 ± 0.09	5.88 ± 0.59	5.25 ± 0.42	4.93 ± 0.17	3.19 ± 0.07
2-10	3.91 ± 1.47	11.88 ± 3.08	8.38 ± 0.67	9.71 ± 3.40	7.73 ± 1.29	25.09 ± 11.13	50.05 ± 9.91
10-20	1.71 ± 0.23	0.53 ± 0.15	18.13 ± 17.52	8.53 ± 6.43	11.15 ± 8.65	104.17 ± 34.53	50.64 ± 47.39
20-50	1.24 ± 0.96	1.49 ± 0.59	0.84 ± 0.07	1.08 ± 0.19	1.51 ± 0.34	1.77 ± 0.48	1.80 ± 0.48
> 50	38.95 ± 6.25	2.60 ± 0.21	4.43 ± 0.42	44.08 ± 13.25	243.10 ± 28.15	55.56 ± 0.09	787.15 ± 69.15
Size-fraction (µm)		Day 8					
		SC	TC	SN	TN	SNP	TNP
< 2		2.00 ± 0.49	0	2.92 ± 0.32	1.13	34.95 ± 4.54	3.31
2-10		0.62 ± 0.62	0.10 ± 0.01	9.24 ± 0.20	17.97	20.92 ± 3.47	5.86
10-20		0.39 ± 0.13	0.74 ± 0.44	9.14 ± 0.37	8.58	47.23 ± 8.96	10.42
20-50		1.43 ± 1.40	0.11 ± 0.01	1.12 ± 0.21	16.33	1.40 ± 0.21	4.33
> 50		2.17 ± 2.04	2.10 ± 0.23	82.66 ± 65.87	363.00	12.77 ± 11.09	275.27

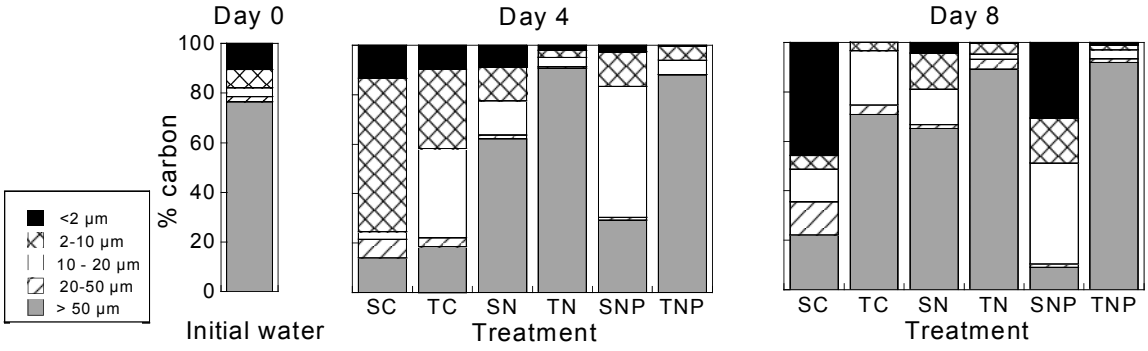

Fig. 5 – Phytoplankton size distribution for the initial water (Day 0), and for the C (control), N (N-surplus) and NP (Redfield ratio) conditions (still and turbulent) on days four and eight. Mean of two replicate microcosms per treatment. The associated errors between replicates are given in Table 3 where absolute values are shown. No replicates for TN and TNP were available on Day 8.

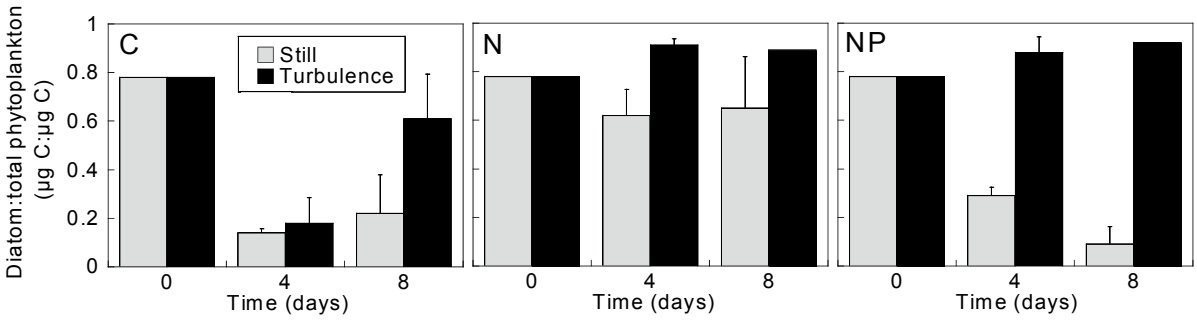

Fig. 6 – Diatom:total phytoplankton ratio for the C (control), N (N-surplus) and NP (Redfield ratio) conditions (still and turbulence) on Days 0, 4 and 8. Mean of two replicate microcosms per treatment ± SE. No replicates for TN and TNP were available on Day 8.

The ratio of diatoms to total phytoplankton (µg C:µg C) was higher in turbulent conditions, especially when nutrients were added (Fig. 6). On Day 4, when nutrients were still available in both treatments, this ratio was 3 times higher in the TNP than in the still Redfield ratio (SNP) containers and around 1.5 times higher in the TN than in the still N-surplus (SN) containers. Although practically no differences were observed in the diatom:total phytoplankton ratio between the turbulence containers of the N and NP treatments (around 90 % in both), in the still containers higher percentages of the ratio were found in the N (62 - 65 %) than in the NP treatments (9 - 29 %). Without nutrient additions (TC and SC treatments), diatoms had a low contribution (see > 50 µm size fraction in Table 3). But

even so, turbulence increased the relative importance of diatoms in relationship to total biomass (2.8 times higher on Day 8).

DISCUSSION

The effect of turbulence on the dynamics of plankton was different depending on the nutrient conditions. No clear effect was found at very low nutrient concentrations (control containers). In these conditions the hypothesised increase in nutrient flux to large cells due to turbulence was not enough to increase significantly the growth of osmotrophic organisms of any size, and therefore not enough to change the relative importance of bacteria to phytoplankton biomass. However, when nutrients were added (N and NP containers), the effect of turbulence was noticeable. Petersen et al. (1998) who examined coastal phytoplankton responses to different levels of turbulence in mesocosms, also found the effect of turbulence to be dependent on nutrient conditions. They observed no differences in the chl *a* concentration between turbulence treatments before nutrient addition. However, after a nutrient pulse, they did observe differences in chl *a* concentration. In our studies, although some trends were coincident for N (P deficient enrichment) and NP (N:P balanced enrichment) treatments, the timing and the magnitude of the response to turbulence were slightly different.

In the TNP containers phytoplankton grew rapidly until Day 4 and then decreased abruptly until the end of the experiment. However, in TN, a continuous growth of phytoplankton was observed (Fig. 2). These differences in phytoplankton growth could be explained by the dynamic of nutrients. In TNP, nitrate and phosphorus were initially added in the Redfield ratio and proportionally consumed by the phytoplankton community until Day 4 when they were almost depleted. After this day, neither nitrate nor phosphate were available and thus phytoplankton biomass started to decrease. However, in TN the initial addition of a surplus of nitrate enabled the growth of phytoplankton at a constant rate until the end of the experiment. Although phosphate was present at very low concentrations, it was probably quickly recycled (see Maar et al. *Chapter V*). Thus, the effects of turbulence on the growth of the phytoplankton community could change depending on the proportion and the concentration of nutrients in the water. The higher autotrophic biomass observed in the water column of the turbulent containers was due to a higher phytoplankton growth since sedimented chl *a* measured on Day 8 was also higher in these containers (Table 2).

Bacterial dynamics were practically the same in turbulent and nonturbulent containers. Bacteria increased initially (Day 1) but then decreased until Day 5 or 6. Afterwards, another increase of

bacteria was observed which was most evident in the NP containers. This initial increase in bacteria followed by a decrease has been observed in other microcosm experiments (Berdalet et al. 1996). The growth of bacteria observed from Day 5 could be explained by the presence of more degradable organic carbon (mostly produced by phytoplankton excretion) and the presence of inorganic nutrients, which in the TNP containers were probably recycled.

Bacteria-phytoplankton relationship

The relationship between bacteria and phytoplankton biomass (as derived from chl *a*, Fig. 4) showed that there were no differences over time between turbulent and still containers when the water was not enriched. However, in the N and NP treatments, lower values of bacteria:phytoplankton were observed with turbulence from Day 3 until the end of the experiment. Thus, turbulence increased the relative importance of phytoplankton to bacteria, as we expected, but only in the microcosms in which nutrients were added. These results are in contrast with those in Peters et al. (1998) who found high bacterial abundance under turbulence. They concluded that the grazing of microflagellates shifted from smaller (bacteria) to larger organisms (autotrophic pico- and nanoplankton). In our experiment, although non-significant differences were observed in bacterial abundance between still and turbulent containers in all the treatments, a higher bacterial abundance was observed under turbulence during the last days of the experiment in NP containers (Fig. 2). This difference was not due to a higher activity of bacteria under turbulence because the specific leucine uptake rates were higher in the still than in the turbulent containers (data not shown). This finding could indicate that top-down interactions dominated bacterial population dynamics during the last days. Peters et al. (2002) found that turbulence increased the heterotrophy in the system, and again argued in favour of a biomass shift to larger heterotrophic components through changes in grazing interactions. However, in terms of nutrient conditions, there are some fundamental differences between those studies and the one described in this paper. We added a relatively high single pulse of nutrients at the beginning of the experiment while no nutrients or low daily nutrient pulses were added in Peters et al. (1998) and (2002), respectively. In this study, the addition of nutrients allowed turbulence to favour large phytoplankton species, while in our previous studies phytoplankton was dominated by pico- and nanoautotrophs.

Phytoplankton size distribution and composition

As expected, the average size of phytoplankton cells was higher under turbulence. This result agrees with theoretical approaches (Lazier & Mann 1989, Karp-Boss et al. 1996) which concluded that the beneficial effect of turbulence on the nutrient flux to the cells increases with cell size. In our

experiments, this differential benefit among sizes was clear, especially in NP treatments. Diatoms were the main component of the highest size fraction observed (> 50 µm) and, within this group, cells from two genera (*Chaetoceros* and *Pseudo-nitzschia*) were the most abundant. These species form chains and could benefit from turbulence and nutrient-rich situations by increasing their advective transport of nutrients or increasing their total length (Pahlow et al. 1997). In turbulence treatments, the chain-length of *Chaetoceros* spp. and *Pseudo-nitzschia* spp. was larger than in still treatments (data not shown). The dominance of diatoms in the turbulent conditions agrees with existing theory (Margalef 1978) and with results from previous experiments (Estrada et al. 1987).

It is also remarkable to note the different responses in still waters depending on nutrient enrichment. We found a much lower diatom contribution to the total phytoplankton biomass in the NP (nutrient balance) than in the N-surplus (P deficient) containers (Fig. 6). These results are in contrast to the findings of Egge (1998) who found that diatoms (in terms of abundance) did not dominate when P was deficient. In our experiment, when the contribution of diatoms is expressed in terms of abundance, the differences between the two still enrichment treatments (N and NP) were smaller (5.5 to 7.7 % and 0.4 to 6.9 %, respectively), but the higher percentages in the N treatment persisted. In contrast, under turbulent conditions, we found a higher diatom:total phytoplankton ratio in the NP than in the N treatments (40 vs. 11 %) on Day 4. The experiments in Egge (1998) were performed in mesocosms in which airlifts were used, therefore producing unquantified turbulence. Thus, Egge's results could be more similar to our turbulence treatment. The species-specific response to nutrient addition should be further studied under different hydrodynamic conditions in order to better understand the competition interactions for nutrient resources among different life-forms.

Several authors have pointed out both bottom-up and top-down effects of turbulence on marine planktonic communities. Bottom-up effects may favour nutrient flux to big cells (Karp-Boss et al. 1996) and top-down effects may increase encounter probability between predators and prey (Rothschild & Osborn 1988, Marrasé et al. 1990, Sundby & Fossum 1990), or influence predator behaviour (Costello et al. 1990, Saiz & Kiørboe 1995, Peters et al. 1998). The combination of these effects rarely compensate each other and turbulence drives the system, at least temporarily, to a different state in relation to still conditions. As shown here, the magnitude and duration of the changes induced by turbulence depend on initial nutrient conditions. Given that turbulence modifies the response of plankton to nutrients, it can be concluded that parameterisations of biological processes (e.g. nutrient uptake and grazing rates) to be used in predictive models should be derived from studies in which the hydrodynamic conditions are considered.

ACKNOWLEDGEMENTS

We are grateful to captain Elías Barrenechea and the staff at the Masnou harbour for letting us use their boat and helping us with sampling. We thank Mercedes Castaño for laboratory assistance, Roser Ventosa for nutrient analysis and Oscar Guadayol for calculation of turbulence intensities in the NW Mediterranean. Marta Estrada provided helpful comments on the manuscript. The comments and suggestions by three anonymous reviewers greatly improved previous versions of the manuscript. Aisling Metcalfe was of great help editing the English. This work was supported by the European projects NTAP (EVK3-CT-2000-00022) and BIOHAB (EVK3-CT99-00015), and the Spanish CICYT project (MAR 98-0854). This is ELOISE contribution Nº 277/40.

Phytoplankton size distribution and growth rates in the Alboran Sea (SW Mediterranean): short-term variability related to mesoscale hydrodynamics

ABSTRACT

The short-term variability of the size distribution and growth rates of the phytoplankton community was studied during several visits at three stations located across the anticyclonic gyre of the Western Alboran Sea in May 1998. Chlorophyll *a* (chl *a*) concentration, was fractionated in three size classes, picoplankton (< 2 µm), nanoplankton (2 - 20 µm) and microplankton (> 20 µm). Biovolume and cell carbon estimations, based on cell cytometry and microscopy counts, image analysis and published conversion values, were carried out for seven groups of autotrophic organisms. Carbon:chlorophyll *a* (C:chl *a*) ratios in combination with ^{14}C uptake experiments were used to calculate phytoplankton growth rates. Temporal differences among stations in the size structure and composition of the phytoplankton community were related to hydrographic phenomena. At the beginning of the survey, the proportion of the three chlorophyll size fractions ranged between 20 and 40 % for all the stations; this situation changed dramatically after a nutrient upwelling event which occurred at the station closest to the coast, located at the northern edge of the anticyclonic gyre, and was associated with an increase of the biomass of the whole phytoplankton community (mainly due to diatoms) and with a shift of the microplankton proportion from 35 to 60 % of the integrated chl *a*. In contrast, the pico- and nanoplankton fractions increased their dominance in the oligotrophic waters of the centre of the gyre (between 75 and 95 % of the integrated total chl *a*, mainly accounted for by *Synechococcus* and small flagellates). At all the stations, picoplanktonic cells were generally more abundant in the upper layers of the photic zone while nano- and microplanktonic organisms tended to be more important with depth. Maximum phytoplankton growth rates ranged from 0.45 to 1.41 d^{-1} and did not present significant differences among stations, in spite of their different hydrographic and nutrient conditions. In particular, average duplication times of 0.9 d at the oligotrophic central station indicate that phytoplankton was actively growing there. Growth rates averaged for the photic layer were not associated to the phytoplankton composition and size distribution but were positively correlated with the available irradiance. These findings suggest a physiological acclimation of the phytoplankton community to the light conditions and may be relevant for the parameterisation of primary production models. The C:chl *a* ratio decreased with depth an increased from high to low nutrient stations and with the fraction size.

INTRODUCTION

The size distribution of the phytoplankton community plays an important role in the carbon cycle and food web dynamics of marine environments (Legendre & Le Fèvre 1991). In turn, the physical and chemical characteristics of a given ecosystem are key factors controlling this size distribution (Parsons & Takahashi 1973, Margalef 1974, Turpin & Harrison 1980, Rodríguez et al. 2001). The accepted paradigm states that the microbial food web predominates in stratified, oligotrophic waters (Azam et al. 1983), in which small autotrophic organisms are comparatively more abundant than other size classes of phytoplankton. In contrast, in turbulent and richer areas, larger size-fractions tend to prevail sustaining the so-called "classical" or "herbivorous" food web (Steele 1974). These extreme situations are, however, simplifications of a more complex scenario, with a continuous functioning of the microbial food web and intermittent departures to the herbivorous food webs when nutrients are injected into the upper layers of the water column (Thingstad & Sakshaug 1990).

The phytoplankton size distribution is commonly described in terms of chlorophyll *a* (e. g. Takahashi & Bienfang 1983) or carbon (e. g. Booth 1988). In the latter case, the cellular volumes of different phytoplanktonic groups are converted to carbon units using reported or empirically determined carbon:volume ratios. Fixed phytoplanktonic carbon to chlorophyll *a* ratios (C:chl *a*) are frequently used to convert the routine measurements of chl *a* into carbon whenever an estimate of algal carbon is needed. C:chl *a* ratios are also used in combination with ^{14}C uptake experiments to calculate phytoplankton growth rates (μ), as an alternative to dilution experiments (Landry & Hassett 1982). However, C:chl *a* ratios are far from constant depending on environmental conditions such as nutrient concentrations, irradiance or temperature (see Geider et al. 1997 and references therein).

The remarkable hydrodynamism found in the Alboran Sea (SW Mediterranean) offers a good scenario to study mesoscale variations of the size structure of the phytoplankton assemblages. This region is characterized by the presence of two quasi-persistent anticyclonic gyres: the Western and Eastern Alboran Sea gyres (Parrilla & Kinder 1985, Minas et al. 1991, Tintoré et al. 1991). These gyres are formed by the superficial inflow of Atlantic waters which enter the Strait of Gibraltar and, upon mixing with the resident Mediterranean waters, form a conspicuous jet of Modified Atlantic Water (MAW). At the frontal zone created around the northern edge of the Western anticyclonic gyre, intermittent upwelling events bring nutrients into the upper layers of the water column (Coste et al. 1988, Packard et al. 1988, Perkins et al. 1990, Minas et al. 1991), in contrast with the more oligotrophic waters found at the centre of the gyre.

In the Eastern Alboran Sea anticyclonic gyre, Videau et al. (1994) found higher phytoplankton cell-sizes in the frontal zone than in the centre of the gyre. In accordance with this observation we would expect the same general trend in the Western Alboran Sea gyre, where information on phytoplankton size structure is only available in relationship with the deep fluorescence maximum (Rodríguez et al. 1998) or with the magnitude of vertical motion (Rodríguez et al. 2001). Owing to the episodic nature of the upwelling phenomena in the frontal zone, notable changes in the phytoplankton size structure could occur on a scale of days, as found by Rodríguez et al. (1994). The effect of these nutrient pulses on algal growth rates has not been addressed by the few primary production surveys carried out in this sub-basin (see references in Morán & Estrada 2001) and is therefore unknown. Information on phytoplankton growth rates is also scarce for other Mediterranean regions. Estrada (1985) and Pedrós-Alió et al. (1999) reported estimates in the NW Mediterranean in summer, while other authors focused on populations of particular organisms such as *Synechococcus* (Agawin et al. 1998, 2000) or *Gyrodinium* (Garcés et al. 1999).

The study of the short-term variability in the physico-chemical and biological properties of the Western Alboran Sea was the objective of a High Frecuency Flux Experiment carried out in May 1998. In this context, the specific aims of the study presented here were (1) to describe the small-scale geographical and temporal variation of the size structure and composition of the phytoplankton community at different stations located across the anticyclonic gyre, (2) to estimate the variability of the C:chl *a* ratio of the various phytoplankton size fractions in the studied coastal-offshore gradient, and (3) to test whether the size structure of the natural phytoplankton assemblages could be related to their ambient and maximum growth rates.

MATERIAL AND METHODS

Sampling

This study was performed during Leg 2 of the R/V *Hespérides* cruise MATER I, carried out in the Alboran Sea between 2 and 16 May, 1998. Three fixed stations (A, B and C), located across the Western Alboran Sea anticyclonic gyre, were visited four times (visits 1 to 4) during the cruise, with an interval of 3 days between visits (Fig.1, Table 1). CTD casts were performed at each station to obtain profiles of temperature, salinity, fluorescence and density (sigma-t). Different subsamples for major inorganic nutrients analysis, total and fractionated chlorophyll *a* (chl *a*) determination and enumeration of diatoms, dinoflagellates, coccolithophorids, autotrophic nanoflagellates, autotrophic picoeukaryotes, *Synechococcus* and *Prochlorococcus* were obtained with Niskin bottles attached at a rosette and closed at selected levels, generally at 10 - 20 m intervals, from the surface down to

100 m depth.

Sample treatment

Nutrient samples were frozen prior to their analysis in the laboratory. Soluble reactive phosphate, nitrate, nitrite, ammonium and silicate concentrations were analyzed using an Evolution II (Alliance Instruments) autoanalyzer (Grasshoff et al. 1983).

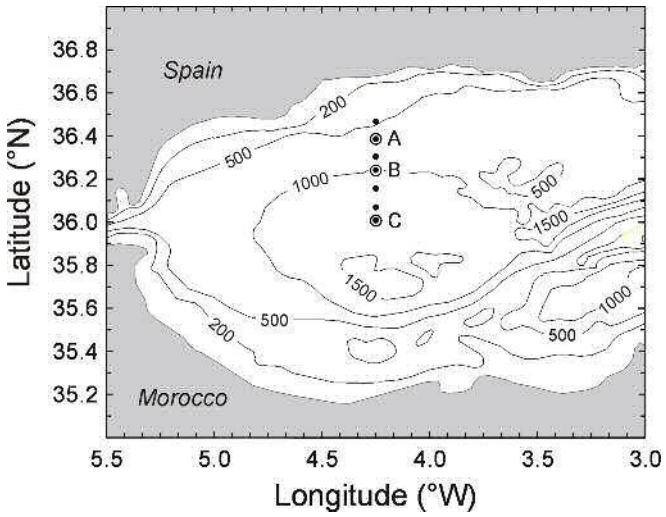

Fig. 1 – Location of the stations sampled (A, B and C) along a transect crossing the northern part of the Western Alboran Sea anticyclonic gyre.

Table 1 – Date and sampling times of the four visits to the sampled stations.

Station	Visit	Date (1998)	Time (GMT)
A	A1	02/05	09:40
	A2	05/05	09:30
	A3	08/05	11:50
	A4	11/05	08:00
B	B1	03/05	09:08
	B2	06/05	09:40
	B3	09/05	09:40
	B4	12/05	08:40
C	C1	04/05	10:00
	C2	07/05	09:05
	C3	10/05	08:10
	C4	13/05	10:15

Chl *a* concentrations (total and fractionated) were measured on board by fluorometry (Yentsch & Menzel 1963). From each depth, 100 ml of water were filtered through Whatman GF/F glass fiber filters (25 mm diameter) for total chl *a* estimation. Parallel samples of 200 and 100 ml of water were filtered, respectively, through polycarbonate 2 µm PORETICS filters (47 mm) and 20 µm mesh net, and the filtrates were collected onto Whatman GF/F filters (25 mm). Therefore, the picoplanktonic chl *a* fraction (< 2 µm) was measured directly, and the nano- and microplankton (2 - 20 µm and > 20 µm, respectively) contributions were calculated by subtracting the < 2 µm from the < 20 µm fraction and the < 20 µm from the total, respectively. All the filtrations were done at low vacuum pressure (< 100 mm Hg) or by gravity (when using 20 µm mesh net) and after the filtrations the GF/F filters were frozen immediately at - 70 ^{o}C for at least 5 hours. The filters were placed subsequently in 6 ml of 90 % acetone for approximately 24 h, in the dark and at 4 ^{o}C. The fluorescence of the extract was measured with a Turner-Designs fluorometer.

Different techniques (Utermöhl-inverted microscopy, epifluorescence microscopy and flow cytometry) were used to quantify the autotrophic organisms according to their size and abundance (García et al. 1994). Subsamples of 120 ml of water for diatom, dinoflagellate and coccolithophorid counts were fixed with formalin-hexamine solution (0.4 % final concentration, Throndsen 1978) and stored in Pyrex bottles. Within a year from sampling, 100 ml of water were sedimented in a composite chamber and examined using the inverted microscope technique (Utermöhl 1958). One transect of the chamber was observed at 400x magnification to enumerate the smaller (< 25 µm) and more abundant organisms. Half of the chamber was additionally observed at 200x to count cells of intermediate size (generally between 25 and 50 µm) and all the chamber was scanned at 200x to count the larger forms. The observed organisms (mainly diatoms, dinoflagellates and coccolithophorids) were classified to the lowest possible taxonomic level.

Samples for nanoflagellate counts (90 ml) were fixed with 10 ml glutaraldehyde (0.5 %, final concentration). On board, a subsample of 40 ml was filtered through 0.6 µm NUCLEPORE black polycarbonate filters and stained with DAPI (1 µg ml^{-1}, final concentration), the filters were then placed on glass slides with a drop of fluorescence oil and a coverslip and kept at - 20 ^{o}C. Autotrophic nanoflagellates were counted with an epifluorescence microscope (Porter & Feig 1980) and sorted into 3 size classes (3.2 - 6.4 µm, 6.4 - 12.8 µm, > 12.8 µm). A mean volume of each size class was used for the biovolume calculations of these organisms. Autotrophic flagellates < 3.2 µm (= autotrophic picoeukaryotes) were analyzed by flow cytometry.

For the flow cytometric enumeration of autotrophic picoeukaryotes and cyanobacteria (*Synechococcus* and *Prochlorococcus*), 1.5 ml samples, fixed with 1% paraformaldehyde + 0.05 %

glutaraldehyde (final concentration), were kept at room temperature during 10 minutes and subsequently deep frozen in liquid nitrogen and stored frozen at - 70 ^{o}C. The samples were then thawed and processed through a flow cytometer FACS-calibur (Becton and Dickinson) with a laser emitting at 488 nm (Gasol & del Giorgio 2000). Samples were run at high speed (approx. 60 µl min^{-1}) and data were acquired in log mode until around 10000 events had been recorded. As an internal standard, we added 10 µl per 600 µl sample of a 10^5 ml^{-1} solution of yellow-green 0.92 Polysciences latex beads. *Synechococcus* cells were detected by their signature in a plot of orange fluorescence (FL2) vs. red fluorescence (FL3). *Prochlorococcus* have a lower FL3 signal and no FL2 signal. Autotrophic picoeukaryotes have higher FL3 signals and no FL2 signal.

Biomass estimates

Autotrophic biomass was estimated for samples taken during the second and fourth visits to each station.

The biovolumes of *Synechococcus* and picoeukaryotes were calculated using the volume values given in Ribes et al. (1999) for samples from the Northwestern Mediterranean Sea. A carbon content of 0.357 pg C μm^{-3} (mean value of Bjørnsen 1986, Kana & Gilbert 1987 and Verity et al. 1992) was used for *Synechococcus*, and the equation pg C $cell^{-1}$ = 0.433 x $(\mu m^3)^{0.863}$ (Verity et al. 1992) was adopted for autotrophic picoeukaryotes. For *Prochloroccocus*, volume calculations were based on a mean size (diameter) of 0.7 µm (Vaulot et al. 1990) and the carbon convertion factor used was 0.133 pg C μm^{-3} (Simon & Azam 1989).

Cell volume of autotrophic nanoflagellates was calculated using the mean dimensions of each size class and assuming an ellipsoid shape for the cells. The carbon conversion equation was the same as for picoeukaryotes.

For diatom, dinoflagellate and coccolithophorid biomass estimation, once a sample had been counted, half of the chamber was observed at 400x, and at least 20 individuals of the most abundant forms were recorded with a video camera Hitachi KPC503. Then, each organism was measured (length and width) using NIH-Image software and its volume calculated using a geometrical approximation of its form. Carbon content was estimated from the conversion factor described in Montagnes et al. (1994, pg C $cell^{-1}$ = 0.109 x $(\mu m^3)^{0.991}$).

Growth rates

Carbon-based ambient growth rates (μ, in units d^{-1}) of phytoplankton during the second and fourth visits were calculated from daily primary production rates (PP) and phytoplankton carbon biomass (PB), obtained from Chl *a* concentrations and the corresponding C:chl *a* ratios. PP was estimated from photosynthesis-irradiance relationships, chl *a* distributions and daily irradiance throughout the water column (see details in Morán & Estrada 2001). Apart from ambient growth rates (μ) at each station, a weighted growth rate for the photic layer ($\mu_{ph\text{-}l}$) was estimated. The depth of the photic layer was defined as that receiving 1 % of the surface incident irradiance, and ranged from 42 m at A4 (fourth visit to station A) to 63 m at C4 (fourth visit to station C).

Maximum growth rates (μ_{max}) were also estimated for the two depths from which samples processed in the photosynthesis-irradiance experiments were taken (Morán & Estrada 2001). μ_{max} was estimated from the hourly maximum photosynthetic rate P^B_m, given in units mg C (mg chl *a*)$^{-1}$ h^{-1}, and a daily photoperiod of 13 h, according to the equation:

$$\mu_{max} = \ln [1 + (13P^B_m / \text{C:chl } a)]$$

RESULTS

Hydrography

The temperature and salinity distribution along the three stations (A, B and C) for the four visits is represented in Figure 2. Shallowing temperature and salinity isolines were observed from station C to A, reflecting the position of the front formed by the jet of MAW and coastal Mediterranean waters. The steeper temperature and salinity isolines during the second visit indicated the occurrence of an upwelling event which affected mainly station A but to some extent also station B. For more details on the hydrography of this zone during the survey see Morán & Estrada (2001).

Nutrients and total chl a distribution

A general decrease in surface nutrient concentrations was observed from the coastalmost station towards the centre of the gyre (Fig. 3). The upwelling event which occurred during the cruise brought high nutrient concentrations into the upper layers of the water column, causing a notable shallowing of the nitrate and phosphate nutriclines (Fig. 3, see also Table 1 in Morán & Estrada, 2001). Station C was homogeneously nutrient-depleted in the upper 100 m along visits.

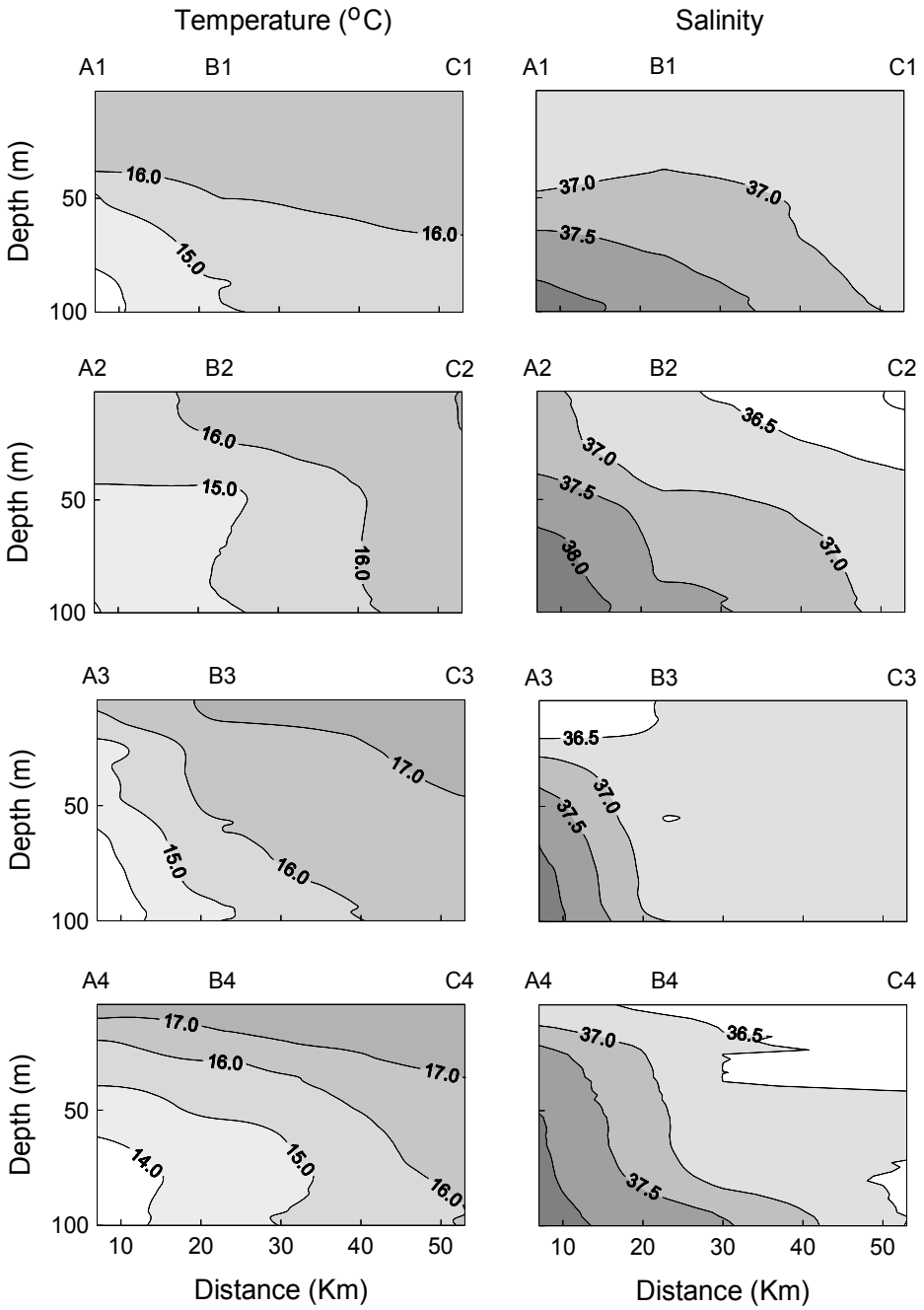

Fig. 2 – Temperature (°C) and salinity distribution across the surveyed transect during the four visits.

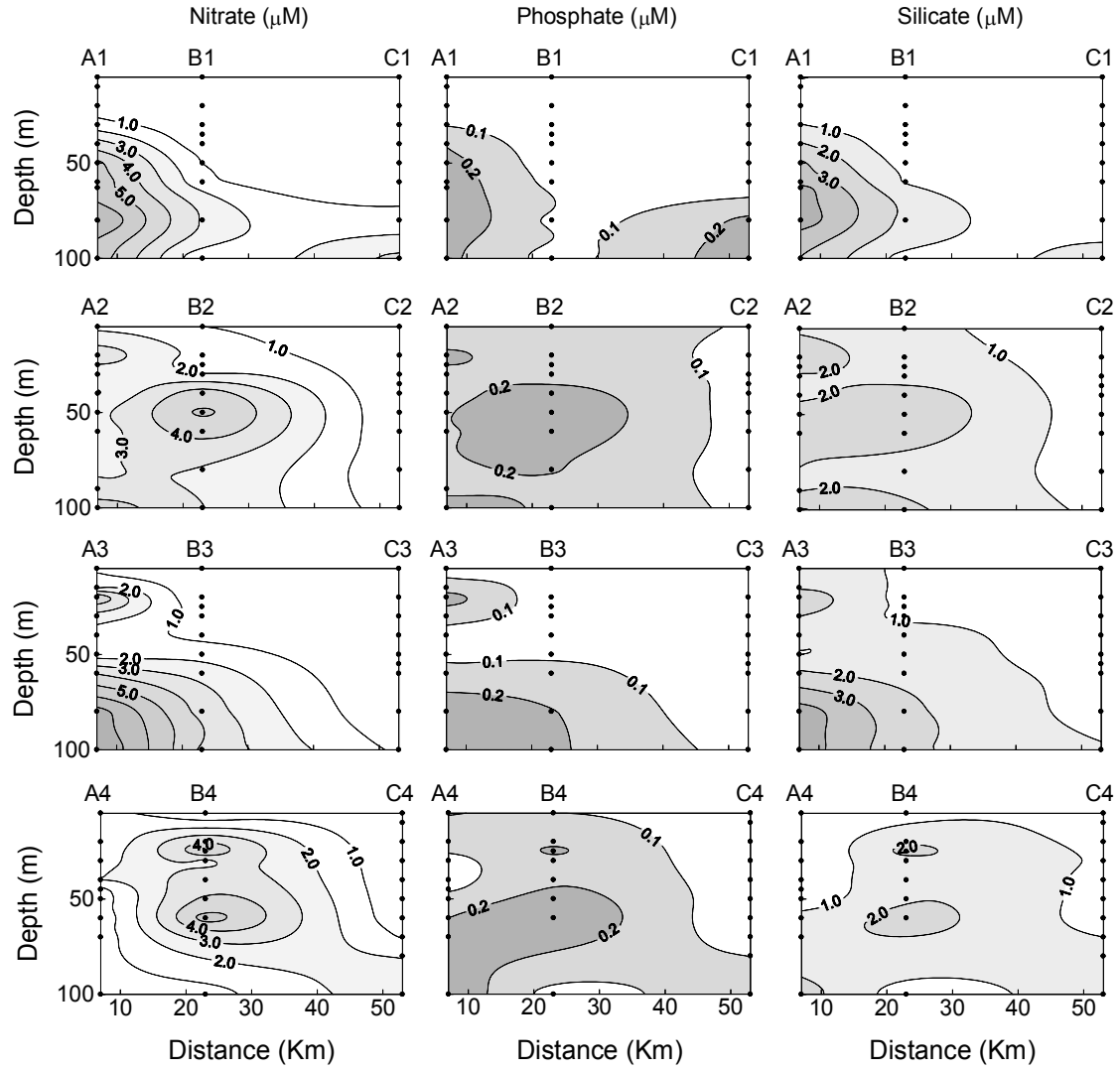

Fig. 3 – Nitrate, phosphate and silicate (all in μM) concentrations across the surveyed transect during the four visits.

The nutrient injection into the upper layers of station A was followed by an increase of chl *a* from a maximum value of 1.3 μg l^{-1} in the first visit to 7.9 μg l^{-1} in the third one (Fig. 4). A pronounced deep chlorophyll maximum (DCM), with chl *a* exceeding 5 μg l^{-1}, was observed at around 40 m depth in the last two visits to this station.

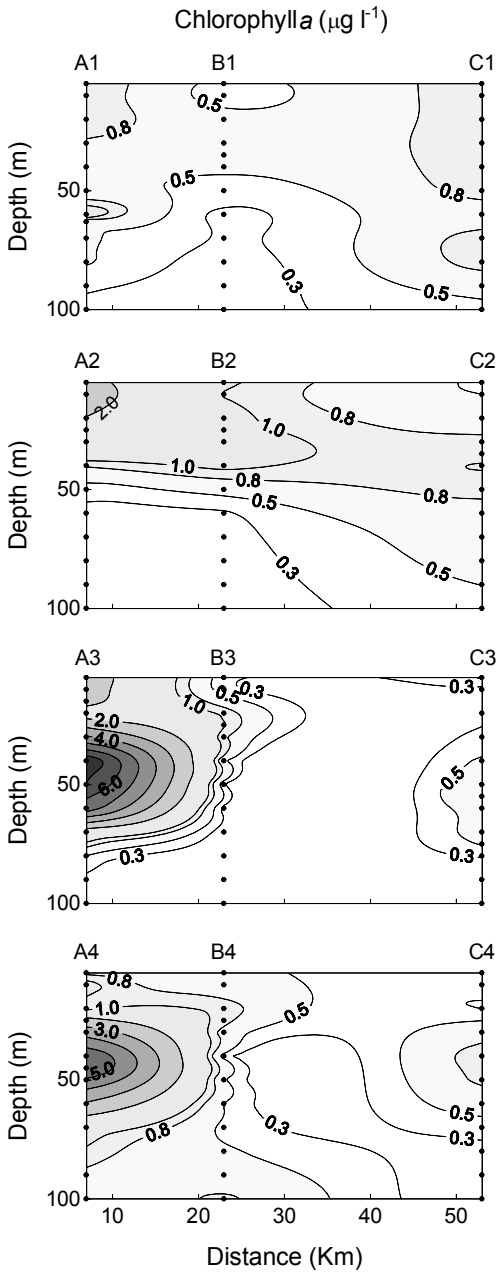

Fig. 4 – Chlorophyll *a* (μg l^{-1}) concentration across the surveyed transect during the different visits.

The DCM was shallower at station B (~20 m), with values below 1 μg l^{-1} except in the second visit. The lowest chl *a* values (always <1 μg l^{-1}) were found at station C and did not show any appreciable DCM structure.

Fractionated chl a distribution

When chl *a* values were integrated for the photic zone, a higher percentage of the larger size fractions (nano- and microplankton) was observed at station A (Fig. 5). At this station, a shift from nano- to microplankton dominance occurred when total chl *a* increased in the third visit, with microplankton chl *a* making up almost 60 % of integrated values.

At station B, nanoplankton formed the highest share of integrated total chl *a* (ca. 40 %) followed (except in the first visit) by picoplankton (between 25 and 40 %). The contribution of picoplankton to total autotrophic biomass was highest at station C, where it increased smoothly from the first (38 %) to the last visit (51 %). At stations B and C the microplankton contribution was always less than 35 % and it decreased steadily with time along visits.

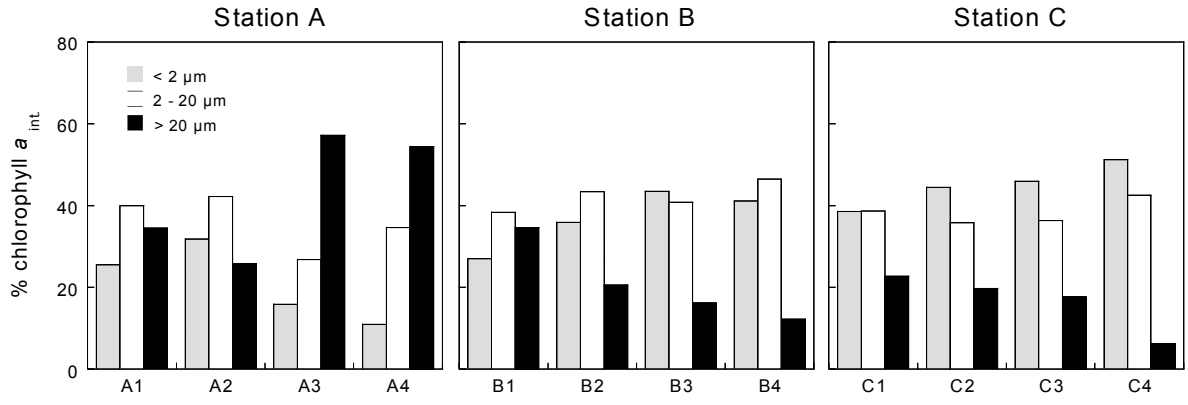

Fig. 5 – Variability of the contribution (%) of picoplankton (< 2 µm), nanoplankton (2 - 20 µm) and microplankton (> 20 µm) size-fractions to integrated total chlorophyll *a* at stations A, B and C.

The relative abundance of the different chl *a* size fractions changed throughout the photic zone (Fig. 6). Higher contributions of picoplankton were generally observed in the upper layers of the water column at the three stations, while nano- and microplankton were, in general, more abundant at deeper layers. In the third and fourth visits, the contribution of chl *a* > 20 µm reached 70 % at the DCM of station A.

For pooled data, the percentage of chl *a* < 2 µm was positively correlated with the percentage of ammonium and negatively correlated with the percentage of nitrate, while the relationships with the percentage of the fractions of chl *a* > 2 µm were of opposite sign (Table 2).

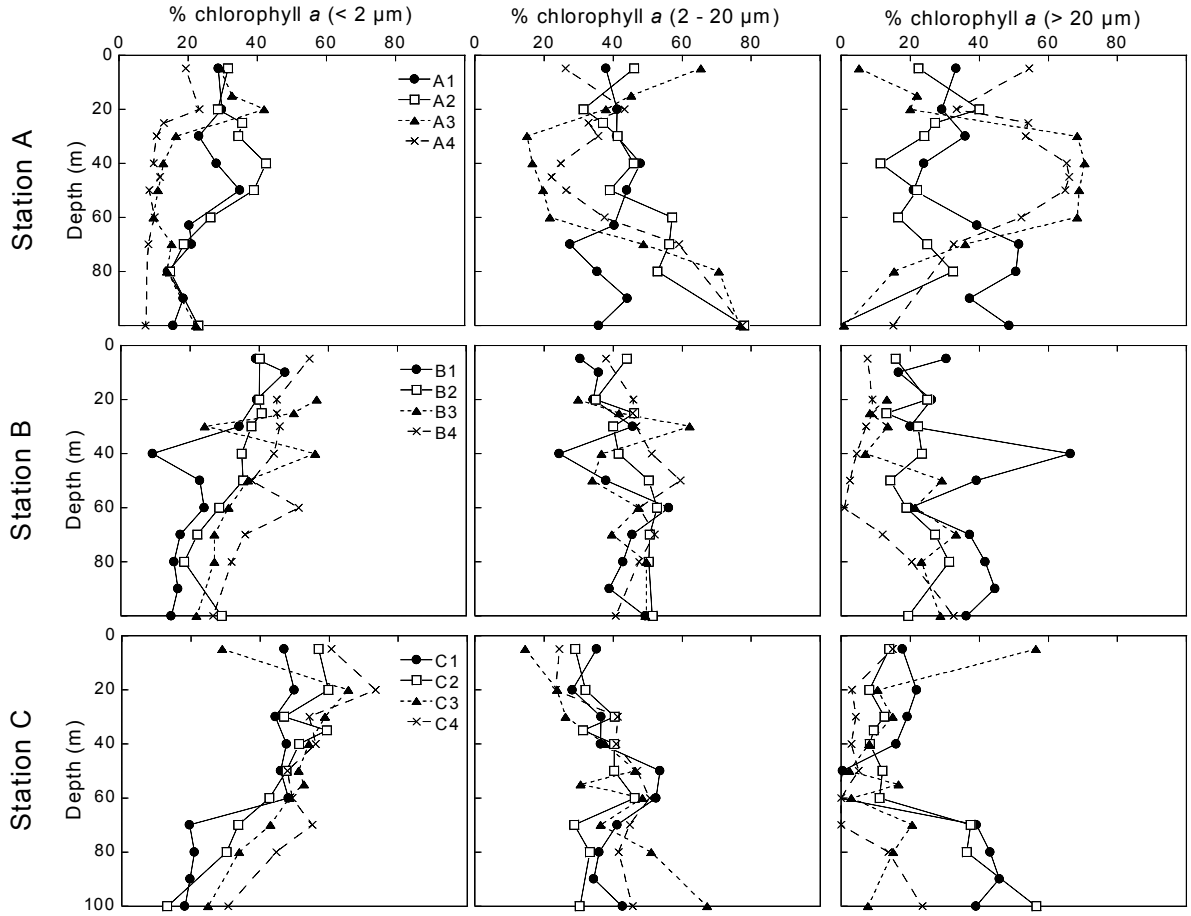

Fig. 6 – Vertical distribution of the percentage of the three size fractions (< 2 µm, 2 - 20 µm and > 20 µm) to total chlorophyll *a* at the three sampled stations.

Phytoplankton size distribution and group composition

A conspicuous shift in the composition of the phytoplankton community was observed at station A between the second (A2) and the fourth (A4) visits (Fig. 7). At A2, the bulk of autotrophic biomass was found between 5 and 20 m with a predominance of autotrophic nanoflagellates (which reached a maximum of 62 % of the total biomass at 20 m depth). Coccolithophorids and picoeukaryotes also contributed appreciably (around 5 µg C l^{-1} each) to autotrophic biomass at these depths. From 40 m downwards, total autotrophic biomass was lower than 8 µg C l^{-1}. In contrast, at A4, a very high contribution of diatoms (mainly from the genus *Chaetoceros* and *Pseudo-nitzschia*) appeared at the

DCM level attaining as much as 64 % of total autotrophic biomass.

Total autotrophic biomass decreased with depth in the two visits to station B. The maximum value (ca. 25 µg C l^{-1}) was observed at 5 m, and no group clearly prevailed. At stations A and B, *Prochlorococcus* biomass generally decreased with depth and did not exceed 0.12 µg C l^{-1}.

Table 2 – Correlation coefficients between the percentage of ammonium, nitrite and nitrate to total dissolved inorganic nitrogen and the percentage of chl *a* < 2 µm, 2 - 20 µm and > 20 µm to total chl *a* for pooled data. * $p < 0.05$; ** $p < 0.01$; n = 102

	% chl *a* < 2 µm	% chl *a* 2 - 20 µm	% chl *a* > 20 µm
% Ammonium	0.58**	- 0.27**	- 0.31**
% Nitrite	0.09	- 0.10	0.05
% Nitrate	- 0.51**	0.26**	0.25*

An increase in the contribution of *Synechococcus* to total biomass was the main difference observed at station C with respect to the other two stations. In the second visit (C2), the contribution of *Synechococcus* varied between 29 and 42 % at depths above 40 m. Below this depth, the observed increase in total biomass was due to the presence of large diatoms (mainly *Guinardia striata* and *Proboscia alata*). Although these diatoms corresponded to less than 0.02 % of the total abundance of photosynthetic cells (data not shown), their relative carbon contribution was up to 84 %, due to their high mean volume per cell (Table 3). In the fourth visit (C4), the contribution of *Synechococcus* biomass was highest at 20 m depth (68 % of the total) while a high proportion of nanoflagellates was observed at 40 m. *Prochlorococcus* was not detected at this station.

Total and fractionated C:chl a ratios

A C:chl *a* ratio was calculated for three layers of the water column (above 30 m, between 30 and 70 m, and below 70 m depth) for total autotrophic biomass and for the < 2 and > 2 µm size fractions (Table 4). This C:chl *a* ratio was generally highest above 30 m depth; below this depth, it tended to increase with size fraction. When all data were considered, the C:chl *a* ratio of the < 2 µm fraction was negatively correlated with depth ($r = -0.5$, $p = 0.003$, n = 33).

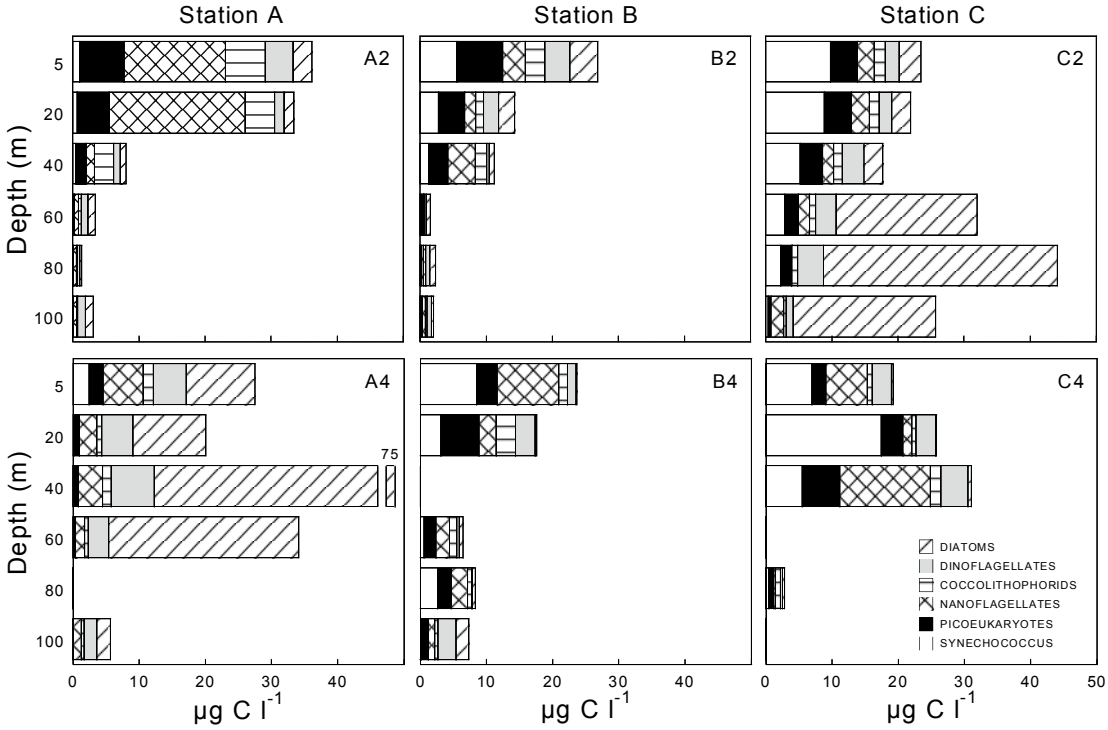

Fig. 7 – Vertical distribution of the biomass (µg C l^{-1}) of the different phytoplankton groups (except *Prochlorococcus*, see text) considered during the second and fourth visits at the three stations. No samples were available for A4 - 80 m, B4 - 40 m and C4 - 60 and 100 m.

A consistent increase of the C:chl *a* ratio was also observed from high-nutrient to low-nutrient stations. Thus, it was 60 %, 75 %, and 53 % higher at station C than at station A, for the total, < 2 µm and > 2 µm fractions, respectively. This trend was further corroborated by the negative correlation found between the C:chl *a* ratio (total and both fractions) and nutrient concentrations (Table 5).

Phytoplankton growth rates

As expected, estimated ambient phytoplankton growth rates (µ) decreased with depth reflecting the decrease in available irradiance (Fig. 8). Phytoplankton was growing at relatively high growth rates (~1 doubling d^{-1}) at the surface of the three stations during the second visit. In general, µ was higher at station B than at the other two stations, although algal biomass was highest at station A (Fig. 4).

Table 3. Average ± SE of the mean volume per organism (μm^3) of nanoflagellates, coccolithophorids, diatoms and dinoflagellates for the second and fourth visits to the three stations.

Station	Nanoflagellates	Coccolithophorids	Diatoms	Dinoflagellates
A2	68 ± 10	482 ± 3	5967 ± 1791	22478 ± 17840
A4	124 ± 38	485 ± 7	5756 ± 1453	6844 ± 1068
B2	48 ± 10	339 ± 5	5597 ± 1503	3778 ± 722
B4	79 ± 24	334 ± 2	6301 ± 3619	14270 ± 9919
C2	77 ± 20	259 ± 0.4	105960 ± 29573	5827 ± 609
C4	109 ± 32	270 ± 7	21925 ± 13172	12981 ± 3296

Table 4 – Average C:chl *a* ratio (± SE) for three layers of the water column (above 30 m, between 30 and 70 m and below 70 m) at the three stations, for the whole phytoplankton community (Total) and two size fractions (< 2 µm and > 2 µm).

		Total	< 2 µm	> 2 µm
St. A	Above 30m	24 ± 5	15 ± 6	27 ± 5
	30 – 70 m	12 ± 1	3 ± 1	25 ± 1
	Below 70 m	11 ± 4	2 ± 0.4	13 ± 5
St. B	Above 30 m	24 ± 6	25 ± 5	24 ± 7
	30 – 70 m	8 ± 3	7 ± 3	13 ± 2
	Below 70 m	11 ± 2	11 ± 5	11 ± 1
St. C	Above 30 m	59 ± 11	59 ± 14	57 ± 7
	30 – 70 m	33 ± 9	19 ± 1	47 ± 16
	Below 70 m	48 ± 19	15 ± 4	58 ± 25

Table 5 – Correlation coefficients between total and two size fractionated C:chl *a* ratios and nutrient concentrations for pooled data. DIN: dissolved inorganic nitrogen; * $p < 0.05$; ** $p < 0.01$; n = 31

	Total C:chl *a*	< 2 µm C:chl *a*	> 2 µm C:chl *a*
Phosphate	- 0.66**	- 0.55**	- 0.65**
DIN	- 0. 59**	- 0.49**	- 0.59**
Silicate	- 0.54**	- 0.42*	- 0.55**

Station C tended to give the lowest µ values, especially during the fourth visit (C4). Photic layer-weighted values ($\mu_{ph\text{-}l}$) ranged between 0.03 and 0.44 d^{-1} and were significantly higher during the second visit (*t*-test, $p = 0.005$), but no significant differences were found between stations. Ambient growth rates were always lower than maximum ones (μ_{max}), which ranged from 0.45 to 1.41 d^{-1} (Table 6). No differences in maximum growth rates were observed either for visits or sampling depth (ANOVA, $p > 0.2$). The size distribution and the composition of phytoplankton did not appear to be correlated with growth rates. Thus, no relationship was found between μ_{max} or $\mu_{ph\text{-}l}$ and the absolute or relative values of the different chl *a* size classes. However, a positive correlation ($r = 0.71$, $p = 0.01$, $n = 12$) was found between μ_{max} and the percentage of picoeukaryotic carbon (i.e. small flagellates as counted with the flow cytometer).

The extremely low ambient growth rates measured at station C4 were undoubtedly related to the low irradiance received due to cloudy conditions (Fig. 9), as μ_{max} did not differ appreciably from the values found at the other two stations (Table 6). Similarly, the notably lower values of the photic layer-weighted growth rates ($\mu_{ph\text{-}l}$) during the fourth visit at the three stations were mainly caused by the comparatively lower irradiance received (Fig. 9). Although averaged C:chl *a* ratios changed notably during the two visits (approximately 1.5 higher in the fourth visit, Table 6), the negative relationship between $\mu_{ph\text{-}l}$ and the C:chl *a* ratio was not significant ($p = 0.15$).

DISCUSSION

The nutrient enrichment into the upper layers of the northern edge of the Western Alboran Sea anticyclonic gyre determined a strong gradient of autotrophic biomass, from high chl *a* values at the coastalmost station to low values in the nutrient-poor waters of the centre of the gyre (St. C, Fig 3). Similar observations have been reported in other studies (Packard et al. 1988, Minas et al. 1991) in the same area of the Alboran Sea.

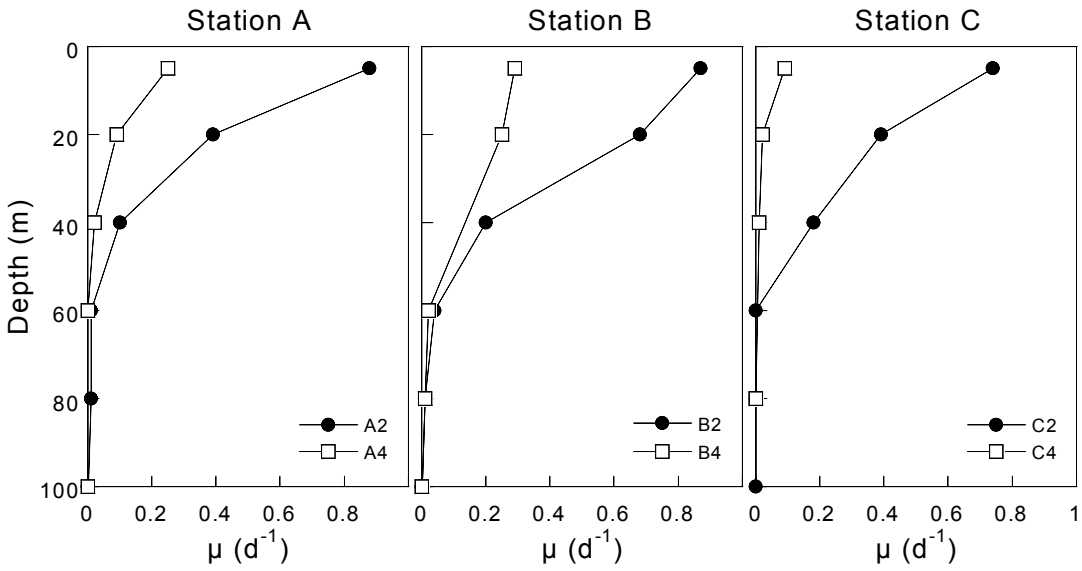

Fig. 8 - Vertical distribution of phytoplankton ambient growth rates (μ) at the three stations during visits 2 and 4.

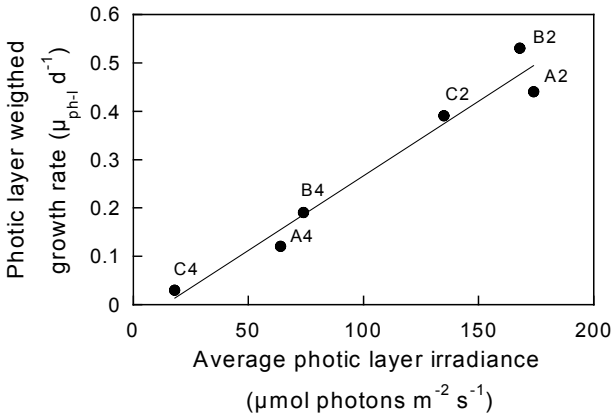

Fig. 9 - Relationship between photic layer weighted phytoplankton growth rates ($\mu_{ph\text{-}l}$) and average daily irradiance received in the photic layer ($E_{ph\text{-}l}$). Linear regression: $\mu_{ph\text{-}l}$ = -0.042 + 0.0031 $E_{ph\text{-}l}$; r^2 = 0.98, p = 0.001, n = 6.

Table 6 - Photic layer-weighted ($\mu_{ph\text{-}l}$) and maximum (μ_{max}) growth rates in visits 2 and 4 to the three stations. The depth of the photic layer ($Z_{ph\text{-}l}$) and the weighted C:Chl *a* ratio (C:Chl $a_{ph\text{-}l}$) is also given. μ_{max} was calculated for the two depths of photosynthesis-irradiance experiments (see the text for details), indicated in a separate column ($Z_{P\text{-}E}$).

Station	$Z_{ph\text{-}l}$ (m)	C:Chl $a_{ph\text{-}l}$	$\mu_{ph\text{-}l}$ (d^{-1})	μ_{max} (d^{-1})	$Z_{P\text{-}E}$ (m)
A2	43	14.7	0.44	0.87	25
				0.54	50
B2	50	14.8	0.53	1.41	25
				1.25	50
C2	49	35.7	0.39	1.04	35
				0.56	50
A4	42	24.4	0.12	0.59	5
				0.69	45
B4	55	22.2	0.19	0.45	5
				1.11	25
C4	63	50.5	0.03	0.91	5
				0.60	50

The high autotrophic biomass observed in the fourth visit to station A was caused by an increased contribution of the nano- and microplankton fractions (Fig. 4), which corresponded mainly to chain-forming diatoms of genus *Chaetoceros* spp and *Pseudo-nitzschia* spp (Fig. 7). The vertical motion produced by the upwelling and the associated introduction of nutrients into the photic layers, could explain the growth of large forms of phytoplankton in the zone. Several processes could be responsible. In nutrient-rich, turbulent environments, non-motile and fast-growing life forms (like diatoms) could be favoured (Margalef 1978) as high nutrient concentrations allow fast division rates and turbulence reduces sedimentation losses out of the photic zone (Kiørboe 1993). The dominance of large cells in relation to high vertical motion intensities has been reported by Semina (1968). Rodríguez et al. (2001), working in the same region, found a significant correlation between the magnitude of the upward velocity and the relative proportion of large cells in the phytoplankton community. In addition, at a small-scale, turbulence could also directly increase the nutrient uptake of large cells (> 60 µm; Karp-Boss et al. 1996) favouring an increase on the proportion of large cells when high nutrient concentrations are present (Arin et al. *Chapter II*). Therefore, both nutrients and turbulence, in combination, could be the main factors that enhancing the growth of large cells in this zone of the Western anticyclonic gyre.

The picoplanktonic fraction was more important at station C (making up to 40 to 50 % of total integrated chlorophyll), where it was located fundamentally in the upper 40 m of the water column (Fig. 5 and 6). The dominant organisms at this station were *Synechococcus*, nanoflagellates and picoeukaryotes, but large diatoms of *Guinardia striata* and *Proboscia alata* were also found below 40 m at station C2. Presumably, the presence of these diatoms was not due to *in situ* growth, but was a result of an intrusion of waters from elsewhere, with an already developed phytoplankton community (see below). Because of its small size and relatively large surface to volume ratio, *Synechococcus* is able to live at low nutrient environments. Motile organisms in the upper nanoflagellate size range could increase their nutrient uptake through swimming, by renewing the nutrient-depleted water surrounding the cell (Kiørboe 1993), or by taking advantages of their motility to approach nutrients patches.

The dominance of large or small cells could also be related to the different forms of dissolved inorganic nitrogen (DIN). At station A, in general, more than 80 % of the DIN was in the form of nitrate (data not shown) which was positively correlated with the fraction of autotrophic biomass > 2 µm (Table 2). In contrast, ammonium was the principal form of DIN at station C (usually more than 40 % in the upper 50 m of the water column, data not shown) and was positively correlated with the fraction of chl *a* < 2 µm (Table 2). This agrees with previous observations (see for instance Chisholm 1992 and references therein) which found an association between large forms of phytoplankton and allochthonous inputs of nitrogen (i.e. nitrate), and a predominance of small organisms in oligotrophic waters, where regenerated ammonium is the principal form of DIN.

Regardless of the importance of each phytoplankton size fraction at the three stations, the overall pattern was a high percentage of small cells (picoplankton) in the upper layers of the photic zone while the largest cell sizes (nano- and microplankton) tended to increase their importance with depth (Fig. 6). Nutrient concentrations in the upper layers of the water column of the three stations ranged from low to almost non-detectable (Fig. 3); under these conditions, as commented above, small organisms would perform better than large ones. The increasing presence of large cells with depth could be explained by several mechanisms. For the intermediate layer considered (30 - 70 m), higher nutrient levels combined with enough irradiance would allow for active growth of these size classes. Below 70 m, where low irradiances would prevent significant photosynthetic activity (Morán & Estrada 2001) high concentrations of nano- and microplankton could be the consequence of sedimentation of senescent cells or of advection of water bodies entrained from shallower depths.

The most remarkable temporal changes in phytoplankton community composition were observed at station A but, unexpectedly, also at station C (Fig. 7). At station A, the community shift from a

dominance of nanoflagellates to large diatoms can be readily explained by the upwelling event and the associated nutrient input, as mentioned above. Nevertheless, at station C, which a priori seemed to be a more stable environment, a marked shift in the composition of the phytoplankton assemblage took place when the diatoms observed at C2 were replaced by nanoflagellates at C4. For the same cruise, Morán & Estrada (2001) reported a large increase in maximum photosynthetic rate and α (initial slope of the P-E curve) at the surface waters of this station, probably as a consequence of this change in the phytoplankton community. Oligotrophic areas can show rather conserved size class biomass distributions with conspicuous changes in the relative production of each size class (Marañón et al. 2001). Here is it shown that despite the dominance of small organisms, noticeable changes in taxonomic composition took place at a scale of days, under invariantly nutrient-depleted conditions. As we mentioned above, this interpretation does not imply that the observed phytoplankton changes occurred *in situ*. It is likely that advection of water masses played an important role in the changes of the phytoplankton composition observed. Transport of organisms through water mass displacement has been suggested in this area and adjacent regions by other authors (Packard et al. 1988, Gómez et al. 2000).

The C:chl *a* ratios obtained for the whole phytoplankton community (Table 4) were in the range reported by Delgado et al. (1992) for the Northwestern Mediterranean Sea. The fact that total C:chl *a* changed 7-fold (with a coefficient of variation of 85 %) and that values were generally below 50 warns against the widespread use of constant values (Strickland 1960). Differences in the C:chl *a* ratio were observed in relation with depth, the nutrient gradient along the three stations and the phytoplankton size class. Lower values of the ratio (for the total and the two fractions considered) were found below 30 m depth, presumably as a consequence of a high chl *a* concentration per cell due to photoacclimation (Jensen & Sakshaug 1973, Latasa et al. 1992) and lower carbon content of cells grown at lower light intensities (Thompson et al. 1991). A decrease of the C:chl *a* ratio with depth was also observed by Delgado et al. (1992). In addition, the C:chl *a* increased from high (station A) to low nutrient waters (station C). Other studies have also reported higher C:chl *a* ratios in oligotrophic than in richer waters (Buck et al. 1996, Chavez et al. 1996). Under nutrient-limited conditions the cells could decrease some metabolic activities while photosynthesis (carbon assimilation) continues. Overconsumption of dissolved inorganic carbon (Sambrotto et al. 1993, Kähler & Koeve 2001), which appears to be higher at low nitrate concentration (Thomas et al. 1999), could result in an increase of the phytoplankton C:N ratio. An elevation of carbohydrate content in diatoms has been observed under nitrate-limiting conditions (Myklestad & Haug 1972, Haug et al. 1973). Thus, it appears that under low nutrient concentrations, the relative proportion of carbon inside the cells could be higher than in richer environments, originating higher C:chl *a* ratios. In

general, in this study, the C:chl *a* ratio increased with cell size. According to Malone (1980), the existence of correlations between chlorophyll per cell and surface area and between carbon content per cell and volume should result in an increase of the C:chl *a* ratio with cell size. However, there are exceptions to this hypothesized relationship. For instance, no relation was observed between cell size and the C:chl *a* ratio in some marine phytoplankton cultures (Blasco et al. 1982, Geider et al. 1986, Montagnes et al. 1994).

Growth rates averaged for the photic layer ($\mu_{ph\text{-}l}$) were higher in the second than in the fourth visit (Table 6); it is likely that after the initial growth pulse and biomass build-up, growth rates had already decreased. In fact, the patches of maximum biomass (40 m depth at stations A3 and A4) coincide with nutrient minima (Fig. 3 and 4). Contrary to some findings along broader spatio-temporal scales in the Atlantic Ocean (e. g. Marañón et al. 2000) no significant relationship was found between $\mu_{ph\text{-}l}$ and nutrient concentrations or the depth of the nutricline for our data set. Moreover, these $\mu_{ph\text{-}l}$ values (Table 6) were very similar to those found in the NW Mediterranean in early summer, where more oligotrophic conditions prevail (Pedrós-Alió et al. 1999). Differences in μ between the two visits were not associated to the observed changes in phytoplankton composition and size distributions, but to changes in irradiance. Virtually all the variability in $\mu_{ph\text{-}l}$ could be explained by the average irradiance received in the photic layer (Fig. 9), in spite of the reported interspecific differences in the growth-irradiance response (Langdon 1988, Gallegos & Jordan 1997). This finding suggests a physiological acclimation of the phytoplankton communities to the environmental light conditions, independently of other environmental factors or of taxonomic composition. In a comparable way, Figueiras et al. (1994) and Figueiras et al. (1998) found that photosynthetic parameters of Antarctic phytoplankton were adjusted to the mean irradiance in the upper water layer and explained it as a phytoplankton adaptation to maximize carbon uptake and growth rates. Furthermore, we did not find any clear evidence of higher growth rates when diatoms were dominant, in contrast with the observations of Furnas (1990) who noted higher *in situ* growth rates in different species of diatoms in comparison with smaller species like flagellates or non-motile ultraplankton. In natural waters, growth rates of diatoms are expected to vary during the successive phases of proliferation following growth pulses caused, for example, by upwelling events: therefore, the dominance of diatoms in natural communities may not always be associated to higher growth rates.

In spite of the oligotrophic conditions found in the middle of the gyre (St. C), the algal assemblage growing there (Fig. 7) showed maximum rates similar to those of the other two stations. However, this similarity of maximum growth rates (μ_{max}) at the three stations, regardless of the different hydrographical and nutrient conditions, is in agreement with the lack of significant differences in photosynthetic parameters between stations, except, as commented above, in the last visit to St. C

(Morán & Estrada 2001). μ_{max} values, corresponding to duplication times lower than 1 d on average (0.9 d ± 0.3 SD), indicate that phytoplankton assemblages were healthy and actively growing during the sampled period, and suggest that ambient growth rates were similarly limited by irradiance at the three stations (Fig. 9).

In conclusion, the differences observed in the hydrography of the Alboran Sea were reflected in the size distribution of the phytoplankton community. The predominance of the largest size fractions in the northern edge of the Western Alboran Sea anticyclonic gyre was related to a higher hydrodynamism and higher nutrient concentrations in this zone, while small organisms dominated the more oligotrophic waters of the centre of the gyre. Phytoplankton growth rates were correlated with available irradiance but not with organism size. This result may be relevant for parameterisation of primary production models. The C:chl *a* ratio varied greatly between the different hydrographical conditions, but also with depth and phytoplankton cell sizes. This variability should caution about the use of constant ratios in models and carbon budget calculations.

ACKNOWLEDGEMENTS

We are grateful to our cruise colleagues for the hydrographycal data and to all the people on board the R/V Hespérides for their help during the cruise. We thank Roser Ventosa for nutrient analyses and Cèlia Marrasé and Lluïsa Cros for helpful discussions and comments. Ted Packard helped editing the English. This work was supported by the MAST Program of the European Union (MAS3-CT96-0051) and by the Spanish CICYT (MAR0932).

Spatio-temporal variability of the size distribution of phytoplankton at the Ebro Shelf (NW Mediterranean)

ABSTRACT

The mesoscale distribution and seasonal variation of the size structure of phytoplankton biomass, as measured by chlorophyll *a* (chl *a*), was studied in the Ebro shelf area (NW Mediterranean) during three different seasons of the year: autumn, winter and summer. In autumn and summer, when the water column was, respectively, slightly or strongly stratified and nutrient concentrations were low at surface, average total chlorophyll *a* (chl *a*) values (± SE) were 0.31 ± 0.02 mg m^{-3} and 0.29 ± 0.01 mg m^{-3}, respectively. In winter, the intrusion of nutrients into the photic zone, by intense vertical mixing and strong riverine inputs, produced an increase of the total autotrophic biomass (0.76 ± 0.05 mg m^{-3}). In the three seasons, the most important contributor to total chl *a* was the picoplanktonic (< 2 µm) size fraction (42 % in winter and around 60 % in autumn and summer). The nanophytoplankton (2 - 20 µm) contribution to total chl *a* showed the lowest variability amongst seasons (between 29 and 39 %) and the microplanktonic (> 20 µm) chl *a* size fraction was higher in winter (27 %) than in the other seasons (less than 13 %). The maximum total chl *a* concentrations were found at surface in winter, at depths of 40 m in autumn and between 50 and 80 m in summer. The relative contribution of the < 2 µm size fraction at these levels of the water column tended to be higher than at other depths in autumn and winter and lower in summer. In autumn and winter, nutrient inputs from Ebro river discharge and mixing processes resulted in an increase on the > 2 µm contribution to total chl *a* in the coastal zone near the Ebro Delta area. In summer, the contribution of the < 2 and > 2 µm chl *a* size fractions was homogeneously distributed through the sampling area. In autumn and summer, when deep chl *a* maxima were observed, the total amount of the autotrophic biomass in the superficial waters (down to 10 m) of most offshore stations was less than 10 % of the whole integrated chl *a* (down to 100 m or to the bottom). In winter, this percentage increased until 20 or 40 %. This finding has implications in the use of remote sensing techniques. The > 2 µm chl *a* increased linearly with total chl *a* values. However, the < 2 µm chl *a* showed a similar linear relationship only at total chl *a* values lower than 1 mg m^{-3} (in autumn and summer) or 2 mg m^{-3} (winter). At higher values of total chl *a*, the contribution of the < 2 µm size fraction remained below an upper limit of roughly 0.5 mg m^{-3}. Our results indicate that the picoplankton fraction of phytoplankton may show higher seasonal and mesoscale variability than is usually acknowledged.

INTRODUCTION

Recent findings have emphasized the importance of the size structure of the phytoplankton communities in relationship with the trophic organization of marine ecosystems and its influence on the magnitude of carbon export from the photic zone to deep waters. The proportion of the picoplanktonic (< 2 µm), nanoplanktonic (2 - 20 µm) and microplanktonic (> 20 µm) phytoplankton size fractions (Sieburth et al. 1978) in a given environment depends of a combination of environmental factors such as nutrient concentrations, light and water movement (Semina 1968, Kiørboe 1993), which could select for different size fractions through effects on growth rates or interactions with advective or turbulent transport of the organisms. Many recent studies about phytoplankton size distribution have pointed out the importance of the picophytoplankton, both in terms of biomass and productivity, in a variety of marine environments (Takahashi & Bienfang 1983, Xiuren et al. 1996, Marañón et al. 2001). Dominance of picophytoplankton (> 50 %) is generally restricted to oligotrophic areas (Chisholm 1992, Magazzù & Decembrini 1995, Agawin et al. 2000) where new nutrients are scarce and water column stability is high (Cushing 1989). In nutrient-rich environments, the < 2 µm size fraction may represent less than 10 % of the total, while globally, in oceans and coastal estuarine areas, it has been reported to account for about 24 % of the total phytoplankton biomass (Agawin et al. 2000). The prevalence of phytoplankton of larger sizes is generally associated to upwelling or coastal areas (Malone 1971, Tundisi 1971, Marañón et al. 2001, Arin et al. 2002b) where a combination of vertical mixing and high nutrient concentrations can be found.

It is generally accepted that the picophytoplankton constitutes the least variable size fraction of phytoplankton (Malone 1980, Raimbault et al. 1988b, Magazzù et al. 1996, Rodríguez et al. 1998) while the pulses of growth of the largest organisms are responsible for the major quantitative increases in the whole phytoplankton community. However, in the Atlantic Ocean, Marañón et al. (2001) found that the picophytoplankton explained 61 % and 73 % of the variability in total chlorophyll *a* and total production, respectively.

In Mediterranean waters, Magazzù & Decembrini (1995) calculated that the average picophytoplankton contribution to the total biomass (measured as chlorophyll *a*) of the phytoplankton community was of 59 %. They reported also that, in spite of the high variability observed, the proportion of picophytoplankton was higher in oligotrophic than in eutrophic waters. However, aspects like the mesoscale heterogeneity of the phytoplankton size distribution and their seasonal variability have been scarcely addressed in Mediterranean waters (Delgado et al. 1992).

The objective of this work was to study the mesoscale distribution and seasonal variation of the phytoplankton size structure in a highly dynamic Mediterranean marine ecosystem. For this purpose, samples were obtained from three cruises, which were carried out in the Ebro shelf area (NW Mediterranean), during three different seasons of the year (autumn, winter and summer). The Ebro continental shelf area (comprised between Cap Salou and the Columbretes Islands) is more than 60 km wide and presents a total surface of about 12000 km^2. In the upper water column of this zone, two distinct water masses can be found: offshore, the Mediterranean Open Sea Water (with high salinity and temperature values) and, inshore, the Continental Shelf Water (with lower salinities than the former due to its more recent Atlantic origin and the local fresh water inputs received along its coastal path). These two water masses are separated by a shelf-slope front which displays a seasonal variability associated with the baroclinic circulation in the area (Font et al. 1995). The Ebro river discharge can be distinguished by an additional low-salinity water mass, referred to as Continentally Influenced Water (CIW), with salinity lower than 37.8 (Salat et al. 2002); CIW distribution depends on both, river discharge and local thermal stratification. The high hydrographic variability of the Ebro shelf area, linked to strong seasonal fluctuations in water column stability and river discharge, provided a suitable scenario to address the relationships between environmental forcing and the size structure of the phytoplankton community.

MATERIALS AND METHODS

Area surveyed

This study was based on three cruises carried out on board the R/V "García del Cid" (Table 1), as part of an interdisciplinary project (FANS) addressing the particulate fluxes in the area of Ebro shelf (NW Mediterranean). The cruises covered an area of about 7500 km^2, from Tarragona to the Columbretes Islands and from the coast to around the 1200 m isobath (Fig. 1). Several aspects of the FANS research have been published in Sánchez-Arcilla & Davies (2002). Information on hydrographic structure and distribution of major nutrients, total chlorophyll *a* (chl *a*) and suspended particulate matter during these cruises has been reported in Salat et al. 2002.

Sampling strategy

An average of 140 CTD casts per cruise, from surface down to near the bottom, were obtained with a GO MkIII C probe, equipped with a GO 12-bottles Rossette sampler, a 25 cm Sea-Tech transmissometer and a Sea-Tech fluorometer. Stations were distributed at regular distances, ranging from 1 to 5 nautical miles according to the bottom topography, along 12 to 14 adjacent

transects across the shelf (Fig. 1). At selected stations of each cruise, water samples for total and fractionated chl *a* and inorganic nutrients were obtained with the Niskin bottles mounted on the Rosette, generally at 5/25/40/60/75/100 m depth in FANS I and 5/10/25/40/60/75/100 m depth in FANS II and III. When the depth was less than 100 m, a sample was taken near the bottom.

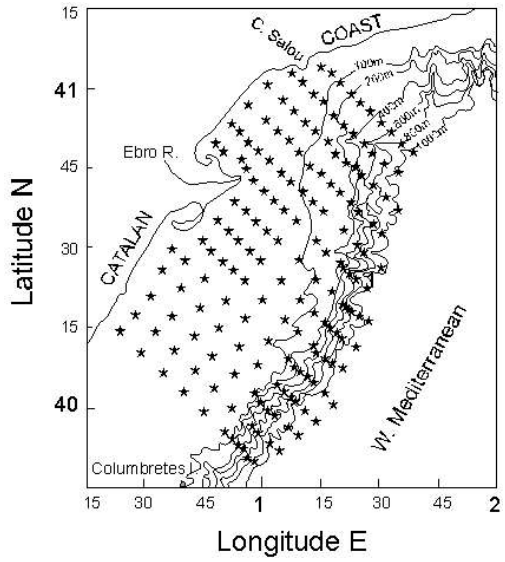

Fig. 1 - Grid of stations sampled for the three FANS cruises.

Chlorophyll a and nutrient analyses

For total chl *a*, 100 ml of water were filtered through Whatman GF/F filters (25 mm diameter, nominal pore size 0.7 µm). Samples of 200 ml and additionally (at a smaller number of stations) of 100 ml of water were filtered, respectively, through polycarbonate 2 µm filters and a 20 µm mesh net and the filtrates were collected onto Whatman GF/F filters. All filtrations were done under low vacuum pressure (< 100 mm Hg); after filtration, the GF/F filters were immediately frozen at - 20 ^{o}C and kept at this temperature for at least five hours until their analysis. Chl *a* was extracted in acetone 90 % (24 h at 4 ^{o}C in the dark) and then measured fluorometrically (Yentsch & Menzel 1963) with a Turner Designs fluorometer (spectrophotometricaly calibrated with chl *a* extracts from the same study area). Samples for < 20 µm chl *a* analyses (from which the > 20 µm chl *a* was calculated) were collected only in part of the stations. Thus, unless otherwise stated, > 2 µm chl *a* will be referred to as the "large" chl *a* fraction.

Nitrite, nitrate, ortophosphate and orthosilicic acid (hereafter referred as silicate) analyses were made on board with a segmented flow continuous analyser (Whitledge et al. 1981).

Data analyses

Integrated chl *a* values down to 10 m depth and down to 100 m depth or to the bottom (at depths lower than 100 m), were calculated by the trapezoidal method. Hereafter, total, < 2 µm or > 2 µm chl *a* integrated down to 10 m or to 100 m (or to the bottom) will be referred to as total, < 2 µm or > 2 µm chl a_{int10m} or total, < 2 µm or > 2 µm chl $a_{int100m}$, respectively.

Correlation coefficients were calculated considering for each cruise all data pairs obtained from integrated values of each station. Total vs. fractionated chl *a* relationships were fitted using a linear regression model.

RESULTS

Hydrography, nutrients and general features of the chl a distribution

Water column temperature in the FANS I cruise decreased gradually with depth; the average value was around 19 ^{o}C at surface and 15 ^{o}C at 100 m depth (Fig. 2a). In this cruise, at 5 m depth, the CIW occupied a horizontal area of about 350 km^2 (Fig. 3a). In general, nitrate, phosphate and silicate showed values lower than 1.0, 0.1 and 2.0 µM, respectively, in the upper 50 - 75 m of the water column. Below this depth, an increase of the three nutrients was generally observed (see example in Fig 4a, b, c). In the coastalmost stations (shallower stations), higher nutrient concentrations were usually observed, specially near the Ebro river outlet. As can be observed in Fig. 5a, depth-averaged total chl *a* concentrations (the graph includes all the stations with depths equal or higher than 100 m), showed a deep maximum (DCM) at 40 m depth. The average total chl *a* concentration at this depth for all the stations was 0.5 mg m^{-3} (Salat et al. 2002). A dominance of the < 2 µm size fraction was observed throughout, with a trend to higher percentages at the DCM level (Fig. 5a). Total chl $a_{int100m}$ ranged between 6 and 40 mg m^{-2}, with values of more than 25 mg m^{-2} at different points of the sampled area (Fig. 6a). The highest (> 15 mg m^{-2}) chl $a_{int100m}$ values of the < 2 µm chl *a* fraction were located in the most oceanic stations of the southern edge of the slope (Fig. 6b), while the > 2 µm size fraction showed its maximum chl $a_{int100m}$ values (in general, > 15 mg m^{-2}) at some southern coastal stations (Fig. 6c).

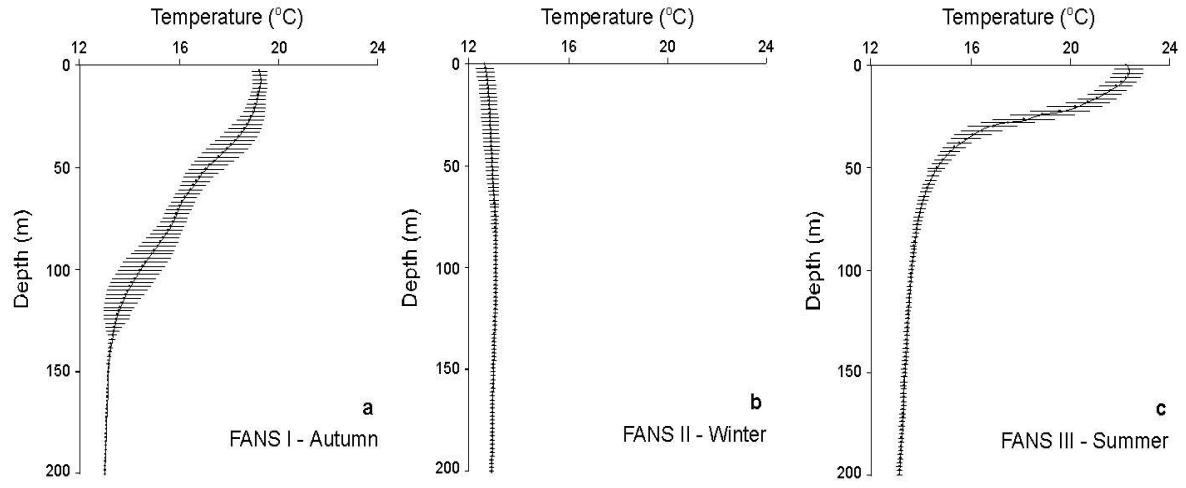

Fig. 2 - Temperature profiles (average with 95% confidence interval, as an indicator of dispersion) for the FANS I (a), FANS II (b) and FANS III (c) cruises.

In FANS II, the average temperature increased smoothly with depth, from around 12.7 °C at surface to around 13.5 °C at 200 m depth (Fig. 2b). In most of the sampled area, surface salinity values were lower than 37.8, corresponding to an area covered by CIW of about 7000 km^2 (Fig. 3b). Nutrients (nitrate, phosphate and silicate) were, in general, fairly homogeneously distributed in the upper 100 m, with a slight increase with depth. Nitrate ranged between 1.0 and 10.0 µM (on average between 1.6 and 3.2 µM), phosphate between 0.001 and 0.6 µM (on average between 0.03 and 0.11) and silicate between 1.0 and 5.4 µM (on average between 2.8 and 3.8 µm). In this cruise, high nutrient concentrations were found in the superficial waters of the coastalmost stations of the transects located to the south of the Ebro river mouth, with around 10 µM of nitrate and 5.5 µM of silicate (see example in Fig 4d, e, f). The highest total chl *a* values were observed at surface (Fig. 5b), where the average total chl *a* value was 1.3 mg m^{-3} (Salat et al. 2002). At this layer (5 – 10 m) the percentages of < 2 and > 2 µm chl *a* were both around 50 % of the total chl *a*. Below these depths, a dominance of the > 2 µm size fraction was observed. Total chl $a_{int100m}$ values (which ranged between 21 and 210 mg m^{-2}) decreased in the offshore direction and were highest at the northern and southern coastal stations of the sampled area (Fig. 6d). The smallest fraction (< 2 µm) of the chl $a_{int100m}$ showed two peaks exceeding 25 mg m^{-2} north and south of the central coastal-offshore transect (Fig. 6e). The highest > 2 µm chl $a_{int100m}$ values (also > 25 mg m^{-2}) in this cruise tended to be found near the coast stations (Fig. 6f). A marked thermocline (with the 15 °C isotherm at its basis) was observed in the FANS III cruise at depths between 40 and 50 m (Fig. 2c).

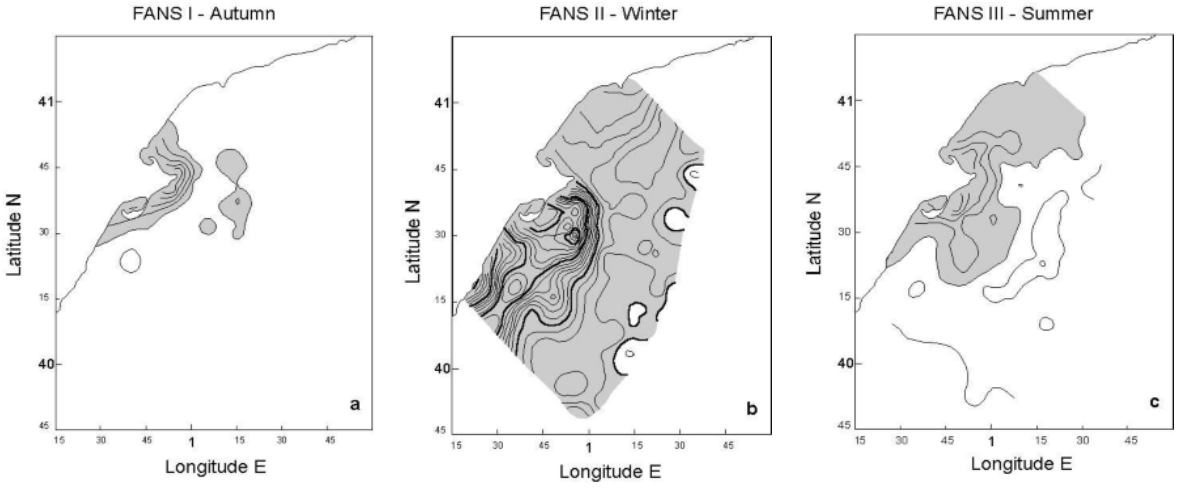

Fig. 3 – Surface salinity distributions for the FANS I (a), FANS II (b) and FANS III (c) cruises. The shaded area shows salinity values below 37.8 to show the extent of the Continental Influenced Waters (CIW). The isolines are drawn every 0.2.

In this cruise, the average sea surface temperature was higher than 22 ^{o}C and the CIW surface area was about 2100 km^{2} (Fig. 3c). In general, nitrate and silicate in the upper 40 - 60 m of the water column were lower than 0.5 µM and 2.0 µM, respectively. Below these depths, a higher concentration of both nutrients was found (see example in Fig 4g, h, i). Phosphate was generally lower than 0.2 µM and its distribution in the upper 100 m depth was more or less homogeneous. A well developed DCM was observed between 50 and 80 m depth (Fig. 5c) with an average value of 0.7 mg m^{-3} for all the stations (Salat et al. 2002). In general, the proportion of < 2 µm chl *a* was higher than 50 % at all depths, with the exception of DCM or near the DCM depths, where both chl *a* fractions (< 2 and > 2 µm) were equally important (Fig. 5c). At the coastal stations, total chl $a_{int100m}$ values were generally lower than 10 mg m^{-2}, while in the southern part of the sampled area and near the slope, they exceeded 30 mg m^{-2} (Fig. 6g). The chl $a_{int100m}$ values of both, the < 2 and > 2 µm size fractions (Fig. 6h, i), showed a similar distribution, with lower values than 10 mg m^{-2} at the coastal stations and between 10 and 20 mg m^{-2} in the remaining ones.

In the three cruises, < 2 and > 2 µm chl $a_{int100m}$ were positively correlated with their respective total chl $a_{int100m}$ (Table 2), except for the < 2 µm size fraction in FANS II. These correlation coefficients were higher for the > 2 µm chl *a*.

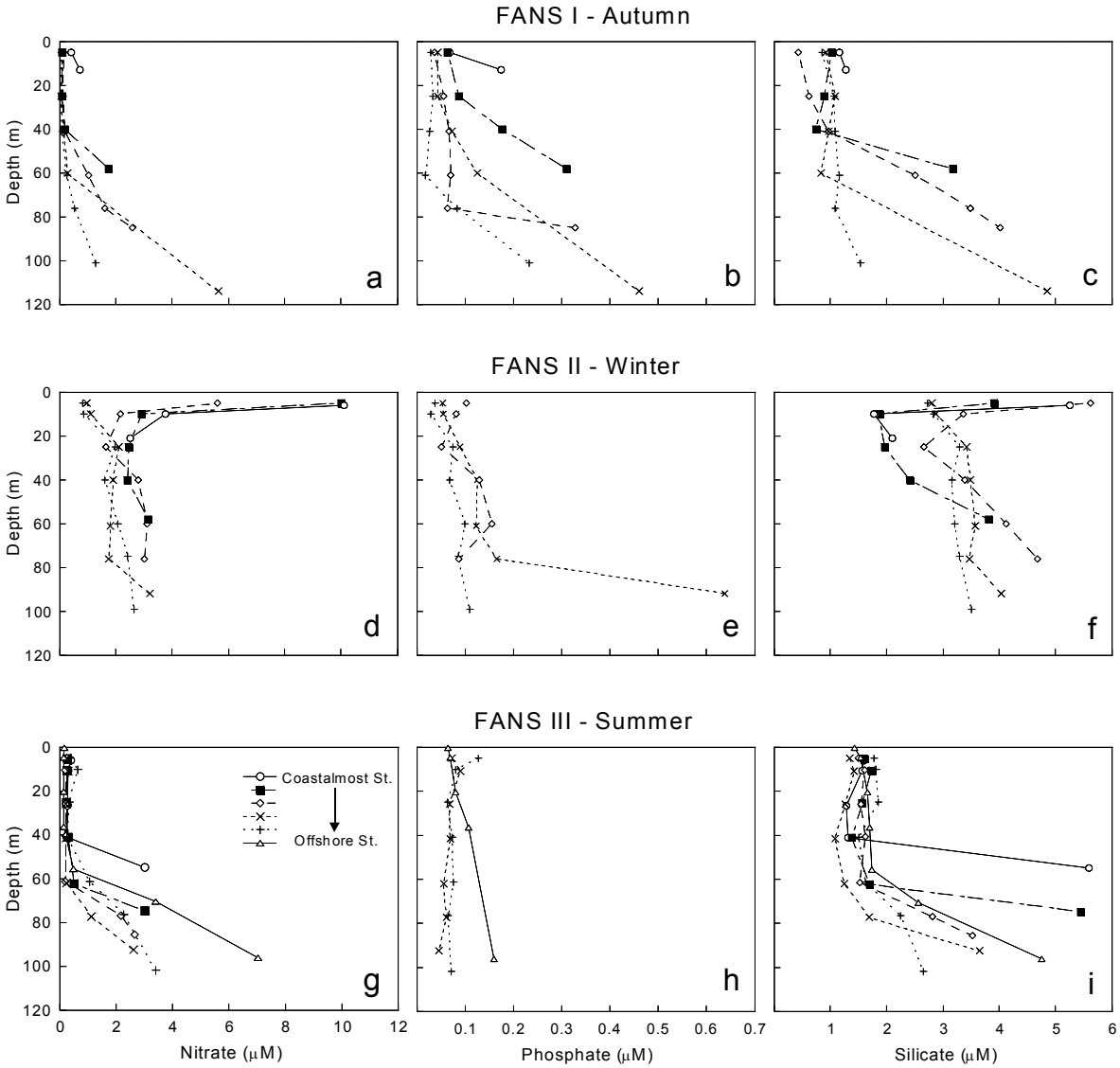

Fig. 4 – Nitrate, phosphate and silicate concentrations (μM) for the FANS I (a, b and c, respectively), FANS II (d, e and f, respectively) and FANS III (g, h and i, respectively) for one of the transects sampled. The transect position in each cruise is shown in Fig. 6. In FANS II and III data for phosphate concentrations at coastal stations were not available.

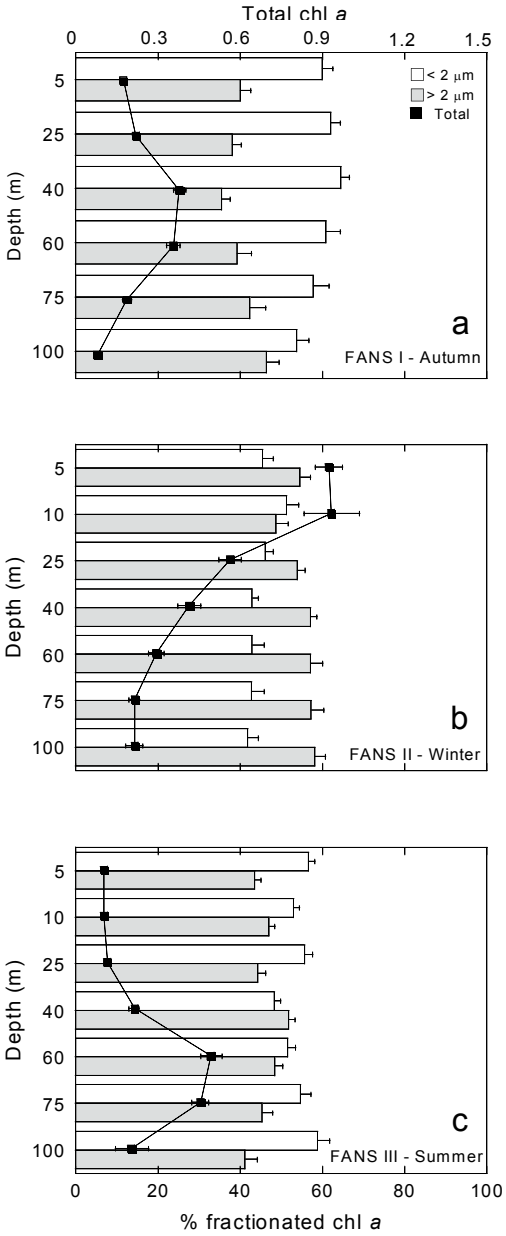

Fig. 5 – Average vertical distribution of total chl *a* and the percentages of < 2 µm and > 2 µm chl *a* (mean ± SE from stations with depths equal or higher than 100 m) for the FANS I (a), FANS II (b) and FANS III (c) cruises.

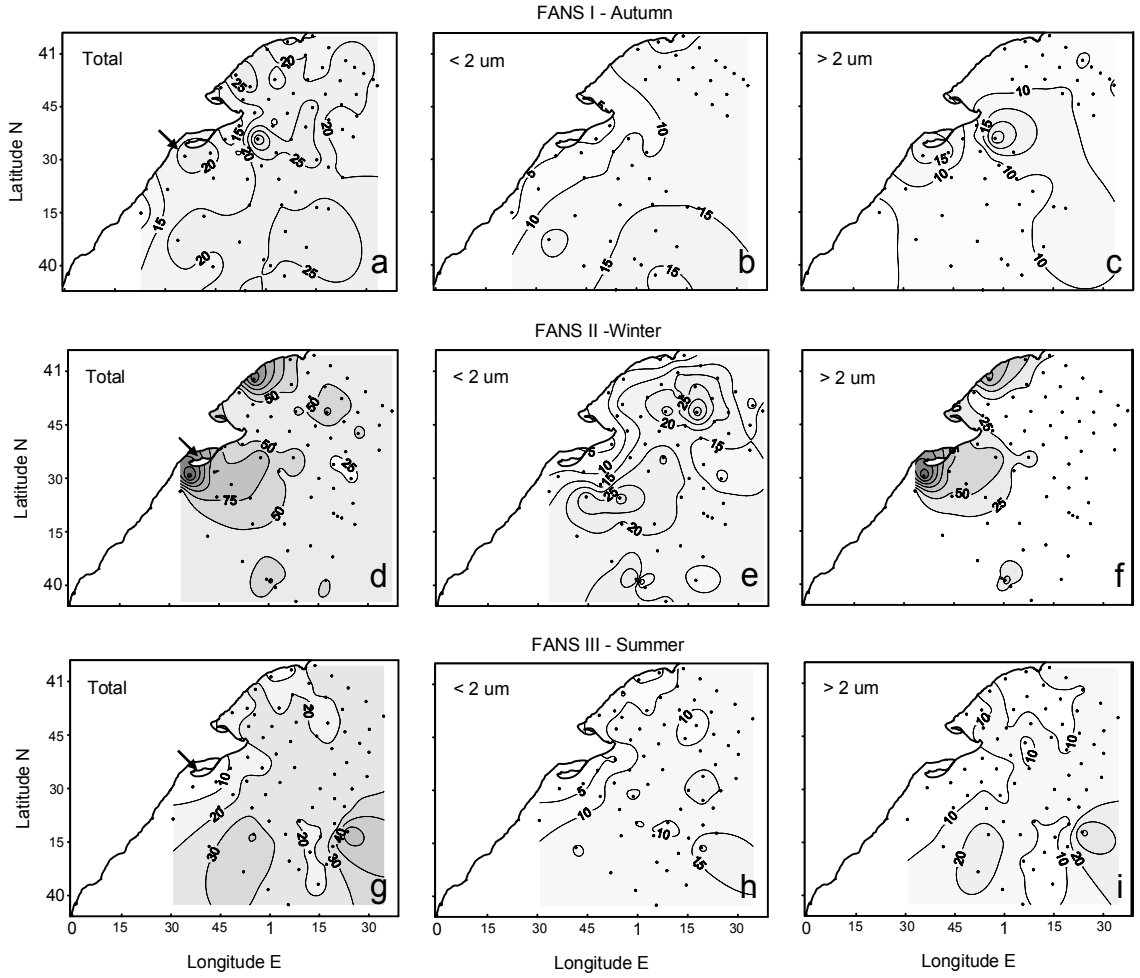

Fig. 6 – Distribution of vertically-integrated total and fractionated (< 2 µm and > 2 µm) chl *a* values (mg m^{-2}) for the FANS I (a, b and c, respectively), FANS II (d, e and f, respectively) and FANS III (g, h and i, respectively) cruises. Arrows show the position of the transects of which nutrient concentrations are illustrated in Fig. 4.

Total and fractionated chl a concentrations in superficial waters in relation to whole water column

For the three seasons, the percentages of total and fractionated (< 2 and > 2 µm) chl a_{int10m} with respect to their respective values of chl $a_{int100m}$ are shown in Fig. 7. As expected, the highest percentages (more than 40 %) were found at the coastal stations, specially around the Ebro Delta, where the bottom was, in general, lower than 40 m. In winter, total autotrophic biomass in the

superficial waters of most stations represented between 20 and 40 % of the total chl *a* or of the < 2 and > 2 µm size fractions (Fig. 7d, e, f). In the other seasons, less than 10 % of the total or fractionated chl *a* was found in the upper 10 m of the water column of most oceanic stations. In summer, in particular, this proportion was generally lower than 5 % (Fig. 7g, h, i). The < 2 µm chl a_{int10m} showed significant negative correlation with its corresponding chl $a_{int100m}$ in all the cruises (Table 2). However, total chl a_{int10m} was negatively correlated with its corresponding chl $a_{int100m}$ only in summer and autumn, and the > 2 µm chl a_{int10m} was negatively correlated with its corresponding chl $a_{int100m}$ only in summer.

Relationship among the total and fractionated chl a concentrations

In the three FANS cruises, < 2 µm chl *a* (Fig. 8a, b, c) increased linearly with total chl *a* only up to total chl *a* values of 1 mg m^{-3} (FANS I: r^2 = 0.81, p = 0.000, n = 222 and FANS III: r^2 = 0.85, p = 0.000, n = 376) or 2 mg m^{-3} (FANS II: r^2 = 0.66, p = 0.000, n = 344), reaching maximum concentrations of 0.72 mg m^{-3} in autumn, 1.11 mg m^{-3} in winter and 0.61 mg m^{-3} in summer. At higher values of total chl *a*, the concentration of the < 2 µm fraction remained approximately stable, with values not exceeding 0.5 mg m^{-3}. The > 2 µm chl *a* fraction increased linearly with respect to total chl *a* through all the range of total values (Fig. 8d, e, f; FANS I: r^2 = 0.90, p = 0.000, n = 236; FANS II: r^2 = 0.96, p = 0.000, n = 369; FANS III: r^2 = 0.88, p = 0.000, n = 384).

Seasonal and mesoscale variability of the relative contribution of the < 2, 2 - 20 and > 20 µm chl a fractions

The highest means of the < 2, 2 - 20 and > 20 µm chl *a* concentrations were observed in winter (FANS II cruise) and the lowest ones in the summer cruise (FANS III, Table 1). However, the relative contribution of the different size fractions to total chl *a* was different in the three cruises (Table 3). Although the fraction of < 2 µm chl *a* was always the most important fraction, its contribution to total chl *a* was higher in autumn and in summer (more than 50 %). The nanophytoplankton (2 - 20 µm) contribution was similar in the three cruises (between 29 and 39 %), while the > 20 µm size fraction was relatively more important in winter (27 % vs. less than 13 % in the other seasons). The relative contributions of the < 2 µm and > 2 µm size fractions showed, respectively, a marked increase or decrease for values of total chl *a* above 1 mg m^{-3} (FANS I and III) or 2 mg m^{-3} (FANS II) (Table 3).

Table 1 – Sample dates of the three FANS cruises and total and fractionated (< 2 µm, 2 - 20 µm and > 20 µm) chl *a* range and mean in each cruise. bd = below detection.

Cruise	Date	Season		Chl *a* (mg m^{-3})			
				Total	< 2 µm	2 - 20 µm	> 20 µm
FANS I	2 - 8 Nov.96	Autumn	Range	0.03 - 2.10	0.01 - 0.72	bd - 1.56	bd - 1.60
			Mean±SE	0.31 ± 0.02	0.16 ± 0.01	0.12 ± 0.02	0.06 ± 0.01
			n	335	236	151	172
FANS II	4 - 13 Feb.97	Winter	Range	0.07 - 8.77	0.03 - 1.11	0.02 - 5.11	bd - 3.19
			Mean±SE	0.76 ± 0.05	0.25 ± 0.01	0.34 ± 0.09	0.31 ± 0.08
			n	374	369	64	64
FANS III	7 - 14 Jul.97	Summer	Range	0.02 - 1.90	0.01 - 0.61	0.01 - 0.64	bd - 0.68
			Mean±SE	0.29 ± 0.01	0.15 ± 0.01	0.11 ± 0.01	0.03 ± 0.01
			n	386	384	53	53

Table 2 – Correlation matrix between integrated chl *a* values for the three FANS cruises. Level of significance: * $p \leq 0.05$; ** $p \leq 0.01$; *** $p \leq 0.001$. FANS I: *n* = 47, FANS II: *n* = 64 and FANS III: *n* = 68. $Chl_{int100m}$ and Chl_{int10m} = integrated chl *a* at 100 m and 10 m depth, respectively.

FANS I

	$Chl_{int100m}$ Tot	$Chl_{int100m}$ < 2 µm	$Chl_{int100m}$ > 2 µm	Chl_{int10m} Tot	Chl_{int10m} < 2 µm	Chl_{int10m} > 2 µm
$Chl_{int100m}$Tot	------					
$Chl_{int100m}$<2 µm	0.60 ***	------				
$Chl_{int100m}$>2 µm	0.72 ***	-0.12	------			
Chl_{int10m}Tot	-0.38 **	-0.75 ***	0.18	------		
Chl_{int10m}<2 µm	-0.34 *	-0.76 ***	0.23	0.99 ***	------	
Chl_{int10m}>2 µm	-0.39 **	-0.72 ***	0.14	0.99 ***	0.97 ***	------

FANS II

	$Chl_{int100m}$ Tot	$Chl_{int100m}$ < 2 µm	$Chl_{int100m}$ > 2 µm	Chl_{int10m} Tot	Chl_{int10m} < 2 µm	Chl_{int10m} > 2 µm
$Chl_{int100m}$Tot	------					
$Chl_{int100m}$<2 µm	0.06	------				
$Chl_{int100m}$>2 µm	0.98 ***	-0.16	------			
Chl_{int10m}Tot	0.04	-0.39 ***	0.13	------		
Chl_{int10m}<2 µm	-0.03	-0.40 ***	0.06	0.87 ***	------	
Chl_{int10m}>2 µm	0.08	-0.35 **	0.15	0.96 ***	0.73 ***	------

FANS III

	$Chl_{int100m}$ Tot	$Chl_{int100m}$ < 2 µm	$Chl_{int100m}$ > 2 µm	Chl_{int10m} Tot	Chl_{int10m} < 2 µm	Chl_{int10m} > 2 µm
$Chl_{int100m}$Tot	------					
$Chl_{int100m}$<2 µm	0.79 ***	------				
$Chl_{int100m}$>2 µm	0.93 ***	0.51 ***	------			
Chl_{int10m}Tot	-0.53 ***	-0.64 ***	-0.37 **	------		
Chl_{int10m}<2 µm	-0.53 ***	-0.66 ***	-0.35 **	0.99 ***	------	
Chl_{int10m}>2 µm	-0.53 ***	-0.62 ***	-0.37 **	0.99 ***	0.99 ***	------

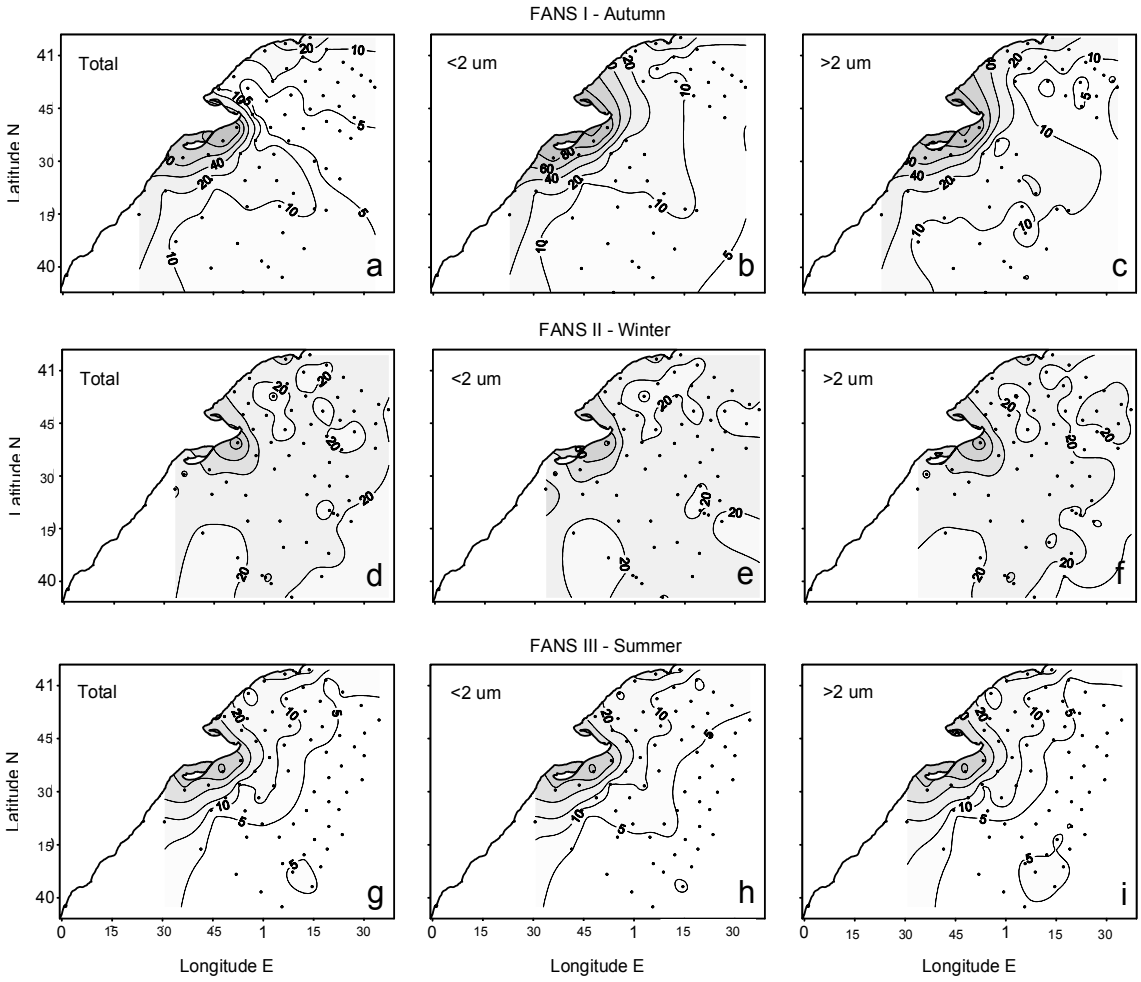

Fig. 7 – Percentage of integrated total and fractionated (< 2 µm and > 2 µm) chl *a* at 10 m depth (related to their respective integrated chl *a* values down to the bottom or 100 m depth) for the FANS I (a, b and c, respectively), FANS II (d, e and f, respectively) and FANS III (g, h and i, respectively) cruises.

The spatial distribution of the relative contribution of the < 2 µm size fraction to total chl *a* (percentages from integrated values) showed different patterns in the three cruises (Fig. 9). In FANS I, the proportion of this size fraction varied from less than 40 % at the stations near the Ebro Delta to more than 60 % in the southern edge of the sampled area, in the most oceanic stations and in some patches of the northern part of the Ebro shelf (Fig. 9a). In FANS II, the maximum percentages of the < 2 µm size fractions (40 %) were found in the middle and southern parts of the sampled area and the lowest in the coastal area (Fig. 9b). In FANS III, most of the stations showed a contribution of the < 2 µm size fraction between 40 and 60 % (Fig. 9c).

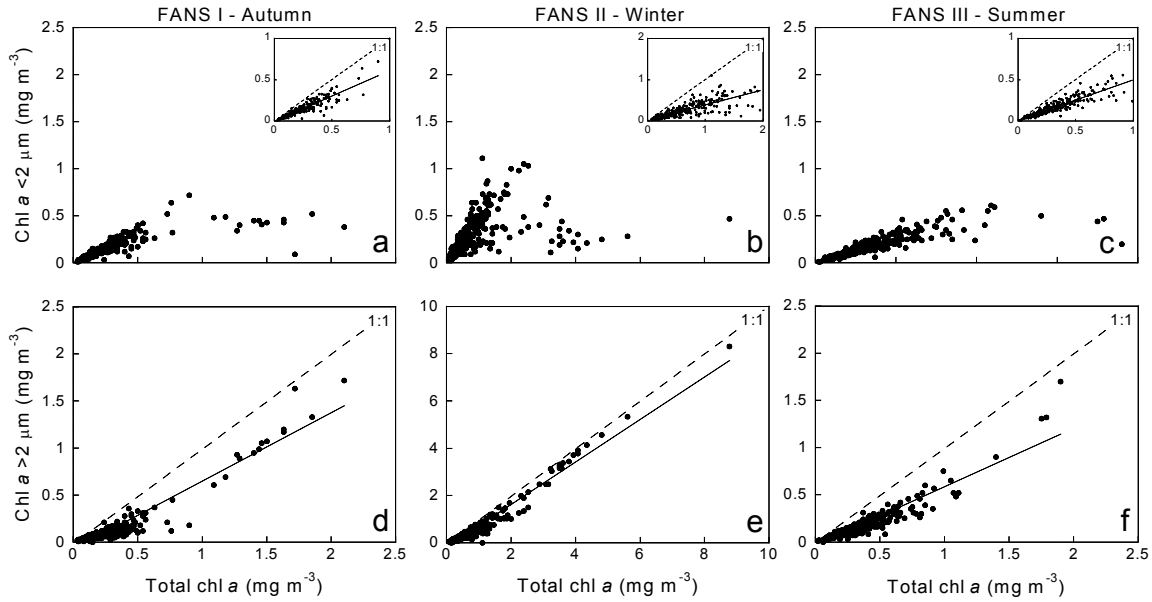

Fig. 8 – Relationship between the total chl *a* and the < 2 µm and > 2 µm size fractions for the FANS I (a and d, respectively), FANS II (b and e, respectively) and FANS III (c and f, respectively) cruises. Plots within the upper graphs show the relationship between the < 2 µm size fraction and total chl *a* values lower than 1 mg m^{-3} (a and c) or 2 mg m^{-3} (b). See the equations in the text. Note the differences in scale for FANS II (b and e).

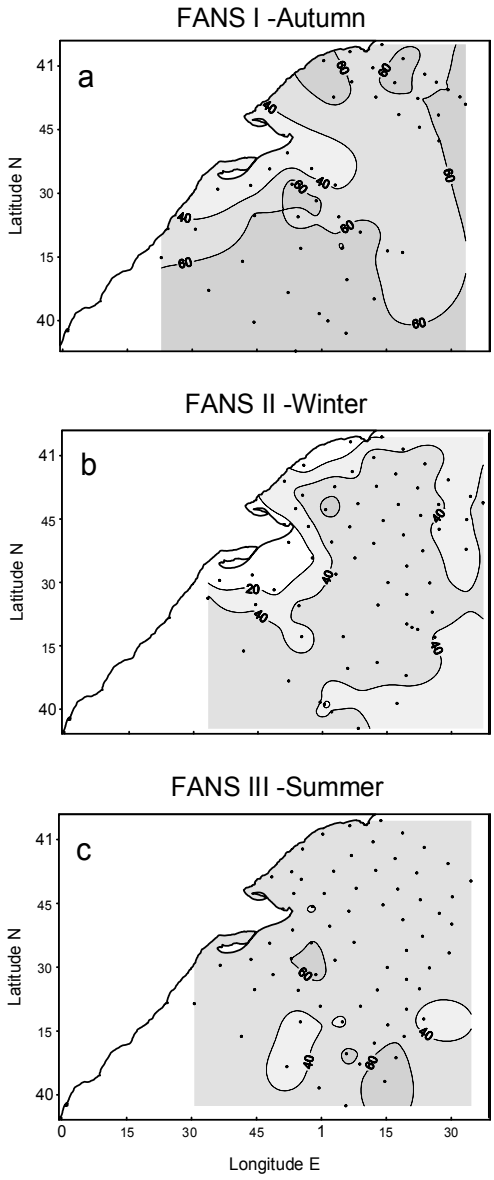

Fig. 9 – Distribution of the percentage of < 2 µm chl *a* for the FANS I (a), FANS II (b) and FANS III (c) cruises.

Table 3 – Percentage (mean ± SE; (n)) of fractionated chl *a* (< 2 µm, 2 - 20 µm and > 20 µm) in relation to the total chl *a* using all data set and for total chl *a* < and > of 1 mg m^{-3} (FANS I and III) or < and > of 2 mg m^{-3} (FANS II).

	Size-fraction	Total chl *a*		
		All data	<1 mg m^{-3} * or <2 mg m^{-3} **	>1 mg m^{-3} * or >2 mg m^{-3} **
FANS I *	< 2 µm	58 ± 1.0 (236)	60 ± 0.9 (223)	28 ± 2.7 (13)
	2-20 µm	29 ± 1.1 (151)	28 ± 1.0 (139)	45 ± 5.3 (12)
	> 20 µm	13 ± 1.0 (172)	12 ± 0.9 (160)	28 ± 6.7 (12)
FANS II **	< 2 µm	42 ± 0.8 (369)	44 ± 0.8 (344)	15 ± 2.8 (25)
	2-20 µm	38 ± 1.8 (64)	38 ± 1.9 (58)	39 ± 7.7 (6)
	> 20 µm	27 ± 2.7 (64)	25 ± 2.7 (58)	45 ± 11.1 (6)
FANS III *	< 2 µm	53 ± 0.6 (384)	54 ± 0.6 (376)	37 ± 5.6 (8)
	2-20 µm	39 ± 1.6 (53)	39 ± 1.6 (52)	36 (1)
	> 20 µm	8 ± 1.2 (53)	7 ± 1.1 (52)	38 (1)

DISCUSSION

Seasonal variability in the contribution of the different size fractions

As expected, the chl *a* distribution and its size structure showed marked differences among the autumn (FANS I), winter (FANS II) and summer (FANS III) cruises. The main patterns of the variability of total chl *a*, during the three cruises, can be related to the hydrographical conditions and nutrient concentrations as discussed in Salat et al. (2002). Briefly, in autumn, thermocline erosion brought nutrients from deep waters into the lower layers of the photic zone, enhancing phytoplankton growth and chl *a* concentrations in subsurface waters (generally at 40 m depth, Fig. 5a). The nutrients provided by the river were also reflected in higher chl *a* at surface near the Ebro river mouth. In winter, due to strong vertical mixing and convection processes, in addition to strong riverine inputs, nutrient concentrations were high at surface, leading to maximum chl *a* at this level (Fig. 5b). In summer, there was limited nutrient supply to the upper layers due to stratification and the availability of nutrients at surface was restricted to the river plume. A DCM was observed generally between 60 and 80 m depth (Fig. 5c).

The highest values of chl $a_{int100m}$ were observed in winter, (between 21 and 210 mg m^{-2}) when, as mentioned above, high nutrient concentrations were observed at surface. In the other two seasons, chl $a_{int100m}$ values ranged only between 6 and 60 mg m^{-2}, due to the low nutrient availability in the upper layers of the water column. The higher total chl *a* values observed in winter, with respect to

the other seasons, were due to an increase in the three measured size fractions (Table 1). However, in winter, the relative contribution of the > 20 µm size fraction was higher than in the other seasons (27 % vs less than 13 %). In all the cruises, the most important contributor to total chl *a* was the < 2 µm size fraction (42 % in winter and between 50 and 60 % in autumn and summer). The nanophytoplankton (2 - 20 µm) contribution showed the lowest seasonal variability (between 29 and 39 % of the total chl *a*, Table 3). The differences observed in this study in the phytoplankton size structure among seasons, agree with those found by Delgado et al. (1992) in the Catalan Sea (NW Mediterranean). These authors reported that the > 20 µm size fraction dominated the autotrophic biomass (in terms of carbon) in winter (55 %), while *Synechococcus* and the 2 - 5 µm size fraction were the main contributors to autotrophic biomass in spring (65 %). However, in the present study, although the highest contribution of the > 20 µm size fraction was observed in winter, the picophytoplankton fraction was always the dominant one. The percentages of chl *a* < 2 µm in the FANS area were similar to (in autumn and summer) or lower than (winter) the mean value (59 %) calculated by Magazzù & Decembrini (1995) for the Mediterranean waters.

Within each season, the variability of the total chl *a* was due to changes in both, the smallest (< 2 µm) and the largest (> 2 µm) size fractions, as indicated by the highly significant positive correlations observed between the integrated values of the total chl *a* and the fractions (except for the < 2 µm size fraction in winter, Table 2). However, the highest correlation coefficients were observed between the total and the > 2 µm size fraction, suggesting a strongest dependence of total chl *a* on this fraction.

In the three seasons, the relative contribution of the < 2 and > 2 µm size fractions to total biomass varied with the total chl *a* concentrations (Table 3). When total chl *a* was lower than 1 mg m^{-3} (autumn and summer) or 2 mg m^{-3} (winter) the chl *a* < 2 µm increased lineally with total chl *a*. However, at total chl *a* values exceeding these thresholds, the < 2 µm size fraction ended to remain stable near an upper limit of 0.5 mg m^{-3} (Fig. 8). The finding that there is an upper concentration of total chl *a*, beyond which the proportion of chl *a* < 2 µm tends to become constant, agrees with the observations of Raimbault et al. (1988b), who found that the biomass of picophytoplankton (defined as the fraction of chl *a* < 1 µm), for Mediterranean waters and other environments, was around 0.5 mg m^{-3}. However, these authors reported that this was the maximum picophytoplankton standing stock through all the range of total chl *a* concentrations, while, in our study, chl *a* < 2 µm could reach higher values when total chl *a* was lower than 1 or 2 mg m^{-3}. The wider range of data used in this study, compared with those of Raimbault et al. (1988b), could explain the observed differences. Our results suggest that, independently of the season (and thus, the physico-chemical conditions of the water), at low total chl *a* concentrations, the amount of < 2 and > 2 µm organisms would increase in

parallel, while at higher concentrations, the contribution of the picoplanktonic fraction would be restricted by competition of the larger phytoplankton fractions.

It is widely accepted that the variability in total autotrophic biomass is associated with changes in large size fractions and that the picoplanktonic fraction is a rather constant component of the phytoplankton community (Malone 1980, Raimbault et al. 1988b, Magazzù et al. 1996, Rodríguez et al. 1998). However, in this study the picophytoplankton contributed significantly to enhance the total chl *a* concentration in winter and it was related with changes in total biomass in each season. In a similar way, in the Atlantic Ocean, Marañón et al. (2001) found that the changes in total phytoplankton abundance and productivity were due to the variability on the picoplanktonic size fraction. As these authors commented, the constancy of picophytoplankton would be true only if concentration changes of several orders of magnitude are considered as a threshold for variability.

The spatial distribution of the contribution of the < 2 µm size fraction to total biomass (from integrated values) showed differences among seasons (Fig. 9). While in autumn there was a trend towards an increasing contribution of this size fraction from coastal to off-shore stations, in winter no clear patterns were observed (although, as in autumn, the lowest contributions of this size fraction was observed in the coastal area) and in summer the picophytoplankton contribution was practically homogeneous throughout the sampling area. The differences observed among seasons in the relative contribution of the < 2 µm chl *a* to total biomass could be related to nutrient inputs from the Ebro river into the coastal zone and to water column stability. In autumn and specially in winter, the nutrient input from the river and mixing processes would be enough to enhance the growth of the largest (> 2 µm) size fractions of the phytoplankton community in the coastal area (Fig. 6c, f). Thus, in this zone, the contribution of the picophytoplankton was lower than in off-shore stations. In summer, although the nutrient inputs from river discharge were in the same order of magnitude than in autumn (Salat et al. 2002), the higher water column stability due to stratification could restrict the growth of the largest fractions of phytoplankton and thus, the size structure of the phytoplankton community was similar in coastal and off-shore regions. Taking into account several Mediterranean ecosystems, Magazzù & Decembrini (1995) observed that, on average, the percentage of the < 2 µm chl *a* fraction was similar in oceanic (57 %) and coastal (64 %) environments. Concretely, in a late-spring cruise, Delgado et al. (1992) observed in the Catalan Sea (NW Mediterranean) that the percentage of < 2 µm chl *a* varied from 21 % (coastalmost st.) to 27 % (oceanic st.). However, in the same area of the Catalan Sea, in summer, Arin (unpublished data) found an increase of the percentage of < 2 µm chl *a* from coastal to off-shore stations (form 31 to 58 % in June 1995 and from 21 to 54 % in June 1996). The results obtained in this study and those observed in other

regions of the NW Mediterranean suggest a high spatio-temporal variability of the size structure of the phytoplankton community.

Vertical distribution patterns

The total amount of the autotrophic biomass was poorly represented in the superficial waters (down to 10 m), specially in autumn and summer, when deep chl *a* maxima were observed. In these seasons, the chl *a* in the upper layers of most of the off-shore stations was less than 10 % of the whole chl $a_{int100m}$. In winter, this percentage increased until 20 or 40 % (Fig. 7). This finding has clear implications in the use of remote sensing techniques. Ocean colour sensors will detect pigments within only one optical depth, which can be defined as the depth at which surface irradiance is attenuated to 1/e = 37 % of its intensity at surface (Joint & Groom 2000). Thus, algorithms used for the estimations of chl *a* and primary production (Eppley et al. 1987, Gitelson et al. 1996) are based on pigment concentrations in the upper euphotic zone, which may represent a small percentage of the total biomass, specially in areas where there are subsuperficial or deep chl *a* maxima. Knowledge of the proportion of small and large fractions in the phytoplankton community is also important for calculations of chl *a* concentration from satellite images due to their different attenuation coefficients. The specific attenuance of phytoplankton chlorophyll is much larger in oligotrophic waters than elsewhere probably by the presence of a high percentage of small phytoplankton, including coccolithophorids, the cells of which are covered by calcareous scales (Megard & Berman 1989, Gitelson et al. 1996). Some coccolithophorids forms tend to inhabit the upper layers of the water column, as found by Cros (2001) in the same cruises of this study and in other areas of the NW Mediterranean Sea.

In autumn and winter, the percentage of < 2 µm chl *a* tended to be higher at depths of maximum total chl *a*, while in summer the lowest percentages of the < 2 µm size fraction were located at or near the DCM depth (Fig. 5). Both types of relationship between the vertical distribution of the < 2 µm size fraction and total chl *a* maxima have been observed in different areas of the Mediterranean (see review of Maggazù & Decembrini 1995) in conditions of marked or moderate water stratification. As deep chl *a* maxima represent, in general, regions of active phytoplankton growth (Estrada 1985), a relatively high proportion of the large fractions could be expected, although factors such as grazing could locally modify the size structure of the phytoplankton community. However, in our case, the vertical variations in the proportion of < 2 µm chl *a* were small, and the different patterns found among cruises must be interpreted with caution. In winter, the dominance of the > 2 µm size fraction at depths below the total chl *a* maxima, where low irradiance probably

impeded the active growth of large organisms, may be a consequence of sedimentation of senescent cells from superficial layers.

In conclusion, the all size fractions of the phytoplankton community of the Ebro shelf area presented a seasonal variability related with changes on the physico-chemical characteristics of the zone. In contrast with the widely accepted paradigm about the constancy on the picophytoplankton abundance, in this study we found that this fraction varied among seasons and contributed markedly to changes of total phytoplankton biomass. In autumn and summer, when deep chl *a* maxima were observed, only less than 10 % of the water column integrated chl *a* values (total and fractions) were represented in the superficial waters. This finding is important for the estimation of chl *a* and primary production by remote sensing techniques.

ACKNOWLEDGEMENTS

We are grateful to all the people on board R/V “García del Cid” and specially to Gustavo Carreras and Susanna Plá for their help during the cruise. This work was supported by the MAST-III Programme (MAST3-CT95-0037). The FANS cruises were cofunded by the Spanish Comisión Interministerial de Ciencia y Tecnología (MAR96-2268-C03-01-CE).

Combined effects of nutrients and small-scale turbulence in a microcosm experiment. II. Dynamics of organic matter and phosphorus

ABSTRACT

In the oligotrophic sea, phytoplankton and bacteria compete for nutrients. Turbulence changes the outcome of this competition by means of an increase in the nutrient flux to cells by the shear fields, which is cell size dependent. This effect is insignificant for small cells such as natural bacteria. The hypothesis is that turbulence will increase the phytoplankton competition-capability for nutrients and reduce the organic matter utilisation by bacteria. Consequently, the composition of particulate organic matter should change. To test this hypothesis we studied the response of natural plankton communities to turbulence enclosed in 15 L microcosms. We evaluate the response in terms of the ratio of heterotrophic:total biomass and the stoichiometry of particulate organic matter. Results under turbulent and still conditions were compared in 3 nutrient-induced conditions: nitrogen surplus (N with initial addition of an excess of nitrogen, N:P ratio = 160), nitrogen:phosphorus ratio balanced (NP with initial addition of nitrogen and phosphorus as Redfield ratio, N:P ratio = 16) and control (C no nutrient addition). In N and NP conditions, turbulence decreased the heterotrophic:total biomass ratio up to two-fold, and induced changes in the stoichiometry of the particulate organic matter. We found higher values of carbon:phosphorus and nitrogen:phosphorus ratios in turbulent than in still treatments. The magnitude of these responses to turbulence depended on the induced nutrient conditions. In the control microcosms we found the maximum differences of carbon:phosphorus ratio between turbulence and still treatments. In terms of biomass the response to turbulence was clear in the enriched conditions and insignificant in the control microcosms.

INTRODUCTION

In the oligotrophic NW Mediterranean Sea, phosphorus (P) has been suggested to be the limiting nutrient for phytoplankton (Margalef 1997, Thingstad et al. 1998) as well as for heterotrophic bacteria (Thingstad et al. 1993, Thingstad et al. 1998, Zweifel et al. 1993, Sala et al. 2002). The outcome of the competition for nutrients between bacteria and different sizes of phytoplankton has implications for the structure and function of the pelagic food web. If small cells dominate the uptake of nutrients, the "microbial" food web will be favoured with respect to the "classical" food chain (Legendre & Le Fèvre 1991). Under P-limiting conditions, the ability of a cell to compete with others will depend, in principle, on its affinity constant for P. Theoretically, the affinity constant (α) for orthophosphate can be calculated from the physical law of diffusion (Thingstad 1998):

$$(1) \qquad \alpha = 3\ D\ \sigma^{-1}\ r^{-2},$$

where D is the diffusion coefficient for phosphate ($\approx 4.8 \times 10^{-6}$ $cm^2\ s^{-1}$), σ is the volume specific P-content (µmol P cm^{-3}) and r is the cell radius (cm). Due to their size, bacteria, pico and nanophytoplankton are expected to outcompete larger phytoplankton species under nutrient limitation (see Table 1). However, the relative advantage of the smaller hetero- and autotrophic components can be reduced in the presence of turbulent mixing. It has been suggested that small-scale turbulence will favour large non-motile phytoplankton cells by keeping them suspended in the euphotic zone of the water-column and by replacing the nutrient-depleted water around them (Pasciak & Gavis 1974, Lazier & Mann 1989, Kiørboe 1993, Karp-Boss et al. 1996).

Studies of nutrient uptake and phytoplankton growth under turbulence are scarce. Pasciak & Gavis (1975) found a Michaelis-Menten type relationship between nitrate uptake rate and shear rate for the large diatom *Ditylum brightwellii* at low nitrate concentrations. Savidge (1981) observed increased growth and uptake of the diatom *Phaedactylum tricornutum* when agitated under P-limited conditions. In natural waters, where other components of plankton are present, turbulence can change the relative importance of autotrophs to heterotrophic bacteria (Arin et al. see *Chapter II*). These two biomass compartments have different nutrient:carbon demands. Thus we speculate that turbulence could change the dynamics of nutrient concentrations. The availability of nutrients has been shown to affect the stoichiometry of organic matter. Guildford & Hecky (2000) found higher carbon:phosphorus ratios in P-limiting conditions. Thomas et al. (1999) found deviations of the Redfield ratio associated with a high contribution of recycling nutrients.

Table 1 - The theoretical affinity constant (α) estimated for different organisms from the physical law of diffusion (Eq. 1) by assuming spherical shapes. The cell carbon contents were calculated as 0.35 pg C μm^{-3} for bacteria (Bjørnsen 1986), 0.433 x $(\mu m^3)^{0.863}$ pg C $cell^{-3}$ for nanoflagellates (Verity et al. 1992) and 0.109 x $(\mu m^3)^{0.991}$ pg C $cell^{-3}$ for diatoms (Montagnes et al. 1994). Carbon contents were converted to phosphorus by a ratio of 50 and 106 for bacteria and phytoplankton, respectively. The literature values of the affinities are from a review by Vadstein & Olsen (1989).

Organism	Radius µm	Volume specific P-content µmol-P cm^{-3}	Theoretical affinity l µmol-$P^{-1}h^{-1}$	Literature affinity l µmol-$P^{-1}h^{-1}$
Bacteria	0.25 - 0.75	583	16 - 142	30 - 146
Pigmented nanoflagellates	1 - 3	515 - 590	1.1 - 8.9	2 - 17
Diatoms	3 - 10	170 - 174	0.3 - 3.3	0.9 - 10

In this paper, we examine the dynamics of nutrients in relation to the response of plankton to turbulence in experiments with Mediterranean coastal waters. As P is often the limiting nutrient in these waters, we studied the variations of P in the particulate (POP) and dissolved (DOP) organic forms, as well as in the soluble reactive phosphorus (SRP). We hypothesise that small-scale turbulence will affect P turnover-rate and plankton structure by favouring large osmotrophic organisms. We also expected these effects on plankton to be reflected in the quality of particulate organic matter. To test these hypotheses we enclosed natural plankton communities in 15 L microcosms and studied their response to turbulence under different N:P ratio conditions.

MATERIAL AND METHODS

The microcosm experiment

Sea water was collected ca 1 km offshore of the Catalan coast north of Barcelona (Spain). The sub-surface water was screened through a 150 µm Nytex mesh to remove mesozooplankton and transported in clean 50 L containers. In the laboratory, water was distributed in twelve 15 L cylindrical containers (made of transparent Plexiglas, 24.2 cm inner diameter and 34.5 cm depth). The enclosures were divided into 3 series: controls with no nutrient addition (C), enriched with a nitrogen-surplus addition (N) and enriched following the nitrogen:phosphorus Redfield ratio (NP), and incubated under still (S) and turbulent (T) conditions (Table 2). Each combination of treatments had two replicates. Nutrients were added at the beginning of the experiment according to Table 2. In N and NP containers, silicate and metals were also added. The metal solution was added in the same proportion to nitrate as in f/2 medium (Guillard 1975). The experiment was carried out in an environmental chamber at 15 ± 1 ^{o}C under a 12h:12h light:dark cycle and at light irradiance of

225 µmol photons m^{-2} s^{-1} within the containers. Small-scale turbulence was generated by a system of vertically oscillating grids as described in Arin et al. *Chapter II*. The turbulent kinetic energy dissipation rate (ε) was estimated as 0.055 cm^2 s^{-3}.

Inorganic and organic nutrients

Inorganic nutrients, namely soluble reactive phosphorus (SRP ≈ PO_4), NO_3, NO_2, NH_4 and SiO_3, were determined daily in all the containers, with an Alliance Evolution II autoanalyzer following standard procedures as described in Grasshoff (1983). Particulate and dissolved organic phosphorus and nitrogen were determined by wet oxidation into SRP and NO_3. Analyses were done in one series of replicates (A) daily from Day 0 until Day 7 except for Day 5. Subsamples of 250 ml were taken in polyethylene bottles and filtered through pre-combusted GF/F filters under gentle vacuum (< 50 mm Hg). The filters were stored in tinfoil envelopes at - 20 ºC. Simultaneous determination of particulate organic phosphorus and nitrogen (POP, PON) was achieved following the persulphate oxidation procedures of Pujo-Pay & Raimbault (1994). In brief, 20 ml Milli-Q water and 2.5 ml persulphate + boric acid reagent were added to the filter in glass vials, and autoclaved at 120 ºC for 30 min. Then, samples were centrifuged to remove filter remains and analysed for PO_4 and NO_3 + NO_2 in the autoanalyser as above. The standard error of analysis was generally within 10 %. The same wet oxidation method was also applied to the total dissolved P (TDP) determination in the filtrates (Koroleff 1983, Valderrama 1995). In glass vials, thirty-ml aliquots were mixed with 4 ml of the oxidant reagent, autoclaved under the same conditions as for POP and autoanalysed. Dissolved organic P (DOP) was calculated by subtracting SRP from TDP. Standard error of analysis replicates for DOP was generally within 25 %.

Sedimented phosphorus

To gain a more complete picture of P dynamics, sedimented particulate phosphorus had to be determined. Accumulation of biomass on the bottom was evident in several of the containers; however, we did not sample and measure it directly as we wanted to avoid disturbing the system. Thus, sedimented POP was estimated as follows. Assuming that P could not be lost from the container because its air-water exchange through volatile forms is insignificant, the value of the P burden for each treatment was fixed as the concentration of total P on Day 0, right after the addition of nutrients. Then, sedimented POP at Day i was estimated by subtracting the measured P pools in the water column from the total P burden, i.e.: sedimented POP_i = P burden - $(PO_4 + DOP + POP)_i$.

Table 2 – Summary of the treatments (each treatment has two replicates) with the initial added nutrient concentrations (µM). No nutrients were added in the control enclosures (SC and TC). Dissolved inorganic nitrogen (DIN) and silicate (Si) concentrations (µM; mean of two replicate microcosms ± SE) at Days 0 and 4 in each treatment and the osmotrophic biomass increase:dissolved inorganic nitrogen consumed (OBI:DINC) and diatom biomass increase:Si consumed (DBI:SiC) ratios (both in µM:µM) from Day 0 to 4. Due to the low inorganic nutrient concentrations and a poor increase in biomass these ratios were not calculated in the control enclosures.

	Initial nutrient addition			DIN		OBI:DINC	Si O_3		DBI:SiC
	PO_4	NO_3	SiO_3	Day 0	Day 4		Day 0	Day 4	
SC	-----	-----	-----	0.24 ± 0.01	0.23 ± 0.04	-----	0.37	0.51 ± 0.03	-----
TC	-----	-----	-----	0.36 ± 0.07	0.16 ± 0.005	-----	0.25 ± 0.005	0.25 ± 0.04	-----
SN	0.1	16	30	21.35 ± 1.71	14.36 ± 0.55	0.49 ± 0.29	35.97 ± 1.32	25.88 ± 0.63	0.07 ± 0.07
TN	0.1	16	30	19.58 ± 0.50	13.44 ± 0.54	5.35 ± 0.42	33.88 ± 0.22	21.65 ± 0.03	1.38 ± 0.17
SNP	1.0	16	30	18.72 ± 0.17	11.04 ± 0.07	2.82 ± 0.46	33.44 ± 0.33	22.83 ± 0.05	0.13
TNP	1.0	16	30	18.97 ± 0.26	1.62 ± 0.76	5.02 ± 0.31	33.00 ± 0.22	19.34 ± 1.02	4.63 ± 0.84

Phosphate turnover-rate

The turnover-rate K (h^{-1}) of phosphate was measured by adding radioactively labelled orthophosphate to subsamples from one series of replicates (A) of each treatment at Day 0 to 7 (except Day 5).

K is defined as the speed of exchange of a phosphate concentration C by a community of uptake rate U:

$$(2) \qquad K = U\, C^{-1}$$

Uptake of radiolabelled orthophosphate was measured by adding 100 μl carrier-free $^{33}PO_4^{3-}$ (Amersham) to 10 ml subsamples in scintillation vials to give a final radioactive concentration of 2 x 10^5 to 4 x 10^5 dpm ml^{-1}. From each microcosm, three or four subsamples were incubated for between 5 min and 5 h depending on the expected turnover-rate. Temperature and light irradiance was similar to the experimental containers. Incubations were terminated by adding a cold chase of 100 μl 0.01 M K_2HPO_4 to the vials. Subsamples of 3.3 ml were filtered through 25 mm polycarbonate filters of 0.2 μm. To minimise cell breakage, filters were supported by Whatman GF/F glass-fibre filters saturated with 0.1 M K_2HPO_4. Suction was applied and increased gradually until all samples had passed through the 0.2 μm filters and then increased to a maximum pump capacity of 0.7 bar until the filters were dry. Blanks were determined each day by adding the cold chase to the subsample before the isotope. The filters were transferred to polyethylene scintillation vials (Zinnsner) and counted in 7 ml Ultima-Gold XR in a Beckmann liquid scintillation counter. The exact start concentration of the added $^{33}PO_4^{3-}$ was determined by transferring 100 μl subsample to each of three plastic vials with 7 ml scintillation fluid. Turnover-rate of phosphate K was calculated from the equation:

$$(3) \qquad K = -\ln (1 - f)\, t^{-1},$$

where t is the incubation time and f the fraction of added isotope retained on the 0.2 μm filters corrected for blanks. The radioactivity of blanks was below 4000 dpm and the signal:blank ratio was higher than 6.2 in C and N containers and higher than 2.5 in NP containers.

Plankton biomass

Phytoplankton biomass was monitored by daily chlorophyll *a* (chl *a*) measurements and converted to carbon biomass using a factor of 30 (Strickland 1960). Chl *a* was analysed fluorometrically (Yentsch

& Menzel 1963) after extraction in 90 % acetone. In addition, phytoplankton biomass was also estimated by their group composition. On Days 0, 4 and 8, abundances were determined for the diatoms, dinoflagellates and coccolithophorids using an inverted microscope (Utermöhl 1958), for the autotrophic picoeukaryotes, *Synechococcus* and *Prochlorococcus* by flow cytometry (Gasol & del Giorgio 2000) and the autotrophic nanoflagellates were enumerated by epifluorescence microscopy (Porter & Feig 1980). Carbon contents were estimated from the following conversion factors: diatoms, dinoflagellates and coccolithophorids: pg C $cell^{-1}$ = 0.109 x $(\mu m^3)^{0.991}$ (Montagnes et al. 1994); *Synechococcus*, 0.357 pg C μm^{-3} (Bjørnsen 1986, Kana & Gilbert 1987, Verity et al. 1992); picoeukaryotic and autotrophic nanoflagellates, pg C $cell^{-1}$ = 0.433 x $(\mu m^3)^{0.863}$ (Verity et al. 1992) and for *Procholococcus,* 0.133 pg C μm^{-3} (Simon & Azam 1989).

The heterotrophic components of the plankton biomass (bacteria + heterotrophic nanoflagellates + ciliates) were also estimated on Days 0, 4 and 8. Abundances were determined for heterotrophic bacterial abundance by flow cytometry (Gasol & del Giorgio 2000), for heterotrophic nanoflagellates using epifluorescence microscopy (Porter & Feig 1980) and for ciliates using an inverted microscope (Utermöhl 1958). Bacterial biomass was estimated using a carbon conversion factor of 0.35 pg C μm^{-3} (Bjørnsen 1986). The same conversion factor as for autotrophic nanoflagellates was used for heterotrophic nanoflagellate organisms. For ciliates, carbon conversion factors of 0.2 pg C μm^3 (Putt & Stoecker 1989) and 0.053 pg C μm^3 (Verity & Langdon 1984) were used for non tintinnids and tintinnids, respectively. More details on plankton counts and biomass calculations are reported in Arin et al. *Chapter II*).

On Day 8, one replicate of the TN and TNP containers was sampled because the other replicate was left for another experiment. In this paper the term “osmotrophic biomass” is used in reference to phytoplankton plus bacterial biomass in terms of carbon, while the term “living carbon” refers to the whole plankton community. The osmotrophic biomass increase (OBI) was calculated during the first four days of the experiment taking into account the estimated sedimented fraction. To estimate the OBI, the biomass of osmotrophs on Day 0 is subtracted from the biomass on Day 4 (biomass in the column water + sedimented biomass). As we only measured the sedimented biomass of osmotrophs on Day 8, we estimated the sedimented biomass on Day 4 in two ways by considering that: (1) sedimentation was constant over the time course of the experiment and (2) the sedimentation across the experiment was proportional to the biomass in the column. As we did not find any significant differences between both estimations, we used the former one to calculate the OBI.

Statistical analyses

All statistical analyses were conducted using the SYSTAT software package. Analysis of covariance (ANCOVA) was applied to different variables using the times of sampling as the covariate. Statistical significance was considered as $p \leq 0.05$ for each of the independent variables (presence or absence of turbulence; nutrient addition treatment). Data are usually presented as means and standard errors of the replicates of each experimental treatment. For organic P and N compounds as well as for P turnover data, the errors are related to the analytical replicates as we only sampled one container of each condition for those variables.

RESULTS

Phosphorus dynamics

The dynamics of phosphorus in the control containers (C) behaved similarly over time (Fig. 1). The suspended particulate fraction (POP) was very low and decreased slightly from 0.1 µM to 0.04 µM between Days 1 and 6. The phosphate concentration varied between 0.02 and 0.13 µM and DOP decreased from 0.08 µM to zero. In the N series, the suspended biomass increased one day after the addition of nutrients (0.11 ± 0.02 and 0.16 ± 0.01 µM in SN and TN, respectively). Sedimentation took place mainly in SN with a final settled biomass on Day 6 of 0.11 µM that corresponds to 55 % of total (suspended + settled) biomass.

There were no significant differences in the phosphate concentration (0.04 - 0.10 µM) and DOP (< 0.13 µM) between the turbulent and still containers. In the NP series, the biomass increased considerably due to the enrichment. The suspended biomass peaked on Day 4 with 0.32 and 0.65 µM in SNP and TNP, respectively, and was followed by a small decrease. Sedimentation was, however, important in both containers, where the estimated settled biomass on Day 6 was 0.56 and 0.62 µM in SNP and TNP, respectively. The higher biomass build-up in TNP resulted in faster depletion of phosphate than in SNP. Phosphate concentrations on Day 6 were below detection limit in TNP and 0.31 µM in SNP.

Initial P turnover-rate before nutrient additions was 1.1 h^{-1} (Fig. 2). In general, we found higher values of P turnover-rate in turbulent treatments (ANCOVA, $p = 0.069$), especially in the NP containers. In the C and N series, the turnover-rate varied between 0.2 and 1.9 h^{-1}. In the NP series, the turnover-rate increased with decreasing P concentrations and was strongest in TNP (from 0.005 to 1.7 h^{-1} between Days 1 and 6).

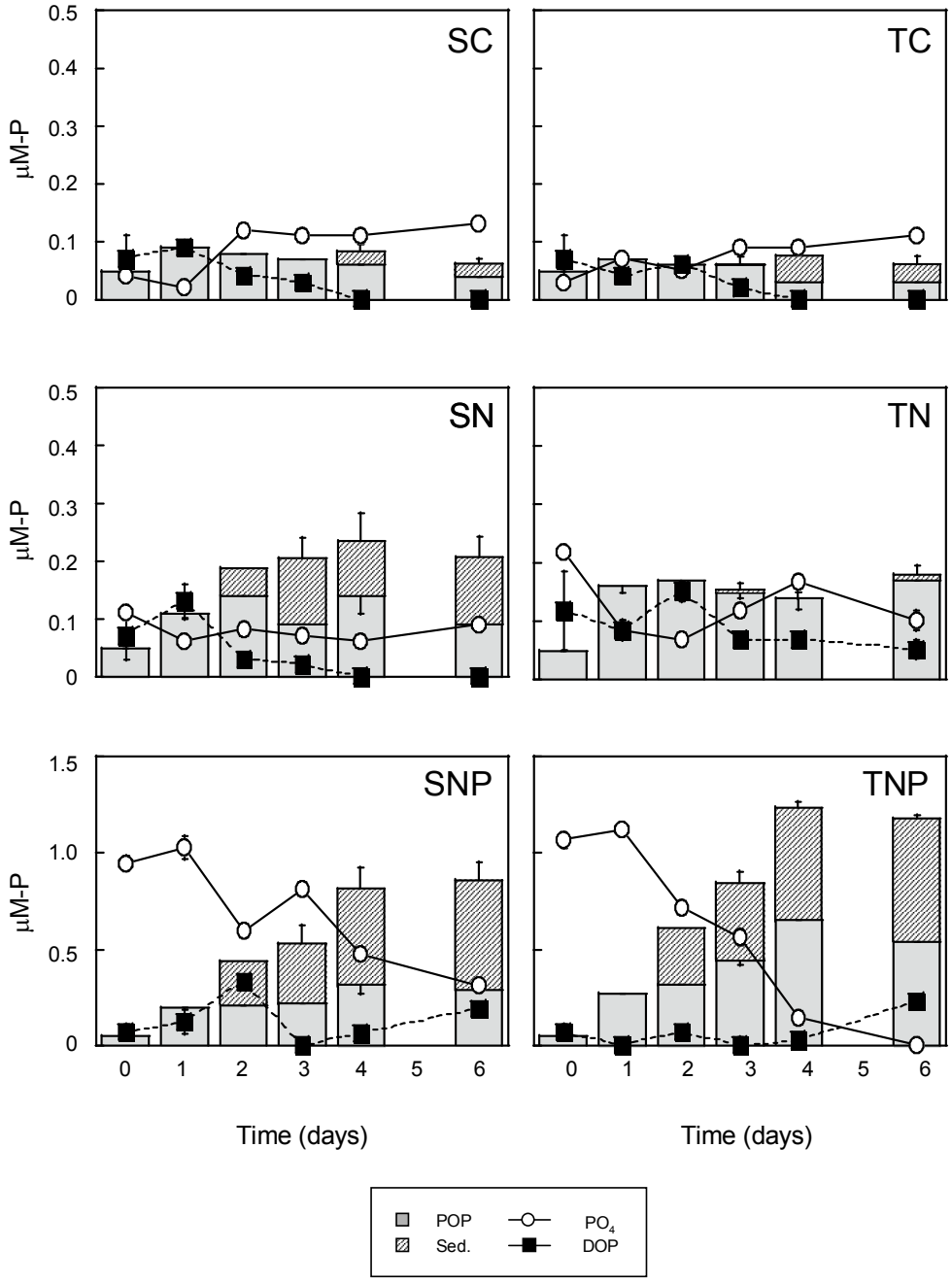

Fig. 1 – The mass balance of phosphorus with time expressed as particulate organic phosphorus (POP), the estimated sedimented phosphorus (Sed), inorganic phosphate (SRP ≈ PO_4) and dissolved organic phosphorus (DOP). (S = still, T = turbulence, C = control, N = N-surplus, NP = nutrient balance). Mean of two replicate microcosms per treatment ± SE for PO_4 values. Analytical means ± SE for POP (below the value) and DOP. Errors transmissions are shown for the calculated sedimented values (above the value).

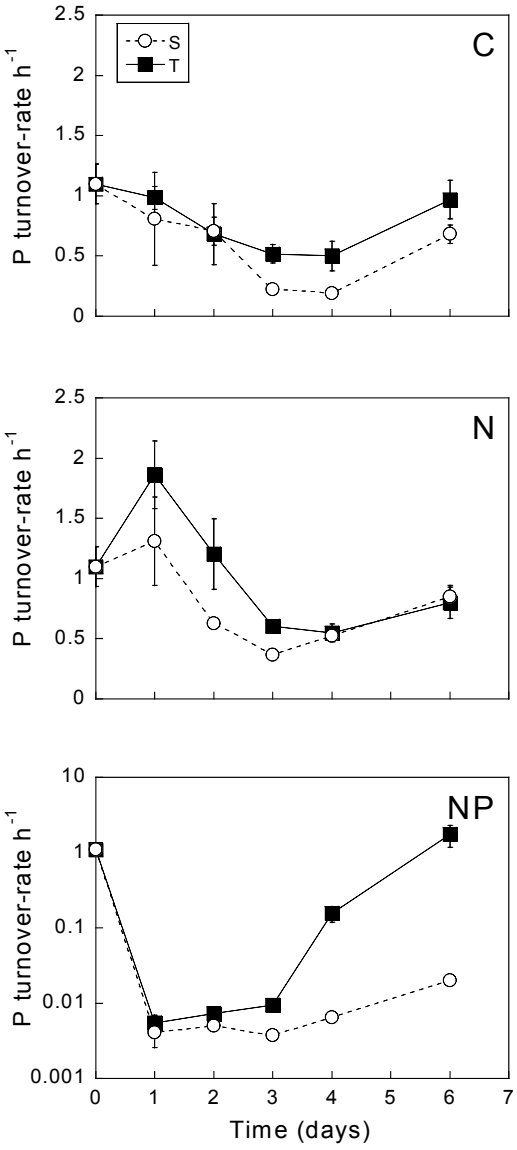

Fig. 2 – The turnover-rate (h^{-1}) of phosphate during the experiment. Symbols are the mean of three to four analytical replicates ± SE. (S = still, T = turbulence, C = control, N = N-surplus, NP = nutrient balance). Note logarithmic scale in the NP treatment graph.

Plankton biomass

The experiment starts with a phytoplankton biomass of around 30 µg C l^{-1} (Fig. 3). A slight increase of this biomass was observed in the control containers at the beginning of the experiment which then decreased to around 1.2 µg C l^{-1}. No significant differences were observed between the still and turbulent containers for this nutrient condition over the course of the experiment. In the enriched

enclosures (N and NP), phytoplankton biomass was significantly higher with turbulence ($p < 0.001$). In the TN containers an increase of phytoplankton was observed during the experiment (up to 304 μg C l^{-1} on Day 8), while in TNP phytoplankton biomass peaked on Day 4 (with 571 ± 32 μg C l^{-1}) and was followed by an abrupt decrease until Day 8. In SN and SNP, phytoplankton biomass increased to a maximum of 110 ± 75 and 125 ± 6.3 μg C l^{-1}, respectively, by the end of the experiment on Day 8. On Day 4, for all nutrient conditions, diatom biomass (in terms of carbon) was higher in the turbulent than in the still treatments (Table 3).

Table 3 – Diatom biomass (μg C l^{-1}) and diatom mean volume per cell (μm^3 $cell^{-1}$) and mean surface:volume ratio (mean of two replicate microcosms ± SE) on Day 4 for the still (S) and turbulent (T) containers of the C (control), N (N-surplus) and NP (Redfield ratio) treatments.

	Biomass (μg C l^{-1})	Mean volume (μm^3 $cell^{-1}$)	Mean Surface:volume
SC	2.6 ± 0.2	647 ± 43	1.04 ± 0.035
TC	4.4 ± 0.4	646 ± 135	1.00 ± 0.070
SN	44 ± 13	644 ± 61	1.04 ± 0.025
TN	243 ± 29	1892 ± 109	0.51 ± 0.005
SNP	55 ± 0.2	669 ± 45	0.98 ± 0.015
TNP	787 ± 69	1688 ± 55	0.47 ± 0.020

Osmotrophic biomass shows practically the same pattern as phytoplankton biomass (Fig. 3). The contribution of bacteria to total osmotrophic biomass was, on average, higher in the control (45 %) than in the nutrient enriched containers (20 %).

The percentage of heterotrophic to total biomass in control containers increased during the experiment to ca. 80 % (Fig. 3). A lower contribution of heterotrophs was observed in N and NP containers. Heterotrophic biomass was lower than 20 % on Day 4 in the TNP treatments and on Day 8 in the TN treatments coinciding with the highest values of phytoplankton biomass. For each nutrient condition, a higher percentage of heterotrophic:total biomass was observed in the still than in turbulent containers ($p \leq 0.05$, analysis of variance considering Days 4 and 8 as levels of a categorical variable), except in the controls where similar values were found (Fig. 3).

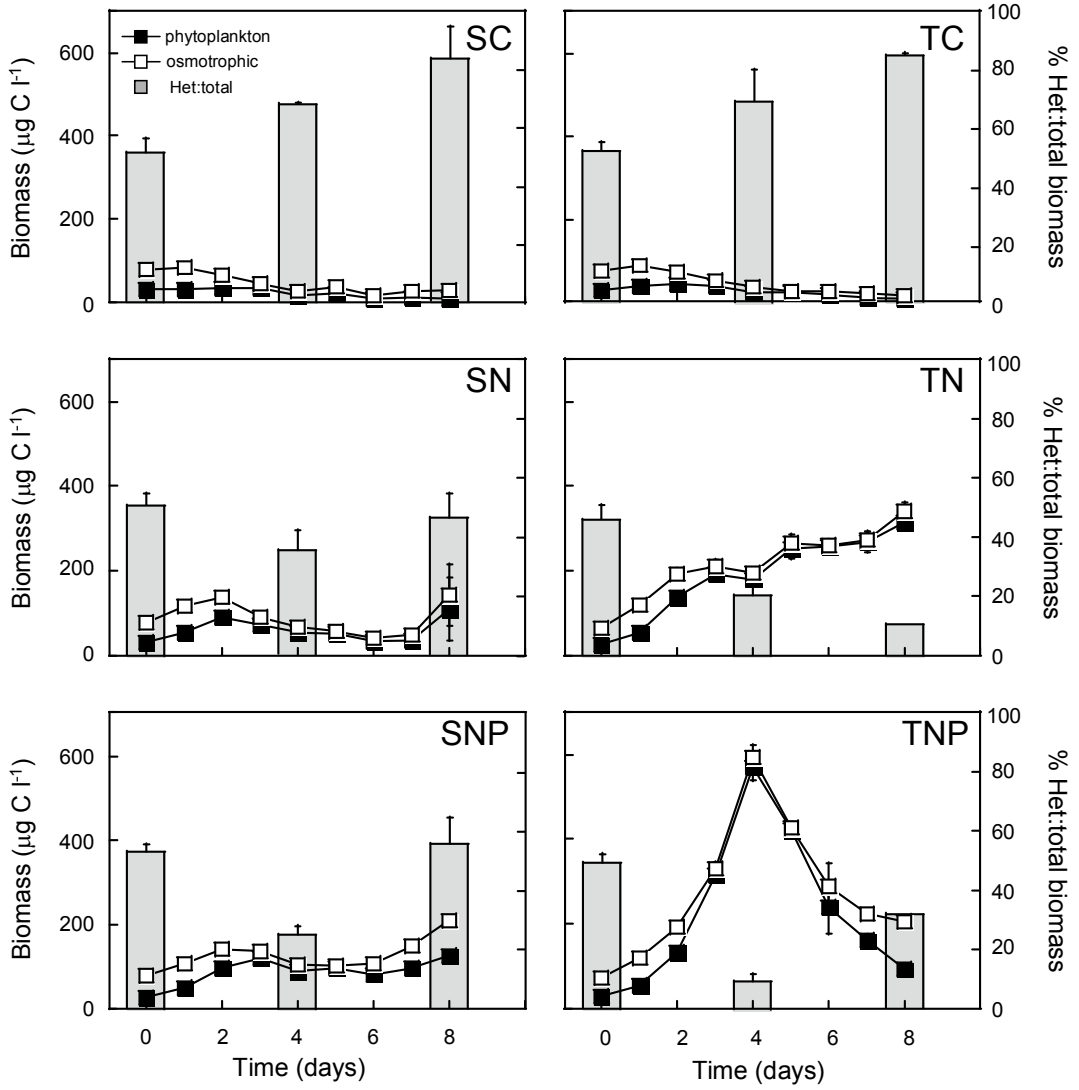

Fig. 3 – Phytoplankton and osmotrophic biomass (µg C l^{-1}) during the experiment and percentage of heterotrophic biomass to total biomass on Days 0, 4 and 8. (S = still, T = turbulence, C = control, N = N-surplus, NP = nutrient balance). Mean of two replicate microcosms per treatment ± SE. No replicates for TN and TNP were available on Day 8.

Particulate organic matter composition and nutrient consumption

In conditions without nutrient additions, the ratio PON:POP showed significantly higher values in turbulent than in still treatments throughout the experiment. In the nutrient added conditions (N and NP) the ratio showed, in general, higher values with turbulence after Day 4, although when analysing the whole data set the differences between still and turbulent treatments were not significant (Fig. 4).

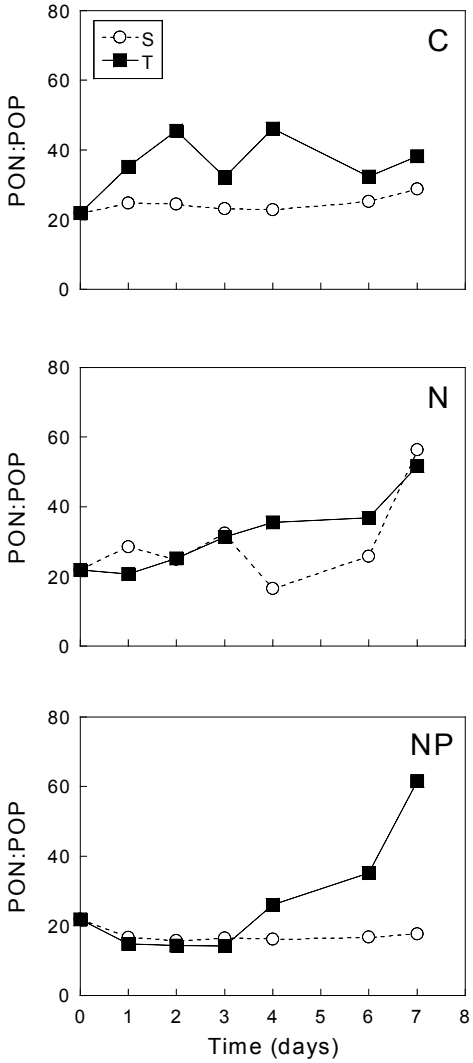

Fig. 4 – Particulate organic nitrogen:particulate organic phosphorus (PON:POP) ratio during the experiment. Symbols are the mean of three analytical replicates ± SE (S = still, T = turbulence, C = control, N = N-surplus, NP = nutrient balance).

We found significant differences from Day 4 to 8 (ANCOVA, $p < 0.01$). In the N and NP conditions, OBI in relation to inorganic phosphate consumed (IPC) was significantly higher in turbulent containers than in the still ones (Fig. 5a, t-test: $p = 0.006$ for N and $p = 0.05$ for NP). Higher values of this ratio were observed in TN than in TNP (12 %, $p = 0.006$) while this was not so clear in SN compared to SNP (1 %, $p = 0.09$).

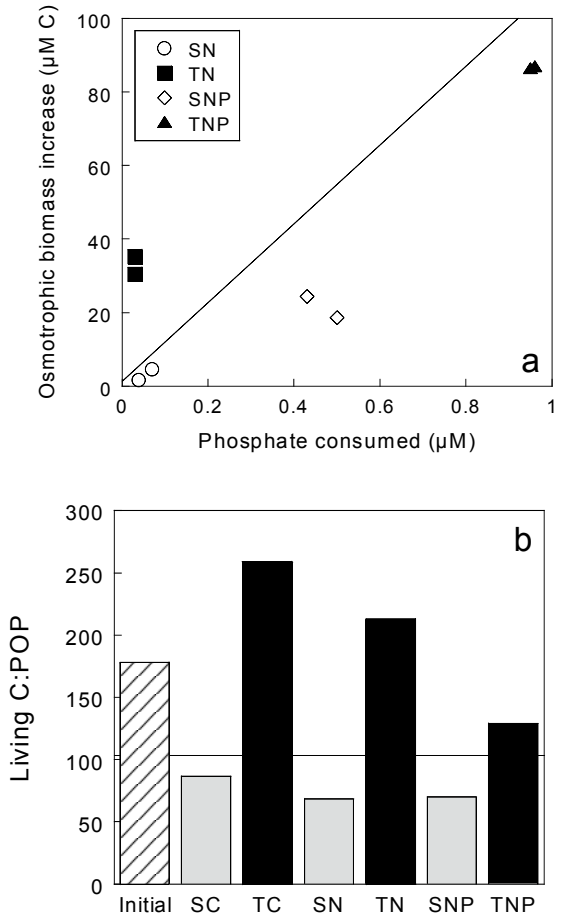

Fig. 5 – (a) Osmotrophic biomass increase (µM carbon) vs. phosphate consumed (µM) from Day 0 to 4. Note the two replicates of each treatment. (b) Living carbon:particulate organic phosphorus (Living C:POP) on Days 0 and 4. Lines indicate the value of Redfield ratio. (S = still, T = turbulence, C = control, N = N-surplus, NP = nutrient balance).

In addition, for each nutrient condition, OBI in relation to dissolved inorganic nitrogen consumed (DINC) was higher in turbulent than in still treatments (Table 2; t-test: $p = 0.01$ and $p = 0.06$ for the N and NP conditions, respectively). The diatom biomass increase (DBI) in relation to the silicate consumed (SiC) was significantly higher with turbulence for the N ($p = 0.02$) and NP ($p = 0.03$) conditions (Table 2). The same tendency was observed in the living C:POP ratio for Day 4 (Fig. 5b) which was higher in turbulent than in the still containers (t-test: $p = 0.03$) and within the turbulent treatments, it was higher in the non-enriched container (C).

DISCUSSION

Despite working with natural communities, the replicates for the different treatments behaved alike. We found no significant differences in nutrient, chl *a* concentrations or bacterial abundance between replicates. The good replicability in similar microcosm experiments has already been found in previous experimental studies (Marrasé et al. 1989, Peters et al. 2002). This argues in favour of the appropriateness of the experimental set-up used here to examine "cause-effect" relationships, when the initial water manipulations are carefully done.

The response to turbulence was different depending on the nutrient conditions. Without nutrient addition (C containers) it was very difficult to attribute changes in biomass to turbulence. Previous experiments also encountered difficulties in seeing an effect owning to turbulence under low nutrient concentrations (Petersen et al. 1998, Peters et al. 2002). The nutrient levels in the experiments conducted by Peters et al. (2002) were similar to those found in our control conditions. They found a slightly higher proportion of heterotrophs under turbulence and an increase of heterotrophy after enclosing the communities in all the treatments, except for the ones where nutrients were added. While in our case, turbulence did not induce a significant increase in heterotrophy in the non-enriched conditions, we did find an increase of heterotrophy towards the end of the experiment. This increase of heterotrophy probably reflects a dominance of recycling and regenerated production.

A different temporal trend of the trophic status of the system was found when nutrients were added. The addition of nutrients induced a phytoplankton increase during the first period of the experiment in all the containers, characterised by a decrease in heterotrophy (Fig. 3). After Day 4, phytoplankton biomass changed little (SN and SNP containers) or decreased abruptly (TNP containers) and an increase in the proportion of heterotrophs was observed in these treatments, except in the TN containers (see below). Thus, for plankton and nutrient dynamics, we detected two phases during the experiment. The first phase was fuelled by new production (phytoplankton absorbing nutrient additions) and the second phase (post-bloom) was driven by regenerated production. A specific response was found in turbulent treatments with N-surplus (TN), where the photosynthetic organisms were growing slowly and the system did not get to the post-bloom phase during the time course of the experiment. This, together with high P turnover-rate (from 1.8 to 0.5 h^{-1} during the first 4 days), seems to indicate a faster P recycling in N-surplus conditions favouring autotrophic growth. Other experiments performed with Mediterranean water also found an anomalous phytoplankton production with N-surplus in comparison with P-surplus additions (Granéli et al. 1999). These authors also attributed the exceptional phytoplankton growth to a fast recycling of P. We found that both nutrients and turbulence influenced the dynamics of plankton.

Changes over time in inorganic nutrients (Si, N and P) indicate a faster nutrient decrease under turbulence (Table 2). This faster consumption matched a faster increase of osmotrophic biomass (Fig. 3). In addition, the increase of osmotrophic biomass with respect to nutrient consumption during this period was clearly different in turbulent and still conditions. The ratio of osmotrophic biomass increase to inorganic nitrogen and phosphorus consumed (OBI:INC and OBI:IPC, respectively) was significantly higher in turbulent conditions (Table 2 and Fig. 5a). As sedimented biomass was taken into account to calculate OBI, we can not attribute the higher values of the ratio in turbulent treatments to differences in sedimentation or resuspension of osmotrophic biomass between treatments. In addition, when we compare the ratio living C:POP in the water column, we also find higher values under turbulent conditions (Fig. 5b). These higher values can not be explained by the differences in the proportion of heterotrophs or diatoms to the total biomass. This is because the controls (without nutrient additions) show the highest differences in living C:POP and no or low differences in the proportion of heterotrophs or diatoms between turbulent and still conditions (Fig. 3 and Table 3). A possible explanation for the high living C:POP in turbulent conditions is that, P was used faster, biomass increased faster and the community reached a P-deficient situation earlier than in still water. In this limiting situation, carbon assimilation and cell division were not affected equally by the limitation. This interpretation is supported by the fact that the values of PON:POP were higher in turbulent treatments compared to still ones after Day 4 (Fig. 4), and also by the higher values of P turnover-rate found in turbulent treatments. Although in principle we expect turnover-rate to increase with biomass, we did not find this trend. Actually, P turnover-rate and biomass were not significantly correlated, indicating that the faster turnover-rate was a response to a combination of factors not linearly associated to biomass.

When comparing the results across different nutrient conditions, both OBI:IPC and living C:POP ratios were higher in the microcosms without P additions. These results agree with Guildford & Hecky (2000), who compiled data from different systems. They found the highest values of the POC:POP ratio (up to five fold Redfield ratio) in systems where the total P (TP) was lower than 0.5 µM. In our study, the conditions with no or low P additions account for a TP of less than 0.3 µM, finding the highest values of the living C:POP ratio. It may be that under P deficiency, cell division decreases or stops while photosynthesis (carbon assimilation) continues. Since these two activities have different P demands (Margalef 1997), the stoichiometry of biomass would change. Guildford & Hecky (2000) found not only the highest values of the POC:POP ratio in systems with low TP but also the highest variability. For systems with less than 0.5 µM of TP, they found values of the POC:POP ratios that ranged from close to 100 to more than 600. In our study, the largest differences in the living C:POP ratio between turbulence and still treatments were found in the

microcosms were no or low amounts of P were added and TP was < 0.3 µM. Our results indicate that one possible cause of the high POC:POP ratio variability in natural systems could be the variability in hydrodynamic conditions.

We also found that the increase in diatom biomass with respect to Si consumed (DBI:SiC, Table 2) was higher in turbulent treatments. The mean diatom cell volume was larger under turbulence and therefore the mean surface:volume ratio was lower (Table 3). This could explain the lower demand for Si compared to carbon (mol:mol). These results, together with the aforementioned differences in P and N dynamics, indicate that the amount of carbon assimilated for one unit of nutrient (P, N or Si) was higher in turbulent conditions and that the stoichiometry of the particulate matter was affected by mixing. It has been shown that nutrient limitation influences the stoichiometry of organic matter, and the POC:POP and PON:POP ratios have already been used as indicators of nutrient limitations. Our observations highlight turbulence as a cause of variability in the stoichiometry of organic matter.

The values of the living C:POP ratio found in turbulent treatments had important deviations from Redfield ratios, especially in non-enriched conditions (2.1 times higher than the Redfield ratio), while in still treatments these values were close to or lower than Redfield. In terms of carbon fluxes, biological factors such as species' composition can influence carbon sedimentation rates. Our results showed larger cell sizes and a higher proportion of diatoms under turbulence (Table 3). This can favour sedimentation and therefore carbon sequestration, once the kinetic energy decays. Therefore, during mixing episodes, carbon assimilation could be underestimated if hydrodynamic factors are not considered. In our experiment, we had only two constant hydrodynamic conditions: still and turbulent (ε = 0.055 cm^2 s^{-3}). In nature, turbulent environments are the norm and mixing events are episodic. Therefore, further experiments varying the level and the duration of the exposure to turbulence will be necessary to elucidate the linearity of the response of the particulate organic matter. Caution should be taken in extrapolating the results of this study to all natural scenarios since we suspect that the response of the particulate organic matter will depend on the characteristics of mixing phenomena (depth of the mixing layer, duration and the intensity of the mixing event, etc). Nevertheless, this finding might be important for the construction of models with biogeochemical fluxes and indicates that hydrodynamic variables like turbulence should be examined when looking for trends in carbon and nutrient fluxes across systems. The significance of our results is that they provide evidence of the link between mechanical energy and geochemical fluxes through biological interactions.

ACKNOWLEDGEMENTS

We thank Mercedes Castaño for laboratory assistance, Roser Ventosa for nutrient analysis and Oscar Guadayol for turbulence intensity calculation for the NW Mediterranean. Further, we are grateful to Frede Thingstad for introducing the ^{33}P-method and to Michael Olesen for fruitful discussions. The comments and suggestions by three anonymous reviewers greatly improved previous versions of the manuscript. Aisling Metcalfe was of great help editing the English. This study was supported by the European projects MEDEA (MAS3-CT95-0016) and NTAP (EVK3-CT-2000-00022) and Spanish CICYT project (MAR 98-0854). MM acknowledges the Knud Højgaards fond, Denmark. This is the ELOISE contribution Nº 278/40.

Particulate DNA and protein relative to microorganisms biomass and detritus in the Catalano-Balearic Sea (NW Mediterranean) during stratification

ABSTRACT

Using microscopic and biochemical approaches, the relative contribution of the main groups of pelagic microorganisms (bacteria, heterotrophic nanoflagellates, phytoplankton and ciliates) and detritus (< 150 µm) to total particulate protein and DNA was investigated at two stations of the Catalano-Balearic Sea (NW Mediterranean) during the stratified period. The two stations, one located in the shelf break front (S) and the other in the open sea, above the central divergence zone (D), were sampled twice in early summer 1993. Both of them showed a well-developed deep chlorophyll maximum (DCM). Maximum DNA concentrations were observed close to the DCM, while protein concentrations were fairly homogeneous from surface to 60 m depth in all samplings. In general, the microorganism distribution showed maximum concentrations at or near the DCM depths. At both stations, bacteria were the most important contributors to living particulate DNA (22.5 to 32.6 %), while phytoplankton and heterotrophic nanoflagellates were the main contributors to living particulate protein (3.8 to 24.4 % and 2.9 to 29.1 %, respectively). In addition, an important amount of detritic DNA and protein was estimated to occur at both stations. Detrital DNA accounted for 23.9 to 42.9 % of the particulate DNA, while detritic protein represented from 63.5 to 84.7 % of the particulate protein. Because both protein and DNA contain nitrogen and DNA is also a phosphorus source, these results indicate that heterotrophic organisms and detritic particles play an important role in the nitrogen and phosphorus cycles in the open sea waters of the NW Mediterranean.

INTRODUCTION

The proportion between heterotrophic and autotrophic organisms, the contribution of the detritic material to the suspended organic matter, and the partitioning between the classic trophic chain and the microbial food web are basic questions about the structure and plankton dynamics in oceans. During the last twenty years many studies have changed some tenets about those topics. For instance, in contrast to the classical idea of a plankton community sustained by a broad base of autotrophs, there is now increasing evidence that the microbial food web dominates in oligotrophic waters (Cho & Azam 1987, 1990) and most biomass is heterotrophic (e.g. Dortch & Packard 1989, Gasol et al. 1997). This suggests that, in oligotrophic ecosystems, the plankton community would have a higher trophic efficiency than in eutrophic ecosystems.

In addition, the proportion of detrital organic matter appears to be relatively high in oligotrophic areas (Winn & Karl 1986, Boehme et al. 1993, Caron et al. 1995). Detrital matter may play an important role in aquatic ecosystems because it serves as food for filter-feeding animals (Posch & Arndt 1996, Wotton 1984), contributes to the vertical transport of organic matter (Passow & Alldredge 1994), and provides important substrates for nutrient remineralization and carbon cycling (Long & Azam 1996). However, data on the proportion of detritus to total particulate organic matter are still scarce.

In the oligotrophic open waters of the Catalano-Balearic Sea (NW Mediterranean) there are few data on the contribution of autotrophic and heterotrophic organisms and detritus to total suspended matter. In this area, the water column is stratified from early spring to late autumn and a deep chlorophyll maximum (DCM) is found at depths ranging from 40 to 90 m, coinciding with the nutricline (Estrada 1985a, 1985b, Estrada et al. 1993). Several studies have provided data on the distribution of different groups of planktonic organisms in relation with the DCM and the associated structures of the water column (Estrada 1985a, Alcaraz et al. 1985, Algarra & Vaqué 1989, Delgado et al. 1992, Dolan & Marrasé 1995, Calbet et al. 1996). However, the relative contribution of particular planktonic groups to total particulate matter (TPM) has only been approached partially by Alcaraz et al. (1985). These researchers found that the ratio of phytoplankton biomass to TPM and phytoplankton to mesozooplankton biomass (in terms of particulate nitrogen and carbon) was lower in the Mediterranean than in upwelling areas. But there are still no data on the relative contribution of the components of the microbial community and detritus to the TPM in the Mediterranean Sea.

Particulate DNA and protein concentrations are often used as indicators of biomass (i.e. living organisms) but there is evidence that in natural environments DNA and protein represent both living and non-living (detritic or non-replicating) particulate matter (Holm-Hansen 1969b, Paul et al. 1985, Winn & Karl 1986, Bailiff & Karl 1991, Boehme et al. 1993). DNA and protein are two important macromolecules in cell. DNA constitutes the genetic material and varies within a factor of two in eucaryotic cells (Berdalet et al. 1992, 1994); proteins, which constitute more than 50 % of the dry weigh in cells (Lehninger 1974) vary with nutrient (fundamentally nitrogen) availability (Dortch 1982, Dortch et al. 1984, 1985). Furthermore, because of their chemical composition, both molecules participate in the dynamics of nitrogen in the aquatic environment and DNA participates, in addition, in that of phosphorus. Additionally, particulate protein has a nutritional implications for animal feeding, because this compound provides a potential nutritive value.

The objective of the present work was to investigate the relative contribution of the autotrophic and heterotrophic components of the microbial community and of detritus to the suspended DNA and protein. This objective was approached by a combination of microscopic and biochemical techniques. The importance of the different DNA and protein partitioning is discussed in the context of nutrient cycles.

MATERIALS AND METHODS

Field sampling

The study was carried out in the Catalano-Balearic Sea, during the VARIMED 1993 cruise on board the R.V. "Hespérides". A transect, perpendicular to the coast of Catalonia (Fig. 1) was repeatedly surveyed between June 1 to 8, 1993 for the estimation of hydrographical parameters and chlorophyll *a* concentration. Two stations, one (S) located in the shelf break front (41°06' N, 2°23' E), and another (D) in the open sea (40°38' N, 2°45' E), above the central divergence zone of the Catalano-Balearic Sea were sampled twice to perform biochemical profiling and other biological studies (Fig. 1). Stations S and D were located approximately 30 km and 85 km offshore, respectively; sampling dates were June, 10 and 14, for station S, and June, 11 and 15, for station D.

At each station, a CTD cast was performed with a Neil Brown Mark III probe down to 1000 m, to obtain profiles of temperature, salinity and sigma-t. Water samples for major inorganic nutrients, oxygen, and chlorophyll *a* were obtained with a rosette of Niskin bottles, at 10 m intervals between 0 and 100 m, and at larger intervals between 100 and 400 m. Aliquots for phytoplankton

identification and estimation of ciliates, autotrophic and heterotrophic flagellates, and bacteria abundance were taken down to 100 m (except for heterotrophic flagellates on June 11). Samples for protein and DNA analyses were obtained at six selected depths (between 0 and 100 m). More details on the sampling strategy and the basic data of the cruise can be found in Masó & VARIMED Group (1995).

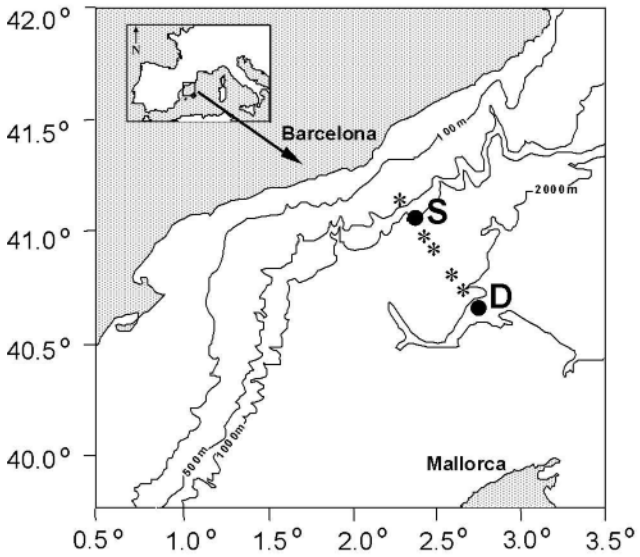

Fig. 1 – Main transect studied in the VARIMED 93 cruise during June. S and D indicate the location of the shelf break front and the open sea station, respectively.

Chlorophyll a analysis and plankton counts

Chlorophyll *a* concentration was estimated fluorometrically (Yentsch & Menzel 1963). Water samples (50 - 100 ml) were filtered through Whatman GF/F (25 mm) glass fiber filters, which were ground in 90 % acetone and left to extract for 30 minutes in the dark at room temperature. The fluorescence of the extract was measured with a Turner Designs fluorometer.

Bacterial samples were fixed with formaldehyde (4 % final concentration) and flagellate samples with glutaraldehyde (1 % final concentration). Samples for determination of bacterial (15 ml) and flagellates (50 ml) abundance were filtered through 0.2 µm and 0.8 µm pore diameter black polycarbonate filters, respectively. Both types of samples were stained with the DNA specific fluorescent stain DAPI and counted with an epifluorescence microscope (Porter & Feig 1980).

Phototrophic and heterotrophic nanoflagellates (PNF and HNF, respectively) were counted separately. Samples for phytoplankton counts (100 ml) were fixed with a formalin-hexamine solution (Throndsen 1978) and examined in an inverted microscope (Utermöhl 1958) as described in Estrada (1985a). The observed organisms (mainly diatoms, dinoflagellates and coccolithophorids) were classified to the lowest possible taxonomic level and sorted in to three size classes (< 10 µm, 10 - 20 µm and > 20 µm). Ciliate samples were preserved with acid Lugol´s (1 - 2 % final concentration). Information regarding the ciliate population can be found in Dolan & Marrasé (1995).

Protein and DNA determination

For particulate protein and DNA determinations, 4 liters of sea water were passed through a 150 µm mesh and then vacuum-filtered (at a pressure < 100 mm Hg) on precombusted (350 °C for 24 h) Whatman GF/F (47 mm) glass fiber filters which were immediately frozen in liquid nitrogen. Protein quantification was carried out using the Lowry et al. (1951) method. DNA was determined using a DNA-specific stain (Hoechst 33258) as described in Berdalet & Dortch (1991); DNA values were divided by 1.46, the conversion factor proposed by Fara et al. (1996), to correct for the overestimation of DNA resulting from the use of this method. Bovine serum albumin and DNA from calf thymus were used as protein and DNA standards, respectively.

To investigate the contribution of the different groups of microorganisms to total DNA and protein, values of DNA and protein content per cell taken from the literature (Tables 1 and 2) were multiplied by the average abundance of each group at three layers of the water column (above the DCM, at the DCM [chlorophyll > 0.6 µg l^{-1}] and below the DCM), on the two sampling days at each station.

Four groups of microorganisms were evaluated: Bacteria, Phytoplankton (including the PNF counted by epifluorescence), HNF and Ciliates (fundamentally heterotrophic, see Dolan & Marrasé 1995).

For bacterial DNA and protein content per cell we used the conversion factors given by Simon & Azam (1989) for 0.05 μm^3 bacteria, which correspond to the average bacterial volume found in this cruise (Massana et al. 1997). Phytoplankton group was classified in 4 classes: PNF, < 10 µm, 10 - 20 µm and 20 - 150 µm, and the average DNA and protein content per cell of each class (using all values for a given class listed in Table 1 and 2) was used for the calculations. Due to the lack of DNA and protein data for HNF, we assumed values of DNA and protein per cell equal to PNF. No data are available on the protein content of ciliates and only one value was found on DNA content.

Table 1. Mean DNA concentration per cell (± SE) for the main groups of microorganisms. The average DNA value (using all studies for a given group) was used for the calculations; N = number of data points; PNF = phototrophic nanoflagellates; HNF = heterotrophic nanoflagellates.

Group		DNA (pg cell^{-1})	N	Reference
Bacteria		0.0025		Simon and Azam 1989
Phytoplankton	PNF	0.6 ± 0.2	12	Holm-Hansen 1969a Wallen & Geen 1971 Cattolico & Gibbs 1975 Madariaga & Joint 1990 Boucher et al. 1991 Fara & Berdalet (unpublished)
	< 10 µm	1.1 ± 0.6	3	Wallen & Geen 1971 Holm-Hansen 1969a* Fara & Berdalet (unpublished)
	10-20 µm	8.5 ± 2.4	13	Rizzo & Noodén 1973 Holm-Hansen 1969a Galleron & Durrand 1978 Berdalet et al. 1994 Oku & Kamatawi 1995 Fara & Berdalet (unpublished) Boucher et al. 1991
	20-150 µm	82.1 ± 16.4	14	Strickland et al. 1969 Holm-Hansen 1969a Werner 1971 Rizzo & Noodén 1973, 1974 Haapala & Soyer 1974 Tappan 1980 Cembella & Taylor 1985 Boucher et al. 1991
HNF		0.6 ± 0.2	12	Idem ref. than PNF
Ciliates		10	1	Mandel 1967

* Data from *N. pelliculosa* were excessively low compared to the average and were not included for our calculations

Detrital DNA and protein were estimated by the difference between the calculated and the analyzed DNA and protein, respectively. Hereafter, the terms calculated DNA and protein will be used for the estimated amounts of DNA and protein in the different groups of microorganisms and analyzed DNA and protein to refer to the results of the biochemical analyses of seston.

As some bacteria can pass through GF/F filters (0.7 µm nominal pore size), we carried out tests to estimate possible bacterial losses. Mediterranean water samples was filtered through GF/F filters and the bacterial abundance in the filtrates were estimated by flow cytometry (Gasol & Morán 1999) and epifluorescence microscopy.

Table 2. Mean protein concentration per cell (± SE) for the main groups of microorganisms. The average protein value (using all studies for a given group) was used for the calculations; N = number of data points; PNF = phototrophic nanoflagellates; HNF = heterotrophic nanoflagellates.

Group		protein (pg cell^{-1})	N	Reference
Bacteria		0.0177		Simon & Azam 1989
Phytoplankton	PNF	25.9 ± 6.7	29	Moal et al. 1987* Thompson et al. 1992 Madariaga & Joint 1990 Montagnes et al. 1994
	< 10 µm	16.6 ± 6.6	15	Thompson et al. 1992 Dortch 1982 Moal et al. 1987 Montagnes et al. 1994
	10-20 µm	271.2 ± 38.4	24	Berdalet et al. 1994 Conover 1975 Moal et al. 1987 Montagnes et al. 1994 Fara & Berdalet (unpublished)
	20-150 µm	933.5 ± 330.6	10	Moal et al. 1987* Montagnes et al. 1994
HNF		25.9 ± 6.7	29	Idem ref. than PNF

* Data from *Cryptomonas* sp. and *Coscinodiscus wailesii* were excessively high compared to the average and were not included for our calculations.

We determined that an average of 14.3 % of the total bacteria passed through the GF/F filters and we used this result to correct the bacterial contribution to the analyzed DNA and protein.

RESULTS

Hydrographic conditions

The S and D stations presented a similar vertical distribution of temperature, salinity and sigma-t during the sampling period (Fig. 2). Thermal stratification was observed at both stations, but was stronger at D; the maximum temperature gradient occured between 10 and 25 m depth (Fig. 2a and b).

Distribution of the biochemical parameters and the main groups of microorganisms

A deep chlorophyll maximum (DCM) was observed between 40 and 50 m depth at the two stations throughout the sampling period (Fig. 3a). At both stations, the chlorophyll *a* concentration at the DCM was > 1 µg l^{-1} and maximum DNA values were observed close to the DCM and generally

above it (Fig. 3b). DNA concentrations ranged from 0.45 to 3.30 µg l^{-1} at station S, and from 0.72 to 4.22 µg l^{-1} at station D.

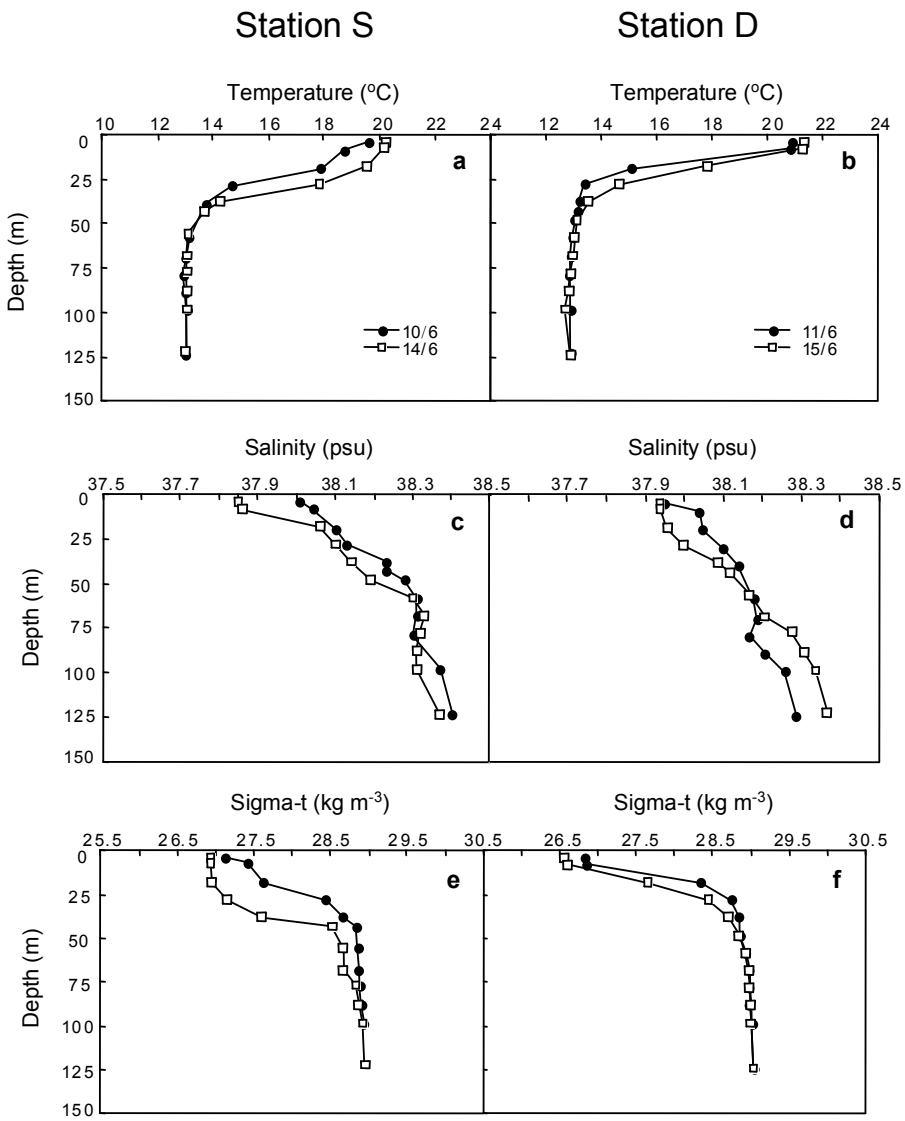

Fig. 2 - Vertical distribution of temperature, salinity and sigma-t at stations S (a, c, e) and D (b, d, f).

The highest protein concentrations were recorded between the surface and 60 m depth at both stations (Fig. 3c), without a deep maximum (station S) or with only a slight increase at or above the DCM depth (station D). Protein concentration ranges were higher at station S (21.1 to 215.9 µg l^{-1}) than at station D (7.8 to 133.7 µg l^{-1}). Phytoplankton, bacteria, heterotrophic flagellates and ciliates

tended to present population peaks at or above the DCM (Fig. 4). However, phytoplankton vertical distribution differed from others. Phytoplankton abundance in surface waters was much lower than at the DCM, while heterotrophic organisms were abundant not only at or near the DCM depth, but also in the upper layers.

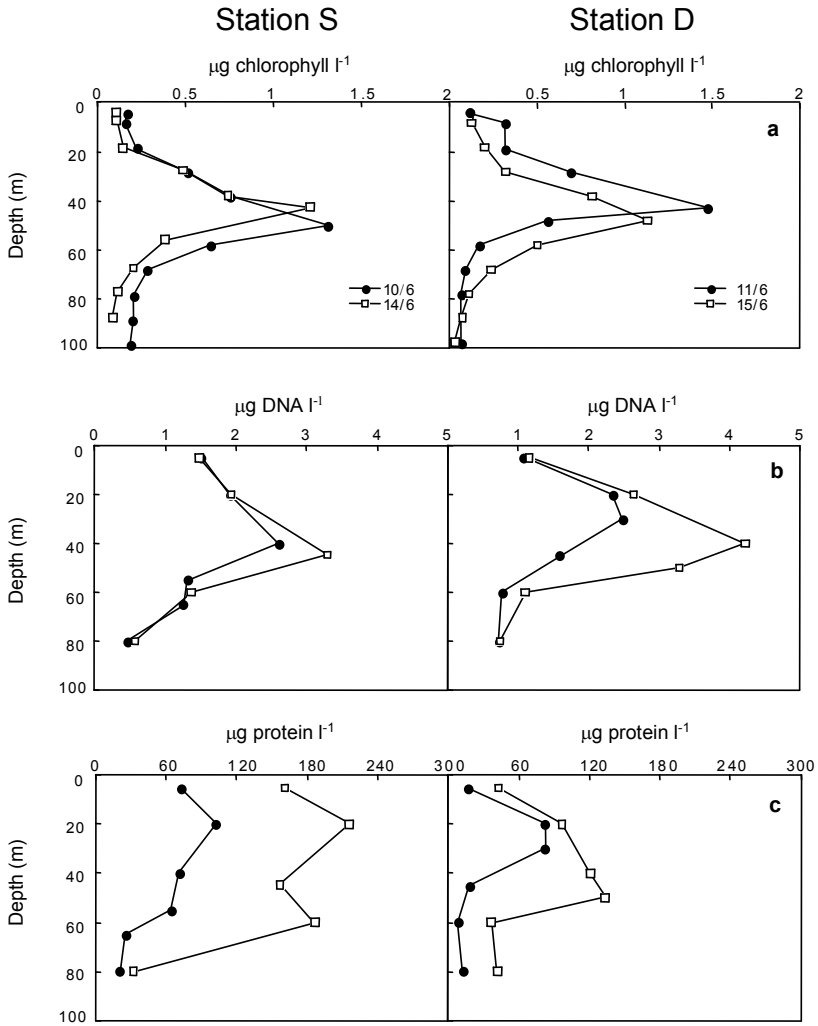

Fig. 3 – Vertical distribution of chlorophyll *a* (a), DNA (b) and protein (c) (all in μg l^{-1}) at stations S and D.

Contribution of microorganisms and detritus to DNA and protein

The distribution of calculated and analyzed DNA values observed at the three layers of the water column (above, at the DCM and below it) was similar at stations S and D (Table 3). Both analyzed

and calculated DNA showed a slight increase at the DCM level and the lowest values of them were found below this level. The highest calculated protein at station S (Table 4) was found at the DCM, while the highest analyzed protein at this station was found above the DCM. At station D, the maximum of analyzed and calculated protein was observed at the DCM level.

At both stations, the heterotrophic (i.e. bacteria + HNF + ciliates) and detritic fraction accounted for 70 to 87 % and for 77 to 96 % of the analyzed DNA and protein, respectively (Tables 3 and 4). In the case of DNA, the main contributor was the bacterial group (23 to 33 %) while for protein, the detritic fraction represented the main protein pool (51 to 85 %) at the three layers of the water column. Less than 30 % of the analyzed DNA and protein corresponded to HNF group, and ciliate contribution to analyzed DNA was only between 0.2 and 0.5 %. The contribution from autotrophic fraction in terms of DNA and protein was < 30 % and < 25 %, respectively.

Table 3. Analyzed and calculated DNA (µg l^{-1}) and DNA contribution (as a percentage) of the main groups of microorganisms and detrital DNA to the total analyzed DNA at stations S and D. In all cases, the given data constitute the average of the parameters obtained at the depths above, at, and below the DCM, on the two sampling dates at each station. Phototrophic nanoflagellates (PNF) were included in the phytoplankton group. HNF = heterotrophic nanoflagellates.

	DNA (µg l^{-1})		**% DNA**				
	Analyzed	Calculated	Bacteria	Phytoplankton	HNF	Ciliates	Detritus
Station S							
Above DCM	1.71	1.02	30.3	12.9	16.4	0.2	40.3
DCM	2.40	1.51	23.9	26.7	12.1	0.3	37.1
Below DCM	0.91	0.55	25.7	30.0	4.8	0.5	39.0
Station D							
Above DCM	1.80	1.37	32.6	20.8	22.4	0.3	23.9
DCM	2.89	1.79	22.5	30.4	8.8	0.2	38.2
Below DCM	0.84	0.48	23.7	28.6	4.6	0.2	42.9

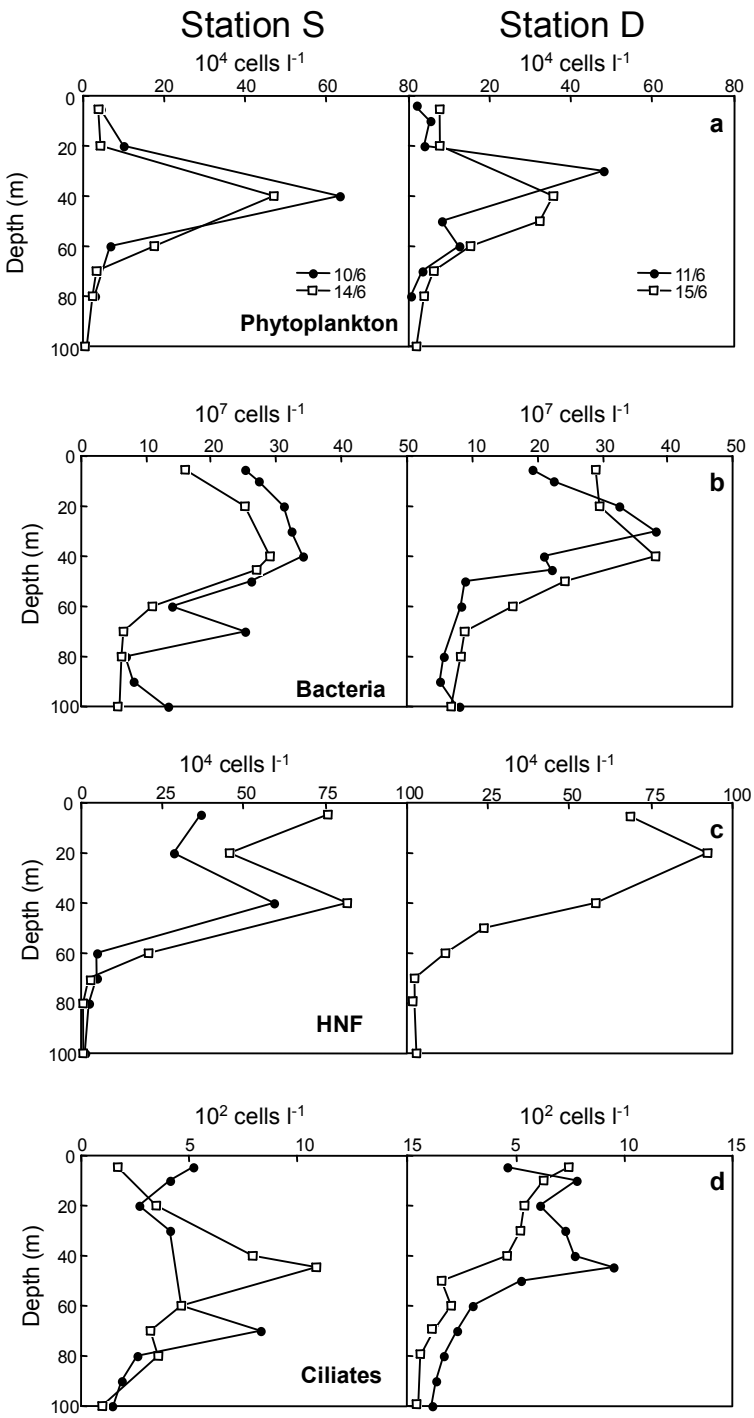

Fig. 4 – Vertical profiles of phytoplankton (a), bacteria (b), heterotrophic nanoflagellates (HNF) (c) and ciliates (d) (cells l^{-1}) at stations S and D.

Table 4. Analyzed and calculated protein (μg l^{-1}) and protein contribution (in percentage) of the main groups of microorganisms and detrital protein to the total analyzed protein at stations S and D. In all cases, the given data constitute the average of the parameters obtained at the depths above, at, and below the DCM, on the two sampling dates at each station. Phototrophic nanoflagellates (PNF) were included in the phytoplankton group. HNF = heterotrophic nanoflagellates.

	protein (μg l^{-1})		% protein			
	Analyzed	Calculated	Bacteria	Phytoplankton	HNF	Detritus
Station S						
Above DCM	137.56	21.01	2.7	3.8	8.8	84.7
DCM	97.17	35.50	4.2	19.5	12.9	63.5
Below DCM	66.05	10.29	2.5	10.2	2.9	84.4
Station D						
Above DCM	59.80	30.74	6.9	12.8	29.1	51.1
DCM	88.73	37.19	5.2	24.4	12.3	58.1
Below DCM	24.73	9.44	5.7	23.6	6.9	63.9

DISCUSSION

The hydrographic conditions (Fig. 2) and the vertical chlorophyll profiles (Fig. 3a), which showed a well-developed DCM, were characteristic of the stratification period in the study area (Delgado et al. 1992, Estrada et al. 1993). The DCM results not only from a higher content of chlorophyll *a* per cell, due to photoacclimation (Jensen & Sakshaug 1973, Latasa et al. 1992), but also from an increase in phytoplankton abundance (Fig. 4a). Our measures of DNA were in the range reported in other oligotrophic areas (i.e. mean chlorophyll < 1.5 μg l^{-1}; mean DNA values < 2 μg l^{-1}), including previous studies conducted in the Catalano-Balearic Sea (Berdalet & Estrada 1993, Table 5). Measured protein values, reported here for the first time in the Catalano-Balearic Sea, were close to those found in other oligotrophic marine areas (i.e. mean chlorophyll < 1.5 μg l^{-1}; mean protein between 30 and 130 μg l^{-1}) including other oligotrophic NW Mediterranean waters (Nival et al. 1976, Table 6).

Compared to chlorophyll, DNA presented a smoother deep maximum near the DCM (Fig. 3a and 3b). Nevertheless, phytoplankton DNA contribution was also high below the DCM (Table 3). This was due to a different size distribution of the phytoplankton cells in the water column. At the DCM

level, around 80 % of the phytoplankton cells corresponded to PNF (with the lowest DNA cell content, Table 1), while below this level bigger cells (> 10 µm) were more abundant (> 36 %). Analyzed protein showed a different vertical distribution than chlorophyll (Fig. 3a and 3c) with high values throughout the euphotic zone, suggesting a low protein contribution from autotrophic organisms in the shallow waters. In addition, above the DCM, the phytoplankton protein contribution was the lowest comparing with the other levels of the water column (Table 4).

We estimated that bacteria were the main contributors to the living DNA at the three layers of the water column, while most living protein was accounted for by phytoplankton or HNF depending on the level of the water column (Table 3 and 4). In other systems a major contribution of bacteria to total DNA has been reported by Paul & Myers (1982), Paul & Carlson (1984) and Paul et al. (1985). In addition, Boehme et al. (1993) found that bacterioplankton provided the largest contribution (> 50 %) to the particulate (> 0.2 µm) DNA pool, whereas phytoplankton accounted for an average of 8 % in the subtropical waters from the Southeastern Gulf of Mexico. In contrast, in terms of protein, we found that bacterioplankton would be a small contributor (3 to 7 % of the total protein) probably as a result of to the high nucleic acid:protein ratio found in small organisms (Skjoldal 1993).

Thus, depending on which biochemical component is considered as indicator of biomass the contribution of the different groups of microorganisms varied. However, the heterotrophic biomass (bacteria + HNF + ciliates), in terms of both DNA and protein, generally, exceeded that of the autotrophs. This results supports the idea that heterotrophy and the microbial food web dominate in oligotrophic planktonic ecosystems, in contrast to eutrophic systems with a much higher proportion of autotrophic biomass (Cho & Azam 1987, Dortch & Packard 1989, Gasol et al. 1997).

Assuming the difference between analyzed and calculated protein as detritus, our approach also revealed a high fraction of detrital protein (> the 50 % of the total), whereas the detrital DNA fraction constituted between the 24 and the 43 % of the total. In eucaryotic cells, protein content is variable and depends on parameters such as nutrient concentration - particularly nitrogen - (Dortch et al. 1984, 1985, Berdalet et al. 1994), light (Wallen & Geen 1971) or stage of growth (Moal et al. 1987). On average the protein content ranges within a factor of two under different physiological or environmental conditions (Moal et al. 1987, Berdalet et al. 1994). Even using twice the amount of protein concentration per cell reported in Table 4 for Phytoplankton and HNF groups (althoug value

Table 5. Mean (± SE) and range of chlorophyll and DNA concentrations (both in μg l^{-1}) in different marine ecosystems and in this study. Note that when mean chlorophyll is < than 1.5 μg l^{-1}, mean DNA values are < 2 μg l^{-1}. N = number of data points

Source	Location	Chl mean ± SE	Chl range	DNA mean ± SE	DNA range	N
Takahashi et al. 1974	North Pacific Ocean	0.45 ± 0.28	0.02 - 7.11	1.65 ± 0.22	0.13 - 5.24	25
Dortch et al. 1985	NE Pacific Ocean	5.10 ± 1.10	1.62 - 11.40	4.88 ± 0.71	2.10 - 10.6	10
Paul et al. 1985	Gulf of Mexico (nearshore, interm. and offshore stations)	2.24 ± 0.95	0.002 - 12.80	10.24 ± 2.72	0.16 - 42.6	16
Fabiano et al. 1993	Ross Sea (Antarctica) - photic layer	1.87 ± 0.60	0.46 - 4.66	31.59 ± 6.46	10.90 - 63.20	9
Berdalet & Estrada 1993	NW Mediterranean Sea					
	-May 1989	0.65 ± 0.14	0.15 - 2.18	1.09 ± 0.13	0.46 - 2.55	21
	-February 1990	0.86 ± 0.07	0.07 - 1.62	1.32 ± 0.09	0.16 - 2.77	30
This study	NW Mediterranean Sea	0.40 ± 0.09	0.04 - 1.43	1.73 ± 0.21	0.45 - 4.22	23

Table 6. Mean (± standard error) and range of chlorophyll and protein concentrations (both in µg l^{-1}) in different marine ecosystems and in this study. Note that when mean chlorophyll is < than 1.5 µg l^{-1}, mean protein ranges between 30 and 130 µg l^{-1}.

Source	Location	Chl mean ± SE	Chl range	Protein mean ± SE	Protein range	N
Takahashi et al. 1974	North Pacific Ocean	0.45 ± 0.28	0.02 - 7.11	48.70 ± 9.01	11.40 - 230.00	25
Packard & Dortch 1975	North Atlantic Ocean					
	- oceanic stations	0.23 ± 0.03	0.02 - 0.64	39.98 ± 5.58	5.04 - 135.24	30
	- upwelling stations	2.42 ± 0.31	0.43 - 4.02	141.68 ± 19.37	36.12 - 297.36	12
Nival et al. 1976	NW Mediterranean Sea (Villefranche-Sur-Mer Bay)	0.66 ± 0.12	0.12 - 1.60	107.19 ± 10.01	60.00 - 200.00	16
Mayzaud & Taguchi 1979	Bedford Basin	3.27 ± 0.72	0.30 - 7.06	437.38 ± 48.18	185.00 - 604.00	8
Hendrickson et al. 1982	Peruvian upwelling	2.25 ± 0.35	0.50 - 5.77	306.90 ± 37.53	82.00 - 764.00	20
Fabiano et al. 1984	Ligurian Sea	0.40 ± 0.04	0.17 - 0.49	95.82 ± 6.00	72.00 - 121.20	8
Dortch et al. 1985	NE Pacific Ocean	5.10 ± 1.10	1.62 - 11.4	104.20 ± 19.30	28.56 - 204.12	10
Dortch & Packard 1989	Washington coast					
	- oligotrophic stations	0.52 ± 0.09	0.15 - 1.03	133.63 ± 27.05	64.29 - 386.42	11
	- eutrophic stations	21.88 ± 8.62	7.72 - 63.74	496.60 ± 136.55	266.21 - 1158.16	6
Bode et al. 1990	Cantabrian Sea	1.12 ± 0.15	0.13 - 2.68	31.79 ± 3.43	13.15 - 79.28	18
Fabiano et al. 1993	Ross Sea (Antarctica) photic layer	1.71 ± 0.56	0.23 - 4.66	169.6 ± 49.18	41.00 - 485.20	10
This study	NW Mediterranean Sea	0.40 ± 0.09	0.04 - 1.43	78.29 ± 12.48	7.80 - 215.90	23

in this table reflect different physiological stages of cells), the detrital protein would still account for a very high percentage of the analyzed protein (41 % on average). In addition, given the lack of data on protein content of ciliates, assuming values similar to those reported for dinoflagellates, ciliates would only account for < 0.5 % of the protein. For cyanobacteria (data not available in our study), we have estimated that they would have contributed up to the 7 % and 1.5 % of the particulate DNA and protein, respectively, based on the data of a previous cruise in this area (Algarra & Vaqué 1989) and assuming the same cellular content as bacteria.

The fact that detritic protein may be an important part of the suspended organic matter has been recently considered by Long & Azam (1996). Using a protein stain, they visualized proteinaceous particles which appeared to constitute an important fraction of the marine snow in natural seawater. With regards to the detritic DNA, its existence was noted as early as this compound was measured in seawater (Holm-Hansen 1969b, Falkowski & Owens 1982, Winn & Karl 1986, Boehme et al. 1993). Most of these studies were concerned with biomass but Winn & Karl (1986) found that non-replicating DNA comprised 75 - 90 % of the total DNA in various locations in the oligotrophic Pacific Ocean. Our data suggest that detritus, in this case in the form of either DNA or protein constitute an important component of particulate matter in the oligotrophic NW Mediterranean in summer. Whether the proportion of detrital protein and DNA is higher in the NW Mediterranean than in other oligotrophic areas is not known. Using a similar indirect approach (i.e. based on particulate carbon and nitrogen conversion factors), in the Sargasso Sea, Caron et al. (1995) estimated that the detrital fraction accounted for the 76 % and 70 % (August 1989) and 45 % and 37 % (March - April 1990) of the total carbon and nitrogen, respectively. Both, this study and our present work reveal the importance of detritus in the oligotrophic food webs, indicating that a major effort is required in quantifying this fraction.

Both detrital protein and detrital DNA may be an important source of organic nitrogen and phosphorus to bacteria and zooplankton in the open sea waters of the NW Mediterranean, where inorganic nutrients are almost undetectable in the euphotic zone during the stratification period. Thingstad & Rassoulzadegan (1995) and Thingstad et al. (1998) argued that the microbial food web in Mediterranean surface waters is characterized by phosphorus-limitation of both phytoplankton and bacteria during the stratified period. In this cruise, very low bacterial production values (between 0.5 and 1.2 µg C l^{-1} d^{-1}, Pedrós-Alió et al. 1999) were found. Thus, we can hypothesize that the utilization of detritic material by the heterotrophic bacteria, limited by phosphorus, occurs at low rates, and therefore a major part of this material is available to grazers; this food source could account for the high zooplankton:phytoplankton biomass ratio found by Alcaraz et al. (1985).

In other words, in the stratification period, the detritic fraction with low sedimentation rates, and degraded slowly by bacteria, can constitute a reservoir of nutritive particles, which can be used by predators. Therefore, we conclude that the quantification of the detritic fraction, specially in periods of low nutrient availability, should be routinely considered in studies addressing nutrient and C fluxes in marine systems.

ACKNOWLEDGEMENTS

We are grateful to our cruise colleagues for the hydrographical data and to M. Vidal for help in the sample collection. A. Cruz provided technical assistance. The comments and suggestions by two anonymous reviewers greatly impoved previous versions of the manuscript. This work was supported by funds from EC Grant Nº MAS2-CT93-0063, EU MAS3-CT95-0016 (MEDEA), and by the ICI (Instituto de Cooperación Iberoamericana) of the Ministerio de Asuntos Exteriores de España fellowship to LA. NG-B. held an FPI fellowship from the Generalitat de Catalunya.

DISCUSIÓN GENERAL

El **primer objetivo** de esta tesis consistía en determinar experimentalmente la importancia de la turbulencia en el desarrollo de organismos osmotróficos (bacterias y fitoplancton) y en la estructura de tamaños y composición taxonómica del fitoplancton, sometido a diferentes condiciones de nutrientes. Las bacterias y el fitoplancton, al ser organismos osmotróficos, incorporan directamente los nutrientes inorgánicos disueltos en el agua. En condiciones de limitación de nutrientes ambos grupos compiten por el nutriente limitante (Bratbak & Thingstad 1985). En teoría, la turbulencia podría incrementar el flujo del nutriente limitante hacia las células aumentando así la tasa de crecimiento potencial de estos organismos (Karp-Boss et al. 1996). Sin embargo, el efecto de la turbulencia sobre el flujo de nutrientes aumenta en función del tamaño celular y sólo sería significativo en células mayores de 60 µm (Karp-Boss et al. 1996). Por lo tanto, era de esperar que en condiciones de turbulencia, el crecimiento de la comunidad fitoplanctónica se viese favorecida con respecto al de la comunidad bacteriana y que, dentro de la comunidad de fitoplancton, aumentase la proporción de organismos en las clases de tamaños mayores.

En el estudio realizado en microcosmos marinos, se ha podido observar que el efecto de la turbulencia sobre el crecimiento de las poblaciones de bacterias y fitoplancton varía en función de las condiciones de nutrientes en que estas poblaciones se desarrollan. En los microcosmos a los que se añadieron inicialmente nutrientes (con una relación N:P deficiente en fósforo o según Redfield), la proporción de biomasa fitoplanctónica en relación a la bacteriana fue mayor en condiciones de turbulencia que en condiciones de calma. (**Capítulo II**, **Fig. 4**). No obstante, en los microcosmos donde no se añadieron inicialmente nutrientes (bajas concentraciones iniciales de nutrientes), la proporción de la biomasa fitoplanctónica con respecto a la bacteriana fue igual en los microcosmos con y sin turbulencia. En este estudio, la teoría de Karp-Boss et al. (1996) sólo se ha podido verificar cuando las condiciones de nutrientes iniciales eran relativamente altas. A bajas concentraciones iniciales de nutrientes, el hipotético aumento del flujo de nutrientes hacia la célula debido a la turbulencia no ha sido suficiente para favorecer el crecimiento de células grandes (véase página 133).

El efecto de la turbulencia sobre la estructura de tamaños y/o la composición taxonómica de la comunidad fitoplanctónica ha sido estudiado en monocultivos algales y en microcosmos marinos. Como primer paso se ha querido saber cuál era el efecto de la turbulencia en el crecimiento de una diatomea grande (*Coscinodiscus* sp., 110 µm) y en el de una pequeña (*Thalassiosira pseudonana*, 6 µm). En cultivos unialgales deficientes en fósforo se ha obtenido una mayor concentración final de

células de *Coscinodiscus* sp. en condiciones de turbulencia que en condiciones de calma. Sin embargo, el crecimiento de la *T. pseudonana* fue prácticamente el mismo en ambas condiciones (**Capítulo I**, **Fig. 1**). Las células de *Coscinodiscus* sp. que crecían en condiciones de calma presentaron una limitación por fósforo mayor que las células que crecían en condiciones turbulentas, lo que se reflejó en una mayor actividad específica de la fosfatasa alcalina (indicadora de limitación de fósforo, Perry 1972). Es de destacar que las células de *Coscinodiscus* sp. presentan una tasa de sedimentación más elevada que la *T. pseudonana* (2.36×10^{-3} y 1.12×10^{-4} cm s^{-1}, respectivamente, según datos de la Fig. 1 en Smayda 1970) y, como consecuencia, las células sedimentadas (con menor superficie de intercambio) podrían haber incorporado menos nutrientes que las que se mantuvieron en suspensión. Con este estudio, se volvió a verificar la teoría de Karp-Boss et al. (1996): el efecto de la turbulencia en la incorporación de nutrientes sólo fue significativo en la diatomea mayor de 60 µm.

En el experimento con microcosmos en el que se encerró una comunidad fitoplanctónica filtrada a través de 150 µm, la evolución de la estructura de tamaños fue diferente según las condiciones físico-químicas del medio (**Capítulo II**, **Fig. 5**). Independientemente de las concentraciones iniciales de nutrientes, el tamaño medio de la comunidad de fitoplancton fue siempre mayor en condiciones de turbulencia que en condiciones de calma. Sin embargo, estas diferencias fueron más marcadas cuando inicialmente se añadieron nutrientes en una relación de Redfield. La fracción mayor de 50 µm fue siempre más importante en condiciones de turbulencia y estuvo formada fundamentalmente por células de diatomeas y, dentro de este grupo, por organismos pertenecientes a dos géneros: *Chaetoceros* y *Pseudo-nitzschia*. Estos organismos forman cadenas por lo que podrían haberse beneficiado aún más de la turbulencia. Pahlow et al. (1997) deduce teóricamente que la formación de cadenas podría, en ciertos casos, aumentar el transporte advectivo de nutrientes hacia la célula, fundamentalmente cuando hay espacios entre las células o cuando su longitud supera la microescala de Kolmogorov. En condiciones de turbulencia la longitud de las cadenas de *Chaetoceros* y *Pseudo-nitzschia* fue mayor que en condiciones de calma.

Con los estudios realizados en los **Capítulos I** y **II** de esta memoria, la importancia de la turbulencia en el crecimiento de células osmotróficas de gran tamaño ha quedado demostrada. Sin embargo, el efecto de la turbulencia sobre estos organismos ha sido poco o no significativo a bajas concentraciones de nutrientes. Este último resultado concuerda con los obtenidos por Peters y colaboradores (Peters et al. 1998, 2002) también en microcosmos marinos. En estos trabajos, en los que no hubo una adición inicial de nutrientes o éstos fueron añadidos diariamente a muy bajas concentraciones, la comunidad fitoplanctónica no se vio favorecida por la presencia de turbulencia sino que, al contrario, se observó un aumento de la heterotrofia en dicha condición. Según Peters et

al. (2002), este aumento de la heterotrofia en condiciones de turbulencia se explicaría por un incremento en las posibles interacciones de predación entre diferentes eslabones de la cadena trófica. En concreto, Peters et al. (1998), concluyeron que el aumento en el número de bacterias en condiciones de turbulencia era debido a un cambio en los hábitos de predación de los microflagelados heterotróficos [quienes pasarían de predar sobre bacteria a predar sobre organismos más grandes y nutritivos (pico- y nanoeucariotas autotróficos)], y no a un efecto directo de la turbulencia sobre el crecimiento bacteriano. Según el modelo conceptual de Marrasé & Peters (2002), a concentraciones muy bajas o a concentraciones saturantes de nutrientes, la presencia de turbulencia no tendría ningún efecto en el crecimiento de los organismos osmotróficos. En el primer caso, el incremento en el flujo de nutrientes hacia la célula debido a la turbulencia no sería suficiente para aumentar significativamente el crecimiento de estos organismos; en el segundo caso, un exceso de nutrientes no sería asimilado por las células incluso en presencia de turbulencia. Bajo concentraciones de nutrientes intermedias la turbulencia afectaría al crecimiento de los organismos osmotróficos.

En el experimento con microcosmos (**Capítulo II**) también se ha podido observar que la composición taxonómica de la comunidad de fitoplancton varía según las condiciones físico-químicas iniciales. La proporción de diatomeas con respecto al resto de la comunidad de fitoplancton fue mayor en condiciones de turbulencia que en condiciones de calma, sobre todo en los microcosmos a los que se añadieron inicialmente nutrientes. En estos últimos, en condiciones de turbulencia, la proporción de diatomeas con respecto al total de fitoplancton fue la misma tanto en los microcosmos donde la adición inicial de nutrientes fue deficiente en fósforo como en los que fue según la relación de Redfield (**Capítulo II**, **Fig. 6**). Sin embargo, en condiciones de calma, la proporción de diatomeas con respecto al resto de la comunidad de fitoplancton fue mayor en los microcosmos cuya adición inicial de nutrientes fue deficiente en fósforo. Estos resultados indican la importancia de estudiar el efecto de las condiciones hidrodinámicas del medio sobre el desarrollo de los diferentes tipos biológicos de fitoplancton.

Con los resultados obtenidos se podría decir que la presencia de turbulencia en aguas naturales, conjuntamente con una concentración relativamente elevada de nutrientes, favorecería el desarrollo de microorganismos autotróficos con respecto a los heterotróficos y, por lo tanto, el desarrollo de la vía trófica clásica sobre la microbiana. Dentro de la comunidad de autótrofos, y principalmente en relación con el grupo de las diatomeas, el crecimiento de las clases de tamaño más grandes se beneficiarían con respecto a las de las menores. Asimismo, los resultados obtenidos indican, también, la importancia de considerar el factor turbulencia a la hora de modelar el crecimiento algal (véase **Capítulo I**).

El **segundo objetivo** de esta tesis era estudiar la estructura de tamaños de comunidades de fitoplancton en sistemas naturales y determinar su variabilidad espacio-temporal. El Giro Occidental del Mar de Alborán fue uno de los escenarios escogidos para realizar este trabajo. Las diferentes condiciones físico-químicas que caracterizan las distintas zonas del giro se vieron reflejadas en la estructura de tamaños de la comunidad de fitoplancton y en su composición taxonómica. En un período de tiempo inferior a 10 días, la comunidad de fitoplancton del borde norte del giro (donde existen aportes intermitentes de aguas profundas ricas en nutrientes) pasó de estar constituida por partes más o menos iguales de células de pico- (< 2 µm), nano- (2 - 20 µm) y microplancton (> 20 µm), a estar prácticamente dominada por células de microplancton (principalmente diatomeas) (**Capítulo III**, **Fig. 5** y **Fig. 7**). El aporte de nutrientes de aguas profundas, conjuntamente con una mayor intensidad de mezcla vertical han sido, posiblemente, las causas de este cambio. En el centro del giro (caracterizado por la presencia de aguas oligotróficas) las fracciones predominantes fueron las del pico- y nanoplancton (constituidas fundamentalmente por *Synechococcus* y pequeños flagelados). Sin embargo, en una de las cuatro visitas a esta zona, se observó la presencia de diatomeas grandes por debajo de los 40 m de profundidad posiblemente como resultado de una intrusión de aguas provenientes de zonas adyacentes. Las diferencias observadas en la composición taxonómica y la estructura de tamaños del fitoplancton de ambas zonas del giro no se vieron reflejadas en las correspondientes tasas de crecimiento, que variaron principalmente en relación a cambios en la irradiancia.

En aguas naturales, las comunidades de fitoplancton van cambiando a lo largo del año y, por lo tanto, también su estructura de tamaños. En la plataforma del Ebro, en invierno, la biomasa fitoplanctónica, en términos de clorofila *a*, fue más elevada que en otoño y verano. Este aumento invernal de la biomasa total fue debido a una mayor abundancia de células de pico-, nano- y microplancton (**Capítulo IV**, **Tabla 1**). Sin embargo, sólo la contribución de la fracción microplanctónica fue más elevada en esta estación, en relación a las otras estaciones observadas. Las condiciones físico-químicas del agua observadas en invierno (fuerte mezcla vertical y, por lo tanto, una elevada concentración de nutrientes en la zona fótica, además de importantes aportes de nutrientes del río Ebro) fueron posiblemente las causas del incremento de esta fracción de fitoplancton. No obstante, en las tres estaciones, la fracción dominante fue la picoplanctónica aunque su importancia fue mayor en otoño y verano (**Capítulo IV**, **Tabla 3**). El porcentaje medio de esta fracción fue similar (otoño y verano), o un poco menor (invierno), al valor medio calculado por Magazzù & Decembrini (1995) a partir de varios estudios realizados en aguas del Mediterráneo. La fracción que presentó menor variabilidad estacional fue la nanoplanctónica. Por otro lado, en las tres estaciones del año observadas, la variabilidad de la biomasa total estuvo relacionada tanto con

la variabilidad de la fracción pequeña (< 2 µm) como con la de las fracciones mayores (> 2 µm), aunque esta última tuvo mayor peso. Generalmente se considera que la variabilidad de la biomasa autotrófica total está asociada con cambios en las clases de tamaños más grandes y que la fracción picoplanctónica es la fracción más constante de la comunidad fitoplanctónica (Malone 1980, Raimbault et al. 1988b, Rodríguez et al. 1998). Sin embargo, en este estudio, el picofitoplancton contribuyó significativamente al aumento de la biomasa total en invierno y estuvo relacionado con los cambios de la biomasa total en cada estación.

Los resultados observados en aguas naturales, así como los obtenidos en el experimento con microcosmos, concuerdan con los modelos conceptuales existentes (Margalef 1978, Legendre & Le Fèvre 1991) los cuales asocian a la turbulencia, conjuntamente con una elevada concentración de nutrientes, a un aumento de células de gran tamaño (principalmente diatomeas), y a las condiciones de calma con el desarrollo de células pequeñas o dotadas de motilidad.

El **tercer y último objetivo** fue estudiar la importancia de la estructura de tamaños y la composición taxonómica de la comunidad de microorganismos planctónicos en relación con la composición química de la materia orgánica formada. En los microcosmos a los que se añadieron inicialmente nutrientes (con una relación N:P deficiente en fósforo o igual a Redfield), la presencia de turbulencia incrementó la incorporación de nutrientes por parte de los organismos osmotróficos. La proporción de estos organismos (en términos de carbono) en relación al fosfato y al nitrato consumidos, así como la proporción de carbono "vivo" (carbono de toda la comunidad planctónica) con respecto al fósforo orgánico particulado (POP), fueron mayores en condiciones de turbulencia que en condiciones de calma (**Capítulo V**, **Tabla 2** y **Fig. 5**). El fitoplancton asimila los nutrientes en una relación C:N y C:P más alta que las bacterias, por lo que la mayor proporción fitoplancton:bacterias encontrada en condiciones de turbulencia (**Capítulo II**, **Fig. 4**) podría haber sido la causa de la mayor cantidad de carbono producido por unidad de nutriente consumido en dicha condición. Sin embargo, esto no justificaría la mayor proporción de carbono "vivo" con respecto al POP observado en condiciones de turbulencia, debido a que el cociente entre ambos fue más alto en los microcosmos en los que no se añadieron inicialmente nutrientes, donde la proporción fitoplancton:bacterias fue la misma en condiciones de turbulencia que en condiciones de calma. Con turbulencia, la tasa de renovación del fósforo (estimada mediante la incorporación de fósforo radioactivo por las células) y el aumento en biomasa fueron más altos que en condiciones de calma. Por lo tanto, en condiciones de turbulencia los organismos quedaron limitados por este nutriente antes que en condiciones de calma. Frente a esta situación de limitación, los organismos autotróficos continuarían realizando la fotosíntesis, mientras que otros procesos metabólicos (incluida la división celular) se enlentecerían (Margalef 1997). Esto explicaría la mayor proporción

de carbono “vivo” en relación al POP observado en condiciones de turbulencia. La proporción de nitrógeno orgánico particulado en relación con el POP también fue más alta en condiciones de turbulencia que en condiciones de calma (**Capítulo V**, **Fig. 4**).

En los microcosmos a los que inicialmente se les añadió nutrientes, el aumento en la biomasa de diatomeas (en términos de carbono) con respecto al silicato consumido también fue mayor en condiciones de turbulencia que en condiciones de calma. Esto se explicaría por un mayor volumen medio de las diatomeas (y por lo tanto una menor relación superficie:volumen) observado en condiciones de turbulencia que en condiciones de calma, lo que requeriría un menor consumo de silicato por parte de la células.

En el estudio realizado en el Giro Occidental del Mar de Alborán, la cantidad de carbono por unidad de clorofila *a* en organismos autotróficos tendió a ser mayor en células grandes (> 2 µm) que en células pequeñas (< 2 µm) (**Capítulo III**, **Tabla 4**). Según Malone (1980), la existencia de correlación entre la cantidad de clorofila por célula y su superficie y, entre el contenido en carbono por célula y su volumen, resultaría en un aumento de la relación carbono:clorofila *a* (C:chl *a*) con el tamaño celular. Sin embargo, en muchas ocasiones otros factores como la intensidad de luz, la temperatura o la concentración de nutrientes (los cuales también influyen en la relación C:chl *a*) podrían interferir en el efecto del tamaño celular sobre esta relación. De hecho, en el Mar de Alborán, las diferencias más importantes en la relación C:chl *a* fueron observadas con respecto a la profundidad y al gradiente horizontal de nutrientes (la relación C:chl *a* disminuyó con la profundidad y con un aumento en la concentración de nutrientes). En cultivos celulares, diversos autores (Blasco et al. 1982, Geider et al. 1986, Montagnes et al. 1994) no encontraron ninguna relación entre el tamaño celular y la relación C:chl *a*. La variabilidad observada en la relación C:chl *a* sugiere cierta precaución en el uso de valores constantes para los cálculos de biomasa en términos de carbono a partir de valores de clorofila.

Se estudió también (**Capítulo VI**) cómo se reflejaba la composición taxonómica de una comunidad de microorganismos planctónicos en su composición química. En las aguas oligotróficas del Mar Catalano-Balear, en el período de estratificación, la contribución de cada grupo de microorganismos planctónicos (bacterias, nanoflagelados heterotróficos, ciliados y fitoplancton) a la concentración total de ADN y proteína particulados fue diferente. Las bacterias fueron quienes presentaron una mayor contribución al ADN particulado “vivo” (no detrítico), mientras que el fitoplancton y los nanoflagelados heterotróficos fueron los principales contribuyentes a la proteína particulada “viva”. Una mayor contribución por parte de las bacterias al ADN particulado total, en aguas naturales, también ha sido observada por otros autores (Paul & Mayers 1982, Paul & Carlson 1984, Boheme

et al. 1993). La contribución por parte de los organismos heterotróficos (bacterias + nanoflagelados heterotróficos + ciliados), ya sea en términos de ADN como en términos de proteína, fue mayor que la de los organismos autotróficos. Este resultado apoya la idea de una mayor biomasa heterotrófica en aguas oligotróficas y, por lo tanto, de la predominancia de la vía trófica microbiana en este tipo aguas (Alcaraz et al. 1985, Cho & Azam 1987, Dortch & Packard 1989, Gasol et al. 1997). En estas condiciones, el alto contenido de ADN de las bacterias haría que su papel en el ciclo del fósforo fuese aún más importante que en condiciones de eutrofia y turbulencia.

CONCLUSIONES

1 – En cultivos deficientes en fósforo, la presencia de turbulencia favoreció el crecimiento de una diatomea grande (*Coscinodiscus* sp., 110 µm) pero no el de una diatomea pequeña (*Thalassiosira pseudonana*, 6 µm). En condiciones de turbulencia, las células de *Coscinodiscus* sp. presentaron una menor limitación por fósforo, reflejada por una menor actividad específica de la fosfatasa alcalina, que en condiciones de calma.

2 – En una comunidad planctónica de componentes capaces de pasar a través de una malla de 150 µm y cultivada en microcosmos, la proporción de los organismos osmotróficos (bacterias y fitoplancton) en condiciones de turbulencia y de calma fue diferente según las condiciones iniciales de nutrientes. La presencia de turbulencia aumentó la importancia relativa del fitoplancton sobre el bacterioplancton en los microcosmos en los que se añadieron inicialmente nutrientes (con una relación N:P según Redfield o deficiente en fósforo), pero no tuvo ningún efecto en los microcosmos sin adición inicial de nutrientes.

3 – En el mismo experimento de microcosmos, la turbulencia tuvo un efecto positivo en el tamaño celular medio de la comunidad fitoplanctónica, independientemente de las condiciones iniciales de nutrientes. La fracción fitoplanctónica mayor de 50 µm fue siempre más importante en los microcosmos sometidos a turbulencia que en los quietos.

4 – En el desarrollo de una comunidad fitoplanctónica la presencia o no de turbulencia, conjuntamente con una determinada concentración inicial de nutrientes, fue un factor determinante en la composición taxonómica de la comunidad. En el estudio realizado en microcosmos, la proporción de diatomeas con respecto al resto de la comunidad fitoplanctónica fue más importante en los contenedores en los que se añadieron inicialmente nutrientes y que además estaban sometidos a la turbulencia. En condiciones de calma, las diatomeas se vieron favorecidas con respecto al resto de la comunidad fitoplanctónica cuando las condiciones iniciales de nutrientes fueron deficientes en fósforo.

5 – El notable hidrodinamismo encontrado en el Giro anticiclónico Occidental del Mar de Alborán se vio reflejado en la estructura de tamaños y en la composición taxonómica de la comunidad fitoplanctónica. En un corto período de tiempo, la comunidad de fitoplancton ubicada en el borde norte del giro, pasó de estar constituida por similares proporciones de células de pico-, nano- y

microplancton a estar dominada prácticamente por células de microplancton (fundamentalmente diatomeas) debido a la intrusión de aguas profundas ricas en nutrientes. En cambio, en la zona central del giro, caracterizado por la presencia de aguas oligotróficas, la comunidad de fitoplancton estuvo dominada por células de pico- y nanoplancton (principalmente *Synechococcus* y pequeños flagelados).

6 – Las diferencias observadas en la composición taxonómica y en la estructura de tamaños de la comunidad fitoplanctónica de las distintas zonas del Giro anticiclónico Occidental del Mar de Alborán no se vieron reflejadas en las correspondientes tasas de crecimiento, que variaron principalmente en relación a cambios en la irradiancia.

7 – La relación carbono:clorofila *a* en la comunidad fitoplanctónica del Giro anticiclónico Occidental del Mar del Alborán tendió a ser mayor en células grandes que en células pequeñas. Sin embargo, esta relación presentó aún una mayor variabilidad en relación a la profundidad y a las condiciones hidrográficas existentes. Una mayor relación carbono:clorofila *a* fue observada en superficie y en aguas más pobres (en un gradiente horizontal).

8 – En la plataforma del Ebro (Mediterráneo Noroccidental) la estructura de tamaños de la comunidad fitoplanctónica presentó una variabilidad estacional marcada. La contribución de la fracción picoplanctónica (< 2 µm) al total de biomasa autotrófica fue la predominante en las tres estaciones del año observadas (otoño, invierno y verano), pero alcanzó los valores más elevados en las estaciones de otoño y verano. En invierno (en que se dio una mayor biomasa autotrófica total), se observaron los mayores porcentajes de la fracción microplanctónica (> 20 µm). La contribución de la fracción nanoplanctónica fue la que presento menor variabilidad estacional.

9 – La contribución de la fracción picoplanctónica a lo largo de un gradiente costa – mar abierto en la plataforma del Ebro fue diferente en las tres estaciones de año muestreadas. En general, en otoño e invierno la contribución de esta fracción al total de fitoplancton en zonas costeras fue menor que en la mayoría de estaciones de mar abierto. Sin embargo, en verano, la contribución del picofitoplancton fue más o menos homogénea en toda el área muestreada. Esta variabilidad estuvo asociada a cambios en las condiciones físico-químicas de la zona.

10 – En el experimento en microcosmos, los cambios producidos por la turbulencia en la estructura de tamaños y en la dinámica de los organismos osmotróficos se vieron reflejados en la composición química de la materia orgánica formada. Independientemente de las concentraciones iniciales de

nutrientes, en condiciones de turbulencia, las relaciones C:P y N:P de la materia orgánica total fueron más altas que en condiciones de calma. Asimismo, en los microcosmos en los que inicialmente se añadieron nutrientes (con una relación N:P según Redfield o deficiente en fósforo) se observó una mayor proporción de biomasa (en términos de carbono) de organismos osmotróficos en relación al fosfato y al nitrato consumido y una mayor biomasa de diatomeas en relación al silicato consumido, en condiciones de turbulencia que en condiciones de calma.

11 – En las aguas estratificadas oligotróficas del Mar Catalano-Balear, cada uno de los principales grupos de micoorganismos planctónicos (bacterias, nanoflagelados heterotróficos, ciliados y fitoplancton) contribuyó de manera diferente a la concentración de ADN y proteína particulados. Las bacterias fueron quienes presentaron una mayor contribución al ADN particulado "vivo" (no detrítico), mientras que el fitoplancton y los nanoflagelados heterotróficos fueron los principales contribuyentes a la proteína particulada "viva". La mayor parte de la proteína particulada total y gran parte del ADN particulado total correspondieron a la fracción detrítica de la materia orgánica.

BIBLIOGRAFÍA

Agawin NSR, Duarte CM, Agustí S (1998) Growth and abundance of *Synechococcus* sp. in a Mediterranean Bay: Seasonality and relationship with temperature. Mar Ecol Prog Ser 170:45-53

Agawin NSR, Duarte CM, Agustí S (2000) Nutrient and temperature control of the contribution of picoplankton to phytoplankton biomass and production. Limnol Oceanogr 45:591-600

Alcaraz M, Estrada M, Flos J, Fraga F (1985) Particulate carbon and nitrogen in plankton biomass in oligotrophic and upwelling systems. Int Symp Upw W Afr Inst Inv Pesq Barcelona V.I:435-448

Algarra P, Vaqué D (1989) Cyanobacteria distribution across the Western Mediterranean divergence: A proof of pigment adaptation in different light conditions. Sci Mar 53:197-202

Arin L, Marrasé C, Maar M, Peters F, Sala MM, Alcaraz M (2002a) Combined effects of nutrients and small-scale turbulence in a microcosms experiment. I. Dynamics and size distribution of osmotrophic plankton. Aquat Microb Ecol 29:51-61

Arin L, Morán XAG, Estrada M (2002b) Phytoplankton size distribution and growth rates in the Alboran Sea (SW Mediterranean): Short-term variability related to mesoscale hydrodynamics. J Plankton Res 24:1019-1033

Azam F, Fenchel T, Field JG, Gray JS, Meyer-Reil LA, Thingstad F (1983) The ecological role of water-column microbes in the sea. Mar Ecol Prog Ser 10:257-263

Bailiff MD, Karl DM (1991) Dissolved and particulate DNA dynamics during a spring bloom in the Antarctic Peninsula region, 1986-87. Deep-Sea Res 3:1077-1095

Banse K (1976) Rates of growth, respiration and photosynthesis of unicellular algae as related to cell size - A review. J Phycol 12:135-140

Banse K (1982) Cell volumes, maximal growth rates of unicellular algae and ciliates, and the role of ciliates in the marine pelagial. Limnol Oceanogr 27:1059-1071

Berdalet E, Dortch Q (1991) New double-staining technique for RNA and DNA measurement in marine phytoplankton. Mar Ecol Prog Ser 73:295-305

Berdalet E (1992) Effects of turbulence on the marine dinoflagellate *Gymnodinium nelsonii*. J Phycol 28:267-272

Berdalet E, Latasa M, Estrada M (1992) Variations in biochemical parameters of *Heterocapsa* sp. and *Olistodiscus luteus* grown in 12:12 light:dark cycles. I. Cell cycle and nucleic acid composition. Hydobiologia 238:139-147

Berdalet E, Estrada M (1993) Relationships between nucleic acid concentrations and primary production in the Catalan Sea (Northwestern Mediterranean). Mar Biol 117:163-170

Berdalet E, Latasa M, Estrada M (1994) Effects of nitrogen and phosphorus starvation on nucleic acid and protein content of *Heterocapsa* sp. J Plankton Res 16:303-316

Berdalet E, Marrasé C, Estrada M, Arin L, MacLean ML (1996) Microbial community responses to nitrogen- and phosphorus- deficient nutrient imputs: microplankton dynamics and biochemical characterization. J Plankton Res 18:1627-1641

Berg HC, Purcell EM (1977) Physics of chemoreception. Biophys J 20:193-219

Berland BR, Maestrini SY, Burlakova ZP, Georgieva L, Kholodov BY, Krupatkina DK (1980) Nutrient limitation of algal growth in ultra-oligotrophic waters of the Eastern Mediterranean Sea. Mem Biol Mar Oceanogr 18:5-28

Bertalanffy LV (1964) Basic concepts in quantitative biology of metabolism. Helgol Wiss Meeresunters 9:5-38

Bienfang PK (1984) Size structure and sedimentation of biogenic microparticulates in a subarctic ecosystem. J Plankton Res 6:983-994

Bjørnsen PK (1986) Automatic determination of bacterioplankton biomass by image analysis. Appl Environ Microbiol 51:1199-1204

Blasco D, Packard TT, Garfield PC (1982) Size dependence of growth rate, respiratory electron transport system activity, and biochemical composition in marine diatoms in laboratory. J Phycol 18:58-63

Bode E, Fernandez E, Botas A, Anadon R (1990) Distribution and composition of suspended particulate matter related to a shelf-break saline intrusion in the Cantabrian Sea (Bay of Biscay). Oceanol Acta 13:219-228

Boehme J, Frischer ME, Jiang SC, Kellogg CA, Pichard S, Rose JB, Steinway C, Paul JH (1993) Viruses, bacterioplankton, and phytoplankton in the southeastern Gulf of Mexico: distribution and contribution to oceanic DNA pools. Mar Ecol Prog Ser 97:1-10

Booth BC (1988) Size classes and major taxonomic groups of phytoplankton at two locations in the subarctic Pacific Ocean in May and August, 1984. Mar Biol 97:275-276

Boucher N, Vaulot D, Partensky F (1991) Flow cytometric determination of phytoplankton DNA in cultures and oceanic populations. Mar Ecol Prog Ser 71:75-84

Bratbak G & Thingstad TF (1985) Phytoplankton-bacteria interactions: an apparent paradox? Analysis of a model system with both competitions and comensalism. Mar Ecol Prog Ser 25:23-30

Brzezinski MA (1985) The Si:C:N ratio of marine diatoms: interspecific variability and the effect of some environmental variables. J Phycol 21:347-357

Buck KR, Chavez FP, Campbell L (1996) Basin-wide distributions of living carbon components and the inverted trophic pyramid of the central gyre of the North Atlantic Ocean, summer 1993. Aquat Microb Ecol 10:283-298

Calbet A, Alcaraz M, Saiz E, Estrada M, Trepat I (1996) Planktonic herbivorous food webs in the Catalan Sea (NW Mediterranean): temporal variability and comparison of indices of phyto-zooplankton coupling based on state variables and rate processes. J Plankton Res 18:2329-2347

Canelli E, Fuhs GW (1976) Effect of the sinking rate of two diatoms (*Thalassiosira* spp.) on the uptake from low concentration of phosphate. J Phycol 12:93-99

Caron DA, Dam HG, Kremer P, Lessard EJ, Madin LP, Malone TC, Napp JM, Peele ER, Roman MR, Youngbluth MJ (1995) The contribution of microorganisms to particulate carbon and nitrogen in surface waters of the Sargasso Sea near Bermuda. Deep-Sea Res 42:943-972

Carpenter SR (1996) Microcosm experiments have limited relevance for community and ecosystem ecology. Ecology 77:677-680

Cattolico RA, Gibbs SP (1975) Rapid filter method for the microfluorometric analysis of DNA. Anal Biochem 69:572-582

Cembella AD, Taylor FJR (1985) Biochemical variability within the *Protogonyaulax tamarensis/catenella* species complex. In: Anderson DM, White AW, Baden DG (eds) Toxic Dinoflagellates. Elsevier Science, New York pp 55-60

Conover SAM (1975) Partitioning of nitrogen and carbon of the marine diatom *Thalassiosira fluviatilis* supplied with nitrate, ammonium or urea. Mar Biol 32:231-246

Coste B, Le Corre P, Minas HJ (1988) Re-evaluation of the nutrient exchanges in the Strait of Gibraltar. Deep-Sea Res 35:765-775

Costello JH, Strickler JR, Marrasé C, Trager G, Zeller R, Freise AJ (1990) Grazing in a turbulent environment: Behavioral response of a calanoid copepod*, Centropages hamatus.* Proc Natl Acad Sci USA 87:1648-1652

Cros L (2001) Planktonic coccolithophores of the NW Mediterranean. PhD Thesis. Universitat de Barcelona pp 1-365

Cushing DH (1989) A difference in structure between ecosystems in strongly stratified waters and in those that are only weakly stratified. J Plankton Res 11:1-13

Chavez FP, Buck KR, Service SK, Newton J, Barber RT (1996) Phytoplankton variability in the central and eastern tropical Pacific. Deep-Sea Res II 43:835-870

Chisholm SW (1992) Phytoplankton size. In: Falkowski PG, Woodhead AD (eds) Primary Productivity and Biogeochemical Cycles in the Sea. Plenum Press, New York pp 213-236

Cho BC, Azam F (1987) Significance of bacterioplankton biomass in the epipelagic and mesopelagic zones in the Pacific Ocean. Eos 68:1729

Cho BC, Azam F (1990) Biogeochemical significance of bacterial biomass in the ocean´s euphotic zone. Mar Ecol Prog Ser 63:253-259

Chrzanowski TH, Kyle M, Elser JJ, Sterner RW (1996) Element ratios and growth dynamics of bacteria in an oligotrophic Canadian shield lake. Aquat Microb Ecol 11:119-125

Delgado M, Latasa M, Estrada M (1992) Variability in the size-fractionated distribution of the phytoplankton across the Catalan front of the north-west Mediterranean. J Plankton Res 14:753-771

Dolan JR, Marrasé C (1995) Planktonic ciliate distribution relative to the deep chlorophyll maximum: Catalan Sea, N.W. Mediterranean, June 1993. Deep-Sea Res 42:1965-1987

Dortch Q (1982) Effect of growth conditions on accumulation of internal pools of nitrate, ammonium, amino acid, and protein in three marine diatoms. J Exp Mar Biol Ecol 61:243-264

Dortch QF, Clayton JRJr, Thoresen SS, Ahmed SI (1984) Species differences in accumulation of nitrogen pools in phytoplankton. Mar Biol 81:237-250

Dortch Q, Clayton JRJr, Thoresen SS, Cleveland JS, Bressler SL, Ahmed SI (1985) Nitrogen storage and use of biochemical indices to assess nitrogen deficiency and growth rate in natural plankton populations. J Mar Res 43:437-464

Dortch Q, Packard TT (1989) Differences in biomass structure between oligotrophic and eutrophic marine ecosystems. Deep-Sea Res 36:223-240

Durbin EG, Krawiec RW, Smayda TJ (1975) Seasonal studies on the relative importance of different size-fractions of phytoplankton in Narragansett Bay, USA. Mar Biol 32:271-288

Egge JK (1998) Are diatoms poor competitors at low phosphate concentration? J Mar Syst 16:191-198

Eppley RW, Sloan PR (1965) Carbon balance experiments with marine phytoplankton. J Fish Res Bd Can 22:1083-1097

Eppley RW, Stewart E, Abbott MR, Owen RW (1987) Estimating ocean production from satellite-derived chlorophyll: insights from the Eastropac data set. Oceanol Acta Nº sp: 109-113

Estrada M (1985a) Deep phytoplankton and chlorophyll maxima in the Western Mediterranean. In: Moraitou-Apostolopoulou M, Kiortsis MV (eds) Mediterranean marine ecosystems. Plenum Press, New York pp 247-277

Estrada M (1985b) Primary production at the deep chlorophyll maximum in the Western Mediterranean. In: Gibbs PE (ed) Proceeding of the 19th European Marine Biology Symposium Plymouth. Cambridge University Press, Cambridge pp 109-121

Estrada M, Alcaraz M, Marrasé C (1987) Effects of turbulence on the composition of phytoplankton assemblages in marine microcosms. Mar Ecol Prog Ser 36:267-281

Estrada M, Marrasé C, Alcaraz M (1988) Phytoplankton response to intermittent stirring and nutrient addition in marine microcosms. Mar Ecol Prog Ser 48:225-234

Estrada M, Marrasé C, Latasa M, Berdalet E (1993) Variability of deep chlorophyll maximum characteristics in the Northwestern Mediterranean. Mar Ecol Prog Ser 92:289-300

Estrada M, Berdalet E (1998) Effects of turbulence on phytoplankton. In: Anderson DM, Cembella AD, Hallegraeff GM (eds) Physiological Ecology of Harmful Algal Blooms. NATO ASI Series, Vol G41. Springer-Verlag, Berlin pp 601-618

Fabiano M, Zavatarelli M, Palmero S (1984) Observations sur la matière organique particulaire (protéines, glucides, lipides, chlorophylle) en Mer Ligure. Téthys 11:133-140

Fabiano M, Povero P, Danovaro R (1993) Distribution and composition of particulate matter in the Ross Sea (Antarctica). Polar Biol 13:525-533

Falkowski PG, Owens TG (1982) A technique for estimating phytoplankton division rates by using a DNA-binding fluorescent dye. Limnol Oceanogr 27:776-782

Fara A, Berdalet E, Arin L (1996) Determination of RNA and DNA concentrations in natural plankton samples using Thiazole orange in combination with DNAse and RNAse digestions. J Phycol 32:1074-1083

Fenchel T (1987) Ecology - Potentials and limitations. Excellence in Ecology 1 pp 1-186

Figueiras FG, Estrada M, López O, Arbones B (1998) Photosynthetic parameters and primary production in the Bransfield Strait: relationships with mesoscale hydrographic structures. J Mar Syst 17:129-141

Figueiras FG, Pérez FF, Pazos Y, Ríos AF (1994) Light and productivity of Antarctic phytoplankton during austral summer in an ice edge region in the Weddell-Scotia Sea. J Plankton Res 16:233-253

Font J, Garcia-Ladona E, Górriz EG (1995) The seasonality of mesoscale motion in the Northern Current of the Western Mediterranean: several years of evidence. Oceanol Acta 18:207-219

Font J, Salat J, Tintoré J (1988) Permanent features of the circulation in the Catalan Sea. Oceanol Acta, Sp Issue 9:51-57

Furnas MJ (1990) *In situ* growth rates of marine phytoplankton: approaches to measurement, community and species growth rates. J Plankton Res 12:1117-1151

Gage MA, Gorham E (1985) Alkaline phosphatase activity and cellular phosphorus as an index of the phosphorus status of phytoplankton in Minnesota lakes. Freshwat Biol 15:227-233

Gallegos CL, Jordan TE (1997) Seasonal progression of factors limiting phytoplankton pigment biomass in the Rhode River estuary, Maryland (USA). 1. Controls on phytoplankton growth. Mar Ecol Prog Ser 161:185-198

Galleron C, Durrand AM (1978) Characterization of a dinoflagellate (*Amphidinium carterae*) DNA. Biochimie 60:1235-1242

Garcés E, Delgado M, Masó M, Camp J (1999) *In situ* growth rate and distribution of the ichthyotoxic dinoflagellate *Gyrodinium corsicum* Paulmier in an estuarine embayment (Alfacs Bay, NW Mediterranean Sea). J Plankton Res 21:1977-1991

García CM, Jiménez-Gómez F, Rodríguez J (Rapporteurs). Bautista B, Estrada M, García Braun J, Gasol JM, Gómez Figueiras F, Guerrero F, Jiménez Montes F, Li WKW, López Díaz JM, Santiago G, Varela M (1994) The size structure and functional composition of ultraplankton and nanoplankton at a frontal station in the Alboran Sea. Working Groups 2 and 3 Report. In: Rodríguez J, Li WKW (eds) The size structure and metabolism of the pelagic ecosystem. Sci Mar 58:43-52

Gasol JM, del Giorgio PA, Duarte CM (1997) Biomass distribution in marine planktonic communities. Limnol Oceanogr 42:1353-1363

Gasol JM, Morán XAG (1999) Effects of filtration on bacterial activity and picoplankton community structure as assessed by flow cytometry. Aquat Microb Ecol 16:251-264

Gasol JM, del Giorgio PA (2000) Using flow cytometry for counting natural planktonic bacteria and understanding the structure of planktonic bacterial communities. Sci Mar 64:197-224

Geider RJ, Platt T, Raven JA (1986) Size dependence of growth and photosynthesis in diatoms: a synthesis. Mar Ecol Prog Ser 30:93-104

Geider RJ, MacIntyre HL, Kana TM (1997) Dynamic model of phytoplankton growth and acclimation: responses of the balanced growth rate and the chlorophyll *a*:carbon ratio to light, nutrient-limitation and temperature. Mar Ecol Prog Ser 148:187-200

Gitelson A, Karnieli A, Goldman N, Yacobi YZ, Mayo M (1996) Chlorophyll estimation in the Southeastern Mediterranean using CZCS images: adaptation of an algorithm and its validation. J Mar Syst 9:283-290

Gómez F, Echevarría F, García CM, Prieto L, Ruiz J, Reul A, Jiménez-Gómez F, Varela M (2000) Microplankton distribution in the Strait of Gibraltar: coupling between organisms and hydrodynamic structure. J Plankton Res 22:603-617

Granéli E, Carlsson P, Turner JT, Tester PA, Béchemin C, Dawson R, Funari E (1999) Effects of N:P:Si ratios and zooplankton grazing on phytoplankton communities in the northern Adriatic Sea. I. Nutrients, phytoplankton biomass, and polysaccharide production. Aquat Microb Ecol 18:37-54

Grasshoff K, Ehrhardt M, Kremling K (1983) Methods of seawater analysis, 2nd edn. Verlag Chemie, Weinheim

Guildford SJ, Hecky RE (2000) Total nitrogen, total phosphorus, and nutrient limitation in lakes and oceans: Is there a common relationship? Limnol Oceanogr 45:1213-1223

Guillard RRL (1975) Culture of phytoplankton for feeding marine invertebrates. In: Smith W, Chanley MH (eds) Culture of Marine Invertebrates. Plenum Publishing Corp, New York pp. 26-60

Haapala OK, Soyer MO (1974) Size of circular chromatids and amount of haploid DNA in the dinoflagellates *Gyrodinium cohnii* and *Prorocentrum micans*. Hereditas 76:83-90

Harris GP (1986) Phytoplankton Ecology. Chapman & Hall Ltd London pp 1-384

Harris GP, Gauf GG, Thomas DP (1987) Productivity, growth rate and cell size distributions of phytoplankton in the SW Tasman Sea: Implications for carbon metabolism in the photic zone. J Plankton Res 9:1003-1030

Hasle GR, Tomas CR (1996) Advanced plankton course taxonomy and systematic. 24 September – 14 October 1995 Napoles, Italia pp 1-385

Haug A, Myklestad S, Sakshaug E (1973) Studies on the phytoplankton ecology of the Trondheimsfjord. I. The chemical composition of phytoplankton populations. J Exp Mar Biol Ecol 11:15-26

Hendrickson P, Sellner KG, de Mendiola BR, Ochoa N, Zimmerman R (1982) The composition of particulate organic matter and biomass in the Peruvian upwelling region during ICANE 1977 (14 Nov-2 Dec). J Plankton Res 4:163-186

Herbland A, Le Bouteiller A (1981) The size distribution of phytoplankton and particulate organic matter in the equatorial Atlantic Ocean: Importance of ultraseston and consequences. J Plankton Res 3:659-673

Holm-Hansen O (1969a) Algae: Amounts of DNA and organic carbon in single cells. Science 163:87-88

Holm-Hansen O (1969b) Determination of microbial biomass in oceans profiles. Limnol Oceanogr 14:740-747

Hopcroft RR, Roff JC (1990) Phytoplankton size fractions in a tropical neritic ecosystem near Kingston, Jamaica. J Plankton Res 12:1069-1088

Jensen A, Sakshaug E (1973) Studies on the phytoplankton ecology of the Trondheimsfjord. II. Chloroplast pigments in relation to abundance physiological state of the phytoplankton. J Exp Mar Biol Ecol 11:137-155

Joint I, Groom SB (2000) Estimation of phytoplankton production from space: current status and future potential of satellite remote sensing. J Exp Mar Biol Ecol 250:233-255

Kähler P, Koeve W (2001) Marine dissolved organic matter: can its C:N ratio explain carbon overconsumption? Deep-Sea Res I 48:49-62

Kahru M, Nomman S, Zeitzschel B (1991) Particle (plankton) size structure across the Azores Front (Joint Global Ocean Flux Study North Atlantic Bloom Experiment). J Geophys Res 96:7083-7088

Kana T, Gilbert PM (1987) Effect on irradiance up to 2000 μE m^{-2} s^{-2} on marine *Synechococcus*WH 7803-I. Growth, pigmentation, and cell composition. Deep-Sea Res 34:479-516

Karp-Boss L, Boss E, Jumars PA (1996) Nutrient fluxes to planktonic osmotrophs in the presence of fluid motion. Oceanogr Mar Biol Annu Rev 34:71-107

Karp-Boss L, Jumars PA (1998) Motion of diatom chains in steady shear flow. Limnol Oceanogr 43:1767-1773

Karp-Boss L, Boss E, Jumars PA (2000) Motion of dinoflagellates in a simple shear flow. Limnol Oceanogr 45:1594-1602

Kiørboe T, Kaas H, Kruse B, Mohlenberg F, Tiselius P, Ærtebjerg G (1990) The structure of the pelagic food web in relation to water column structure in Skagerrak. Mar Ecol Prog Ser 59:19-32

Kiørboe T (1993) Turbulence, phytoplankton cell size, and the structure of pelagic food webs. Adv Mar Biol 29:1-73

Kiørboe T, Saiz E (1995) Planktivorous feeding in calm and turbulent environments, with emphasis on copepods. Mar Ecol Prog Ser 122:135-145

Köhler J (1997) Measurement of *in situ* growth rates of phytoplankton under conditions of simulated turbulence. J Plankton Res 19:849-862

Koroleff F (1983) Determination of total nitrogen and phosphorus. In: Grasshoff K, Ehrhardt M, Kremling K (eds) Methods for seawater analysis, 2nd edition. Verlag Chemie, Weinheim pp 162-173

Krom MD, Kress N, Brenner S, Gordon LI (1991) Phosphorus limitation of primary productivity in the eastern Mediterranean Sea. Limnol Oceanogr 36:424-432

Landry MR, Hassett RP (1982) Estimating the grazing impact of marine micro-zooplankton. Mar Biol 67:283-288

Langdon C (1988) On the causes of interspecific differences in the growth-irradiance relationship for phytoplankton. 2. A general review. J Plankton Res 10:1291-1312

Latasa M, Estrada M, Delgado M (1992) Plankton-pigment relationships in the Northwestern Mediterranean during stratification. Mar Ecol Prog Ser 88:61-73

Lazier JRN, Mann KH (1989) Turbulence and the diffusive layer around small organisms. Deep-Sea Res 36:1721-1733

Legendre L (1990) The significance of microbial blooms for fisheries and for the export of particulate organic carbon in oceans. J Plankton Res 12:681-699

Legendre L, Le Fèvre J (1991) From individual plankton cells to pelagic marine ecosystems and to global biogeochemical cycles. NATO ASI Series Particle Analysis and Oceanography. Demers S (ed) Springer-Verlag, Berlin Vol G27 pp 261-300

Legendre L, Gosselin M, Hirche H-J, Kattner G, Rosenberg G (1993) Environmental control and potential fate of size-fractionated phytoplankton production in the Greenland Sea (75ºN). Mar Ecol Prog Ser 98:297-313

Legendre L, Rassoulzadegan F (1995) Plankton and nutrient dynamics in marine waters. Ophelia 41:153-172

Lehninger AL (1974) Bioquímica. Ed Omega SA, Barcelona

Li WKW, Dickie PM, Irwin BP, Wood AM (1992) Biomass of bacteria, cianobacteria, prochlorophytes and photosynthetic eukaryotic in the Sargasso Sea. Deep-Sea Res 39:501-519

Li H, Veldhuis MJW, Post AF (1998) Alkaline phosphatase activities among planktonic communities in the northern Red Sea, Mar Ecol Prog Ser 173:107-115

Lohmann H (1911) Über das Nannoplankton und die Zentrifugierung kleinster Wasserproben zur Gewinnung desselben in lebendem Zustand. Int Rev Gesamten Hydrobiol Hydrog 4:1-38

Long RA, Azam F (1996) Abundant protein-containing particles in the sea. Aquat Microb Ecol 10:213-221

Lowry OH, Rosebrough NJ, Farr AL, Randall RJ (1951) Protein measurement with the folin phenol reagent. J Biol Chem 193:265-280

Maar M, Arin L, Simó R, Sala MM, Peters F, Marrasé C (2002) Combined effects of nutrients and small-scale turbulence in a microcosms experiment. II. Dynamics of organic matter and phosphorus. Aquat Microb Ecol 29:63-72

MacKenzie BR, Leggett WC (1993) Wind-based models for estimating the dissipation rates of turbulent energy in aquatic environments: empirical comparisons. Mar Ecol Prog Ser 94:207-216

Madariaga I de, Joint I (1992) A comparative study of phytoplankton physiological indicators. J Exp Mar Biol Ecol 158:149-165

Magazzù G, Decembrini F (1995) Primary production, biomass and abundance of phototrophic picoplankton in the Mediterranean Sea: a review. Aquat Microb Ecol 9:97-104

Magazzù G, Panella S, Decembrini F (1996) Seasonal variability of fractionated phytoplankton, biomass and primary production in the Straits of Magellan. J Mar Syst 9:249-267

Malone TC (1971) The relative importance of nannoplankton and netplankton as primary producers in the California current system. Fish Bull 69:799-820

Malone TC (1977) Light-saturated photosynthesis by phytoplankton size fractions in the New York Bight. Mar Biol 42:281-292

Malone TC (1980) Algal Size. In: Morris I (ed) The Physiological Ecology of Phytoplankton. Blackwell Scientific Publications, Oxford. pp 433-463

Mandel M (1967) Nucleic acid of protozoa. In: Kidder GW (ed) Chemical Zoology. New York Academic Press Vol.1 pp 541-572

Mann KH, Lazier JRN (1991) Dynamics of marine ecosystems. Blackwell Scientific Publication, Boston

Marañón E, Holligan PM, Varela M, Mouriño B, Bale AJ (2000) Basin-scale variability of phytoplankton biomass production and growth in the Atlantic Ocean. Deep-Sea Res Part I Oceanogr Res Pap 47:825-857

Marañón E, Holligan PM, Barciela R, González N, Mouriño B, Pazó MJ, Varela M (2001) Patterns of phytoplankton size structure and productivity in contrasting open-ocean environments. Mar Ecol Prog Ser 216:43-56

Margalef R (1974) Ecología. Omega, Barcelona

Margalef R (1978) Life-forms of phytoplankton as survival alternatives in an unstable environment. Oceanol Acta 1:493-509

Margalef R (1997) Our biosphere. In: Kinne O (ed) Excellence in ecology. Ecology Institute, Oldendorf/Luhe

Marrasé C, Duarte CM, Vaqué D (1989) Succession patterns of phytoplankton blooms: directionality and influence of algal cell size. Mar Biol 102:43-48

Marrasé C, Costello JH, Granata T, Strickler JR (1990) Grazing in a turbulent environment: Energy dissipation, encounter rates, and efficacy of feeding currents in *Centrophages hamatus*. Proc Natl Acad Sci USA 87:1653-1657

Marrasé C, Peters F (2002) Towards building a conceptual framework of physical-biological interactions at small scales. GLOBEC 2nd Open Science Meeting, Quingdao, China

Masó M, Grupo VARIMED (1995) Datos Oceanográficos Básicos de las Campañas "Fronts 1992" (octubre- noviembre 1992) y "Variabilidad de Mesoescala en el Mediterrráneo Occidental" (junio 1993). Institut de Ciènces del Mar (CSIC). Barcelona, Spain.

Massana R, Gasol JM, Bjørnsen PK, Blackburn N, Hagström Å, Hietanen S, Hygum BH, Kuparinen J, Pedrós-Alió C (1997) Measurement of bacterial size via image analysis of epifluorescence preparations: description of an inexpensive system and solutions to some of the most common problems. Sci Mar 61:397-407

Mayzaud P, Taguchi S (1979) Spectral and biochemical characteristics of the particulate matter in Bedford Basin. J Fish Res Board Can 36:211-218

Megard RO, Berman T (1989) Effects of algae on the Secchi transparency of the Southeastern Mediterranean Sea. Limnol Oceanogr 34:1640-1655

Minas HJ, Coste B, Le Corre P, Minas M, Raimbault P (1991) Biological and geochemical signatures associated with the water circulation through the Strait of Gibraltar and in the western Alboran Sea. J Geophys Res 96:8755-8771

Moal J, Martin-Jezequel V, Harris RP, Samain J-F, Poulet SA (1987) Interespecific and intraspecific variability of the chemical composition of marine phytoplankton. Oceanol Acta 10:339-346

Moloney CL, Field JG (1989) General allometric equations for rates of nutrient uptake, ingestion, and respiration in plankton organisms. Limnol Oceanogr 34:1290-1299

Montagnes DJ, Berges SJA, Harrison PJ, Taylor FJR (1994) Estimating carbon, nitrogen, protein and chlorophyll *a* from volume in marine phytoplankton. Limnol Oceanogr 39:1044-1060

Montesino V, Quiroz D (2000) Specific primary production and phytoplankton cell size structure in an upwelling area off the coast of Chile (30^{o}S). Aquat Sci 62:364-380

Morán XAG, Estrada M (2001) Short-term variability of photosynthetic parameters and particulate and dissolved primary production in the Alboran Sea (SW Mediterranean). Mar Ecol Prog Ser 212:53-67

Mullin MM, Sloan PR, Eppley RW (1966) Relationship between carbon content, cell volume and area in phytoplankton. Limnol Oceanogr 11:307-311

Murphy LS, Haugen EM (1985) The distribution and abundance of phototrophic ultraplankton in the North Atlantic. Limnol Oceanogr 30:47-58

Myklestad S, Haug A (1972) Production of carbohydrates by the marine diatom *Chaetoceros affinis* var. *willei* (Gran) Hustedt. I. Effect of the concentration of nutrients in the culture medium. J Exp Mar Biol Ecol 9:125-136

Nival J, Gostan J, Malara G, Charra R (1976) Évolution du plancton dans la Baie de Villefranche-Sur-Mer a la fin du printemps (Mai et Juin 1971). II. Biomasse de phytoplancton, production primaire. Vie Milieu 26:47-76

Odate T, Maita Y (1988) Regional variation in the size composition of phytoplankton communities in the Western North Pacific Ocean, Spring 1985. Biol Oceanogr 6:65-77

Oku O, Kamatawi A (1995) Resting spores formation and phosphorus composition of the marine diatom *Chaetoceros pseudocurvisetus* under various nutrient conditions. Mar Biol 123:393-399

Olson RJD, Vaulot D, Chisholm SW (1985) Marine phytoplankton distributions measured using shipboard flow cytometry. Deep-Sea Res 32:1273-1280

Oviatt CA (1981) Effects of different mixing schedules on phytoplankton, zooplankton and nutrients on marine microcosms. Mar Ecol Progr Ser 4:57-67

Ozmidov RV (1965) Certain features of the oceanic turbulent energy spectrum. Dokl Acad Nauk SSSR 161:828-832

Packard TT, Dortch Q (1975) Particulate protein-nitrogen in North Atlantic surface waters. Mar Biol 33:345-354

Packard TT, Minas HJ, Coste B, Martinez R, Bonin MC, Gostan J, Garfield P, Christensen J, Dortch Q, Minas M, Copin-Montegut G, Copin-Montegut C (1988) Formation of the Alboran oxygen minimum zone. Deep-Sea Res 35:1111-1118

Pahlow M, Riebesell U, Wolf-Gladrow DA (1997) Impact of cell shape and chain formation on nutrient acquisition by marine diatoms. Limnol Oceanogr 42:1660-1672

Parrilla G, Kinder TH (1985) The physical oceanography of the Alboran Sea. NATO Advanced Research Workshop. La Spezia, 7-14 September 1983. Proceedings. In: Charnock H (ed). pp 1-23

Parsons TR, Takahashi M (1973) Environmental control of phytoplankton cell size. Limnol Oceanogr 18:511-515

Pasciak WJ, Gavis J (1974) Transport limitations of nutrient uptake in phytoplankton. Limnol Oceanogr 19:881-888

Pasciak WJ, Gavis J (1975) Transport limited nutrient uptake rates in *Ditylum brightwellii.* Limnol Oceanogr 20:604-617

Passow U, Alldredge AL (1994) Distribution, size and bacterial colonization of transparent exopolymer particles (TEP) in the ocean. Mar Ecol Prog Ser 113:185-198

Paul JH, Myers B (1982) Fluorometric determination of DNA in aquatic microorganisms by use of Hoechst 33258. Appl Envirom Microbiol 43:1393-1399

Paul JH, Carlson DJ (1984) Genetic material in the marine environment: Implication for bacterial DNA. Limnol Oceanogr 29:1091-1097

Paul JH, Jeffrey WH, DeFlaun M (1985) Particulate DNA in subtropical oceanic and estuarine planktonic environments. Mar Biol 90:95-101

Pedrós-Alió C, Calderón-Paz J-I, Guixa-Boixereu N, Estrada M, Gasol JM (1999) Bacterioplankton and phytoplankton biomass and production during summer stratification in the northwestern Mediterranean Sea. Deep-Sea I 46:985-1019

Perkins H, Kinder T, La Violette P (1990) The Atlantic inflow in the western Alboran Sea. J Phys Oceanogr 20:242-263

Perry MJ (1972) Alkaline phosphatase activity in subtropical central North Pacific waters using a sensitive fluorometric method. Mar Biol 15:113-119

Perry MJ (1976) Phosphate utilization by an oceanic diatom in phosphorus-limited chemostat culture and in the oligotrophic water of the central North Pacific. Limnol Oceanogr 21:88-107

Peters F, Gross T (1994) Increased grazing rates of microplankton in response to small-scale turbulence. Mar Ecol Prog Ser 115:299-307

Peters F, Marrasé C, Gasol JM, Sala MM, Arin L (1998) Effects of turbulence on bacterial growth mediates through food web interactions. Mar Ecol Prog Ser 172:293-303

Peters F, Marrasé C (2000) Effects of turbulence on plankton: an overview of experimental evidence and some theoretical considerations. Mar Ecol Prog Ser 205:291-306

Peters F, Marrasé C, Havskum H, Rassoulzadegan F, Dolan J, Alcaraz M, Gasol JM (2002) Turbulence and the microbial food web: effects on bacterial losses to predation and on community structure. J Plankton Res 24:321-331

Petersen JE, Sanford LP, Kemp WM (1998) Coastal plankton responses to turbulence mixing in experimental ecosystem. Mar Ecol Prog Ser 171:23-41

Platt H (1985) Structure of marine ecosystem: Its allometric basis. Can Bull Fish Aquat Sci 213:55-64

Platt T, Mann KH, Ulanowicz RE (1981) Mathematical models in biological oceanography. UNESCO, Paris.

Porter KG, Feig YS (1980) The use of DAPI for identifying and counting aquatic microflora. Limnol Oceanogr 25:943-948

Posch T, Arndt H (1996) Uptake of sub-micrometer- and- micrometer-sized detrital particles by bacteriovorous and omnivorous ciliates. Aquat Microb Ecol 10:45-53

Pujo-Pay M, Raimbault P (1994) Improvement of the wet-oxidation procedure for simultaneous determination of particulate organic nitrogen and phosphorus collected on filters. Mar Ecol Prog Ser 105:203-207

Putt M, Stoecker DK (1989) An experimentally determined carbon:volume ratio for marine "oligotrichous" ciliates from estuarine and coastal waters. Limnol Oceanogr 34:1097-1103

Raimbault P, Taupier-Letage I, Rodier M (1988a) Vertical size distribution of phytoplankton in the western Mediterranean Sea during early summer. Mar Ecol Prog Ser 45:153-158

Raimbault P, Rodier M, Taupier-Letage I (1988b) Size fraction of phytoplankton in the Ligurian Sea and the Algerian Basin (Mediterranean Sea): size distribution versus total concentration. Mar Microb Food Webs 3:1-7

Redfield AC, Ketchum BH, Richards FA (1963) The infuence of organisms on the composition of sea-water. In: Hill MN (ed) The Sea. Vol 2 Wiley Interscience New York pp 26-79

Ribes M, Coma R, Gili JM (1999) Seasonal variation of particulate organic carbon, dissolved organic carbon and the contribution of microbial communities to the live particulate organic carbon in a shallow near-bottom ecosystem at the Northwestern Mediterranean Sea. J Plankton Res 21:1077-1100

Rizzo PJ, Noodén LD (1973) Isolation and chemical composition of dinoflagellate nuclei. J Protozool 20:666-672

Rodríguez J, Blanco JM, Jiménez-Gómez F, Echevarría F, Gil J, Rodríguez V, Ruiz J, Bautista B, Guerrero F (1998) Patterns in the size structure of the phytoplankton community in the deep fluorescence maximum of the Alboran Sea (southwestern Mediterranean). Deep-Sea Res I 45:1577-1593

Rodríguez J, Tintoré J, Allen JT, Blanco JM, Gomis D, Reul A, Ruiz J, Rodríguez V, Echevarría F, Jiménez-Gómez F (2001) Mesoscale vertical motion and the size structure of phytoplankton in the ocean. Nature 410:360-363

Rodríguez V (Repporteur) Bautista B, Blanco JM, Figueroa FL, Cano N, Ruiz J (1994) Hydrological structure, optical characteristics and size distribution of pigments and particles at a frontal station in the Albora Sea. Working group 1 Report. In: Rodríguez J, Li WKW (eds) The size structure and metabolism of the pelagic ecosystem. Sci Mar 58:31-41

Rothschild BJ, Osborn TR (1988) Small-scale turbulence and plankton contact rates. J Plankton Res 10:465-474

Ruiz J, García CM, Rodríguez J (1996) Sedimentation loss of phytoplankton cells from the mixed layer: effects of turbulence levels. J Plankton Res 18:1727-1734

Saiz E, Kiørboe T (1995) Predatory and suspension feeding on the copepod *Acartia tonsa* in turbulent environments. Mar Ecol Prog Ser 122:147-158

Sala MM, Karner M, Arin L, Marrasé C (2001) Measurement of ectoenzyme activities as an indication of inorganic nutrient imbalance in microbial communities. Aquat Microb Ecol 23:301-311

Sala MM, Peters F, Gasol JM, Pedrós-Alió C, Marrasé C, Vaqué D (2002) Seasonal and spatial variations in the nutrient limitation of bacterioplankton growth in the northwestern Mediterranean. Aquat Microb Ecol 27:47-56

Salat J, Cruzado A (1981) Masses d`eau dans la Méditerranée occidentale: Mer Catalane et eaux adjacentes. In Rapp Comm int Médit 27:201-209

Salat J, Garcia MA, Cruzado A, Palanques A, Arin L, Gomis D, Guillen J, de León A, Puigdefàbregas J, Sospedra J, Velásquez ZR (2002) Seasonal changes of water mass structure and shelf slope exchanges at the Ebro Shelf (NW Mediterranean). Cont Shelf Res 22:327-248

Sambrotto RN, Savidge G, Robinson C, Boyd P, Takahashi T, Karl DM, Langdon C, Chipman D, Marra J, Codispoti L (1993) Elevated consumption of carbon relative to nitrogen in the surface ocean. Nature 363:248-250

Sánchez-Arcilla A, Davies AM (2002) Fluxes Across a Narrow Shelf. Cont Shelf Res 22:151

Savidge G (1981) Studies of the effects of small-scale turbulence on phytoplankton. J Mar Biol Ass UK 61:477-488

Schütt F (1892) Analytische Planktonstudien. Lipsius & Tischer

Semina HJ (1968) Water movement and the size of phytoplankton cells. Sarsia 34:267-272

Sheldon RW, Prakash A, Sutcliffe WH Jr (1972) The size distribution of particles in the ocean. Limnol Oceanogr 17:327-340

Sieburth JMcN, Smetacek V, Lenz J (1978) Pelagic ecosystem structure: Heterotrophic compartments of the plankton and their relationship to plankton size fractions. Limnol Oceanogr 23:1256-1263

Siegenthaler U, Sarmiento JL (1993) Atmospheric carbon dioxide and the ocean. Nature 365:119-125

Simon M, Azam F (1989) Protein content and protein synthesis rates of planktonic marine bacteria. Mar Ecol Prog Ser 51:201-213

Simon N, Barlow RG, Marie F, Partensky F, Vaulot D (1994) Characterization of oceanic photosynthetic picoeukaryotes by flow cytometry. J Phycol 30:922-935

Skjoldal HR (1993) Eutrophication and algal growth in the North Sea. In: Della Croce NFR (ed) *Symposium Mediterranean Seas 2000.* Univ. of Genova, Instituto Scienze Ambientali Marine- Santa Margherita, Ligure pp 445-478

Smayda TJ (1970) The suspension and sinking of phytoplankton in the sea. Oceanogr Mar Biol Ann Rev 8:353-414

Smetacek V (1980) Annual cycle of sedimentation in relation to plankton ecology in western Kiel Bight. Ophelia Suppl 1:65-76

Smetacek V (1985) Role of sinking in diatom life-history cycles: ecological, evolutionary and geological significance. Mar Biol 84:239-251

Sommer U (1989) Maximal growth rates of Antarctic phytoplankton: only weak dependence of cell size. Limnol Oceanogr 34:1109-1112

Steele JH (1974) The structure of marine ecosystems. Harvard University Press, Cambridge.

Strickland JDH (1960) Measuring the production of marine phytoplankton. Bull Fish Res Bd Canada 122:1-172

Strickland JDH, Holm-Hansen O, Eppley RW, Linn RJ (1969) The use of a deep tank in plankton ecology. I. Studies of the growth and composition of phytoplankton crops at low nutrient levels. Limnol Oceanogr 14:23-34

Sundby S, Fossum P (1990) Feeding conditions of Arco-norwegian cod larvae compared with the Rothschild-Osborn theory on small-scale turbulence and plankton contact rates. J Plankton Res 12:1153-1162

Svensen C, Egge JK, Stiansen JE (2001) Can silicate and turbulence regulate the vertical flux of biogenic matter? A mesocosms study. Mar Ecol Prog Ser 217:67-80

Sverdrup HU, Johnson MW, Fleming RH (1942). The Oceans. Prentice-Hall

Takahashi M, Nagal H, Yamaguchi Y, Ichimura Y (1974) The distribution of chlorophyll a, protein, RNA and DNA in the North Pacific Ocean. J Oceanogr Soc Japan 30:137-150

Takahashi M, Bienfang PK (1983) Size structure of phytoplankton biomass and photosynthesis in subtropical Hawaiian waters. Mar Biol 76:203-211

Takahashi M, Hori T (1984) Abundance of picophytoplankton in the subsurface chlorophyll maximum layer in subtropical and tropical waters. Mar Biol 79:177-186

Tappan H (1980) *The Paleobiology of Plant Protists*. Freeman and company, San Francisco, California

Teira E, Serret P, Fernández E (2001) Phytoplankton size-structure, particulate and dissolved organic carbon production and oxygen fluxes through microbial communities in the NW Iberian coastal transition zone. Mar Ecol Prog Ser 219:65-83

Tenekes H, Lumley JL (1972) A first course in turbulence. MIT Press, Cambridge, MA

Thingstad TF, Sakshaug E (1990) Control of phytoplankton growth in nutrient recycling ecosystems. Theory and terminology. Mar Ecol Prog Ser 63:261-272

Thingstad TF, Skjoldal E, Bohne RA (1993) Phosphorus cycling and algal-bacterial competition in Sandsfjord, western Norway. Mar Ecol Prog Ser 99:239-259

Thingstad TF, Rassoulzadegan F (1995) Nutrient limitations, microbial food webs, and `biological C-pumps´: suggested interactions in a P-limited Mediterranean. Mar Ecol Prog Ser 117:299-306

Thingstad TF (1998) A theoretical approach to structuring mechanisms in the pelagic food web. Hydrobiologia 363:59-72

Thingstad TF, Zweifel UL, Rassoulzadegan F (1998) P limitation of heterotrophic bacteria and phytoplankton in the northwest Mediterranean. Limnol Oceanogr 43:88-94

Thomas H, Ittekkot V, Osterroht C, Schneider B (1999) Preferential recycling of nutrients- the ocean´s way to increase new production and to pass nutrient limitation? Limnol Oceanogr 44:1999-2004

Thomas WH, Gibson CH (1990) Effects of small-scale turbulence on microalgae. J Appl Phycol 2:71-77

Thomas WH, Vernet M, Gibson CH (1995) Effects of small-scale turbulence on photosynthesis, pigmentation, cell division, and cell size in the marine dinoflagellate *Gonyaulax polyedra* (Dinophyceae). J Phycol 31:50-59

Thompson PA, Harrison PJ, Parslow JS (1991) Influence of irradiance on cell volume and carbon quota for ten species of marine phytoplankton. J Phycol 27:351-360

Thompson PA, Guo M-x, Harrison PJ (1992) Effects of variation in temperature. I. On the biochemical composition of eight species of marine phytoplankton. J Plankton Res 28:481-488

Throndsen J (1978) Preservation and storage. In: Sournia A (ed) Phytoplankton Manual. UNESCO, Paris pp 69-74

Tintoré J, Gomis D, Alonso S, Parrilla G (1991) Mesoscale dynamics and vertical motion in the Alborán Sea. J Phys Oceanogr 21:811-823

Tundisi JG (1971) Size distribution of the phytoplankton and its ecological significance in tropical waters. In: Costlow JD (ed) Fertility of the Sea. Gordon & Breach, New York pp 603-612

Turpin DH, Harrison PJ (1980) Cell size manipulation in natural marine, planktonic, diatom communities. Can J Fish Aquat Sciencies 37:1193-1195

Utermöhl H (1958) Zur Vervollkommung der quantitativen Phytoplankton-Methodik. Mitt Int Ver Theor Angew Limnol 9:1-38

Vadstein O, Olsen Y (1989) Chemical composition and phosphate uptake kinetics of limnetic bacterial communities cultured in chemostats under phosphorus limitation. Limnol Oceanogr 34:939-946

Valderrama JC (1995) Methods of nutrient analysis. In: Hallegraeff GM, Anderson DM, Cembella AD (eds) Manual on harmful marine Microalgae. IOC Manuals and Guides No. 33, UNESCO, Paris pp 251-268

Vaulot D, Partensky F, Neveus J, Mantoura RFC, Llewellyn C (1990) Winter presence of prochlorophytes in surface waters of the northwestern Mediterranean Sea. Limnol Oceanogr 35:1156-1164

Verity PG, Langdon C (1984) Relationships between lorica volume, carbon, nitrogen, and ATP content of tintinnids in Narrangasett Bay. J Plankton Res 6:859-868

Verity PG, Robertson CY, Tronzo CR, Andrews MG, Nelson JR, Sieracki ME (1992) Relationships between cell volume and the carbon and nitrogen content of marine photosynthetic nanoplankton. Limnol Oceanogr 37:1434-1446

Videau C, Sournia A, Prieur L, Fiala M (1994) Phytoplankton and primary production characteristics at selected sites in the geostrophic Almeria-Oran front system (SW Mediterranean Sea). J Mar Syst 5:235-250

Wallen DG, Geen GH (1971) Light quality and concentration of protein, RNA, DNA and photosynthetic pigments in two species of marine plankton algae. Mar Biol 10:44-51

Weber LH, El-Sayed SZ (1987) Contributions of the net, nano- and picoplankton to the phytoplankton standing crop and primary productivity in the Southern Ocean. J Plankton Res 9:973-994

Werner D (1971) Der Entwicklungscyclus mit Sexualphase bei der marinem Diatomee *Coscinodiscus asteromphalus.* II. Oberflächenabhängige Differenzierung während der vegetativen Zellverkleinerung. Archiv Mikrobiol 80:115-133

Wheeler PA, Kirchman DL (1986) Utilization of inorganic and organic nitrogen by bacteria in marine systems. Limnol Oceanogr 31:998-1009

Whitledge TE, Malloy SC, Patton CJ, Wirick CD (1981) Automated nutrient analyses in seawater. Brookhaven National Laboratory, US Department of Energy and Environment, Upton, New York pp 1-216

Winn CD, Karl DM (1986) Diel nucleic acid synthesis and particulate DNA concentrations: Conflicts with division rate estimates by DNA accumulation. Limnol Oceanogr 31:637-645

Wotton RS (1984) The importance of identifying the origins of microfine particles in aquatic systems. OIKOS 43:217-221

Xiuren N, Zilin L, Genhai Z, Junxian S (1996) Size-fractionated biomass and productivity of phytoplankton and particulate organic carbon in the South Ocean. Polar Biol 16:1-11

Yentsch CS, Menzel DW (1963) A method for the determination of phytoplankton chlorophyll and phaeophytin by fluorescence. Deep Sea Res 10:221-231

Zirbel MJ, Veron F, Latz MI (2000) The reversible effect of flow on the morphology of *Ceratocorys horrida* (Peridiniales, Dinophyta). J Phycol 36:46-58

Zweifel UL, Norrman B, Hagström Å (1993) Consumption of dissolved organic carbon by marine bacteria and demand for inorganic nutrients. Mar Ecol Prog Ser 101:23-32

INTRODUCCIÓN

El conocimiento de la estructura de tamaños de las comunidades de microorganismos planctónicos y de su composición química es importante debido, entre otros aspectos, a la implicación que tienen ambos en el flujo de materia y energía entre los distintos eslabones de la cadena trófica. En un ambiente determinado, el desarrollo de un tipo de red trófica depende, fundamentalmente, de los factores físico-químicos del medio. Según el esquema generalmente aceptado, en aguas ricas en nutrientes y con cierta intensidad de mezcla turbulenta, el desarrollo de autótrofos grandes haría que predominase la vía trófica "clásica" (Steele 1974), mientas que en ambientes oligotróficos y estratificados, el desarrollo de autótrofos pequeños favorecería la vía trófica "microbiana" (Azam et al. 1983). La dominancia de una vía trófica u otra determinaría, a su vez, el destino final del carbono fijado fotosintéticamente.

El establecimiento de una determinada estructura de tamaños dentro de la comunidad de fitoplancton influye, a su vez, en el desarrollo de otros componentes de la comunidad de microorganismos planctónicos (bacterias heterotróficas, flagelados heterotróficos y ciliados). Por ejemplo, las bacterias heterotróficas y el fitoplancton (considerados como organismos osmotróficos, es decir, que asimilan directamente los nutrientes inorgánicos disueltos en el agua y en el caso de la bacterias, además, los nutrientes orgánicos) compiten por el nutriente limitante ante una situación de limitación de nutrientes (Bratbak & Thingstad 1985). Bajo esta situación, el flujo del nutriente limitante hacia la célula sería menor que la tasa potencial de incorporación de dicho nutriente por parte de la misma y, en ausencia de mecanismos activos de transporte, ésta pasaría a estar limitada por difusión. Cuando no hay movimiento del agua o de los microorganismos, los de menor tamaño, debido a su mayor relación superficie:volumen, tendrían ventajas competitivas sobre los grandes. Un movimiento de la células (ya sea por sedimentación o por natación) o del agua circundante, produce una renovación del nutriente limitante en el medio que las rodea, con lo que la incorporación de este nutriente hacia la célula puede aumentar en una cantidad denominada "transporte advectivo". La relación entre la cantidad total de nutriente que llega a la célula (por transporte advectivo y difusivo) y el que llegaría sólo por difusión (denominada número de Sherwood) depende del tamaño celular (Karp-Boss et al. 1996). Por lo tanto, en condiciones de mezcla o movimiento turbulento del agua, las células más grandes experimentarían un mayor aumento en la incorporación de nutrientes que las células pequeñas. Este aumento sería significativo a partir de un tamaño de unas 60 µm (Karp-Boss et al. 1996).

La estructura de tamaños de los productores primarios ha sido ampliamente estudiada debido a su gran importancia en relación con el funcionamiento de las redes tróficas pelágicas y el ciclo del carbono. En base a muchos de los trabajos realizados se pueden hacer ciertas generalizaciones. En aguas oligotróficas, las células de fitoplancton menores a 2 µm (picofitoplancton) constituyen más de un 50 % de la biomasa y de la producción primaria, mientas que en aguas eutróficas representan menos del 10 % (Agawin et al. 2000). Cuanto mayor es la biomasa de fitoplancton, menor es la contribución relativa del picofitoplancton. Esta fracción del fitoplancton ha sido considerada como prácticamente invariable en el espacio y en el tiempo (Raimbault et al. 1988b) aunque, en algunos casos, se ha observado que puede explicar la mayor parte de la variabilidad de la biomasa autotrófica total (Marañón et al. 2001).

La distribución de tamaños y/o los diferentes morfotipos que desarrollan las comunidades de fitoplancton según las condiciones ambientales, están definidas en algunos modelos conceptuales ("Mandala" de Margalef 1978, Legendre & Le Fèvre 1991). Estos modelos asocian la turbulencia, conjuntamente con una elevada concentración de nutrientes, con la predominancia de células de gran tamaño, y las condiciones de calma con el desarrollo de células pequeñas o dotadas de motilidad.

Dentro de una comunidad de fitoplancton, muchos procesos fisiológicos como el crecimiento y la respiración, así como el contenido en carbono, nitrógeno, proteína y clorofila *a*, son dependientes del tamaño celular (Banse 1976, Blasco et al. 1982, Montagnes et al. 1994). Por lo tanto, la estructura de tamaños de esta comunidad se verá reflejada en su composición química. Por otro lado, la proporción relativa de los grupos de microorganismos planctónicos (fitoplancton, bacterias heterotróficas, flagelados heterotróficos y ciliados) también se verá reflejada en la composición química de toda la comunidad. Por ejemplo, las bacterias asimilan los elementos C:N y N:P en una relación más baja que el fitoplancton (Redfield 1963, Chrzanowski et al. 1996). Además, estos organismos constituyen la mayor parte del ADN particulado en ambientes marinos (Holm-Hansen 1969a, b, Paul et al. 1985, Boehme et al. 1993). Por ello, una mayor o menor proporción de los distintos componentes de una determinada comunidad de microorganismos también influirá en su composición química.

En la presente memoria se han estudiado diversos aspectos ecológicos de las relaciones entre la caracterización taxonómica, la composición química y la distribución de tamaños de comunidades de microorganismos planctónicos bajo diferentes condiciones físico-químicas del ambiente.

Los principales objetivos de esta memoria han sido los siguientes:

A) Determinar experimentalmente la importancia de la turbulencia en el desarrollo de organismos osmotróficos (bacterias y fitoplancton) y en la estructura de tamaños y composición taxonómica del fitoplancton bajo diferentes condiciones iniciales de nutrientes.

B) Estudiar la estructura de tamaños de comunidades de fitoplancton y su composición taxonómica en sistemas naturales, así como su variabilidad espacio-temporal.

C) Estudiar cómo influye la estructura de tamaños y la composición taxonómica de la comunidad de microorganismos planctónicos en la composición química de la materia orgánica formada ya sea en experimentos de laboratorio como en sistemas naturales.

Los resultados expuestos en los distintos capítulos de esta tesis se resumen a continuación.

.

RESULTADOS

Efecto de la turbulencia en el crecimiento de dos diatomeas de diferente tamaño

El efecto de la turbulencia en el crecimiento de dos diatomeas marinas (*Thalassiosira pseudonana*, y *Coscinodiscus* sp.) ha sido observado en cultivos deficientes en fósforo durante aproximadamente 5 días. Al final del experimento, se observó un mayor número de células de *Coscinodiscus* sp. (110 µm de diámetro) en condiciones de turbulencia que en condiciones de calma (1.7 veces más células en condiciones de turbulencia). Sin embargo, el crecimiento de la *T. pseudonana* (6 µm de diámetro), ha sido prácticamente el mismo en ambos tratamientos. La relación entre la actividad específica de la fosfatasa alcalina (APA) en condiciones de calma y su actividad en condiciones de turbulencia (APA_s:APA_t) en los cultivos de *Coscinodiscus* sp. aumentó en el transcurso del tiempo hasta alcanzar valores entre aproximadamente 2 y 5 veces más elevados al final del experimento que a las 40 h del mismo. En cambio, en los cultivos de *T. pseudonana*, la relación APA_s:APA_t fue generalmente cercana a 1 durante todo el experimento. Se puso a punto un modelo dinámico del proceso de incorporación de fósfato y su transformación en biomasa de diatomea (en términos de fósforo) que se ajustó con parámetros experimentales y tomados de la literatura y produjo resultados similares a los observados experimentalmente. Según el modelo, la intensidad de turbulencia utilizada en los experimentos incrementaría en un 118 % la tasa de crecimiento de las células de *Coscinodiscus* sp. y sólo en un 19 % la de *T. pseudonana*.

Efecto de la turbulencia y los nutrientes en la dinámica de los organismos osmotróficos y su distribución de tamaños.

El efecto de la turbulencia sobre el desarrollo de la comunidad de fitoplancton y de bacterias, así como la estructura de tamaños del fitoplancton y su composición taxonómica, han sido estudiados en microcosmos marinos bajo diferentes condiciones iniciales de nutrientes. La presencia de turbulencia aumentó la importancia relativa de la comunidad fitoplanctónica con respecto a la bacteriana en los microcosmos en los que se añadieron inicialmente nutrientes, ya sea en una relación N:P deficiente en fósforo (microcosmos N) o en una relación N:P según Redfield (microcosmos NP). En cambio, en los microcosmos controles (C, sin adición inicial de nutrientes) la relación bacterias:fitoplancton fue la misma en condiciones de turbulencia que en condiciones de calma. La presencia de turbulencia en el medio también se vio reflejada en la composición taxonómica y en la distribución de tamaños de la comunidad fitoplanctónica. La importancia relativa de las diatomeas con respecto al total de fitoplancton fue mayor en condiciones de turbulencia que en condiciones de calma. Estas diferencias fueron más marcadas en los microcosmos NP. En estos microcosmos la relación entre la concentración de diatomeas y la de fitoplancton total fue 3 veces mayor en condiciones de turbulencia que en condiciones de calma. El tamaño celular medio de la comunidad fitoplanctónica fue mayor con turbulencia que sin ella. Este aumento se ha debido fundamentalmente a un incremento de la fracción mayor a 50 µm. Dentro de esta fracción, el grupo predominante fue el de las diatomeas, principalmente el de dos géneros formadores de cadenas: *Chaetoceros* y *Pseudo-nitzschia*.

Distribución de tamaños y tasas de crecimiento del fitoplancton en el Mar de Alborán y su variabilidad a corto plazo

En el Giro anticiclónico Occidental del Mar de Alborán (Mediterráneo Suroccidental), se comprobó que la estructura de tamaños y la composición taxonómica de la comunidad de fitoplancton era diferente en el borde norte del giro y en la zona central. Al principio de la campaña, en las tres estaciones muestreadas (ubicadas en el borde norte del Giro, en la zona central y una en una zona intermedia entre ambas), la contribución de las diferentes clases de tamaño de clorofila *a* analizadas (< 2 µm = picofitoplancton, 2 - 20 µm = nanofitoplancton y > 20 µm = microfitoplancton) a la clorofila *a* integrada total, osciló entre el 20 y el 40 %. Transcurridos 9 días, un pulso de afloramiento en la estación situada en el borde norte del giro se reflejó en un aumento de la biomasa fitoplanctónica total debido principalmente a un incremento en la fracción > 20 µm (principalmente diatomeas de los géneros *Chaetoceros* y *Pseudo-nitzschia*), que pasó a constituir el 60 % de la comunidad de fitoplancton. En cambio, en las aguas oligotróficas del centro del giro, en

el mismo intervalo de tiempo, se observó un aumento en las fracciones de pico- y nanofitoplancton (entre un 75 y un 95 % de la clorofila *a* total integrada) constituidas principalmente por *Synechococcus* y pequeños flagelados. En todas las estaciones, los organismos picoplanctónicos fueron relativamente más abundantes en las capas superficiales de la columna de agua, mientras que los organismos nano- y microplanctónicos tendieron a ser más importantes a mayor profundidad. Las tasas de crecimiento máximas de la comunidad fitoplanctónica oscilaron entre 0.45 y 1.41 d^{-1} y no presentaron diferencias significativas entre las distintas localidades muestreadas, a pesar de las diferencias físico-químicas observadas entre estaciones. Las tasas medias de crecimiento para la zona fótica se correlacionaron positivamente con la irradiancia recibida pero no presentaron correlaciones significativas ni con la composición taxonómica del fitoplancton ni con su estructura de tamaños. La relación carbono:clorofila disminuyó con la profundidad y con el aumento de la concentración de nutrientes (en un gradiente horizontal) y tendió a ser más alta en la fracción mayor de 2 µm.

Variabilidad espacio-temporal de la distribución de tamaños del fitoplancton en el Delta del Ebro

En la plataforma del Ebro (Mediterráneo Noroccidental), se estudió la distribución de mesoescala y la variación estacional de la estructura de tamaños de la biomasa fitoplanctónica (medida como clorofila *a*) durante tres estaciones del año: otoño, invierno y verano. En otoño y verano, la columna de agua se mostró estratificada y las concentraciones de nutrientes en la zona fótica fueron muy bajas (generalmente menos de 1.0, 0.1 y 2.0 µM de nitrato, fosfato y silicato, respectivamente, en los primeros 50 - 60 m de la columna de agua). Bajo estas condiciones, las concentraciones medias de clorofila *a* (± SE) para la zona fótica fueron de 0.31 ± 0.02 mg m^{-3} (otoño) y 0.29 ± 0.01 mg m^{-3} (verano). En invierno, el aporte de aguas ricas en nutrientes provenientes del río Ebro y de aguas profundas (llevadas a la superficie por una intensa mezcla vertical), se vieron reflejadas en un aumento en la biomasa de fitoplancton (0.76 ± 0.05 mg m^{-3}). En las tres estaciones del año, el picofitoplancton (< 2 µm) fue la fracción más importante de la biomasa total y constituyó un 42 % de la clorofila *a* en invierno y cerca de un 60 % en los meses de otoño y verano. La contribución de la fracción microplanctónica (> 20 µm) al total de clorofila *a* fue más elevada en invierno (27 %) que en otoño y verano (menos del 13 %). El porcentaje de nanofitoplancton (2 - 20 µm) fue el que varió menos entre las tres estaciones muestreadas (entre un 29 y un 39 % de la biomasa total). La fracción de clorofila *a* > 2 µm aumentó de forma lineal con la biomasa total. Sin embargo, la clorofila *a* < 2 µm aumentó linealmente con la clorofila *a* total sólo para concentraciones de ésta menores a 1 mg m^{-3} (en otoño y verano) o 2 mg m^{-3} (en invierno). Para valores más altos de clorofila *a* total, la fracción < 2 µm se mantuvo más o menos estable y no superó los 0.5 mg m^{-3}. En

otoño e invierno, el aporte de nutrientes provenientes del río Ebro y los procesos de mezcla vertical produjeron un aumento de la fracción de clorofila *a* > 2 µm en la zona costera cercana al Delta del Ebro. Como consecuencia, en estas estaciones, la contribución de la fracción < 2 µm al total de clorofila *a* fue menor en áreas costeras (menos del 40 % de la clorofila *a* total integrada) que mar afuera. En verano, la contribución de la fracción < 2 µm fue similar en toda la zona muestreada y constituyó entre un 40 y el 60 % de la biomasa total. La distribución vertical de la clorofila *a* total presentó sus máximos valores en superficie en invierno, a profundidades cercanas a los 40 m en otoño, y entre los 50 y 80 m en verano. La contribución relativa de la fracción < 2 µm en los máximos de biomasa total tendió a ser mayor que en otras profundidades en otoño e invierno y menor en verano. En otoño y verano, cuando se observó un máximo profundo de clorofila, la cantidad de biomasa autotrófica (ya sea total o fraccionada) correspondiente a los primeros 10 m de profundidad de la mayoría de las estaciones de mar afuera, constituyó menos de un 10 % de la biomasa fitoplanctónica integrada en toda la columna de agua (hasta el fondo o hasta los 100 m de profundidad).

Efecto de la turbulencia y los nutrientes en la dinámica de la materia orgánica y del fósforo.

En microcosmos marinos, los cambios producidos por la turbulencia sobre la dinámica de los organismos osmotróficos y su estructura de tamaños (y como consecuencia el de toda la comunidad) se vieron reflejados en la composición química de la materia orgánica formada. De hecho, en los microcosmos a los que se añadieron inicialmente nutrientes [ya sea en una relación N:P deficiente en fósforo (microcosmos N) o según Redfield (microcosmos NP)] la relación entre biomasa de organismos heterotróficos y la biomasa total fue hasta dos veces menor en condiciones de turbulencia que en condiciones de calma. En estos mismos microcosmos, la biomasa (en términos de carbono) de organismos osmotróficos producida en relación al fosfato y al nitrato consumidos fue mayor en condiciones de turbulencia que en condiciones de calma. En estos experimentos, se observó también que el aumento en la biomasa de diatomeas (también en términos de carbono) con respecto al silicato consumido fue mayor en tratamientos de turbulencia que de calma. Para las tres condiciones de nutrientes (microcosmos N, microcosmos NP y microcosmos C, estos últimos sin adición inicial de nutrientes), la aplicación de turbulencia se tradujo en una mayor proporción de C:P y N:P orgánicos que en condiciones de calma. En general, se observó una mayor tasa de renovación del fósforo (estimada mediante la incorporación de fósforo radiactivo por las células) en condiciones de turbulencia que de calma, especialmente en los microcosmos NP.

ADN y proteína particulados en relación a la biomasa de microorganismos y a la concentración de detritus en el Mar Catalano-Balear

En dos estaciones de diferentes características hidrográficas, ubicadas en el Mar Catalano-Balear (Mediterráneo Noroccidental), se estudió la contribución relativa de los principales grupos de microorganismos planctónicos a la concentración total de ADN y proteína particulados. Ambas estaciones presentaron un máximo profundo de clorofila (MPC) entre los 40 y 50 m de profundidad, cerca del cual se ubicaron las concentraciones máximas de ADN. En cambio, las concentraciones de proteína fueron más o menos constantes en los primeros 60 m de profundidad. La distribución de organismos presentó sus máximas concentraciones (en número) a profundidades coincidentes con las del MPC o cercanas a las del mismo. En las dos estaciones muestreadas, las bacterias fueron las principales contribuyentes al ADN particulado "vivo" (no detrítico) total (entre un 22.5 y un 32.6 %), mientras que el fitoplancton y los nanoflagelados heterotróficos lo fueron a la proteína particulada "viva" total (entre un 3.8 y 24.4 % y entre un 2.9 y 29.1 %, respectivamente). La fracción detrítica del ADN correspondió entre un 23.9 y un 42.9 % del total de ADN particulado, mientras que la proteína detrítica resulto ser entre un 63.5 y un 84.7 % de la proteína particulada total.

DISCUSIÓN

Los resultados obtenidos en esta memoria han mostrado la importancia de la turbulencia en el crecimiento de células osmotróficas de tamaño superior a un determinado umbral. En condiciones experimentales y, de acuerdo con las teorías generalmente aceptadas (Karp-Boss et al. 1996), la presencia de turbulencia favoreció el crecimiento de las células osmotróficas grandes sobre las pequeñas, con lo que cambió la proporción bacterias:fitoplancton y la estructura de tamaños de la comunidad fitoplanctónica. Sin embargo, el efecto de la turbulencia estuvo condicionado por la concentración de nutrientes del medio. Según Marrasé & Peters (2002), a concentraciones de nutrientes muy bajas o muy altas, la presencia de turbulencia no tendría ningún efecto directo sobre el crecimiento de los organismos osmotróficos. Los resultados obtenidos indican, también, la importancia de considerar el factor turbulencia en la modelización del crecimiento algal.

En ambientes naturales, una mayor proporción de células grandes (> 2 µm) en la comunidad fitoplanctónica estuvo siempre asociada a concentraciones elevadas de nutrientes y a una importante intensidad de mezcla vertical de la columna de agua. Al igual que lo observado en los experimentos, los principales componentes de esta fracción de fitoplancton (fundamentalmente

> 20 µm) fueron organismos pertenecientes al grupo de las diatomeas. En cambio, en aguas oligotróficas y/o estratificadas, la fracción picoplanctónica (< 2 µm) del fitoplancton fue la más importante. Bajo condiciones de limitación de nutrientes, los organismos pequeños, con mayor relación superficie:volumen que los de mayor tamaño, tendrían ventajas competitivas sobre éstos últimos. En contraste con el existente paradigma de la constancia de la fracción picoplanctónica, en esta memoria se ha observado que ésta puede variar de manera significativa tanto entre las distintas estaciones del año como en diversas situaciones hidrográficas dentro de cada estación.

Los resultados obtenidos concuerdan con los modelos conceptuales existentes (Margalef 1978, Legendre & Le Fèvre 1991), los cuales asocian la turbulencia, acompañada por una elevada concentración de nutrientes, con un aumento de células de gran tamaño, y las condiciones de calma, con el desarrollo de células pequeñas o dotadas de motilidad.

Como se ha visto anteriormente, las condiciones hidrodinámicas y la concentración de nutrientes en el medio condicionan el establecimiento de comunidades de microorganismos de características diversas (ya sea a nivel de composición taxonómica o de estructura de tamaños). Esta variabilidad se refleja en diferencias en la composición química de la comunidad por lo que refiere a la proporción de carbono y nitrógeno orgánicos y a la contribución de clorofila, proteína y ADN. Estos resultados indican la importancia de considerar los distintos niveles de interacción entre las condiciones físico-químicas del medio y los organismos.